

THE PAST AND FUTURE IMPACT OF ICE TONGUE LOSS
ON OUTLET GLACIERS IN NORTHERN GREENLAND

EMILY ANN HILL

Thesis submitted for the degree of
Doctor of Philosophy



*School of Geography, Politics & Sociology
Newcastle University
Newcastle upon Tyne
United Kingdom*

March 2020

Abstract

Ice discharge from fast-flowing outlet glaciers across the Greenland Ice Sheet (GrIS) has increased in response to 21st century climate warming. These outlets are sensitive to changes at their terminus, particularly iceberg calving from floating tongues. Many glaciers have accelerated and thinned in response to recent retreat, but the impact of major calving events and ice tongue loss on ice discharge and sea level rise remains poorly constrained. Northern Greenland is the last region with floating ice tongues, but remains understudied compared to other regions of the ice sheet. The aim of this thesis is to quantify outlet glacier change across northern Greenland and assess the role of ice tongues in modulating past and future glacier dynamics. To address this aim I use: i) remote sensing to assess past glacier change across northern Greenland, and ii) two sets of numerical modelling experiments to simulate future ice tongue loss at Petermann Glacier. The key findings are that outlet glacier retreat rates have increased in the last two decades, but the dynamic response to retreat was dependent on terminus type (grounded vs floating) and glacier geometry. Grounded outlet glaciers retreated, accelerated and thinned, while the response of glaciers with ice tongues was more varied, and dependent on tongue confinement and bed topography inland of the grounding line. Modelling experiments on Petermann Glacier further corroborate these findings, demonstrating that unconfined portions of the tongue had little impact on dynamics, but removing confined sections closer to the grounding line accelerated ice flow. However, the long-term response (up to 100-years) to ice tongue loss was muted by the absence of a retrograde bed-slope in the grounding zone, which limited grounding line retreat. Overall, this thesis highlights the complexity of outlet glacier behaviour in northern Greenland. It also notes the variability between individual glacier responses to ice tongue loss. These factors require careful consideration when assessing future glacier sensitivity to ice tongue/shelf loss in both Greenland and Antarctica in order to accurately project accelerated ice discharge and ultimately global sea level rise.

Declaration

This thesis is the result of my own work done under the supervision of J. R. Carr, C. R. Stokes and G. H. Gudmundsson. It has not been previously submitted for a degree or other qualification in this or any other University. Chapters 2, 3 and 4 are all based on published papers in which J. R. Carr, C. R. Stokes and G. H. Gudmundsson are co-authors. The details of these papers are included in the summary sections at the beginning of each chapter. In all cases I conducted all of the analysis and writing, and co-authors provided editorial input.

Emily Hill

July 2019

Acknowledgements

First and foremost I would like to thank my supervisors Rachel Carr, Chris Stokes, and Hilmar Gudmundsson for their academic guidance throughout, but also for the pastoral support and personal development that inevitably come hand in hand with completing a PhD. Rachel, thank you for your constant support in all aspects, be it writing, modelling, or teaching, and additionally for the memories made on trips both overseas and down to Cambridge. Chris, thank you for all your input, in particular for taking the time to provide such detailed feedback and guidance which greatly improved my research and writing ability. Hilmar, thank you for your patience and guidance throughout the modelling aspects of this thesis, I've learnt a huge amount, that extends beyond just how glaciers flow. I would also like to thank Prof. Pete Nienow and Dr Stuart Dunning for their constructive feedback and interesting discussion during the examination of this thesis.

This thesis was made possible by funding from the IAPETUS Doctoral Training Partnership through Newcastle University, and I am grateful for the opportunities provided through this scheme, including the experiences shared with other members of the DTP. I would also like to thank my CASE partner, the British Antarctic Survey, who provided financial support for visits to Cambridge. Thanks must also go to all the lecturing and support staff and students within the School of Geography, Politics, and Sociology - thank you for making me feel welcome and providing a safe and supportive environment to do research.

I'd like to thank PGR colleagues that have become great friends during the last years. To begin, I want to thank Arminel Lovell for being a constant sounding board, for all the coffee break chats/pub trips etc., and for the amazing memories made on fieldwork to Nepal - they will last a lifetime. I'd equally like to thank Izzy Williams for the support she has given me, often without me even realising I needed it, and for all the great memories shared both inside and outside of the office. This journey wouldn't have been the same without either of you. I'd also like to make special mentions to Ryan Dick and Jake Collins-May for the hilariously inappropriate puns, constant laughs, putting up with my rants, and at the same time (perhaps unknowingly) providing me with a whole load of strength when I needed it. Also a big thank you to anyone (PGRs in Newcastle or elsewhere) that I haven't mentioned by name here, if you've taken the time to read this then you know who you are!

Two final thanks. A huge thank you to my family for their continued support in any venture I pursue, in particular to my parents whose resilience and perseverance has set me on the path I am today. Finally, Devin, thank you not only for the encouragement you have given me during this PhD, but for the selfless unconditional support you provide me with daily. Thank you for having the strength to take on my baggage alongside your own challenges, I'm so grateful.

Contents

| | | |
|----------|---|-----------|
| 1 | Introduction | 1 |
| 1.1 | Research Background | 1 |
| 1.1.1 | Ice sheets and outlet glaciers | 1 |
| 1.1.2 | Glacier force balance and terminus change | 5 |
| 1.1.3 | Ice shelves and buttressing | 8 |
| 1.1.4 | Northern Greenland | 9 |
| 1.2 | Rationale | 10 |
| 1.3 | Aim and objectives | 11 |
| 1.4 | Thesis outline | 12 |
| 2 | A review of recent changes in major marine-terminating outlet glaciers in northern Greenland | 14 |
| 2.1 | Chapter summary | 14 |
| 2.2 | Introduction | 15 |
| 2.3 | Regional changes in glacier dynamics | 19 |
| 2.3.1 | Northwest Greenland | 21 |
| 2.3.2 | North Greenland | 25 |
| 2.3.3 | Northeast Greenland | 35 |
| 2.3.4 | Summary of northern Greenland outlet glacier changes | 39 |
| 2.4 | Discussion | 40 |
| 2.4.1 | Atmospheric and oceanic forcing | 41 |
| 2.4.1.1 | Subaerial ice melt | 41 |
| 2.4.1.2 | Submarine melt | 43 |
| 2.4.2 | Sea ice influence | 44 |
| 2.4.3 | Glacier-specific factors | 45 |
| 2.4.3.1 | Fjord width | 45 |
| 2.4.3.2 | Floating ice tongues | 46 |

| | | |
|----------|--|-----------|
| 2.4.3.3 | Basal topography | 46 |
| 2.4.4 | Glacier surging | 47 |
| 2.5 | Future changes | 49 |
| 2.6 | Conclusions | 50 |
| 3 | Dynamic changes in outlet glaciers in northern Greenland from 1948 to 2015 | 52 |
| 3.1 | Chapter summary | 52 |
| 3.2 | Introduction | 53 |
| 3.3 | Methods | 55 |
| 3.3.1 | Study region | 55 |
| 3.3.2 | Terminus change | 56 |
| 3.3.2.1 | Data sources | 56 |
| 3.3.2.2 | Front position mapping | 57 |
| 3.3.2.3 | Changepoint analysis | 60 |
| 3.3.3 | Ice velocity and surface elevation | 61 |
| 3.3.4 | Fjord width and basal topography | 63 |
| 3.4 | Results | 64 |
| 3.4.1 | Changes in glacier frontal position (1948-2015) | 64 |
| 3.4.2 | Frontal position change according to terminus type | 66 |
| 3.4.3 | Ice velocity change | 70 |
| 3.4.4 | Surface elevation change | 73 |
| 3.4.5 | Topographic factors | 74 |
| 3.5 | Discussion | 77 |
| 3.5.1 | Timing of glacier change between 1948 and 2016 | 77 |
| 3.5.2 | Dynamic glacier response to terminus change | 80 |
| 3.5.3 | Influence of glacier geometry | 82 |
| 3.5.4 | Glacier surging | 84 |
| 3.6 | Conclusions | 85 |
| 4 | Velocity response of Petermann Glacier, northwest Greenland to past and future calving events | 87 |
| 4.1 | Chapter summary | 87 |
| 4.2 | Introduction | 88 |
| 4.3 | Methodology | 91 |
| 4.3.1 | Data Input | 91 |
| 4.3.2 | Model Initialization | 93 |

| | | |
|----------|--|------------|
| 4.3.3 | Model Inversion | 96 |
| 4.3.4 | Boundary Conditions | 98 |
| 4.3.5 | Model Experiments | 101 |
| 4.4 | Results | 103 |
| 4.4.1 | Response to 2010 and 2012 calving | 103 |
| 4.4.2 | Response to future calving events | 105 |
| 4.5 | Discussion and Conclusions | 108 |
| 5 | Grounding line stability limits 21st century sea level rise from Petermann Glacier in response to ice tongue loss | 110 |
| 5.1 | Chapter summary | 110 |
| 5.2 | Introduction | 111 |
| 5.3 | Methods | 112 |
| 5.3.1 | Model set-up | 112 |
| 5.3.2 | Model initialization and control run | 116 |
| 5.4 | Results | 119 |
| 5.5 | Discussion | 125 |
| 5.6 | Conclusions | 128 |
| 6 | Discussion | 129 |
| 6.1 | Recent retreat of glaciers in northern Greenland and the role of ocean-climate forcing | 129 |
| 6.2 | Glacier sensitivity to ice tongue loss | 134 |
| 6.3 | Role of bed geometry in modulating glacier dynamics | 137 |
| 6.4 | Future work | 140 |
| 7 | Conclusions | 143 |
| A | Bed slope direction and errors in basal topography | 146 |
| B | Sensitivity of our model results to the slipperiness exponent value (m) in the Weertman sliding law | 149 |
| B.1 | Diagnostic experiments | 150 |
| B.2 | Transient experiments | 150 |
| | References | 152 |

List of Figures

| | | |
|-----|--|---|
| 1.1 | Cumulative ice mass loss (and sea level equivalent SLE) of the Greenland (a) and Antarctic (b) ice sheets between 1991 and 2012 derived from numerous recent studies incorporated into the Fifth IPCC report Chapter 4 [Vaughan <i>et al.</i> , 2013]. | 2 |
| 1.2 | Modified from the IPCC AR5 report Chapter 4 [a-c: Vaughan <i>et al.</i> , 2013] and [d: Murray <i>et al.</i> , 2015]. a) is mean surface mass balance for the period 1989 to 2003 from regional atmospheric climate modelling [Ettema <i>et al.</i> , 2009]. b) ice sheet velocity for 2007 to 2009 from satellite data where red is fast flow and slower flow is in yellow [Rignot & Mouginot, 2012]. c) changes in ice sheet surface elevation for 2003 to 2008 from ICESat altimetry, where red is elevation decrease and blue is increase [Pritchard <i>et al.</i> , 2009]. d) changes in frontal position between 2000-2010 from Murray <i>et al.</i> [2015] for 199 glaciers, where proportional sized circles represent the magnitude of frontal position change, and red is retreat and blue is glacier advance. . . . | 4 |
| 1.3 | Glacier forces acting on a block of ice (modified from Cuffey & Paterson [2010]). Glacier flows in the direction X, the base is irregular to reflect subglacial topography (β), surface slope is α , and ice thickness is H . Lateral drag (τ_w) occurs along planes A and A' (sidewalls), while longitudinal resistive stress (τ_L) acts on the front and back of the ice block (planes B and B'). | 5 |
| 1.4 | Schematic diagrams of changes in force balance at grounded outlet glaciers (left diagrams) and glaciers that terminate in a floating ice tongue (right diagrams). Larger arrows represent greater resistance (lateral and basal) or greater driving stress. Top panels show the glacier before an initial thinning of the surface at the grounded terminus or along the floating ice tongue. Bottom panels show the change in glacier force balance due to perturbations of the terminus: i.e. surface lowering, a reduction in basal and lateral drag, an increase in driving stress and calving. | 7 |

| | | |
|-----|---|----|
| 1.5 | Photographs of Antarctic and Arctic ice shelves. (a) Larsen C Ice Shelf and Gipps Ice Rise, eastern Antarctic Peninsula (Photo: C.W.M. Swithinbank). The ice rise is about 18 km long. (b) A floating glacier tongue, 2–4 km wide, embedded in sea ice immediately north of the larger Aviator Glacier Tongue, Victoria Land Coast, Antarctica (Photo: J.A. Dowdeswell). (c) The floating margin of Daugaard Jensen Gletscher, East Greenland (Photo: J.A. Dowdeswell). (d) The Ward Hunt Ice Shelf, northern Ellesmere Island, Arctic Canada (Photo: D.R. Mueller). Taken from Dowdeswell & Jeffries [2017]. | 10 |
| 2.1 | Location map of Northern Greenland showing the glaciers reviewed in this paper. The study area has been split into three geographical regions which are Northwest Greenland (2.3.1), North Greenland (2.3.2) and Northeast Greenland (2.3.3). Colored circles show a first order classification of potential surge-type glaciers across northern Greenland. Red circles show glaciers which are likely to be surge type based on clear surge-cycles having been recorded within the literature. Yellow circles show glaciers at which surging is possible based on glaciers which may have shown surge-characteristics, but either have not been referred to as surge-type or have not undergone a large surge event. Green circles show glaciers at which no evidence of surging has been recorded in the literature. Background image derived from NASA EOSDIS Worldview (16.07.15 and 21.07.15). | 16 |
| 2.2 | A) Location of large floating ice tongues around the northern Greenland study region based on a review of the literature. Glacier abbreviations relate to Table 2.1. B) Bed topography data across Greenland displayed as areas below sea level (< 0 m), deep areas in red, shallower bed topography in blue. Both bed topography and floating ice tongue data were derived from the IceBridge BedMachine Greenland, Version 2 dataset in 2015 [Morlighem <i>et al.</i> , 2014]. C) glacier velocities (m a^{-1}) during 2009/10 acquired from the MEaSUREs v2 Greenland velocity dataset [Joughin <i>et al.</i> , 2010b] and catchment areas of northern Greenland outlet glaciers derived from hydrological analysis using the Morlighem <i>et al.</i> [2014] bed elevation and ice thickness datasets. | 18 |

| | | |
|-----|--|----|
| 2.3 | A) Location of studied glaciers in Northwest Greenland, including Harald Moltke Bræ, Heilprin and Tracy Glaciers (green circles) and grounded ice (black line). Velocity data were acquired from the 2005/2006 MEaSUREs v2 Greenland velocity [Joughin <i>et al.</i> , 2010b]. Background imagery is from Landsat 8 (late summer 2015). B) estimated terminus positions from Wright [1939], showing changes between 1916 and 1932, and its position in 2015 (green). C) previous terminus positions for Tracy and Heilprin Glaciers [Dawes & As, 2010] and the 2015 position (light blue). | 22 |
| 2.4 | Several dramatic retreat events observed at northern Greenland outlet glaciers. Panels a) and b) show Tracy Glacier retreat between 2000 and 2006. Petermann Glacier's large calving event in 2010 is shown in c/d. Steensby Glacier retreat in e/f. A significant disintegration of C. H. Ostenfeld floating ice tongue is shown in g/h. All background Landsat imagery was derived from USGS Earth Explorer from the years shown in the panels. | 24 |
| 2.5 | North Greenland region. A) Humboldt and Petermann Glaciers. B) Seven outlet glaciers in the most northern part of the study region between Steensby Glacier and Henson Glacier. C) Marie-Sophie, Academy and Hagen Bræ Glaciers. Grounded ice is shown in a black outline. Velocity is shown on each glacier in m a^{-1} . Velocity data was acquired from the 2008/2009 MEaSUREs v2 Greenland velocity [Joughin <i>et al.</i> , 2010b]. Background imagery is from Landsat 8 (late summer 2015). | 29 |
| 2.6 | Northeast Greenland region that includes Nioghalvfjærdsfjorden (79North), Zachariæ Isstrøm, Kofoed-Hansen Bræ, Storstrømmen, and L. Bistrup Bræ. Grounded ice is shown in a black outline. Velocity is shown on each glacier in m a^{-1} . Velocity data was acquired from the 2008/2009 MEaSUREs v2 Greenland velocity [Joughin <i>et al.</i> , 2010b]. Background imagery is from Landsat 8 (late summer 2015). | 36 |
| 2.7 | A summary of recorded changes at northern Greenland outlet glaciers based on a review of the literature. Key events of terminus change (circles, red for retreat, blue for advance), velocity change (triangle), grounding line retreat (cross) and glacier thinning (square), that have occurred at all northern Greenland focus glaciers between 1880 and present (2015) are recorded. Data points are shown in the middle of study periods and the grey lines show the duration over which the change refers to. All data points are converted to m a^{-1} across the study period and the size of all data points are based on m a^{-1} magnitude. The legend shows the symbol sizes and their corresponding values for each category of data shown. | 40 |

| | | |
|-----|--|----|
| 2.8 | Velocity change between winters 2000/01 and 2008/09 using MEaSUREs v2 Greenland velocity data [Joughin <i>et al.</i> , 2010b]. Orange and red colors show velocity increase, and green and blue show velocity decrease. | 41 |
| 3.1 | Study region of northern Greenland. Green circles show the location of each of 18 northern Greenland study outlet glaciers. Average glacier velocities (m a^{-1}) are shown between 1993 and 2015 derived from the multi-year mosaic dataset [Joughin <i>et al.</i> , 2010b]. Black outlines show glacier drainage catchments. Symbols represents the state of the glacier terminus. Stars show glaciers which currently have floating ice tongues, circles represent glaciers which lost their ice tongues (during 1995 to 2015), squares denote glaciers which have some previous literature record of a floating ice tongue, and triangles are glaciers which are grounded at their termini and have been throughout the study record. | 56 |
| 3.2 | Rectilinear box method used to measure glacier terminus positions. An example at Harald Moltke Bræ, NW Greenland. This includes: reference box (pink), and roughly decadal terminus positions (green to red). The glacier centreline profile is shown in white and the location of 500 m sample points (white circles). Background image is Landsat 8 band 8 from the USGS Earth Explorer. | 59 |
| 3.3 | Schematic diagram of terminus position behaviour in northern Greenland. Two categories of behaviour determined from changepoint detection, which align to the differences in terminus type. The first (a) is an example of a glacier front position switching from minimal terminus change to a period of steady terminus retreat (grey), the second (b) shows a glacier which undergoes a period of rapid retreat (grey) after minimal terminus change. | 61 |
| 3.4 | Overall mean rate of terminus change (m a^{-1}) at 18 outlet glaciers in northern Greenland from 1948 to 2015. Green circles represent glaciers which have undergone overall advance during the record, while yellow to red circles represent increasing retreat rates from 0 to larger than -300 m a^{-1} | 65 |
| 3.5 | Mean decadal rates of terminus change across northern Greenland. These are shown for five epochs between 1948 and 2015. Increasing red circles represent glacier retreat rates between 0 and exceeding -1000 m a^{-1} . Increasing blue circles represent advance rates between 0 and exceeding $+1000 \text{ m a}^{-1}$ | 67 |

| | | |
|------|--|----|
| 3.6 | Retreat rates during identified periods of either minimal frontal position change or periods of either steady or rapid retreat and displayed by either grounded or floating termini. Glaciers are then ordered based on their overall (1948-2015: Table 3.2) frontal position change rates within each of these categories. Grey bars show their periods of minimal/variable terminus change (in some cases advance) and turquoise bars show the period of higher magnitude frontal position change. | 68 |
| 3.7 | Front position, velocity and elevation change at nine outlet glaciers grounded at their terminus in northern Greenland. Left axes show relative front position (black line) between 1948 and 2015 relative to their initial position in 1948. Grounding line velocities (purple) on right axes one between 1996 and 2015. Surface elevation changes averaged across the glacier centreline profile (green) for 1996 to 2015. | 70 |
| 3.8 | Front position, velocity and elevation change at nine outlet glaciers which terminate in floating ice tongues in northern Greenland. Left axes show relative front position (black line) between 1948 and 2015 relative to their initial position in 1948. Grounding line velocities (purple) on right axes one between 1996 and 2015. Surface elevation changes averaged across the glacier centreline profile (green) for 1996 to 2015. | 72 |
| 3.9 | Annual surface elevation change, annual velocity and surface/bed topography for two outlet glaciers in northeast Greenland: Storstrømmen (a) and L. Bistrup Bræ (b). Blue to green coloured lines represent annual surface elevation through time (1992-96 to 2014-15) and yellow through to red lines represent annual winter velocity from 1991/92 to 2015/16. | 75 |
| 3.10 | Basal topography from Operation IceBridge BedMachine v3 [Morlighem <i>et al.</i> , 2017] beneath nine study glaciers with grounded termini in northern Greenland. Red points represent the position of the terminus/grounding line at each glacier from our most recent record of their terminus position (2015). Black lines are glacier centreline profiles. Profile plots show basal elevations along each glacier centreline profile and solid red lines nearest to zero show the terminus location. | 76 |

| | | |
|------|---|----|
| 3.11 | Basal topography from Operation IceBridge BedMachine v3 [Morlighem <i>et al.</i> , 2017] beneath nine study glaciers which terminate in floating ice tongues in northern Greenland. Red points represent the most recent recorded terminus position (2015) from this study. Green points represent the location of the grounding line along the centreline profile from the GIMP DEM mask [Howat <i>et al.</i> , 2014]. Profile plots show basal elevations along each glacier centreline profile, where closest to zero red lines show the terminus locations, and further inland green lines shown the grounding line. | 78 |
| 3.12 | Landsat imagery of three glaciers which terminate in floating ice tongues in northern Greenland before their ice tongue collapse. (a) Steensby Glacier in 2013, (b) C. H. Ostenfeld Glacier in 2002, (c) Hagen Bræ in 2005. Purple lines denote the location of the grounding line. | 83 |
| 4.1 | Study location, Petermann Glacier, northwest Greenland. Observed ice speeds from the MEaSUREs program (winter 2009/10: Joughin <i>et al.</i> 2010 <i>b</i>) across the Petermann Glacier catchment, which corresponds with the model domain. White lines show 300 m ice surface contours across the catchment. The thick black line is the glacier centerline and the thick red line is the glacier grounding line. Inset shows the location of newly prescribed terminus positions for each diagnostic perturbation experiment (A-H). Light green shows floating ice, and white is grounded ice. | 90 |
| 4.2 | Spatial distribution of observed and modeled changes in flow speeds across the Petermann Glacier ice tongue after calving events in 2010 and 2012. Left two plots show the observed changes in speed between initial pre-calving observed speed (winter 2009/10, MEaSUREs Joughin <i>et al.</i> [2010 <i>b</i>]) and observed speeds after the 2010 calving event (top) and 2012 calving event (bottom). Right hand plots show the corresponding modeled change in speed between initial modeled flow speeds and speeds after removing sections of the ice tongue in 2010 (top) and 2012 (bottom). xpsn and ypsn are x and y kms in polar stereographic north projection, respectively | 94 |

-
- 4.3 Observed and modeled velocities along the Petermann Glacier centerline before and after calving events in 2010 **a)** and 2012 **b)**. Observed initial speed (MEaSURES InSAR winter 2009/10) is shown with a solid black line. Observed post-calving speeds after the 2010 calving event (PALSAR and TerraSAR-X winter 2010/11) and the 2012 calving event (MEaSURES InSAR winter 2012/13) are shown with solid purple lines. Modeled initial speeds are shown in dashed black, and speeds after each respective modeled calving event are shown in dashed purple. Note the small change in both observed and modeled velocities, particularly inland of the grounding line. . 95
- 4.4 Finite element mesh for Petermann Glacier. The inset shows the mesh across the entire Petermann catchment and the red square highlights the areas shown in the main figure. Element sizes are smallest in the areas of fastest flow (see Figure 4.1), and larger towards the slower flowing inland regions of the glacier catchment. The thick black line is the model domain. 97
- 4.5 Observed (U_{obs}) winter velocities 2009/10 **(a)** in the proximity of the grounding line, **(b)** Modeled (U_{mod}) velocities. **(c)** shows a normalized bivariate histogram of the velocity residuals which are the difference between modeled and observed velocities in the vicinity of the grounding line (magenta). $\Delta u = u_{\text{mod}} - u_{\text{obs}}$ and $\Delta v = v_{\text{mod}} - v_{\text{obs}}$. u and v are x and y components of the velocity vectors, respectively. 98
- 4.6 Inversion experiments using three sets of boundary conditions along the floating ice tongue. **a-c** show logarithmic calculated basal slipperiness (C) for boundary condition Scenarios 1 to 3 respectively, where orange represents highly slippery areas. Glen's flow law rate factor A (**d-f**), where light blue represents soft ice, and brown is stiff ice. The final column (**g-i**) is the absolute difference between observed (U_{obs}) and modeled velocities (U_{mod}) after inversion using each set of boundary conditions. 100
- 4.7 Diagnostic perturbation experiments for the 2010 calving event, using three scenarios of boundary conditions applied along the floating ice tongue (**a-c**). Graduated white to red shows speed increase between initial modeled velocities (U_{initial}) and modeled velocities post-2010 calving (U_{calving}). Bottom plots show observed velocities (U_{obs}) post-calving (winter 2010/11), and modeled velocities (U_{mod}) post-2010 calving along the glacier centerline. 103

| | | |
|-----|---|-----|
| 4.8 | Diagnostic perturbation experiments at Petermann Glacier. Top panel shows a cross-sectional centerline profile of Petermann Glacier from the BedMachine v3 dataset [Morlighem <i>et al.</i> , 2017]. Letters A to H represent the points along the glacier centerline at which sections of the terminus were removed for each experiment. A is the 2010 calving event, B is the 2012 calving event, and C is the location of a large rift that formed in 2016. D to G are successive 8 km splices and H is the current grounding line location. Bottom panels (a-h) show the modeled instantaneous increase in speed after each experiment with respect to initial pre-calving (before 2010) speeds. | 104 |
| 4.9 | Modeled experiment parameters for Petermann Glacier, for each diagnostic experiment (A-H), also shown in Figure 4.8. (a) Black line shows iceberg area lost between each experiment [km^2] and magenta is the average ice thickness [m] of each section of ice removed. (b) green is the average ice rate factor [$\log_{10}A$] across the section of ice removed in each diagnostic experiment. Orange and purple lines represent the cumulative grounding line flux with respect to an initial ice flux of 10.12 Gt a^{-1} and sea level equivalent contribution after the removal of each section of ice. (c) Average increases in ice speed across the entire ice tongue (red) and average ice speed within 10 km inland of the grounding line (blue) after each diagnostic experiment. | 106 |
| 5.1 | a) Bed topography [m] across the lower portion of the Petermann Glacier catchment, b) is initially perscribed steady-state melt rates beneath the ice tongue (red) and green is observed surface elevation change (SEC) from Cryosat-2 between 2011 and 2016, both of which are in m yr^{-1} . Inset map shows Greenland ice flow speed [m day^{-1}] in orange and the Petermann catchment outlined in black. | 113 |
| 5.2 | Initial finite linear-element mesh across the Petermann Glacier catchment (black line) which acts as our model domain. This mesh has 111391 elements, and 56340 nodes, and is refined in areas of low elevation, along the floating ice tongue, and where the ice is flowing fastest. Inset shows the mesh refinement along the ice tongue (300 m element size) and around the grounding line (100 m element size) shown in green. | 114 |

-
- 5.3 Results from model inversion. Top left panel shows observed ice flow speeds, where flow speeds reach up to 1200 m a^{-1} along the ice tongue. Top right panel shows the misfit between observed and modeled ice flow speeds after inversion. The bottom left panel shows basal slipperiness (C) using $m=3$. Light blue through to light and dark orange show areas of slipperiest ice. Note the slippery bed within $\sim 10 \text{ km}$ inland of the grounding line. Bottom right panel shows ice rheology parameter (A) from Glen's flow law using $n=3$. Areas of light to dark turquoise represent the softest ice, while dark brown is the areas of stiffest ice. 115
- 5.4 Observed and modelled thinning rates of elevation change. Left plot is observed surface elevation change from the Cryosat 2.2 satellite averaged between 2012-2016, which is similar to the date range of our input SMB from RACMO (2011-2016). Middle plot shows modelled surface elevation change at the beginning of our control run (10-11 yrs). As expected, due to prescribing lower basal melt rates than observed during 2012-2016 [Wilson *et al.*, 2017], our thinning rates underestimate observations. As way of comparison, the right hand plot shows thinning rates during our enhanced basal melt rates (at the point at which the glacier begins to respond dynamically to higher melt rates: 30yrs), which show a better fit to observed elevation changes. 118
- 5.5 Percentage change ($10^{-3} \%$) in total mass balance relative to initial conditions (time=0) during the model relaxation period of 10-years. 118
- 5.6 Change in ice volume above flotation (VAF) over 100 yrs in Gt for control runs executed using different sized elements within 2 km of the grounding line. 119
- 5.7 Top line shows initial ice thickness [m] at time = 0 (a) and plots b-e show the change in ice thickness [m] after 100 years for each of our experiments. The middle line of plots shows initial ice speed (f) in m yr^{-1} and plots g-j show change in speed [m yr^{-1}] after 100 years. The final line shows initial thinning rates (k) in m yr^{-1} where red is thinning and blue is thickening, and plots l-o show thinning rates at 100 years [m yr^{-1}]. In plots a, f and k, the green line represents the initial grounding line position. In all other plots the green line is the position of the grounding line after 100-years for each experiment. The dotted grey line in d,i and n is the previous PGIT extent removed at the beginning of the experiment. In e,j and o, the dotted lines represent calved icebergs at 5-year intervals between 5 and 25 years. . 120

| | | |
|------|--|-----|
| 5.8 | Annual speed (blue) and elevation change (red) along the Petermann Glacier centerline (sampled at 100 m intervals) for each of our model experiments (a-d). Pale to dark blue and pale to dark red represent each year between 0 and 100 for speed and elevation respectively. The dotted grey line represents the initial grounding line position and the ice ocean and bed extents are from the Operation IceBridge BedMachine v3 dataset [Morlighem <i>et al.</i> , 2017]. In plot d, the grey lines are sections of the PGIT removed at 5 year intervals between 5 and 25 years. | 123 |
| 5.9 | Model results for each of our experiments; control run (green), enhanced basal melt (purple), ice tongue collapse (orange) and retreat and enhanced basal melt (pink). a) change in volume above flotation (VAF) in mm of global sea level equivalent. b) change in grounded area [km ²]. c) width-averaged grounding line retreat [km], note some advance associated with re-grounding downstream of the main grounding line position. d) annual ice flux [Gt yr ⁻¹] across the grounding line. e) average annual ice flow speeds [m yr ⁻¹] within a 134 km ² square ~ 17 km inland of the grounding line (Figure 5.1). f) average annual thinning rates (change in thickness (h) over time (t)) in m yr ⁻¹ within our sample square. | 124 |
| 5.10 | Left panel shows the basal slipperiness from our inversion (C), where orange represents high basal slipperiness, and blue is low basal slipperiness. The right panel shows the bed topography from the Operation IceBridge BedMachine v3 dataset [Morlighem <i>et al.</i> , 2017], where blue is elevation below sea level and green-brown is above sea level. The initial grounding line position at time=0 is shown in black. Grounding line positions after 100 years for each model run are: control run (green), enhanced basal melt (purple), ice tongue collapse (orange), and retreat and enhanced basal melt (pink). | 126 |

- 6.1 Climate data for northern Greenland provided by the Danish Meteorological Institute. A) Annual (dark blue) and summer June July August (light blue) air temperatures from the Pituffik (PK) ($76^{\circ}32'N$, $68^{\circ}45'W$) automatic weather station in northwest Greenland. B) Annual (dark blue) and summer June July August (light blue) air temperatures from the Danmarkshavn (DK) ($76^{\circ}46'N$, $18^{\circ}40'W$) automatic weather station, in northeast Greenland. For both plots the black line represents the 5-year moving average of air temperature time series and solid vertical lines (blue and red) represent a statistically significant change point between the mean air temperature either side (shown in grey). Blue and red bars represent positive degree days from available daily air temperatures from both weather stations. 132
- A.1 (a) categorised source data of bed topography from the BedMachine v3 for northern Greenland (b) bed elevation error (m) map from the BedMachine v3 dataset. Grey outlines show glacier surface drainage catchments, and black lines show glacier centreline profiles. 147
- A.2 Bed topography profiles for each of 18 study outlet glaciers in northern Greenland. Bed topography was sampled along glacier centreline profiles and subsampled from the grounding line to 20 km inland to determine the local bed slope direction inland of the grounding line. Each profile was fit with a linear regression model (red). The direction of the linear fit was used to determine if the bed slope was seaward or landward sloping 148
- B.1 Left two panels show normalized increase in speed along the Petermann Glacier centerline from the grounding line to 40 km inland where $\Delta U_{(x)}$ is the change in velocity at each point along the transect and $\Delta U_{(GL)}$ is the change in speed at the grounding line. Each colored line is a different value of m . The final panel shows the percentage change in speed at the grounding line $\Delta U_{(GL)}$ for each slipperiness exponent value of m . Circles show percentage change after the 2010 calving event and squares after removing the entire ice tongue 150
- B.2 Left panel shows volume above flotation (VAF) loss during our control run for different values of m . Right panel, same as left but for our perturbed model run, incorporating both enhanced basal melt rates and episodic calving of Petermann Glacier's ice tongue. 151

List of Tables

| | | |
|-----|---|----|
| 2.1 | Key data on 21 Northern Greenland glaciers reviewed in this chapter. Widths and ice tongue lengths were measured in Landsat 8 2015 late summer imagery. Glacier width was measured at the grounding line. Floating ice tongue lengths are recorded for glaciers at which floating tongues are still present. Drainage basin areas were derived from hydrological catchment analysis using ice thickness and bed elevation from the Morlighem <i>et al.</i> [2014] dataset. Estimated ice discharge is derived from ^a Rignot <i>et al.</i> [2001] from 1992 to 1996 or ^b Rignot <i>et al.</i> [1997] from 1995 to 1996. Surge-type relates to a first order classification of surge-type glaciers in northern Greenland (see also Figure 2.1). | 20 |
| 3.1 | List of data sources used in this study. Data is split by usage and shown for each year | 58 |
| 3.2 | Mean decadal frontal position change for all study outlet glaciers in northern Greenland, and split based on our two glacier categories of terminus type: grounded terminus or terminating in a floating ice tongue. | 66 |
| 3.3 | Mean decadal frontal position change for all study outlet glaciers in northern Greenland, and split based on our two glacier categories of terminus type: grounded terminus or terminating in a floating ice tongue. | 69 |
| 3.4 | Glacier-specific factors at 18 northern Greenland study glaciers ordered by terminus type and then based on high-low magnitude retreat rates. This includes the size and percentage of each surface drainage basin below sea level, the direction of the bed slope 20 km inland of the grounding line (inland or seaward), and whether the fjord widens or narrows with distance inland. ^a Combined drainage catchment of Hagen Bræ and Academy Glacier. ^b Northeast Greenland Ice Stream (NEGIS) drainage catchment. | 79 |
| 4.1 | Velocity data sources for Petermann Glacier. ^a is from [Joughin <i>et al.</i> , 2010b] and ^b is from [Nagler <i>et al.</i> , 2016] | 93 |

| | | |
|-----|--|-----|
| 4.2 | Misfit between observed and modeled velocity for each boundary condition scenario | 99 |
| 5.1 | dhdt, speed and acceleration calculated within a square upstream of the grounding line. Acceleration is relative to initial velocities after 10-year relaxation period (after 0-10 CtrlRun). Flux is average GL flux for 0-100 yrs. Total mass loss is the volume of ice above flotation lost by the end of the 100 year period. | 121 |
| A.1 | Mean elevation error for each glacier across either the grounded portion of the glacier centreline profile, or the seaward (bathymetry) section of the glacier centreline profile | 147 |

Chapter 1

Introduction

1.1 Research Background

1.1.1 Ice sheets and outlet glaciers

The Greenland and Antarctic ice sheets are currently losing mass and contributing substantially to global sea level rise [Shepherd *et al.*, 2012; Vaughan *et al.*, 2013]. Since the early 1990s, they have discharged approximately 2900 and 2000 Gt of ice into the ocean respectively, contributing ~ 14 mm to global sea level rise by 2012 (Figure 1.1 Vaughan *et al.* 2013). In particular, recent estimates from the GrIS showed mass loss has increased 2.5 times in recent years [2011-2014: Helm *et al.*, 2014] compared to records from 2003 to 2009 [Shepherd *et al.*, 2012]. If accelerated ice loss continues, the Greenland and Antarctic ice sheets could contribute up to a further 2 m of global sea level rise by 2100 [Bamber *et al.*, 2019], impacting upon coastal communities across the world. However, future projections have large uncertainties based on the non-linear and poorly-understood processes relating to West Antarctic Ice Sheet (WAIS) collapse and accelerated discharge from the GrIS [Vaughan & Arthern, 2007; Church *et al.*, 2013].

Recent mass loss from the GrIS is via: i) negative surface mass balance (SMB), and ii) discharge from marine-terminating outlet glaciers [van den Broeke *et al.*, 2016; Rignot *et al.*, 2008; Sasgen *et al.*, 2012; Rignot *et al.*, 2011]. SMB, is the difference between accumulation from precipitation, and mass loss from ablation (e.g. surface melting and runoff). A number of studies have quantified recent changes in the SMB of the GrIS [e.g., Khan *et al.*, 2015, 2014; van den Broeke *et al.*, 2016; Enderlin *et al.*, 2014; Box & Colgan,

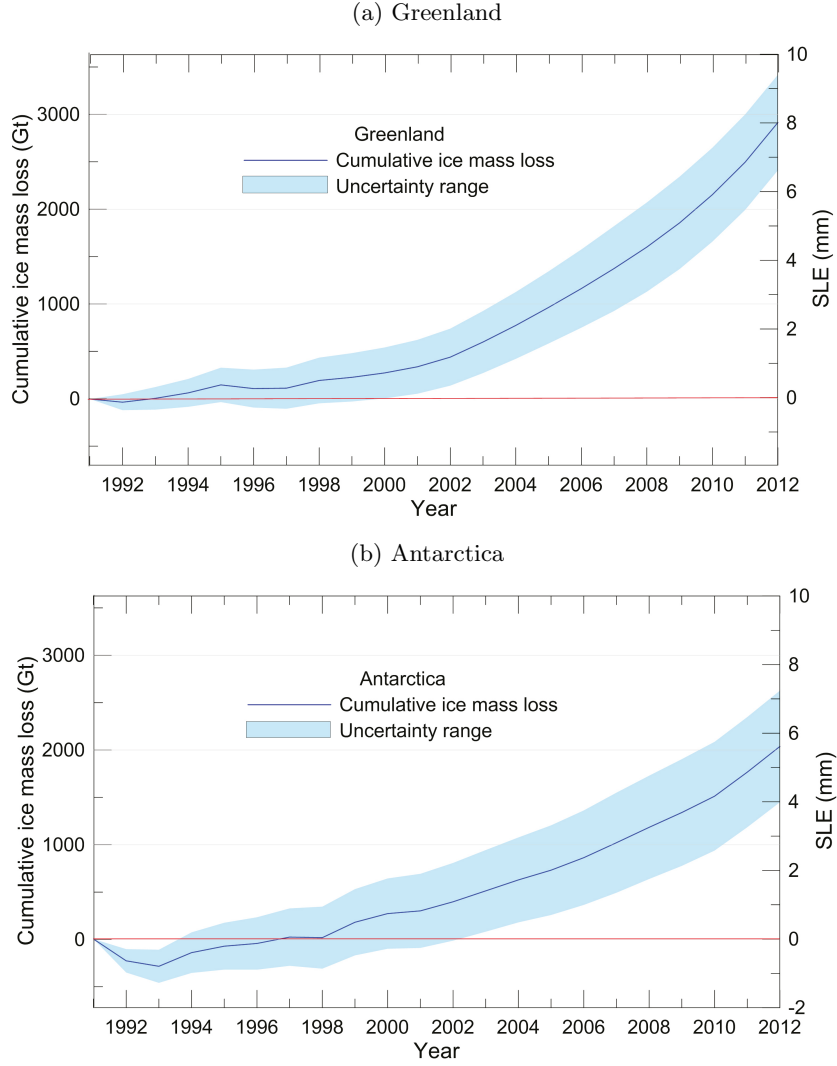


Figure 1.1: Cumulative ice mass loss (and sea level equivalent SLE) of the Greenland (a) and Antarctic (b) ice sheets between 1991 and 2012 derived from numerous recent studies incorporated into the Fifth IPCC report Chapter 4 [Vaughan *et al.*, 2013].

2013; Ettema *et al.*, 2009; Mouginot *et al.*, 2019] and it is clear that SMB has become increasingly negative since the early 1990s. In total SMB has contributed to around 60% of recent mass loss from the GrIS [van den Broeke *et al.*, 2016; Fettweis *et al.*, 2017; Enderlin *et al.*, 2014; Andersen *et al.*, 2015]. As expected, increases in surface runoff were greatest at lower elevations (Figure 1.2), below 2000 m above sea level [van den Broeke *et al.*, 2016; Ettema *et al.*, 2009], which also coincides with regions of fast flow and ice-surface thinning [Krabill *et al.*, 2000; Pritchard *et al.*, 2009].

The second component of mass loss is dynamic ice discharge from marine-terminating outlet glaciers, which is thought to account for approximately one third to 40% of total ice

loss [Enderlin *et al.*, 2014; Velicogna *et al.*, 2014; Andersen *et al.*, 2015]. Outlet glaciers act as fast-flowing conveyor belts, that rapidly drain ice from the interior to the ocean. In recent years, significant efforts have been made to better constrain the processes by which outlet glaciers respond to climate warming across Greenland. Some studies have compiled aerial photographs from the 1940s-1980s to provide long-term estimates (1900 - 2010) of dynamic mass loss and retreat [Kjeldsen *et al.*, 2015; Bjørk *et al.*, 2012]. These long-term records show Greenland wide mass loss throughout the 20th century, that contributed to approximately 25 mm of global sea level rise [Kjeldsen *et al.*, 2015]. A number of studies have quantified recent outlet glacier retreat at high temporal resolutions [Box & Decker, 2011; Murray *et al.*, 2015; Moon & Joughin, 2008; Bunce *et al.*, 2018; Carr *et al.*, 2017b; Howat & Eddy, 2011] with a particular focus on the northwest and southeast regions. Figure 1.2d shows a trend of ice sheet wide glacier retreat between 2000 and 2010 [Murray *et al.*, 2015]. Alongside widespread glacier retreat, several studies also recorded glacier acceleration [Moon *et al.*, 2012; Rignot & Kanagaratnam, 2006; Joughin *et al.*, 2010b; McFadden *et al.*, 2011] and thinning [Pritchard *et al.*, 2009; Thomas *et al.*, 2009; Felikson *et al.*, 2017] at marine-margins (Figure 1.2). This synchronous acceleration and thinning is thought to occur as the glacier adjusts to an imbalance of forces associated with retreat (see discussion in Section 1.1.2). However, compared to SMB, the future of ice loss and ice discharge remain poorly constrained in model simulations.

Initial observations suggested synchronous glacier speed-up and retreat were related to a common forcing, likely to be the onset of ocean-climate warming [Vieli & Nick, 2011; Moon *et al.*, 2012]. Rising air temperatures from the early-mid-1990s over Greenland [Box *et al.*, 2009; Cappelen *et al.*, 2010] have been linked to the synchronous retreat around several parts of the ice sheet [e.g., Bevan *et al.*, 2012; Howat & Eddy, 2011; Moon & Joughin, 2008]. Increased surface melt due to atmospheric warming can contribute to glacier retreat via three main mechanisms. Firstly, transport of meltwater to the base of the ice sheet can lubricate and accelerate ice flow [Zwally *et al.*, 2002; Moon *et al.*, 2015], but this is often only on short time-scales during the summer when the subglacial drainage system is pressurised [Tedstone *et al.*, 2015; Bartholomew *et al.*, 2010]. Second, an increase in subglacial discharge at the glacier front via plumes can promote submarine melt at the front [Jenkins, 2011; Slater *et al.*, 2015]. Finally, increased surface meltwater could promote crevasse propagation, which enhances calving as they propagate towards the ice front [van der Veen *et al.*, 2011] and also weakens the ice along the shear margins [Vieli & Nick, 2011].

Ocean warming has also been strongly linked to recent retreat across many regions of the ice sheet [Straneo & Heimbach, 2013; Rignot & Mouginot, 2012; Holland *et al.*, 2008;

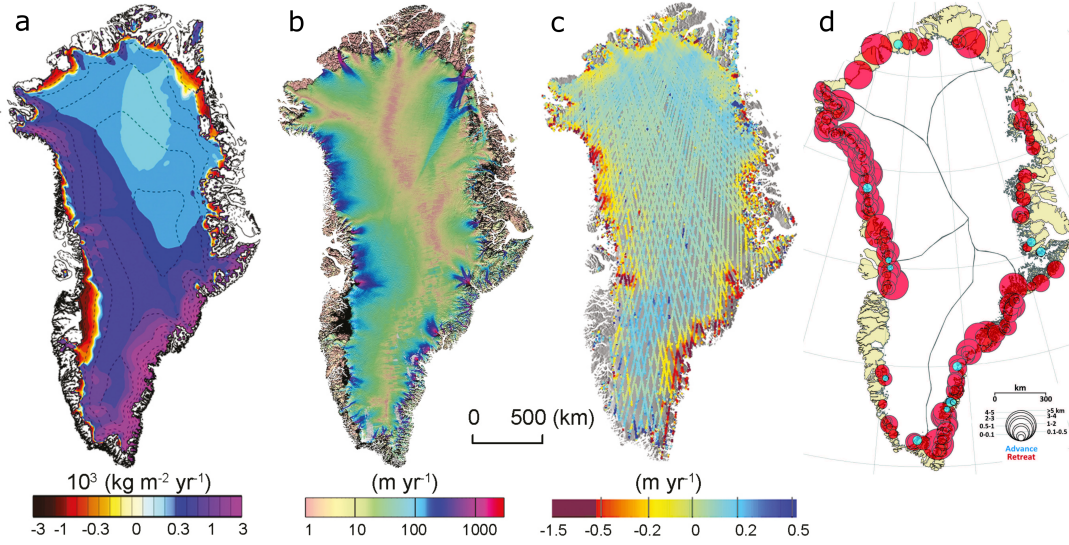


Figure 1.2: Modified from the IPCC AR5 report Chapter 4 [a-c: Vaughan *et al.*, 2013] and [d: Murray *et al.*, 2015]. a) is mean surface mass balance for the period 1989 to 2003 from regional atmospheric climate modelling [Ettema *et al.*, 2009]. b) ice sheet velocity for 2007 to 2009 from satellite data where red is fast flow and slower flow is in yellow [Rignot & Mouginot, 2012]. c) changes in ice sheet surface elevation for 2003 to 2008 from ICESat altimetry, where red is elevation decrease and blue is increase [Pritchard *et al.*, 2009]. d) changes in frontal position between 2000-2010 from Murray *et al.* [2015] for 199 glaciers, where proportional sized circles represent the magnitude of frontal position change, and red is retreat and blue is glacier advance.

Millan *et al.*, 2018; Murray *et al.*, 2010; Motyka *et al.*, 2011; Johnson *et al.*, 2011; Wood *et al.*, 2018]. Warm Atlantic waters transported from the continental shelf into the fjords, promote submarine melt at grounded ice faces or beneath floating ice shelves [Rignot *et al.*, 2010; Khan *et al.*, 2014; Rignot & Steffen, 2008]. In addition, the recent break up of sea ice and/or ice mélange, and the associated loss of backstress on the terminus, coincided with retreat, thinning and acceleration at Jakobshavn Isbræ [Amundson *et al.*, 2010], in northwest Greenland [Carr *et al.*, 2013b; Moon *et al.*, 2015], and at glaciers draining the Northeast Greenland Ice Stream (NEGIS) [Khan *et al.*, 2014; Reeh *et al.*, 2001]. While links between the timing of past ocean-climate warming and terminus change have been established, there exists high variability between individual regions and glaciers across the ice sheet. Despite some recent progress towards parameterising glacier retreat under ocean-climate warming [Cowton *et al.*, 2018; Slater *et al.*, 2019], the mass loss associated with glacier retreat remains poorly constrained in model simulations of future climate change and projections of sea level rise.

Ultimately, ocean-climate warming can act as the initial ‘push’ that destabilises marine-margins but the glacier response to climate-ocean forcing is highly non-linear. Importantly, the long-term response of any given outlet glacier is also dependent on its geom-

etry/topography which can modulate the time for a glacier to reach a new equilibrium, following an initial perturbation. Indeed, a number of studies have attributed heterogeneity in glacier response to climate to individual glacier geometry [Bunce *et al.*, 2018; Catania *et al.*, 2018; Howat *et al.*, 2007; McFadden *et al.*, 2011; Carr *et al.*, 2013b]. The following section discusses the role of geometry on glacier response to terminus changes further.

1.1.2 Glacier force balance and terminus change

Glacier flow is driven by the gravitational driving stress (τ_d) which is a function of local ice thickness and surface slope [Cuffey & Paterson, 2010]. The glacier driving force is resisted by basal drag (τ_b), lateral drag along the glacier side-walls (τ_w), and longitudinal resistive stresses (τ_L) that stretch or compress the ice (Figure 1.3). Glacier force balance can therefore be written simply as: $\tau_d = \tau_b + \tau_w + \tau_L$ [Cuffey & Paterson, 2010].

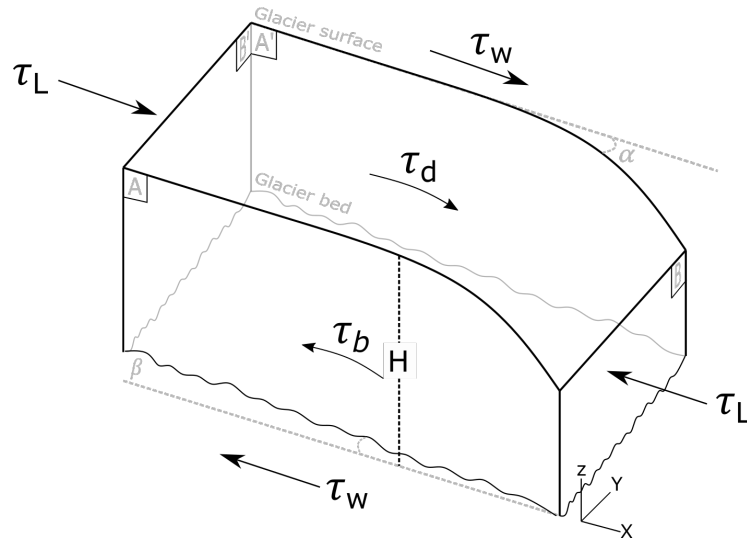


Figure 1.3: Glacier forces acting on a block of ice (modified from Cuffey & Paterson [2010]). Glacier flows in the direction X, the base is irregular to reflect subglacial topography (β), surface slope is α , and ice thickness is H . Lateral drag (τ_w) occurs along planes A and A' (sidewalls), while longitudinal resistive stress (τ_L) acts on the front and back of the ice block (planes B and B').

In the case of fast-flowing marine-terminating glaciers, it is important to consider the role that changes at the termini exert on the glacier force balance [Cuffey & Paterson, 2010]. Changes in the terminus position or extent of a floating ice shelf (see Section 1.1.3) can create an imbalance in the glacier forces leading to acceleration (or deceleration) and dynamic thinning (or thickening). Indeed a number of observational [Thomas, 2004; Howat

et al., 2005; Joughin *et al.*, 2004] and modelling studies [Nick *et al.*, 2009; Vieli & Nick, 2011] have documented positive feedbacks between terminus retreat and glacier thinning and acceleration further inland. Perturbations in driving stress due to changes at the terminus are dependent on three main factors: i) changes in surface slope ii) increasing basal slipperiness, and iii) glacier width and bed topography.

First, initial retreat and thinning at the glacier terminus forced by air/ocean warming, sea level rise, or submarine melting of floating termini, increases the surface slope up-glacier. Ice flow then accelerates down-slope, and thinning propagates inland as a diffusive wave. This causes longitudinal stretching and thinning of the ice that promotes further retreat of the terminus and decreases in τ_b , τ_L and τ_w , which leads to a positive feedback. This process has been observed at several outlet glaciers in Greenland [Joughin *et al.*, 2008b; Howat *et al.*, 2005, 2007].

Second, regions of slippery bed inland of the glacier terminus/grounding line can reduce basal drag, making the glacier more sensitive to terminus changes than in the case of a non-slippery bed. Slippery beds have been identified beneath both Antarctic ice streams [Alley *et al.*, 1986; Bindshadler *et al.*, 1987], and major outlet glaciers in Greenland [Shapero *et al.*, 2016; MacGregor *et al.*, 2016]. When thinning occurs, ice overburden pressure decreases, increasing basal slipperiness [van der Veen *et al.*, 2011], and promoting greater acceleration and thinning. Shapero *et al.* [2016] also showed that weak slippery beds at three major outlet glaciers in Greenland provide little resistance to the driving stress, allowing fast flow and rapid ice discharge. Ultimately, this means that if thinning (or some other process) causes glacier beds to become slipperier in the future, it could increase their ice discharge and contribution to sea level rise.

Finally, as ice at grounded termini is resisted by both side-wall and basal drag, the geometry of the fjord, i.e. width and bed-slope direction can control the magnitude of resistive stress lost when the glacier retreats. Indeed, both observations [Carr *et al.*, 2015; McFadden *et al.*, 2011; Lüthi *et al.*, 2016; Catania *et al.*, 2018; Bunce *et al.*, 2018], and modelling studies [Jamieson *et al.*, 2012; Enderlin *et al.*, 2013; Åkesson *et al.*, 2018; Morlighem *et al.*, 2016a] have shown that topography can strongly affect glacier dynamic response to changes at the terminus. Firstly, there is a greater reduction in lateral resistive stresses when the glacier terminus retreats into a widening fjord, compared to a narrowing one [Raymond, 1996; Jamieson *et al.*, 2012]. Thereafter, mass conservation requires thinning and surface lowering in order to maintain the same flux at the grounding line as the ice moves into the wider fjord [Jamieson *et al.*, 2012; Enderlin *et al.*, 2013; Åkesson *et al.*, 2018]. This reduction in side drag ultimately leads to an increase in driving stress and speed-up of inland ice [Cuffey & Paterson, 2010]. Loss of thicker ice, where everything else

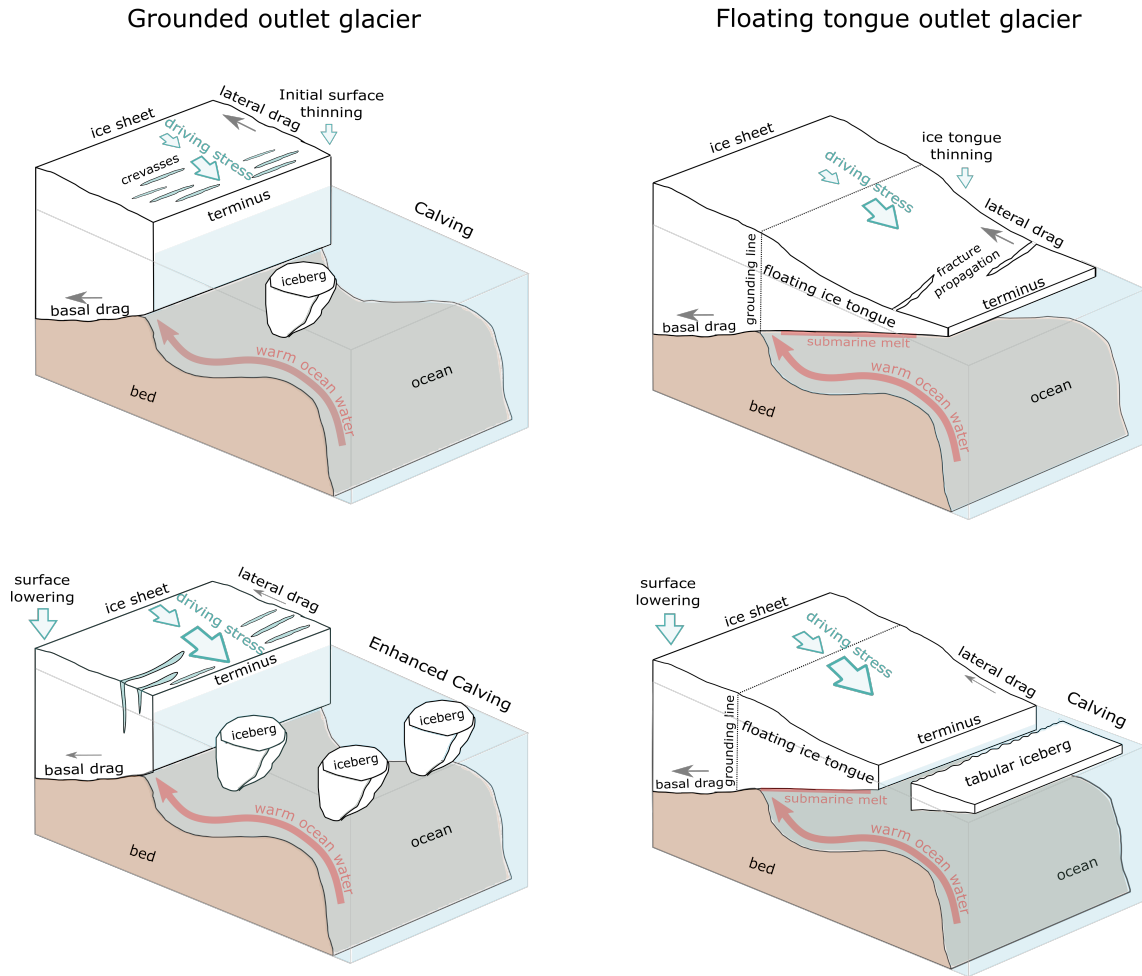


Figure 1.4: Schematic diagrams of changes in force balance at grounded outlet glaciers (left diagrams) and glaciers that terminate in a floating ice tongue (right diagrams). Larger arrows represent greater resistance (lateral and basal) or greater driving stress. Top panels show the glacier before an initial thinning of the surface at the grounded terminus or along the floating ice tongue. Bottom panels show the change in glacier force balance due to perturbations of the terminus: i.e. surface lowering, a reduction in basal and lateral drag, an increase in driving stress and calving.

remains constant, will cause a larger perturbation in the force balance due to a greater loss of contact with the side-walls.

After a marine-terminating glacier front has been initially destabilised by external forcing (Section 1.1.1), the likelihood of continued retreat and dynamic instability is strongly influenced by bed slope. Retreat of the glacier terminus into deeper water has three main effects on the glacier force balance: i) an increase in ice thickness leads to greater ice flux, and driving stress, ii) longitudinal stretching at the terminus promotes crevasse formation and increased calving, iii) effective pressure at the bed decreases due to greater water

pressure at depth. Collectively, these factors lead to thinning at the terminus, accelerated ice flow, and un-grounding of ice. This causes further down-slope retreat, and the initiation of a positive feedback [Cuffey & Paterson, 2010], which is termed marine-ice sheet instability (MISI: see Mercer [1978]; Pattyn *et al.* [2018]). MISI studies have focused on the potential future instability of the West Antarctic Ice Sheet [Joughin *et al.*, 2014; Favier *et al.*, 2014; Pattyn *et al.*, 2018], but conditions for MISI are satisfied at numerous marine-terminating outlet glaciers in Greenland [e.g., Moon *et al.*, 2012], including those with floating ice tongues [e.g., Khan *et al.*, 2014]. Indeed, a number of studies have observed rapid retreat down retrograde bed-slopes, for example at grounded glaciers in northwest Greenland [Porter *et al.*, 2014] and at the formerly floating Zachariæ Isstrøm in northeast Greenland [Mouginot *et al.*, 2015]. However, in many regions of the GrIS, glacier sensitivity to bed slope has not been systematically assessed.

1.1.3 Ice shelves and buttressing

Ice shelves or ice tongues are large floating extensions of outlet glaciers that restrain the flow of grounded ice inland, and are most commonly found in Antarctica (Figure 1.5). The elevation of the ice shelf/tongue above water level (freeboard) is what drives ice flow down-slope [Cuffey & Paterson, 2010]. In contrast to grounded ice, the base of ice shelves are not in contact with the bed (except in the case of local grounding on pinning points), meaning that there is no basal resistance to ice flow. Therefore, the driving stress is only resisted by ice shelf backstress that is primarily related to the amount of side-wall drag exerted along the lateral shelf margins. Buttressing is, therefore, simply the ratio between ice shelf driving force and the amount of backstress [Cuffey & Paterson, 2010].

Ice is lost from floating ice shelves via fracture driven calving and submarine melting along the base. Ocean-climate warming has the potential to de-stabilise floating termini by thinning and/or disintegrating an ice shelf. Such thinning/collapse reduces backstress on ice in the grounding zone, increases stretching, thinning the ice and ultimately increasing the driving force. Thinning also brings the ice close to flotation which forces grounding line retreat, and also reduces basal/lateral drag provided by formerly grounded ice. When this grounding line retreat occurs into deeper water down a retrograde bed-slope it can prevent the glacier from reaching a new equilibrium, and instead prolongs glacier instability via MISI. However, it is important to note that there are some cases where laterally confined ice shelves provide enough buttressing that the grounding line can be stable on a reverse slope [Haseloff & Sergienko, 2018; Gudmundsson *et al.*, 2012], and marine ice sheet instability may not necessarily be the case. One of the key examples of MISI is at Pine

Island Glacier, Antarctica, where substantial grounding line retreat down a retrograde bed slope led to inland acceleration, and increased ice loss [Favier *et al.*, 2014]. The NEGIS may also be susceptible to MISI, because the glaciers rest on a retrograde bed that is below sea level [Khan *et al.*, 2014]. However the process of MISI remains less studied at floating termini in Greenland.

In the last two decades several large ice shelves collapsed around the Antarctic Ice Sheet, particularly from the Antarctic Peninsula [Rott *et al.*, 2002; Scambos *et al.*, 2004; Rignot *et al.*, 2004]. As a result, a number of studies have demonstrated the important impact of ice shelf buttressing on the dynamics of inland grounded ice flow, ice flux, and ultimately the potential contribution to sea level rise [Schoof, 2007; Goldberg *et al.*, 2009; Gudmundsson, 2013; Fürst *et al.*, 2016; Favier *et al.*, 2014; Reese *et al.*, 2018a; Miles *et al.*, 2018; De Rydt *et al.*, 2015; Scambos *et al.*, 2004]. However, similarly detailed work has not yet been conducted in the Arctic and, particularly Greenland, where smaller, elongated ice shelves, that are often constrained by fjord walls (and therefore referred to as ice tongues), exist [Reeh, 2017]. In particular the collapse of Jakobshavn Isbræ’s ice tongue in the early 2000s drew attention to the role of ice tongue buttressing in Greenland [Holland *et al.*, 2008; Joughin *et al.*, 2004]. Since then, some recent work has focused on the floating extensions of the glaciers draining the fast-flowing NEGIS [Khan *et al.*, 2014; Rathmann *et al.*, 2017; Mouginot *et al.*, 2015; Choi *et al.*, 2017] and on Petermann Glacier in northwest Greenland [Nick *et al.*, 2012], but otherwise floating ice tongues in Greenland remain understudied.

1.1.4 Northern Greenland

Northern Greenland represents a large component of the GrIS, collectively draining approximately $\sim 40\%$ of the ice sheet by area [Rignot & Kanagaratnam, 2006]. A substantial portion of these drainage basins also rest below sea level [Morlighem *et al.*, 2017], and could therefore be inherently unstable. Total mass balance in the region has become increasingly negative since the 1900s, with increasing dynamic discharge from the northeast and northwest sectors, but remaining relatively constant in the far north [Kjeldsen *et al.*, 2015]. In the near future northern Greenland is expected to become a greater contributor to sea level rise in the future [Mouginot *et al.*, 2019]. Outlet glacier behaviour in the region has not been well studied compared to the central, north-west, and south-east regions of the ice sheet [e.g., Bunce *et al.*, 2018; Moon & Joughin, 2008; Moon *et al.*, 2012; Carr *et al.*, 2013b]. As such, our process understanding of recent glacier behaviour remains

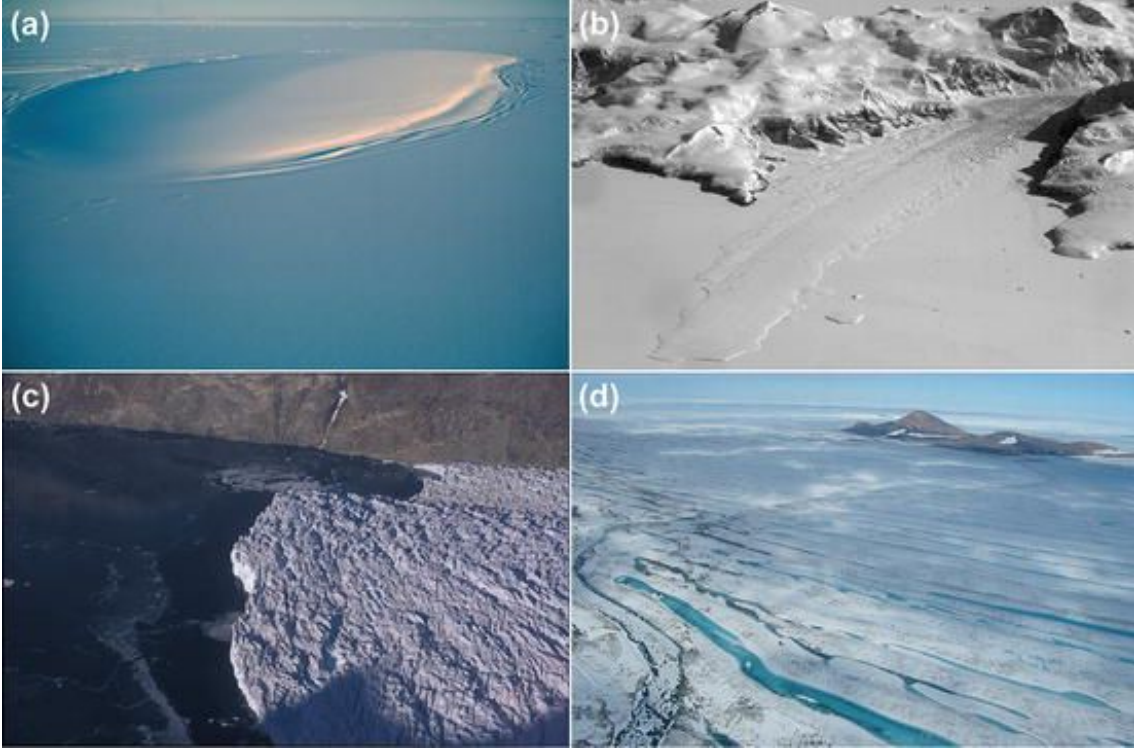


Figure 1.5: Photographs of Antarctic and Arctic ice shelves. (a) Larsen C Ice Shelf and Gipps Ice Rise, eastern Antarctic Peninsula (Photo: C.W.M. Swithinbank). The ice rise is about 18 km long. (b) A floating glacier tongue, 2–4 km wide, embedded in sea ice immediately north of the larger Aviator Glacier Tongue, Victoria Land Coast, Antarctica (Photo: J.A. Dowdeswell). (c) The floating margin of Daugaard Jensen Gletscher, East Greenland (Photo: J.A. Dowdeswell). (d) The Ward Hunt Ice Shelf, northern Ellesmere Island, Arctic Canada (Photo: D.R. Mueller). Taken from Dowdeswell & Jeffries [2017].

poor. Alongside this, it is the last region of the GrIS with floating ice tongues [Reeh, 2017]. Despite the fact that flow speeds along glaciers with floating ice tongues have shown little change since 2000 [Moon *et al.*, 2012], ice tongue collapse could cause substantial loss of buttressing, ice acceleration, and increased discharge (see Section 1.1.3), which could add to northern Greenland becoming a more important contributor to ice loss and global sea level rise in the future. A more detailed overview of the study region is given in Chapter 2.

1.2 Rationale

To summarise the above, there is an ice sheet wide signal of glacier thinning, retreat and acceleration across the GrIS which is coincident with 21st century warming. However, high variability exists in climatic/oceanic forcing between regions and the geometric setting of

individual glaciers. Hence, there are a number of uncertainties in our understanding of Greenland outlet glacier behaviour that remain, particularly in the northern regions of the ice sheet, which impacts our ability to accurately forecast its contribution to 21st century sea level rise. More specifically, there are a number of key areas of uncertainty that provide the motivation for this thesis:

- Ice tongues can restrain ice flow, but the buttressing effect of floating ice tongues in northern Greenland is uncertain. The question remains: how did glaciers respond to past ice tongue loss, and how might they response to future loss? Hence, there is a need for improved understanding on the role of tongue loss, using long-term observations of ice tongue extent, and numerical modelling to simulate future ice tongue loss and glacier response.
- Ocean-climate warming in the future could force rapid retreat and accelerate ice flow and ice discharge in northern Greenland. To determine glacier sensitivity to retreat there is a need for a longer-term context to determine whether recent terminus changes are dynamically important and part of a sustained trend, or part of a natural cycle. Despite the fact that northern Greenland constitutes a large region of the GrIS, recent retreat remains unknown, and there is a need for long-term records of ice front change, that extend further back in time than satellite records.
- While ocean-climate forcing may initialise retreat, geometry can modulate the duration of glacier instability. Some recent efforts have assessed glacier sensitivity to geometry [e.g., Catania *et al.*, 2018], but this needs to be extended to other regions of the ice sheet. Hence, there is a need for quantitative assessment of geometry on modulating the past behaviour of glaciers with or without ice tongues in northern Greenland.

1.3 Aim and objectives

The aim of this thesis is to quantify outlet glacier change in northern Greenland and assess the role of floating ice tongues in modulating past, and potential future dynamic glacier behaviour. The research targets three main objectives:

1. Review and synthesise the past behaviour of outlet glaciers in north Greenland and identify gaps in the current understanding of region-wide glacier behaviour.

2. Provide a new long-term record (1948 to 2015) of region-wide outlet glacier change, with a particular focus on comparing glaciers with or without floating ice tongues, and on assessing the role of glacier geometry on modulating glacier dynamic behaviour.
3. Assess the past and future response of a large ice-tongue terminating glacier in north Greenland (Petermann Glacier) to ice tongue loss.

1.4 Thesis outline

This thesis is outlined as follows: Chapter 2 provides a review of northern Greenland glacier behaviour, and Chapters 3 to 5 present new data in which a combination of remote sensing and numerical modelling are used to address the three main objectives outlined above. Note that these chapters have been published or prepared as journal papers and hence, they each include the methods, results and discussion instead of dedicated thesis chapters for each of these sections. The final Chapters (6 and 7) synthesise the results and discussion from all of the previous chapters, and provide an outlook for future change in northern Greenland, and suggestions of areas for further research.

Chapter 2 addresses Objective 1 by providing a comprehensive review of the ‘state-of-knowledge’ of outlet glacier behaviour in north Greenland and was published in Hill *et al.* [2017, *Frontiers in Earth Science*]. Chapter 3 achieves the second objective of this thesis, by using remotely sensed imagery in combination with historical map charts to provide a novel long-term record (1948 to 2015) of terminus change across northern Greenland. This new dataset was then combined with existing velocity and surface elevation change records to assess the feedback between terminus change and perturbations on the glacier force balance, i.e. acceleration and surface thinning. This focused on the key differences between the two terminus types (grounded and floating), as well as assessing the role of fjord width and bed topography on the sensitivity of each group of glaciers. This chapter was published in Hill *et al.* [2018a, *The Cryosphere*].

To attain the final objective of this thesis, Chapters 4 and 5 assess glacier sensitivity to future ice tongue loss. This was achieved by performing two sets of numerical modelling experiments on Petermann Glacier, which is one of the last remaining ice-tongue-terminating glaciers in northern Greenland. These experiments were done using the existing two horizontal dimensional ice flow model *Úa* [Gudmundsson *et al.*, 2012, see Chapter 4 Section 4.3.2]. Chapter 4 removes sections of the ice tongue similar in size to previous large calving

events, to assess the glaciers' instantaneous sensitivity to the associated loss of buttressing. This chapter was published in Hill *et al.* [2018b, *The Cryosphere*]. Chapter 5 follows on from this, by performing time dependent simulations, in which the glacier geometry is able to evolve over 100-years in response to a perturbation in ice tongue conditions, e.g. enhanced submarine melt and ice tongue calving. This chapter therefore assesses the continued glacier response over time to the loss of buttressing and the role of geometry on modulating ice loss and grounding line retreat.

Chapter 2

A review of recent changes in major marine-terminating outlet glaciers in northern Greenland

2.1 Chapter summary

Over the past two decades, mass loss from the Greenland Ice Sheet (GrIS) has accelerated and contributed to global sea level rise. This has been partly attributed to dynamic changes in marine terminating outlet glaciers. Outlet glaciers at the northern margin of the ice sheet drain 40% of its area but are comparatively less well-studied than elsewhere on the ice sheet (e.g. central-west or south-east). This chapter addresses the first objective of this thesis, which is to review and synthesize outlet glacier behaviour in northern Greenland. The primary aim of this chapter was therefore to provide an up-to-date record of the current knowledge on 21 major marine-terminating outlet glaciers in northern Greenland, and identify gaps in our current understanding. This Chapter was published as a journal paper in *Frontiers in Earth Science* in January 2017 (see reference below), in which I carried out all the analysis, produced all the figures, and wrote the manuscript. Co-authors helped to develop the research ideas, and provided editorial input.

HILL, E. A., CARR, J. R. & STOKES, C. R. 2017 A Review of Recent Changes in Major Marine-Terminating Outlet Glaciers in Northern Greenland. *Frontiers in Earth Science* **4** (111), 1–23

The key findings of this chapter were that over the last 130 years, there has been a clear pattern of glacier retreat, particularly over the last two decades. This was accompanied by velocity increases on the majority of glaciers for which records exist. Despite a distinct signal of retreat, however, there is clear variability within the region, which has complicated efforts to determine the precise drivers of recent changes, such as changes in ice tongue buttressing, atmospheric and /or oceanic warming, in addition to the possibility of glacier surging. Thus, there is an important need for further work to ascertain the precise drivers of glacier change, which is likely to require datasets on recent changes in the ocean-climate system (particularly sub-surface ocean temperatures) and numerical modelling of glacier sensitivity to these various forcings. Objective identification of surge-type glaciers is also required. These findings provided the motivation for the research conducted in the subsequent chapters of this thesis. Given that Northern Greenland is predicted to undergo greater warming due to Arctic Amplification during the 21st century, we conclude that the region has the potential to become an increasingly important source of mass loss.

2.2 Introduction

Mass loss from the Greenland Ice Sheet (GrIS) has doubled in the last two decades [Shepherd *et al.*, 2012] as a result of both increased ice discharge and increased surface melt [van den Broeke *et al.*, 2016]. Together, these processes currently contribute approximately 0.6 mm per year to global sea level rise [Fürst *et al.*, 2015]. The increased ice discharge is associated in part with marine-terminating outlet glaciers that have undergone thinning, retreat and acceleration since the mid-1990s [Rignot & Kanagaratnam, 2006; Moon & Joughin, 2008; Joughin *et al.*, 2010b]. Their retreat between 2000 and 2010 was considered exceptional over the past half century [Howat & Eddy, 2011], and dynamic discharge from outlet glaciers was thought to be responsible for approximately 40% of mass loss from the ice sheet between 1991 and 2015 [van den Broeke *et al.*, 2016]. The recent rapid outlet glacier retreat and flow acceleration is understood to be in response to ocean-climate forcing [McFadden *et al.*, 2011; Cook *et al.*, 2014]. Potential mechanisms by which atmospheric temperatures may promote retreat through glacier calving are the drainage of supraglacial lakes or water-filled crevasses fracturing through the full ice thickness [van der Veen, 2007; Das *et al.*, 2008]. Alongside this, ocean warming may increase rates of submarine melting at marine-terminating glaciers [Holland *et al.*, 2008], which may be further enhanced by submarine meltwater plume discharge [Motyka *et al.*, 2013; Jenkins, 2011]. In addition, sea ice removal or decline may promote calving and a longer ice-free season may allow greater volumes of ice to be lost during the year [e.g., Carr *et al.*,

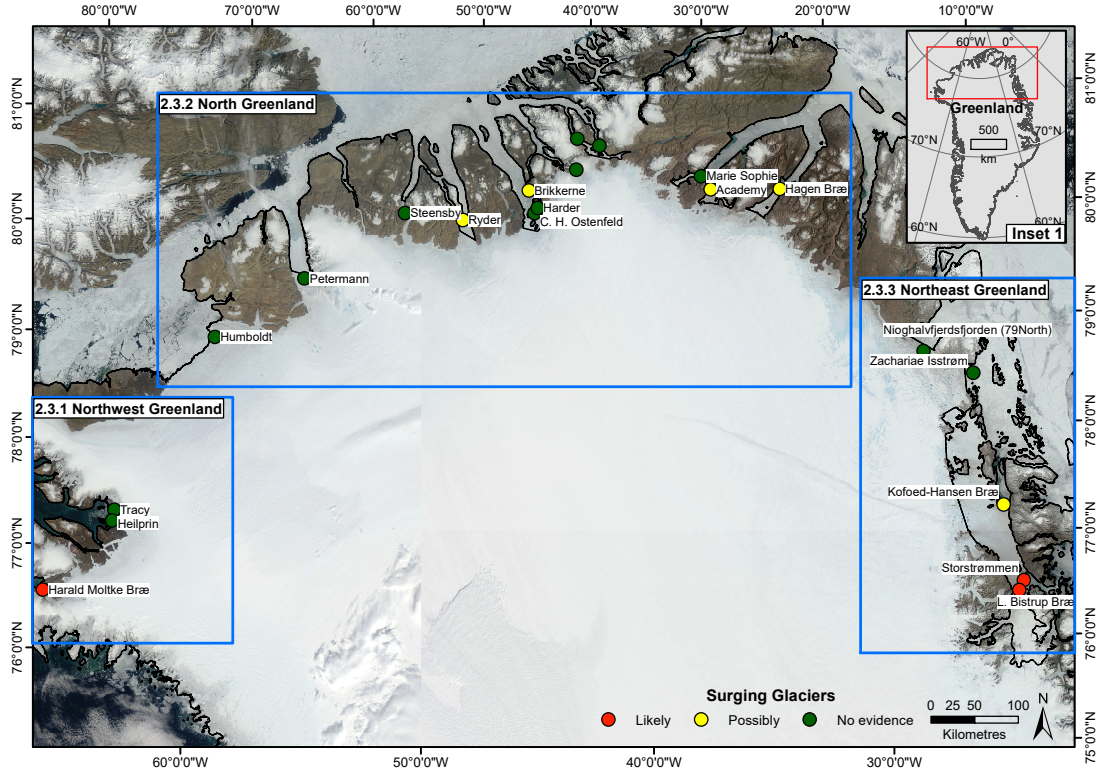


Figure 2.1: Location map of Northern Greenland showing the glaciers reviewed in this paper. The study area has been split into three geographical regions which are Northwest Greenland (2.3.1), North Greenland (2.3.2) and Northeast Greenland (2.3.3). Colored circles show a first order classification of potential surge-type glaciers across northern Greenland. Red circles show glaciers which are likely to be surge type based on clear surge-cycles having been recorded within the literature. Yellow circles show glaciers at which surging is possible based on glaciers which may have shown surge-characteristics, but either have not been referred to as surge-type or have not undergone a large surge event. Green circles show glaciers at which no evidence of surging has been recorded in the literature. Background image derived from NASA EOSDIS Worldview (16.07.15 and 21.07.15).

2013b, 2014; Moon *et al.*, 2015].

However, the magnitude of individual glacier responses to these forcings is known to be modulated by local topographic factors [Howat *et al.*, 2007; Moon *et al.*, 2012; Carr *et al.*, 2013b]. For example, fjord width is a key local control on glacier retreat, where a narrow fjord can delay the removal of icebergs from the terminus [e.g., Warren & Glasser, 2006; Jamieson *et al.*, 2012; Carr *et al.*, 2014]. Another important glacier-specific factor is basal topography, whereby a reverse inland bed slope can make a glacier vulnerable to feedbacks between rapid thinning, acceleration and retreat [e.g., Thomas *et al.*, 2009]. The relative contribution of external factors (oceanic and climatic) versus localized glacier-specific factors (most notably fjord geometry and basal topography) remains poorly understood and

identifying their respective influence on outlet glacier retreat is of paramount importance for estimating future glacier response to climate change and sea level rise [Nick *et al.*, 2013; Porter *et al.*, 2014; Carr *et al.*, 2015].

Over the last two decades, several areas of the ice sheet have been the focus of regional to local scale studies of glacier change, particularly Jakobshavn Isbræ in west Greenland [Joughin *et al.*, 2008*b*, 2012*b*; Podrasky *et al.*, 2012], and Kangerdlugssuaq and Helheim Glaciers in south east Greenland [Howat *et al.*, 2007; Joughin *et al.*, 2008*a*]. However, with the possible exception of Petermann Glacier and the NEGIS, major outlet glaciers in northern Greenland have received much less attention. This is despite several studies documenting large calving events from northern Greenland ice tongues during the past decade [Moon & Joughin, 2008; Johannessen *et al.*, 2013; Murray *et al.*, 2015], the most notable of which was the 270 km² retreat of Petermann Glacier’s floating tongue in 2010 [Nick *et al.*, 2012; Johannessen *et al.*, 2013]. Thus, there is a paucity of data from northern Greenland, compared to other areas. It remains unclear how these glaciers are responding to climate change compared to other areas of Greenland and in the context of their longer-term behavior over the last 100 years. There is also uncertainty about the forcing of glacier retreat (atmospheric versus oceanic warming) and how these glaciers might respond to future changes at their terminus (such as ice tongue losses) and whether these changes have the potential to trigger substantial inland ice loss and glacier acceleration, similar to that experienced at Jakobshavn Isbræ [Joughin *et al.*, 2004; Amundson *et al.*, 2010], and on the Antarctic Peninsula [Scambos *et al.*, 2004]. Further complexity in the region arises from surge-dynamics and the literature highlights that several glaciers in this region as potentially surge-type [Mock, 1966; Reeh *et al.*, 1994; Joughin *et al.*, 1996*b*]. We define surges here as the periodic fluctuation between long periods of slow glacier flow (quiescent phase) and short-lived rapid flow, which results in at least an order of magnitude increase (active phase) [Meier & Post, 1969; Sharp, 1988]. These surge events can be either thermally or hydrologically controlled [Murray *et al.*, 2003] driven by basal temperatures [Fowler *et al.*, 2001] or changes in basal hydrology [Kamb *et al.*, 1985] respectively.

Given that northern Greenland glaciers collectively drain 40% of the GrIS by area [Rignot & Kanagaratnam, 2006] and consist of large catchments, some grounded well below sea-level up to 100s of km inland [Morlighem *et al.*, 2014], this region has the potential to be a large contributor to future dynamic change, mass loss, and sea level rise.

Here, we review previous research in this region, with a particular focus on recent changes in marine-terminating outlet glaciers and their links to ocean-climate forcing. Our study area is defined by a coastline that is ~2000 km long (Figure 2.1). This is drained by around 40 marine-terminating outlet glaciers and we focus on a sample of

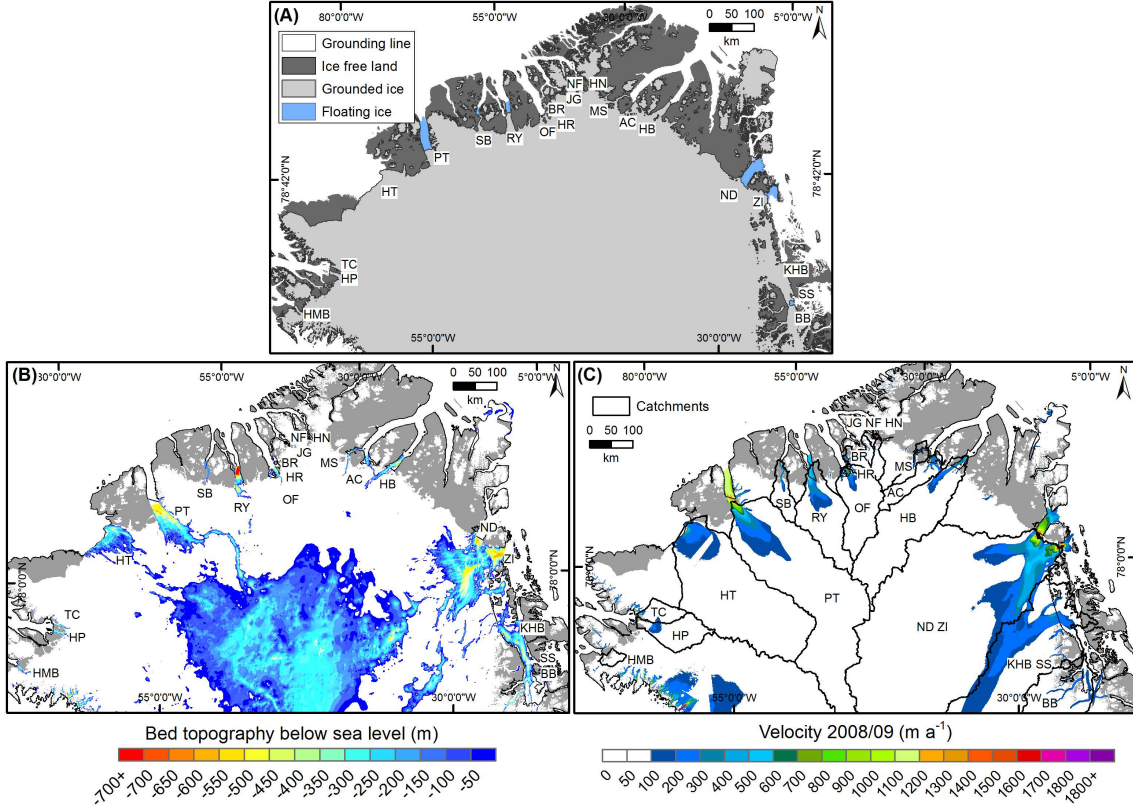


Figure 2.2: A) Location of large floating ice tongues around the northern Greenland study region based on a review of the literature. Glacier abbreviations relate to Table 2.1. B) Bed topography data across Greenland displayed as areas below sea level (< 0 m), deep areas in red, shallower bed topography in blue. Both bed topography and floating ice tongue data were derived from the IceBridge BedMachine Greenland, Version 2 dataset in 2015 [Morlighem *et al.*, 2014]. C) glacier velocities (m a^{-1}) during 2009/10 acquired from the MEaSUREs v2 Greenland velocity dataset [Joughin *et al.*, 2010b] and catchment areas of northern Greenland outlet glaciers derived from hydrological analysis using the Morlighem *et al.* [2014] bed elevation and ice thickness datasets.

21 of these glaciers (Figure 2.1), which represent the primary ice drainage routes where previous work has been undertaken [Higgins, 1990; Rignot *et al.*, 1997, 2001]. Many of these glaciers have large catchments overlying deep basal topography, and exhibit high ice velocities [up to 1200 m a^{-1} : Joughin *et al.*, 2010b] that are comparable to fast-flowing outlets elsewhere on the ice sheet (Figure 2.2). Thus, they have the potential to be large contributors to dynamic mass loss in the future.

2.3 Regional changes in glacier dynamics

Early scientific explorations of northern Greenland by [Peary, 1892] and the First (1912) and Second (1916-1918) Thule expeditions led by Knud Rasmussen [Rasmussen, 1912, 1919] sought to improve understanding of the northern margin of the ice sheet. Subsequent studies identified large floating ice tongues, up to 50 km long, on many northern Greenland glaciers [Koch, 1928; Higgins, 1990]. In this respect, they are unique in comparison to other regions of the ice sheet, where floating ice tongues are generally much shorter or absent. Historically, a significant proportion of northern Greenland glaciers are documented to have retreated, particularly between 1894 and 1962 [Davies & Krinsley, 1962]. More recently, estimates of ice discharge in the late 1990s indicated widespread thinning [Rignot *et al.*, 1997]. Using historical photographs Kjeldsen *et al.* [2015] provided a long-term record (1900-2010) of mass balance changes, which showed relatively constant ($\sim 24 \text{ Gt yr}^{-1}$) dynamic thinning throughout the 20th century in northern Greenland. Studies by Higgins [1990], Rignot *et al.* [1997], and Rignot *et al.* [2001] provided more comprehensive observations of glacier width, length, the presence of floating tongues, as well as initial velocity measurements and grounding line positions. Since then, a comprehensive analysis of northern Greenland glacier retreat and velocity fluctuations has not been conducted, although outlet glaciers from this region are often incorporated into GrIS wide studies [Moon & Joughin, 2008; Joughin *et al.*, 2010b; Box & Decker, 2011; Murray *et al.*, 2015]. These syntheses reported significant increases in outlet glacier retreat rates across Greenland (for 1992-2006) [Moon & Joughin, 2008] and that the largest cumulative area changes (during 2000-2010) occurred in northern Greenland, particularly at glaciers with the largest floating portions (e.g. Petermann, Humboldt and Zachariæ Isstrøm) [Box & Decker, 2011].

An outline of the characteristics of each of the outlet glaciers in our study region is provided in Table 2.1, which also includes glacier catchment sizes delineated using bedrock topography and ice thickness data [Morlighem *et al.*, 2014] input into the Shreve hydropotential formula [Shreve, 1972] to determine subglacial water routing and thus glacier drainage catchments. The following sections are a synthesis of previous work on each of the glaciers by region (Figure 2.1), with a focus on describing the key characteristics of each glacier and setting recent observations in a broader historical context. For comparison between sub-sections, we focus on terminus length changes, but in some cases where length is not reported in the literature, we refer to terminus change as it is reported in area.

| Code | Glacier | Width (km) | Ice tongue length (km) | Drainage Area (km ²) | Area of north GrIS (%) | Area of GrIS (%) | Ice discharge (km ³ a ⁻¹) | Surge-type |
|------|-----------------------|------------|------------------------|----------------------------------|------------------------|------------------|--|-------------|
| HMB | Harold Moltke Bræ | 6.3 | - | 1,401 | 0.28 | 0.12 | - | Likely |
| HP | Heilprin | 6.7 | - | 8,408 | 1.66 | 0.70 | 2.19 ^a | No evidence |
| TC | Tracy | 5.0 | - | 3,835 | 0.76 | 0.32 | 1.43 ^a | No evidence |
| HT | Humboldt | 91 | - | 56,357 | 11.16 | 4.66 | 6.25 ^a | No evidence |
| PT | Petermann | 21 | 48 | 71,305 | 14.11 | 5.90 | 12.82 ^a | No evidence |
| SB | Steensby | 4.8 | 5.1 | 4,694 | 0.93 | 0.39 | 0.63 ^b | No evidence |
| RY | Ryder | 10 | 26 | 17,265 | 3.42 | 1.43 | 3.88 ^a | Possibly |
| OF | C.H. Ostenfeld | 7.9 | 1.5 | 14,494 | 2.87 | 1.20 | 2.32 ^a | No evidence |
| HR | Harder | 5.1 | - | 726 | 0.14 | 0.06 | 0.34 ^b | No evidence |
| BR | Brikkerne | 6.1 | 1.2 | 2,058 | 0.41 | 0.17 | 0.44 ^b | Likely |
| JG | Jungersen | 2.0 | - | 993 | 0.20 | 0.08 | 0.20 ^b | No evidence |
| NF | Naravana Fjord | 2.5 | - | 676 | 0.13 | 0.06 | 0.02 ^b | No evidence |
| HN | Henson | 2.7 | - | 1,975 | 0.39 | 0.16 | 0.08 ^b | No evidence |
| MS | Marie Sophie | 3.9 | - | 2,565 | 0.51 | 0.21 | 0.02 ^b | No evidence |
| AC | Academy | 8.4 | - | 6,184 | 1.22 | 0.51 | 0.69 ^a | Possibly |
| HB | Hagen Bræ | 9.4 | 0.5 | 30,741 | 6.08 | 2.54 | 1.03 ^a | Possibly |
| ND | Nioghalvfjordsfjorden | 24 | 69 | 145,562 | 28.81 | 12.04 | 14.27 ^a | No evidence |
| ZI | Zachariæ Isstrøm | 27 | - | - | 23.05 | 9.63 | 11.65 ^a | No evidence |
| KHB | Kofoed-Hansen Bræ | 10 | - | 116,440 | - | - | - | Possibly |
| SS | Storstrømmen | 12 | 8.4 | - | - | - | 5.80 ^a | Likely |
| BB | L. Bistrup Bræ | 11 | 6.2 | 19,525 | 3.86 | 1.61 | - | Likely |

Table 2.1: Key data on 21 Northern Greenland glaciers reviewed in this chapter. Widths and ice tongue lengths were measured in Landsat 8 2015 late summer imagery. Glacier width was measured at the grounding line. Floating ice tongue lengths are recorded for glaciers at which floating tongues are still present. Drainage basin areas were derived from hydrological catchment analysis using ice thickness and bed elevation from the Morlighem *et al.* [2014] dataset. Estimated ice discharge is derived from ^a Rignot *et al.* [2001] from 1992 to 1996 or ^b Rignot *et al.* [1997] from 1995 to 1996. Surge-type relates to a first order classification of surge-type glaciers in northern Greenland (see also Figure 2.1).

2.3.1 Northwest Greenland

Northwest Greenland (Figure 2.1), has recently undergone glacier retreat, particularly between 2000 and 2010 [Murray *et al.*, 2015]. Most outlets in this region have undergone long-term thinning (1994-2014) [Csatho *et al.*, 2014] and have accelerated by 28% between 2000 and 2010 [Moon *et al.*, 2012]. Three of the largest outlet glaciers in the far northwestern region are Harald Moltke Bræ, which drains into Wolstenholme Fjord, and Heilprin and Tracy Glaciers, which terminate in the neighboring Inglefield Bay (Figure 2.3).

Harald Moltke Bræ

Harald Moltke Bræ is an outlet glacier in northwest Greenland that is 6.3 km wide at its grounded terminus [Koch, 1928; Wright, 1939; Davies & Krinsley, 1962; Rignot *et al.*, 2001] (Figure 2.2). Early observations suggested that the terminus had two calving lobes [Wright, 1939] shown in Figure 2.3b. However, recent imagery shows this is no longer the case (Figure 2.3b). The catchment area of Harald Moltke Bræ is smaller than most other glaciers in the study area, draining only 1,400 km² (Table 2.1).

Early studies provided a detailed historical account of terminus change for the period 1916-1965 [Wright, 1939; Davies & Krinsley, 1962; Mock, 1966] (Figure 2.3b). Between 1916 and 1926 the glacier retreated, which was followed by advance until 1932 when it reached a similar position as in 1916 [Wright, 1939; Davies & Krinsley, 1962; Mock, 1966]. Between 1932 and 1937, the calving of large tabular icebergs was observed [Wright, 1939] and, by 1959, the terminus had retreated 5.5 km from its 1932 position [Davies & Krinsley, 1962]. It is also known that the glacier underwent net retreat of 2.9 km between 2000 and 2010 [Murray *et al.*, 2015].

From 1916 to 1965 the velocity of Harald Moltke Bræ fluctuated greatly between 30 and 1000 m a⁻¹ [Mock, 1966]. More recently, in 2000/01, the glacier was flowing at 30-100 m a⁻¹ at the terminus, reaching up to a maximum of 300 m a⁻¹ further up glacier [Joughin *et al.*, 2010b]. By 2005, the velocity at the terminus increased to 2000 m a⁻¹ [Joughin *et al.*, 2010b]. Several authors have suggested these recent changes in velocity reflect surge behavior at Harald Moltke Bræ [Rignot & Kanagaratnam, 2006; Moon *et al.*, 2012]. In particular, velocity increase during 2005 coincided with terminus advance (1.2 km) in 2004/2005 [Murray *et al.*, 2015].

Since the detailed work of Mock [1966], few studies have specifically focused on Harald

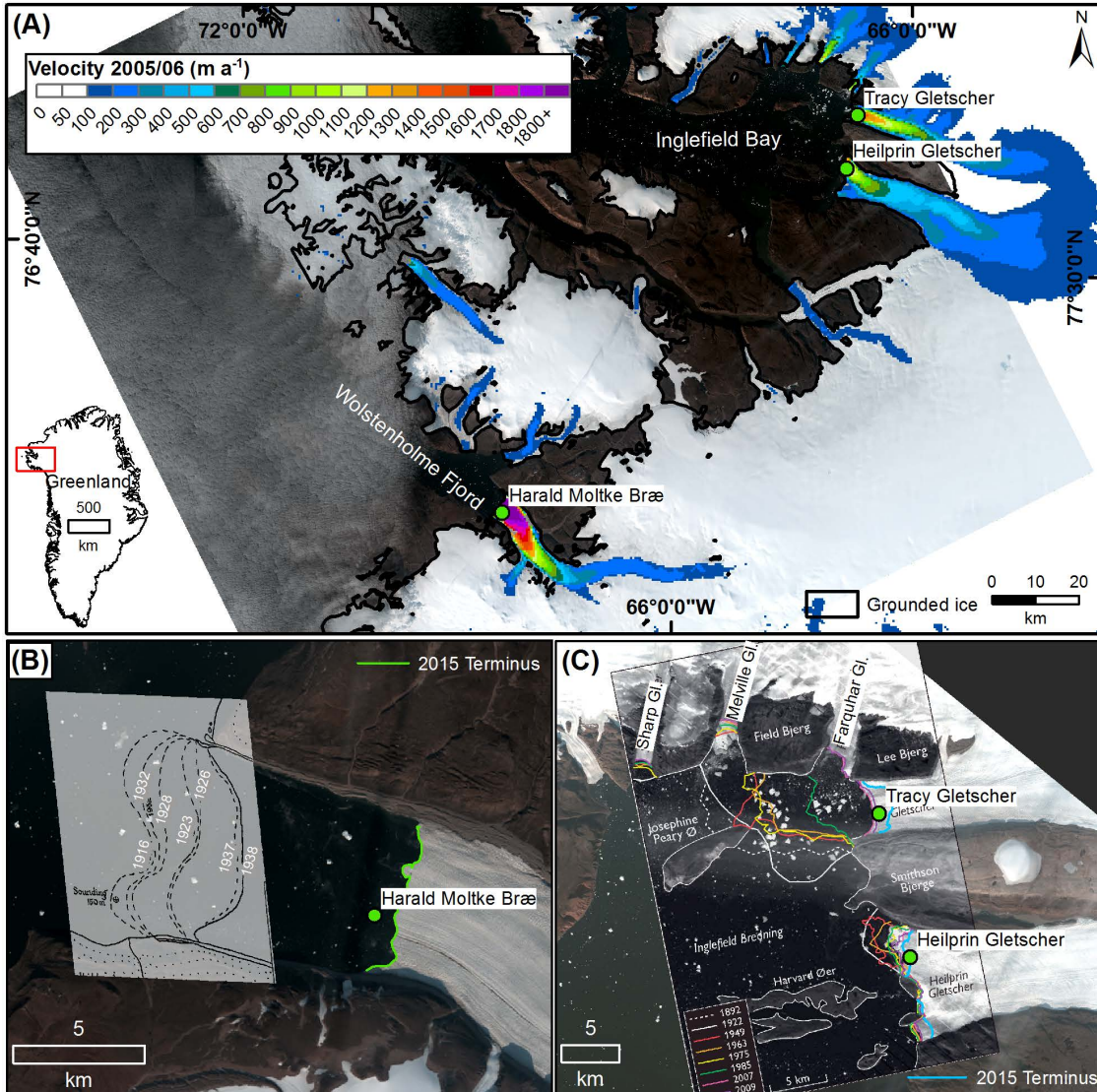


Figure 2.3: A) Location of studied glaciers in Northwest Greenland, including Harald Moltke Bræ, Heilprin and Tracy Glaciers (green circles) and grounded ice (black line). Velocity data were acquired from the 2005/2006 MEaSUREs v2 Greenland velocity [Joughin *et al.*, 2010b]. Background imagery is from Landsat 8 (late summer 2015). B) estimated terminus positions from Wright [1939], showing changes between 1916 and 1932, and its position in 2015 (green). C) previous terminus positions for Tracy and Heilprin Glaciers [Dawes & As, 2010] and the 2015 position (light blue).

Moltke Bræ. Its surge-like behavior is unusual in comparison to nearby outlet glaciers. Despite showing marked increases in velocity and advance during proposed surge events [Rignot & Kanagaratnam, 2006; Joughin *et al.*, 2010b; Murray *et al.*, 2015], the glacier has undergone large net retreat following surge events [Murray *et al.*, 2015]. This has led to a retreat of ~ 12 km compared to its position in 1916 (Figure 2.3b) and hints that the glacier has been influenced by longer-term external environmental drivers.

Heilprin and Tracy Glaciers

Heilprin and Tracy Glaciers are two large outlet glaciers in northwest Greenland that are 6.7 km and 5 km wide, respectively (Table 2.1), and collectively drain an area of approximately 12,000 km² into Inglefield Bay (Figure 2.3a). Davies & Krinsley [1962] noted that both glaciers had floating ice tongues in 1892, although early observations with limited data make this difficult to verify. Rignot *et al.* [2001] later found floating sections absent from both glaciers, which recent grounding line data confirms [Morlighem *et al.*, 2014] (Figure 2.2a). Basal topographic data from these glaciers (Figure 2.2b), shows they both lie below sea level for a distance of 36-42 km inland of the terminus [Morlighem *et al.*, 2014].

Both Heilprin and Tracy Glaciers have undergone net retreat in the 20th Century [Kollmeyer, 1980]. Tracy Glacier retreated by 7 km between 1892 and 1959 [Davies & Krinsley, 1962] and between 1949 and 2009 the glacier retreated a further 15 km away from Josephine Peary Øer Island (Figure 2.3c) [Dawes & As, 2010]. In contrast, Heilprin Glacier, retreated only 4 km between 1892 and 2009 [Porter *et al.*, 2014]. The retreat of Tracy Glacier has increased over the last two decades: between 2000 and 2005, Tracy Glacier lost 8 km of its terminus (Figure 2.4a, b) followed by 2 km retreat between 2005 and 2013 [Porter *et al.*, 2014]. These differing rates of retreat were attributed at least partly to fjord geometry, and primarily deeper basal topography below Tracy Glacier which could allow warm water intrusion [Porter *et al.*, 2014]. Surprisingly, despite an inland-sloping bed at Heilprin, it is undergoing slower dynamic change than Tracy Glacier [Porter *et al.*, 2014].

Estimates of ice discharge from European Remote Sensing (ERS) data in the mid-1990s at these glaciers are given in Table 2.1. Porter *et al.* [2014] recorded a doubling in thinning rates between 2011 and 2012 at Tracy Glacier. In terms of ice velocity fluctuations, both Heilprin and Tracy Glaciers experienced increases in speed between 2000/01 and 2005/06 of 20 and 40%, respectively [Joughin *et al.*, 2010b], and coincided with the large retreat observed at Tracy Glacier (Figure 2.4). There is no record of surging at these glaciers. Despite retreat taking place at both glaciers, and aside from study by Porter *et al.* [2014], Tracy and Heilprin Glaciers have been subject to little in-depth research in comparison to other northern Greenland areas. The differing responses of these neighboring glaciers, potentially attributed to fjord geometry, suggests uncertainty remains regarding the controls on these outlet glaciers.



Figure 2.4: Several dramatic retreat events observed at northern Greenland outlet glaciers. Panels a) and b) show Tracy Glacier retreat between 2000 and 2006. Petermann Glacier's large calving event in 2010 is shown in c/d. Steensby Glacier retreat in e/f. A significant disintegration of C. H. Ostenfeld floating ice tongue is shown in g/h. All background Landsat imagery was derived from USGS Earth Explorer from the years shown in the panels.

2.3.2 North Greenland

The northern sub-region extends from Humboldt Glacier (79°22'N, 64°57'W) to Hagen Bræ (81°17'N, 28°30'W) (Figure 2.1) and contains 13 outlet glaciers.

Humboldt Glacier

Humboldt Glacier drains ~5% of the GrIS by area [Rignot & Kanagaratnam, 2006] and has a ~91 km wide calving front (Table 2.1), making it the widest outlet glacier in Greenland. The majority of the terminus is thought to be grounded [Higgins, 1989; Joughin *et al.*, 1999], but the northern bay possesses a floating section [Rignot *et al.*, 2001; Carr *et al.*, 2015]. The glacier terminus rests significantly below sea level, extending ~100 km distance inland (Figure 2.2b).

Early work by Davies & Krinsley [1962] using early expedition maps [Koch, 1928], suggested that the frontal position changed little between 1922 and 1960. A more recent synthesis of 2000-2010 calving positions with results from Rignot *et al.* [2001], concluded that Humboldt Glacier has been retreating since the 1990s [Box & Decker, 2011]. Carr *et al.* [2015] confirmed accelerated retreat since 1999 of 162 m yr⁻¹ compared to only 37 m yr⁻¹ between 1975 and 1999. Between 2000 and 2010, Humboldt Glacier underwent the largest area change (-311 km²) of the 39 glaciers studied in Box and Decker's [2011] ice sheet wide dataset.

Several studies have identified differences between the northern and southern sections of Humboldt Glacier's terminus. Ice flow velocities vary spatially across the glacier front [Rignot *et al.*, 2001; Carr *et al.*, 2015], with up to 4 times faster flow, and increased glacier thinning in the north section compared to the south [Joughin *et al.*, 1996a; Abdalati *et al.*, 2001; Rignot *et al.*, 2001] (Figure 2.5a). Joughin *et al.* [1996a] first hypothesized that this was due to a bedrock channel beneath this northern section and later work by Carr *et al.* [2015] confirmed the presence of a large deep basal trough (>300 m) that extends 72 km into the ice sheet interior (Figure 2.2b).

Recent modelling suggests that both reduced sea-ice buttressing, particularly in the northern sector, and enhanced meltwater availability derived from increased surface temperatures are responsible for the recent retreat of Humboldt Glacier's terminus [Carr *et al.*, 2015]. Observations and modelling also suggest regional differences in glacier response to external forcing may occur along the calving front, largely controlled by underlying to-

pography [Rignot *et al.*, 2001; Carr *et al.*, 2015]. This glacier is significant in terms of its wide terminus and catchment area. It is hypothesized that if it retreats past a potential pinning point, which is located close to the northern portion of the terminus, into a deep trough extending ~ 70 km inland, rapid retreat and acceleration and subsequent increased mass loss may be expected in future [Carr *et al.*, 2015]. Thus, Humboldt Glacier may be particularly susceptible to external forcing.

Petermann Glacier

Petermann Glacier was first documented during the US Polaris Expedition by Hall in 1871 [Kollmeyer, 1980] and has since become one of the most studied glaciers in northern Greenland [Johannessen *et al.*, 2013]. The glacier is approximately 21 km wide at the grounding line (Table 2.1), narrowing down-fjord to between 15 and 20 km at the current floating terminus [Rignot, 1996; Johannessen *et al.*, 2013] (Figure 2.5a). Its floating ice tongue is one of the most extensive in northern Greenland, previously up to 70 km long, [Rignot *et al.*, 2001; Nick *et al.*, 2012], and now 48 km in length (Table 2.1). The glacier drains approximately 6% of the GrIS by area into Hall Basin [Rignot & Kanagaratnam, 2006] (Table 2.1). Large sections of this catchment are grounded well below sea level [Rignot & Steffen, 2008; Johnson *et al.*, 2011] and a deep subglacial trough extends far (100 km) into the ice sheet interior [Morlighem *et al.*, 2014]. The trough is approximately 200-400 m deep and coincides with the fastest ice flow [Joughin *et al.*, 1999] (Figure 2.2).

At the grounding line the ice is approximately 600 m thick [Johannessen *et al.*, 2013], thinning considerably to 200 m towards the front of the ice tongue [Falkner *et al.*, 2011]. There are large differences in estimated ice discharge, depending on whether calculations are made at the glacier front [Higgins, 1990] or the grounding line [Rignot *et al.*, 1997]. Estimates at the grounding line, give a value of $13.2 \text{ km}^3 \text{ a}^{-1}$ [Rignot *et al.*, 1997], much higher than estimated calving fluxes at the glacier terminus ($0.59 \text{ km}^3 \text{ a}^{-1}$) [Higgins, 1990]. These different estimates are likely to be due to increasing rates of mass loss through extreme melting beneath the floating ice tongue [Rignot *et al.*, 1997]. However, it could also be in part attributed to different measurement accuracy between using aerial photographs [Higgins, 1990] and radar satellite imagery accompanied by digital elevation models [Rignot *et al.*, 1997].

The majority of mass loss (80%) at Petermann is via high rates of submarine melting beneath the floating ice tongue [Rignot *et al.*, 2001; Rignot & Steffen, 2008]. This explains relatively low iceberg calving rates [Higgins, 1990], despite its large grounding line flux

[Rignot *et al.*, 1997; Reeh *et al.*, 1999]. Melt rates vary spatially beneath the ice tongue, from 0 m a⁻¹ at the grounding line, to a peak of 25 m a⁻¹ at 10 km downstream of the grounding line [Rignot & Steffen, 2008]. Ocean heat transported into the fjord is likely to account for these high rates of submarine melt [Johnson *et al.*, 2011]. Rignot & Steffen [2008] also observed several channels on the underside of the tongue, aligned in the direction of ice flow, which are believed to have formed from submarine melt and warm ocean water having been transported beneath the ice. Recently, it has been suggested that ice thinning in these channels may have weakened the ice shelf and been a precursor to recent calving events in 2010 and 2012 [Münchow *et al.*, 2014].

Terminus retreat normally occurs via the calving of large, tabular icebergs [Johnson *et al.*, 2011], and early studies observed sporadic calving of tabular icebergs up to 50 m thick and up to 120 km² [Dunbar, 1978; Kollmeyer, 1980]. The frontal position of Petermann remained relatively stationary between 1876 [Koch, 1928; Davies & Krinsley, 1962] and the 1980s, which suggests that iceberg calving is an important component of the longer-term mass balance of the glacier as opposed to solely losing mass via submarine melt [Higgins, 1989]. A large calving event took place in August 2010 and attracted substantial scientific attention due to its size [Box & Decker, 2011; Falkner *et al.*, 2011; Nick *et al.*, 2012; Johannessen *et al.*, 2013]. This event removed 25% of the glacier tongue by area [Falkner *et al.*, 2011], creating a tabular iceberg approximately 27 km in length and 270 km² in area [Johannessen *et al.*, 2013] (Figure 2.4c,d). This was followed by another large retreat in 2012 of 10 km (approx. ~130 km² in area) [Johannessen *et al.*, 2013]. To put these events into context, Johannessen *et al.* [2013] found that 5 major calving events occurred over the past 50 years. A particularly large event occurred in 1991 (153 km²), but the magnitude of the 2010 event exceeds all others in this 50 year record [Johannessen *et al.*, 2013]. Alongside observed terminus changes, grounding line retreat of 450 m was observed between 1992 and 1996 [Rignot *et al.*, 2001]. Future grounding line retreat could allow warm water to be transported greater distances inland, enhancing submarine melt and increasing the instability of Petermann Glacier [Nick *et al.*, 2012]. That said, large uncertainty remains over whether large calving events in recent years were part of a natural cycle or in response to climate-induced forcing [Johannessen *et al.*, 2013].

This glacier is one of the fastest flowing outlets in northern Greenland, with velocities of 1000 m a⁻¹ close to the grounding line [Johnson *et al.*, 2011; Nick *et al.*, 2012; Johannessen *et al.*, 2013] (see Figure 2.5a). However, mean annual velocity has changed little since early estimates (950 m a⁻¹) [Higgins, 1990], and has been relatively stable over recent decades (1985-2011) [Rignot & Steffen, 2008; Johannessen *et al.*, 2013]. Following the 2010 calving event, only marginal acceleration was observed at the glacier terminus, which could be

due to weak attachment of the floating ice tongue to the fjord walls, and suggests that glacier velocities may be largely insensitive to ice tongue retreat [Nick *et al.*, 2012]. Warm ocean water, accompanied by the absence of sea ice in Hall Basin prior to the 2010 calving event could be responsible for the magnitude of the 2010 calving event [Johannessen *et al.*, 2013].

In summary, Petermann Glacier is one of the major outlets in Greenland and has lost large portions of its floating tongue over the last two decades. The occurrence of several large calving events over the last 50 years suggest these recent changes may be part of a natural cycle [Nick *et al.*, 2012; Johannessen *et al.*, 2013]. However, the terminus now resides at its furthest position inland since 1953 [Johannessen *et al.*, 2013]. This retreat is likely due to increased submarine melt under the floating portion of its terminus as a result of recent ocean warming [Nick *et al.*, 2012].

Steensby Glacier

Steensby Glacier is a 4.8 km wide glacier that has a catchment area of 4,700 km² and has a 5.1 km long floating tongue (Table 2.1). Previous observations suggested this floating ice tongue was formerly between 48 and 62 km long [Ahnert, 1963]. Some of the first observations were made by Ahnert [1963] and terminus changes were later recorded by Higgins [1990]. Aerial photographs in 1947 showed the terminus to be floating [Ahnert, 1963], and later oblique photographs from 1953 suggested that it advanced between 1947 and 1953 [Higgins, 1990]. By 1996, the grounding line had advanced slightly, and the glacier thickened between these two studies [Rignot *et al.*, 2001]. Grounding line data between 1993 and 2013 [Morlighem *et al.*, 2014] showed a more extensive, 16 km-long floating tongue at Steensby Glacier (Figure 2.2a). However, recent satellite imagery shows 15 km of retreat between 1999 and 2015 (Figure 2.4e, f).

Few records of ice velocities at Steensby Glacier exist. Ice velocities showed little fluctuation between estimates made in the 1970s (430 m a⁻¹: Higgins [1990]) and in 1996 [Rignot *et al.*, 2001]. More recently, velocities decreased by 10-15% between 2000/01 and 2005/06 [Joughin *et al.*, 2010b]. Steensby Glacier has often been absent from regional to ice-sheet-wide studies of glacier retreat and flow acceleration, despite having retreated a substantial 1 km a⁻¹ over the last 15 years (Figure 2.4e, f).

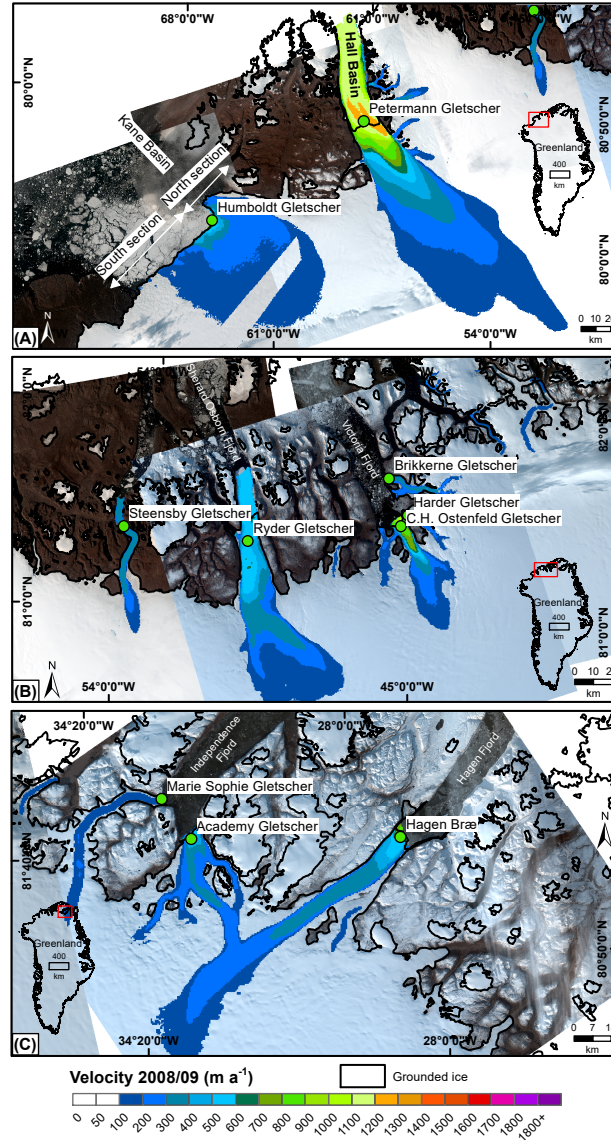


Figure 2.5: North Greenland region. A) Humboldt and Petermann Glaciers. B) Seven outlet glaciers in the most northern part of the study region between Steensby Glacier and Henson Glacier. C) Marie-Sophie, Academy and Hagen Bræ Glaciers. Grounded ice is shown in a black outline. Velocity is shown on each glacier in m a^{-1} . Velocity data was acquired from the 2008/2009 MEaSUREs v2 Greenland velocity [Joughin *et al.*, 2010b]. Background imagery is from Landsat 8 (late summer 2015).

Ryder Glacier

Ryder Glacier is a 10 km wide outlet glacier that drains approximately 3.5% of the ice sheet by area (Table 2.1) into Sherard Osborn Fjord (Figure 2.5b). The glacier comprises two tributaries that combine at 1000 m elevation [Joughin *et al.*, 1996b, 1999], and it currently has a 29 km long floating tongue (Table 2.1). An early estimate (1978) of discharge at

the terminus was $0.66 \text{ km}^3 \text{ a}^{-1}$, making it one of the more important northern Greenland glaciers [Higgins, 1990]. Later work found a substantially larger grounding line flux of $3.88 \text{ km}^3 \text{ a}^{-1}$, confirming its high discharge [Rignot *et al.*, 2001].

Relatively few records of terminus change are available for Ryder Glacier. Some of the first observations, from 1917, suggested that the floating tongue extended further north than at present [Koch, 1928], but then retreated by 5 km between 1947 and 1956 [Davies & Krinsley, 1962]. The position of the grounding line also showed retreat during 1992-1996, along with 4 m a^{-1} of ice surface thinning [Rignot *et al.*, 2001]. Following this period, the glacier thinned by $2\text{-}4 \text{ m a}^{-1}$ between 1997 and 1999 [Abdalati *et al.*, 2001]. More recent observations of terminus change are limited, although Murray *et al.* [2015] documented $0.43\text{-}0.55 \text{ km a}^{-1}$ of glacier advance between 2002 and 2006, followed by a substantial retreat of 3 km in 2006/07. This was followed by advance during 2007-2010 [Box & Decker, 2011]. Should observed thinning continue at Ryder Glacier, large areas of ice may become ungrounded [Thomas *et al.*, 2009; Csatho *et al.*, 2014] making it more susceptible to retreat and further large ice losses. Recent work by Joughin *et al.* [2010b], however, found no notable changes in velocity at Ryder Glacier between the winters of 2000/01 and 2005/06, with flow speeds similar to those of earlier studies [Joughin *et al.*, 1999; Rignot *et al.*, 2001].

The majority of reported velocity changes recorded at Ryder Glacier focused on a postulated mini-surge event in 1995 during which velocity increased three-fold [Joughin *et al.*, 1996b, 1999]. This suggested event occurred between September and October 1995, when ice velocity in the slower upstream areas of the glacier was recorded to have increased from 20 m a^{-1} to 150 m a^{-1} and then returned to normal in just a seven-week period [Joughin *et al.*, 1996b]. However, as velocity change for the faster main trunk of the glacier was not available during this period, uncertainty remains as to the true magnitude of this mini-surge. It was also unclear if the glacier simultaneously advanced during this interval [Joughin *et al.*, 1996b, 1999; Rignot *et al.*, 2001], although it was hypothesized that this acceleration may have caused a substantial increase in ice discharge [Joughin *et al.*, 1996b; Abdalati *et al.*, 2001]. Whether this ‘mini-surge’ reflects true surge-behavior at Ryder Glacier is ambiguous and is discussed in more detail in Section 2.4.4.

C. H. Ostenfeld Glacier

C. H. Ostenfeld Glacier is approximately 7.9 km wide (Table 2.1) and has a drainage area of approximately $14,000 \text{ km}^2$. Of the three outlet glaciers draining into Victoria Fjord, it

is the largest and has the highest ice discharge [Higgins, 1989; Rignot *et al.*, 2001] (Figure 2.5b).

Limited information is available on past terminus changes at C.H. Ostenfeld Glacier. Over the past two decades, the terminus shows variable periods of advance and retreat [Box & Decker, 2011; Murray *et al.*, 2015]. The floating glacier tongue previously extended ~ 25 km down fjord of the grounding line [Higgins, 1989, 1990]. It still has a floating ice tongue, but it is now only 1.5 km long (Table 2.1). During 1992-1996, the grounding line retreated 500 ± 200 m [Rignot *et al.*, 2001]. More recently, an advance of 5.6 km^2 occurred in 2001/02, followed by an annual retreat of 20.6 km^2 in 2002/03 [Box & Decker, 2011]. Between the years 2000 and 2006, the majority of the ice tongue disintegrated (Figure 2.4g, h), removing an estimated total area of 350 km^2 [Moon & Joughin, 2008]. Following this, a further 1.2 km retreat occurred (2006 -2007) [Murray *et al.*, 2015].

Ice velocities have shown little increase between 2000/01 and 2005/06 [Joughin *et al.*, 2010b] and were consistent with earlier velocity values from 1978 and the 1990s of around 800 m a^{-1} [Higgins, 1989, 1990; Rignot *et al.*, 2001]. Consequently, ice tongue collapse appeared not to significantly affect up-glacier ice velocities during 2000-2006. This could be due to its fragmented nature (Figure 2.4g), which would provide little resistive stress to the grounded inland ice. There are no documented surges at C. H. Ostenfeld Glacier although a large advance followed by retreat between 2000 and 2003 could suggest surge activity, but this remains untested.

C. H. Ostenfeld is one of the main outlet glaciers in northern Greenland. A large area of its floating tongue has been lost over the past two decades, yet ice velocities have changed little. However, it has recently lost the majority of its floating ice tongue and it may soon retreat back to become grounded, and then discharge grounded ice into the ocean. Thus, there is potential for enhanced velocities and ice discharge from the C. H. Ostenfeld catchment in the near-future, but large uncertainty remains on the glacier's current and future behavior.

Harder and Brikkerne Glaciers

Harder and Brikkerne are two outlet glaciers also draining into Victoria fjord (Figure 2.5b) which are 5.1 and 6.1 km wide, respectively (Table 2.1). Collectively, they drain an area of $\sim 3,000 \text{ km}^2$ (Table 2.1) from local ice domes. Both glaciers previously coalesced with the floating tongue of C. H. Ostenfeld, with Harder Glacier merging on the eastern side. Brikkerne Glacier sits further north, has three branches, and a small floating ice tongue

which is 1.2 km long (Table 2.1).

Little record of these glaciers exists in the literature and there are no records of terminus change at Harder Glacier. At Brikkerne, the only frontal position data available show that the northern and central sections of the glacier advanced 11 km and 8 km, respectively, between 1953 and 1978 [Higgins, 1990]. Data from the 1970s showed relatively low velocities at Harder Glacier ($84\text{--}122\text{ m a}^{-1}$) [Higgins, 1990]. At Brikkerne Glacier, velocity was considered to be very slow in 1947, increasing to $150\text{--}360\text{ m a}^{-1}$ in 1963 and 500 m a^{-1} between 1971 and 1978 [Higgins, 1990]. This velocity increase coincided with periods of glacier advance [Higgins, 1990]. No records of surging exist for Harder Glacier, but Brikkerne Glacier was identified as surge-type glacier on the basis of variable velocity records [Higgins, 1990; Rignot *et al.*, 2001]. Since the early studies [Higgins, 1990; Rignot *et al.*, 2001], little attention has been paid to these glaciers, despite their potential dynamic changes such as surging at Brikkerne Glacier.

Jungersen, Naravana Fjord and Henson Glaciers

Further north from Victoria fjord lie three further outlet glaciers, Jungersen, Naravana Fjord and Henson, which collectively drain 0.7% of northern Greenland (Table 2.1). Both Jungersen and Henson Glaciers are approximately 2 km wide [Higgins, 1990] and previously had floating sections [Rignot *et al.*, 2001], although their length has not been reported in the literature. Naravana Fjord, located between these glaciers, is 2.5 km wide and has no floating section. Little is known about terminus changes at these glaciers. Grounding line data [Morlighem *et al.*, 2014] shows they no longer have floating ice tongues (Figure 2.2a), suggesting their termini have retreated since previous observations [Rignot *et al.*, 2001]. Ice velocity data are limited, although Jungersen Glacier was estimated to flow at 350 m a^{-1} in the 1970s, whereas Henson was barely moving (1.7 m a^{-1} : Higgins [1990]). More recent velocity estimates suggested similar velocities at Jungersen Glacier (395 m a^{-1}), slower flow at Naravana Fjord (59 m a^{-1}), and a much higher estimate for Henson Glacier (286 m a^{-1} : Rignot *et al.* [1997]).

These glaciers have received little research attention and Rignot *et al.* [2001] suggested that their significance in terms of ice discharge may have been previously overstated by [Koch, 1928]. This may explain their absence from the majority of northern Greenland research. Nevertheless, they collectively drain a similar area to Tracy Glacier ($\sim 3,800\text{ km}^2$), and thus represent an important component of the mass budget of the region.

Academy and Marie Sophie Glaciers

Academy and Marie Sophie Glaciers collectively drain an area of $\sim 9,000 \text{ km}^2$ into Independence Fjord (Figure 2.5c). Academy Glacier has a much wider terminus (8.4 km), compared to Marie Sophie (3.9 km) (Table 2.1), and neither glacier has a floating ice tongue (Figure 2.2a) [Higgins, 1990; Rignot *et al.*, 2001]. Relatively few records of terminus change exist for either glacier. At Marie Sophie, early records showed minimal retreat of 0.06-0.09 km between 1921 and 1956 and sketches by Peary [1892] suggest that Academy Glacier retreated 12 km between 1892 and 1956 [Davies & Krinsley, 1962]. More recently, terminus changes showed substantial inter-annual variability between 2000 and 2010 [Murray *et al.*, 2015]. Academy Glacier, in particular, advanced (0.59 km) between 2008 and 2009, and subsequently retreated by a similar magnitude (0.49 km) in the following year (2009-2010) [Murray *et al.*, 2015]. Overall, between 2000 and 2010, both Academy and Marie Sophie Glaciers underwent retreat of 0.9 km and 0.2 km, respectively [Murray *et al.*, 2015].

Early work in the 1970s estimated velocities of 220 m a^{-1} at Marie Sophie Glacier [Higgins, 1990]. This contrasts markedly with more recent values of only 40 m a^{-1} in 1996 [Rignot *et al.*, 1997] and $< 100 \text{ m a}^{-1}$ in 2006 [Joughin *et al.*, 2010b]. Initial velocity estimates (1970s) at Academy Glacier found values of 256 to 290 m a^{-1} at the terminus [Higgins, 1990; Rignot *et al.*, 1997]. It then maintained a steady velocity of 270 m a^{-1} from the 1970s to the mid-1990s [Rignot *et al.*, 2001], followed by deceleration between 1996 and 2000/01 [Rignot & Kanagaratnam, 2006]. More recently, both Marie Sophie and Academy Glaciers accelerated between 2000/01 and 2005/06 (from 200 m a^{-1} to 600 m a^{-1} at Academy) [Joughin *et al.*, 2010b]. It has been suggested that recent increases in glacier velocity could reflect surge behavior on Academy Glacier [Rignot & Kanagaratnam, 2006]. However, as the glacier has not shown multi-year advance (despite reduced retreat rates between 2004/05 and 2005/06 of approximately 500 m) [Murray *et al.*, 2015], this is questionable. No record of surging exists for Marie Sophie Glacier.

Both glaciers are significant within northern Greenland in terms of their drainage areas, and because they have both shown variable ice velocities and retreat rates throughout the historical record. Whether variable terminus positions and flow speeds are representative of a cyclic process or surge activity remains unknown. Thus they require future consideration, particularly in terms of deciphering the impacts of external forcing versus internal glacier dynamics.

Hagen Bræ

Hagen Bræ is a large outlet glacier that is 9.4 km wide at the grounding line (Table 2.1) and drains $\sim 31,000$ km² of ice area into Hagen Fjord (Figure 2.5c). Previously, the terminus was pinned on two islands [Higgins, 1989, 1990]. Early studies also documented a floating ice tongue approximately 18 km in length between 1947 and 1978 [Davies & Krinsley, 1962; Higgins, 1989, 1990], but recent imagery (2015) suggests the floating section is only 2.1 km long (Table 2.1). Academy and Hagen Bræ Glaciers lie within two basal troughs that deepen inland, approximately 10 km wide that extend approximately 100 km inland [Morlighem *et al.*, 2014] (Figure 2.2b).

Relatively few studies have considered terminus changes at Hagen Bræ. Early work by Higgins [1989] found the glacier terminus advanced at 0.5 km a⁻¹ during the 1970s. In 2008/09, Hagen Bræ underwent the largest retreat in a single year out of 199 outlet glaciers across Greenland during the period 2000-2010 (15 km) [Murray *et al.*, 2015]. However, the glacier also experienced 3.8 km of total advance between 2001 and 2007 [Murray *et al.*, 2015].

In 1996, velocities at the terminus were 94 m a⁻¹ [Rignot *et al.*, 2001]. More recently, the glacier has accelerated substantially close to the grounding line: relatively low velocities in 2000/01 (200 m a⁻¹ inland and 60 m a⁻¹ at the grounding line) increased to over 600 m a⁻¹ by 2005/06 and 2007 [Joughin *et al.*, 2010b; Moon *et al.*, 2012]. Moon *et al.* [2012] hypothesized that these large velocity increases may have been due to glacier surging. Several other studies have noted potential surge-type behavior at Hagen Bræ [Abdalati *et al.*, 2001; Rignot *et al.*, 2001]. Ice velocities were higher in the 1970s [Higgins, 1990] than in 1996 [Rignot *et al.*, 2001]. In 1996, velocity decreased between the equilibrium line altitude and the glacier terminus [Rignot *et al.*, 2001]. In addition, the grounding line retreated 400 m [Rignot *et al.*, 2001] between 1992 and 1996. Based on these observations, Rignot *et al.* [2001] suggested surging occurred in the 1970s and that the glacier was then in quiescence between 1992 and 1996. Between 2000 and 2007, large increases in velocity [Joughin *et al.*, 2010b] coincided with 3.8 km of advance [Murray *et al.*, 2015]. This may suggest a second surge of Hagen Bræ. Following this potential surge event, however, the glacier retreated substantially (15 km) [Murray *et al.*, 2015]. However, velocities remained high (2008/09) (Figure 2.5c). This behavior is not usually associated with the quiescent phase of a surge-cycle [Meier & Post, 1969]. Thus, it could be that external forcing, or retreat from a stable position in the fjord, as opposed to internal, surge-related changes have become the primary control on terminus position at Hagen Bræ in more recent years.

Recent large retreat at Hagen Bræ and its location in a deep basal trough below sea level, might suggest the glacier is vulnerable to rapid retreat in the near-future. This glacier is significant in terms of discharge, draining 6% of northern Greenland by area and it is surprising that this glacier has not been studied in more detail.

2.3.3 Northeast Greenland

The northeast region (Figure 2.1) consists of five outlet glaciers which are Nioghalvfjærdsfjorden (also known as 79 North), Zachariæ Isstrøm, Storstrømmen, Kofoed-Hansen Bræ and L. Bistrup Bræ. These glaciers are associated with the NEGIS, which is a large, fast flowing portion of the GrIS that rests substantially below sea level (Figure 2.2b) and drains ice some 600 km into the interior of the ice sheet [Joughin *et al.*, 2001; Reeh *et al.*, 2001]. The entire NEGIS is considered potentially unstable, having undergone substantial ice thinning since the beginning of the 21st century [Khan *et al.*, 2014].

Nioghalvfjærdsfjorden (79 North Glacier) and Zachariæ Isstrøm

Nioghalvfjærdsfjorden and Zachariæ Isstrøm are the two main outlets of the NEGIS [Khan *et al.*, 2014] and collectively drain around 30% of the northern GrIS by area [Rignot & Kanagaratnam, 2006] (Table 2.1). Nioghalvfjærdsfjorden is 24 km wide, and has an extensive (approx. 69 km long) floating ice tongue (Figure 2.2a), that widens down-fjord to 30 km at the terminus [Thomsen *et al.*, 1997]. Zachariæ Isstrøm is 27 km wide and terminates in an embayment typically surrounded by calved icebergs [Box & Decker, 2011]. Zachariæ Isstrøm previously terminated as a floating ice tongue (Figure 2.2a), but this dramatically disintegrated between 2000 and 2006, meaning that the glacier terminus is currently grounded [Khan *et al.*, 2014]. Both glaciers lie above deep basal troughs, which rest significantly below sea level [Mayer *et al.*, 2000], and have a reverse bed slope [Bamber *et al.*, 2013] (Figure 2.2b).

Information on the frontal positions of these two glaciers has been comparatively limited due to year-round ice mélange in the fjords, resulting in an ambiguous calving region and therefore making it difficult to accurately identify the true calving front [Bevan *et al.*, 2012; Murray *et al.*, 2015]. In 1976, the two glaciers were thought to have coalescing ice tongues [Weidick *et al.*, 1995], which suggests they have since retreated substantially and become separated [Rignot *et al.*, 2001]. Early records from Nioghalvfjærdsfjorden found 20 km of retreat between 1950 and 1963 [Thomsen *et al.*, 1997]. Subsequently, the terminus

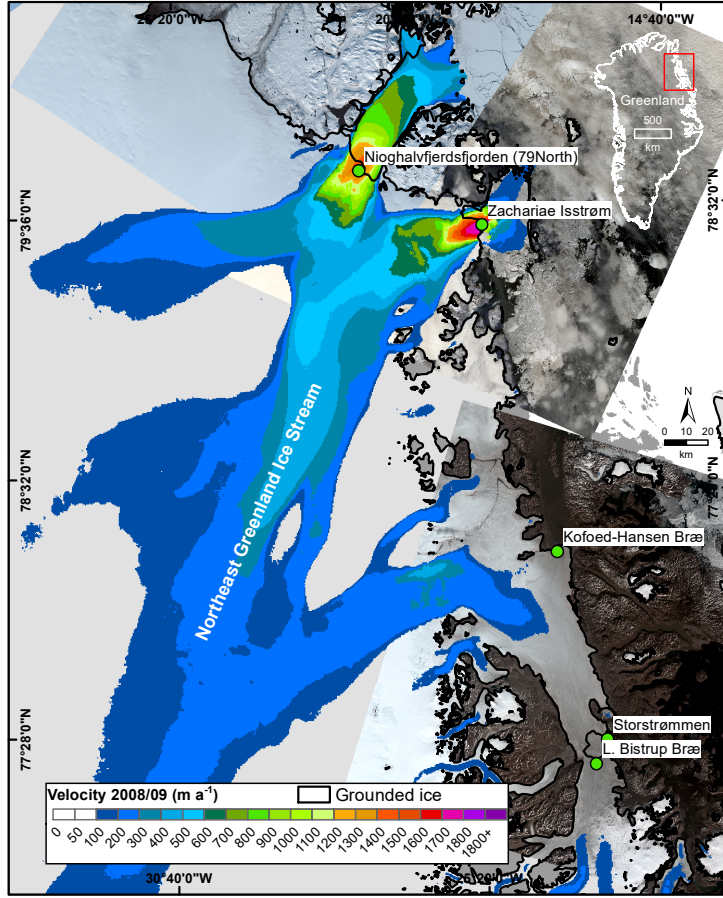


Figure 2.6: Northeast Greenland region that includes Nioghalvfjærdsfjorden (79North), Zachariae Isstrøm, Kofoed-Hansen Bræ, Storstrømmen, and L. Bistrup Bræ. Grounded ice is shown in a black outline. Velocity is shown on each glacier in m a^{-1} . Velocity data was acquired from the 2008/2009 MEaSUREs v2 Greenland velocity [Joughin *et al.*, 2010b]. Background imagery is from Landsat 8 (late summer 2015).

retreated 5-7 km during 1978-2003 [Khan *et al.*, 2014]. Zachariae Isstrøm, lost 1400 km^2 of its ice shelf between 2000 and 2006 [Moon & Joughin, 2008] and its grounding line has begun to rapidly retreat downslope [Mouginot *et al.*, 2015]. Both glaciers underwent similar ice loss in 2004/05, with 60 km^2 of ice lost at Nioghalvfjærdsfjorden and 67 km^2 at Zachariae Isstrøm [Box & Decker, 2011]. Two years later, during 2006/07, both glaciers advanced, although of differing magnitudes: 8.4 km^2 at Nioghalvfjærdsfjorden and 45.8 km^2 at Zachariae Isstrøm [Box & Decker, 2011]. Subsequently, between 2009 and 2012, sections of the Nioghalvfjærdsfjorden retreated by a further 2-3 km [Khan *et al.*, 2014].

Nioghalvfjærdsfjorden and Zachariae Isstrøm were considered slow-moving in the early 1950s [Helk & Dunbar, 2014], although no specific velocity values were given. However, more recent data show that they are relatively fast-flowing reaching speeds of $>1 \text{ km a}^{-1}$

at their termini [Khan *et al.*, 2014] (Figure 2.6). No significant acceleration or deceleration was detected between 2000 and 2006 on Nioghalvfjærdsfjorden [Rignot & Kanagaratnam, 2006; Joughin *et al.*, 2010b]. However, a more recent study observed an acceleration of 100 m a^{-1} between 2000 and 2011 [Khan *et al.*, 2014]. Zachariæ Isstrøm has been accelerating since the early 2000s, increasing by up to 200 m a^{-2} , following the disintegration of part of the ice shelf in 2004/05 [Rignot & Kanagaratnam, 2006; Moon & Joughin, 2008; Joughin *et al.*, 2010b]. Acceleration then continued, although more steadily, until 2012 [Khan *et al.*, 2014; Mouginot *et al.*, 2015]. Since 2012, ice velocities on Zachariæ Isstrøm have increased by 25%, accompanied by accelerated frontal retreat [Mouginot *et al.*, 2015].

Estimates suggest that these glaciers must have experienced submarine melt rates of between $6\text{--}8 \text{ m a}^{-1}$ to explain their 1996 ice flux [Rignot *et al.*, 1997]. This is similar to submarine melt rates recorded at other northern Greenland outlet glaciers e.g. Petermann Glacier [Rignot & Steffen, 2008]. The break-up of fast ice offshore of Nioghalvfjærdsfjorden in 1997 was followed by a large glacier calving event and is thus considered an important control on the rates of calving [Reeh *et al.*, 2001].

More generally, the NEGIS is thought to be undergoing dynamic thinning as a result of climate change, losing mass at a rate of $>10 \text{ Gt a}^{-1}$ [Khan *et al.*, 2014]. As the NEGIS extends far into the ice sheet interior [Khan *et al.*, 2014] (Figure 2.2c) and sits on a reverse bed slope, these glaciers have the potential to discharge large volumes of ice. Should retreat continue at the present or increased rates (particularly at Zachariæ Isstrøm) [Khan *et al.*, 2014], subsequent ice flow speed-ups could cause significant mass loss from a large inland area of the GrIS [Csatho *et al.*, 2014]. This could further destabilize this region and increase its contribution to 21st century sea level rise.

Storstrømmen, Kofoed-Hansen Bræ and L. Bistrup Bræ

Storstrømmen is another large outlet of the NEGIS that, along with Kofoed-Hansen Bræ, drains $\sim 120,000 \text{ km}^2$ (Table 2.1). The catchment extends to the summit of the GrIS [Reeh *et al.*, 2003] (Figure 2.2c). Kofoed-Hansen Bræ is the northeastern branch of Storstrømmen which discharges approximately 25% of the Storstrømmen ice flux [Mohr *et al.*, 1998]. Storstrømmen has a two-lobed calving front, one of which drains directly into the ocean and the other of which joins with L. Bistrup Bræ to the south (Figure 2.6) [Khan *et al.*, 2014]. L. Bistrup Bræ terminates alongside Storstrømmen and is approximately 11 km wide with a catchment of $\sim 20,000 \text{ km}^2$ (Table 2.1). Within this embayment, both Storstrømmen and L. Bistrup Bræ have floating ice sections (Figure 2.2a) that are 8.4 and 6.2 km long,

respectively, whereas data suggests Kofoed-Hansen Bræ is grounded [Morlighem *et al.*, 2014].

Relatively little is known about frontal position changes at these glaciers. Available data show that all three glaciers retreated between 2001 and 2005 [Seale *et al.*, 2011]. In total, this resulted in retreat of 0.3 km at Storstrømmen, and 0.76 km at both Kofoed-Hansen Bræ and L. Bistrup Bræ [Seale *et al.*, 2011]. However, during this period Storstrømmen underwent a short term advance of 0.4 km² in 2001/02 [Box & Decker, 2011]. Later, between 2005 and 2008, only Storstrømmen glacier continued to retreat, while L. Bistrup Bræ and Kofoed-Hansen Bræ both advanced by 0.29 km [Seale *et al.*, 2011].

The velocity of Storstrømmen was thought to be approximately 230 m a⁻¹ in 1996 [Rignot *et al.*, 2001]. L. Bistrup Bræ is considered slow moving, although specific values were not documented in the literature [Rignot *et al.*, 2001], with almost zero velocity between 2000/01 and 2009/10 at the terminus [Joughin *et al.*, 2010b]. However, further inland the glacier flows at ~ 100 m a⁻¹ in 2008/09 (Figure 2.6). During this same period (2000/01 – 2009/10) Storstrømmen Glacier decelerated by 60 m a⁻² [Joughin *et al.*, 2010b]. Evidence of surging exists for all three glaciers. A surge was documented at Storstrømmen between 1978 and 1984 [Reeh *et al.*, 1994], when the glacier advanced approximately 12 km. By the 1990s it was considered to be quiescent [Mohr *et al.*, 1998], and has remained so since that time [Reeh *et al.*, 2003; Rignot & Kanagaratnam, 2006]. L. Bistrup Bræ is also likely to be a surge-type glacier, based on thickening at the grounding line, although there is no direct evidence of an actual surge event. The glacier is instead hypothesized to have surged in the past and now be quiescent [Rignot *et al.*, 2001]. Both L. Bistrup Bræ and Storstrømmen have experienced very low flow speeds over the past decade, potentially indicative of quiescence [Moon *et al.*, 2012], as well as a characteristic pattern of thickening inland, where the surge may have initiated, and thinning towards the terminus [Abdalati *et al.*, 2001; Csatho *et al.*, 2014]. Surveys between 1995 and 1999 found thinning rates of 2 m a⁻¹ in the lower reaches of both glaciers and thickening up to 3 m a⁻¹ further inland [Thomas *et al.*, 2009]. Following this, however, thickening rates on the upper reaches of Storstrømmen began to decrease [Thomas *et al.*, 2009].

Despite these three outlet glaciers collectively draining an area (27%) of the GrIS, which is far greater than the well-studied Petermann Glacier (Table 2.1), little previous work has focused on their dynamics. Considerable variability in terminus positions have taken place over the last two decades, particularly at Storstrømmen and L. Bistrup Bræ, which has been linked to surge activity. These glaciers are important in terms of draining a large proportion of the NEGIS and it is necessary for further work to better understand their surge-nature and their implications for increased ice discharge from potentially unstable

regions.

2.3.4 Summary of northern Greenland outlet glacier changes

Overall, substantial changes have taken place in northern Greenland, particularly during the past two decades, and there has been considerable variability between sub-regions and individual glaciers. Figure 2.7 summarizes the events recorded from the literature at the selected outlet glaciers in northern Greenland between 1880 and 2015. For all glaciers where records exist (17 out of 21 in Figure 2.7), retreat has occurred at some stage between 2000 and 2015, with the most substantial at Humboldt, Tracy, Hagen Bræ, C. H. Ostenfeld, and Petermann Glaciers. In the case of the latter three glaciers, this retreat resulted in substantial loss of their floating ice tongues. For example, Petermann Glacier lost 27 km of its floating ice tongue in 2010 [Falkner *et al.*, 2011], and Hagen Bræ lost a 15 km floating section in 2008/09 [Murray *et al.*, 2015]. However, glacier retreat is not uniform across the region, and several glaciers underwent advance between 2000 and 2010 (e.g. L. Bistrup Bræ, Kofoed-Hansen Bræ, and Harald Moltke Bræ). This could either reflect surge behavior (which has been hypothesized at all three of these glaciers) or a differing response to external environmental forcing, perhaps due to local topographic controls. Nevertheless, over the last 20 years, all glaciers have experienced some retreat, which would suggest a common response to external forcing.

Alongside terminus changes, our review has shown that several of the study glaciers have accelerated, particularly over the last two decades (Figure 2.7). However, this has not been the case at all study glaciers. This is evident in Figure 2.8, which uses MEaSUREs velocity data [Joughin *et al.*, 2010b] from 2000/01 and 2008/09 to show changes in velocity between these two periods across northern Greenland. These two datasets are winter velocities, between 3 September and 24 January 2000 - 2001 and 1 December and 28 February 2008 - 2009. Instead, velocity change is highly variable, with several glaciers accelerating substantially (e.g. Hagen Bræ and Academy Glacier) and others slowing (e.g. Petermann and Ryder Glaciers). Recent velocity increases were often accompanied by glacier retreat (Figure 2.7), namely at Hagen Bræ, Academy, Marie Sophie, Tracy, and Heilprin Glaciers. Apart from Hagen Bræ, the retreat of large floating ice tongues (e.g. Petermann and C.H. Ostenfeld) did not appear to coincide with increased velocities. The impact of major ice tongue losses on ice velocities is therefore complex.

Figure 2.7 also shows that there are several glaciers in northern Greenland for which measurements of retreat, advance, and other glacier changes have not been made, par-

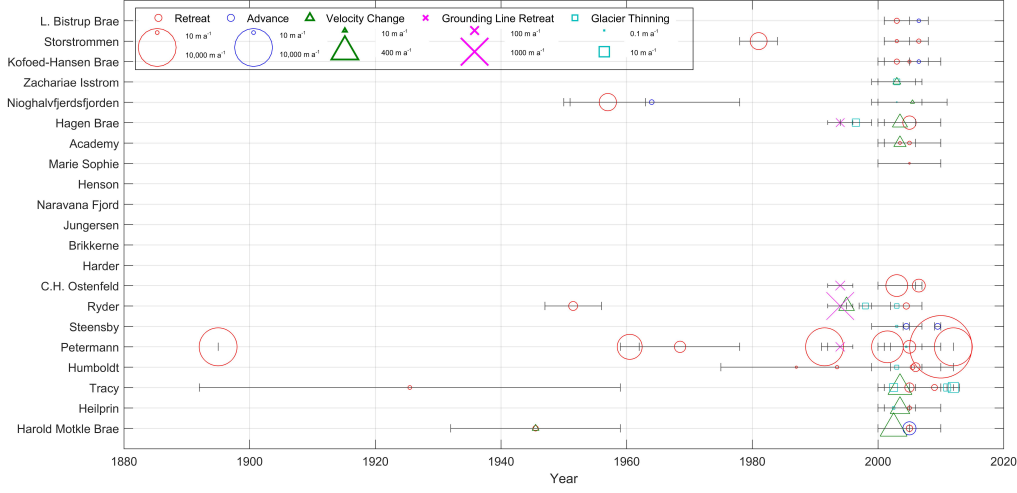


Figure 2.7: A summary of recorded changes at northern Greenland outlet glaciers based on a review of the literature. Key events of terminus change (circles, red for retreat, blue for advance), velocity change (triangle), grounding line retreat (cross) and glacier thinning (square), that have occurred at all northern Greenland focus glaciers between 1880 and present (2015) are recorded. Data points are shown in the middle of study periods and the grey lines show the duration over which the change refers to. All data points are converted to m a^{-1} across the study period and the size of all data points are based on m a^{-1} magnitude. The legend shows the symbol sizes and their corresponding values for each category of data shown.

ticularly at the smaller glaciers such as Henson, Naravana Fjord, Jungersen, Brikkerne and Harder. Several other glaciers have very few measurements. Further research into these large and potentially important outlet glaciers including frontal retreat and ice velocity measurements would help to improve understanding of region wide drivers on glacier retreat.

2.4 Discussion

In the following sections we discuss the potential factors which may have driven recent changes in the dynamics of outlet glaciers in northern Greenland. This begins with external forcing via increasing atmospheric and oceanic temperatures, and the impact of reductions in sea ice. Following that we consider the role of glacier-specific factors as well as the potential surge-dynamics of several of the study glaciers in this region. we also assess the future implications of mass loss in northern Greenland.

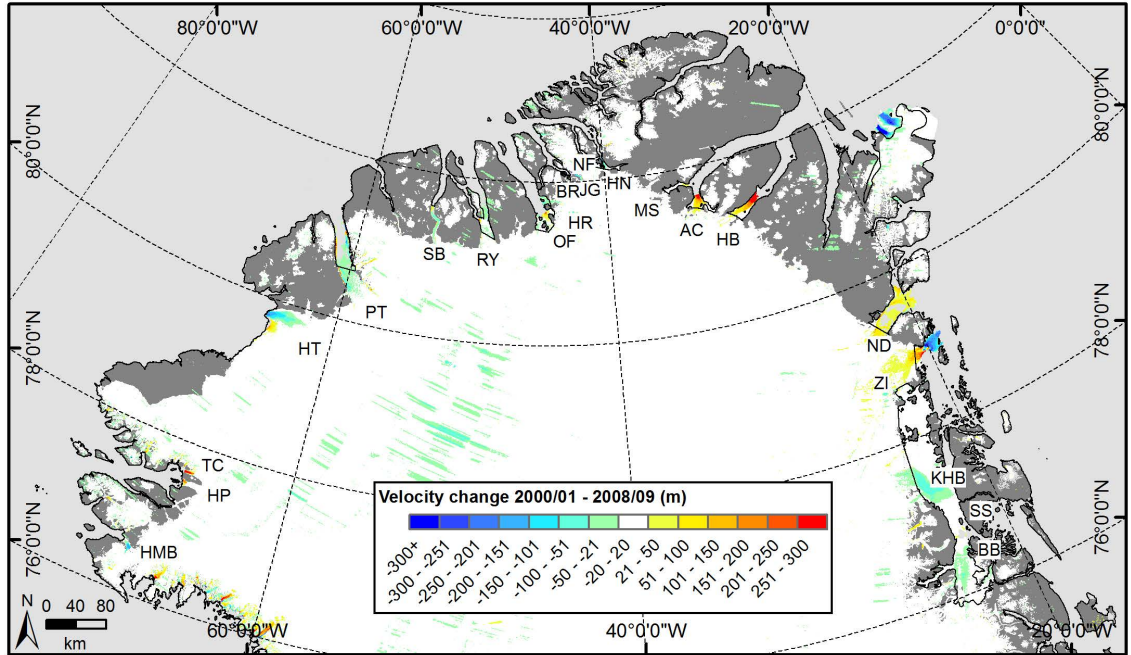


Figure 2.8: Velocity change between winters 2000/01 and 2008/09 using MEaSUREs v2 Greenland velocity data [Joughin *et al.*, 2010b]. Orange and red colors show velocity increase, and green and blue show velocity decrease.

2.4.1 Atmospheric and oceanic forcing

Recently observed changes at northern Greenland outlet glaciers may have been driven by changes in atmospheric and oceanic temperatures. Here we discuss these potential external controls on surface ice and submarine melting and their links to observed outlet glacier change across northern Greenland.

2.4.1.1 Subaerial ice melt

Atmospheric temperatures over the GrIS have increased significantly since the early 1990s, increasing by 1.7°C between 1991 and 2006 [Hanna *et al.*, 2008; Box *et al.*, 2009], which appears to have coincided with widespread glacier retreat [Moon & Joughin, 2008]. Northern Greenland experienced negative mass balance between 2006 and 2012 [Khan *et al.*, 2015], primarily due to enhanced surface melting and runoff [van den Broeke *et al.*, 2009]. Carr *et al.* [2013a] showed air temperatures at NW and NE Greenland meteorological stations between 1990 and 2010 increased linearly which coincides with the dominant pattern of retreat at outlet glaciers in the region (Figure 2.7). In particular, the northeast region of Greenland has experienced increased discharge and melting between 2003 and 2012,

which has been correlated to atmospheric warming [Khan *et al.*, 2014]. This coincides with substantial retreat of both Nioghalvfjærdsfjorden and Zachariæ Isstrøm. While the majority of glaciers have shown retreat, the response is clearly non-uniform. Several of the study glaciers showed large variability in their terminus positions and sometimes advance (Storstrømmen, Kofoed-Hansen Bræ and L. Bistrup Bræ) [Box & Decker, 2011]. Others showed a velocity increase of a factor of ten (e.g. Harald Moltke Bræ and Hagen Bræ). Some of this behavior (e.g. periods of order of magnitude increased velocities accompanied by glacier advance) may be attributed to internal surging dynamics (Section 2.4.4). Thus, whilst it is likely that increased air temperatures in northern Greenland have influenced glacier retreat over the last two decades, there has not been a coherent response.

In northern Greenland, greater surface meltwater production due to increased air temperatures has been linked to inter-annual retreat at Humboldt Glacier [Carr *et al.*, 2015]. Here, hydrofracture of crevasses a few kilometers inland of the glacier terminus may have caused weakening and promoted calving once the ice reached the terminus [Carr *et al.*, 2015]. At several glaciers, the presence of supraglacial lakes has also been noted (Humboldt, Ryder, Nioghalvfjærdsfjorden) [Joughin *et al.*, 1996b; Thomsen *et al.*, 1997; Carr *et al.*, 2015], and they are likely to be present on other outlet glaciers across northern Greenland. These lakes may enhance rates of calving through hydrofracture [e.g., Sohn *et al.*, 1998; van der Veen, 1998; Carr *et al.*, 2015], and the role of supraglacial lakes in northern Greenland, particularly across the NEGIS, could become increasingly important in the future [Ignéczi *et al.*, 2016].

In other areas of the ice sheet it was initially thought that increased meltwater inputs led to seasonal-scale velocity increases [Zwally *et al.*, 2002; Pimentel & Flowers, 2010]. However, more recent work has linked increased meltwater production to a net annual slowdown in velocity, due to the drainage systems capacity to adjust and more efficiently drain adjacent high pressure areas via larger subglacial channels [Sole *et al.*, 2013; Tedstone *et al.*, 2015]. Numerical modelling results suggest that the influence of meltwater inputs on seasonal velocity variations at Peterman Glacier is substantial [Nick *et al.*, 2012], but little is known about this effect elsewhere in northern Greenland. To date, the potential impact of supraglacial lakes on northern Greenland outlet glaciers and their floating ice tongues has not been assessed. Based on observations from Antarctic ice shelves [Banwell *et al.*, 2013], supraglacial lake drainages may play a role in calving events from large floating ice tongues by fracturing and weakening the ice. Further work to measure the occurrence, volume, and timing of supraglacial lake drainages is required due to the abundance of floating ice tongues in northern Greenland.

2.4.1.2 Submarine melt

Alongside the role of surface meltwater induced changes discussed above, rates of submarine melt, primarily along the base of floating ice tongues, is likely to be an important control on glacier dynamics in northern Greenland. Submarine melt is likely to depend on both ocean temperature trends and topographic controls, whereby fjord configuration and depth control the access of sub-surface waters to glacier fronts. Submarine melt may be further enhanced by submarine meltwater plumes discharged at the grounding line [Motyka *et al.*, 2003; Jenkins, 2011], where the more buoyant freshwater discharge promotes the circulation of deep warm water towards the grounding line [Motyka *et al.*, 2003, 2011]. Subglacial discharge is considered another primary control on submarine melt rates [Jenkins, 2011; Xu *et al.*, 2012; Motyka *et al.*, 2013; Sciascia *et al.*, 2013], which could be strongly influenced by the amount of meltwater produced at the glacier surface and thus ultimately forced by atmospheric temperature changes.

Across the study region, ocean temperatures have been identified as a key control on outlet glacier behavior and ice tongue disintegration. In contrast to other areas of the GrIS, ice loss is thought to be dominated by submarine melting on large floating ice tongues [Reeh *et al.*, 1999; Rignot *et al.*, 2001]. At Nioghalvfjærdsfjorden and Zachariæ Isstrøm, recent retreat rates may be due to high rates of submarine melt (approx. 6-8 m a⁻¹) [Rignot *et al.*, 1997]. Similarly, at Petermann and Tracy Glaciers, the intrusion of warm ocean water beneath floating ice tongues could have contributed to high rates of submarine melting, reaching up to 25 m a⁻¹ beneath Petermann Glacier [Rignot & Steffen, 2008], and subsequent ice tongue disintegration [Johnson *et al.*, 2011; Johannessen *et al.*, 2013; Porter *et al.*, 2014]. At Petermann Glacier, it was hypothesized that warmer ocean waters may have been a precursor to the large calving event in 2010 [Johannessen *et al.*, 2013], where basal channels beneath the floating ice tongue underwent the greatest thinning [Münchow *et al.*, 2014]. Thus, Petermann Glacier's floating ice tongue is considered vulnerable to the temperature of relatively warm subsurface water entering the fjord [Johnson *et al.*, 2011]. We thus suggest the interaction between floating ice tongues and the ocean could have important implications for submarine-melt induced ice tongue collapse elsewhere in northern Greenland. However, limited in-situ measurements of submarine melt rates, ocean temperatures [Thomsen *et al.*, 1997], fjord circulation, and meltwater plumes means the extent of this process across northern Greenland remains unknown.

Forecasts suggest that ocean temperatures and submarine melt rates are likely to increase with future climate warming [e.g., Collins *et al.*, 2013]. As submarine melt rates of between 6-25 m a⁻¹ dominate mass loss at several northern Greenland outlet glaciers

(e.g. Petermann, Nioghalvfjærdsfjorden, and Zachariæ Isstrøm) [Rignot *et al.*, 2001], and have the potential to greatly influence glacier stability, there is need for improved fjord temperature data to better estimate submarine melt rates and the role of subglacial melt-water plumes [Nick *et al.*, 2012]. Systematic measurements of surface mass balance versus submarine melting and calving are also required to better understand the importance of these processes of mass loss for many glaciers in northern Greenland. Northern Greenland glaciers are likely to be particularly vulnerable to ocean warming, due to the presence of extensive floating ice tongues, with large surface areas susceptible to submarine-melt induced collapse.

2.4.2 Sea ice influence

Sea ice has previously been identified as an important control on glacier stability and calving rates, both in Greenland [Joughin *et al.*, 2008b; Amundson *et al.*, 2010] and elsewhere [e.g., Miles *et al.*, 2016]. Northern Greenland glaciers may be particularly susceptible to this control, as they have long floating ice tongues, which are likely to be more sensitive to changes in buttressing provided by sea ice than grounded glaciers [Reeh *et al.*, 2001]. Indeed, this was first hypothesized in northern Greenland by Higgins [1989], who suggested that icebergs discharged from outlet glaciers in this region are held in place by semi-permanent sea ice for extended periods of time. Northern Greenland is characterized by multi-year sea ice, which undergoes periodic disintegration events. These are thought to allow the release of icebergs and to reduce back stress, thus promoting calving events and glacier retreat [Higgins, 1990; Reeh *et al.*, 2001]. Subsequent studies at Humboldt [Carr *et al.*, 2015] and Petermann [Johannessen *et al.*, 2013] have partly supported this theory, although the relationship appears to be more complex. At Petermann, the impact of sea ice buttressing appears to be less important than surface melt on seasonal velocity increases [Nick *et al.*, 2012], whilst at Humboldt, icebergs were able to move away from the terminus, despite the formation of winter sea ice [Carr *et al.*, 2015].

The outlets of the NEGIS are thought to be particularly susceptible to the effects of sea ice buttressing [Khan *et al.*, 2014]. At Nioghalvfjærdsfjorden, evidence suggests that sea ice holds icebergs in place at the calving front [Helk & Dunbar, 2014; Reeh *et al.*, 2001], and that sea ice disintegration led to a large calving event in August 1997 [Reeh *et al.*, 2001]. 10 km of frontal retreat occurred at Zachariæ Isstrøm during 2002-2003, which led to the complete loss of its floating ice tongue [Mouginot *et al.*, 2015]. Khan *et al.* [2014] linked this to reduced sea ice concentration, due to high atmospheric temperatures, however, others have suggested it was primarily due to warmer subsurface temperatures

[Mouginot *et al.*, 2015]. With Arctic sea ice predicted to decrease in the near-future [e.g., Collins *et al.*, 2013], there is clear potential for reduced sea ice buttressing on glacier termini to allow for faster, enhanced ice discharge from the northern regions of the ice sheet. However, uncertainty remains as to the importance of sea ice buttressing on all outlet glaciers in northern Greenland. There is therefore a need for more detailed study of the impact of these processes on glacier retreat and inland ice velocities.

2.4.3 Glacier-specific factors

Across the GrIS, glacier-specific factors (basal topography and fjord geometry) have been identified as the cause of differing glacier responses to external climatic forcing [Howat & Eddy, 2011; Enderlin *et al.*, 2013], and research suggests that this is also the case in northern Greenland [e.g., Carr *et al.*, 2015; Porter *et al.*, 2014]. This section presents evidence for the effect of glacier geometry, the presence of floating ice tongues, and basal topography, on outlet glacier dynamics in northern Greenland.

2.4.3.1 Fjord width

Fjord width has been shown to have a strong influence on glacier dynamics [e.g., Jamieson *et al.*, 2012; Enderlin *et al.*, 2013; Carr *et al.*, 2015]. Fjord width variations can influence the stability of marine-terminating outlet glacier front positions by either promoting equilibrium or advance in a narrowing fjord, or rapid retreat in a widening fjord [e.g., Benn *et al.*, 2007; Carr *et al.*, 2014]. At Petermann Glacier, the narrow fjord is thought to hinder the movement of icebergs away from the glacier front, which may facilitate ice mélange formation, which, also referred to as sikussak, is defined as a mixture of calved icebergs and sea ice. This mélange may ‘choke’ the fjord with icebergs, which could exert resistive back-stress on the glacier tongue [Johnson *et al.*, 2011]. This ice mélange has been identified as a key control on iceberg calving rates elsewhere in Greenland [Amundson *et al.*, 2010; Cassotto *et al.*, 2015]. Narrow fjords may also result in more ice contact with the fjord walls and, consequently, greater lateral drag exerted on the glacier sides [Raymond, 1996]. These processes may apply to other glaciers in the region, several of which also terminate in narrow fjords (e.g. Ryder, Steensby, and Hagen Bræ), and there is large variability in fjord geometries across northern Greenland, ranging from the wide Humboldt Glacier to the narrow sinuous fjord at Steensby Glacier. Thus, contrasting fjord widths between glaciers in northern Greenland could contribute to their varying response to external drivers.

2.4.3.2 Floating ice tongues

Changes in the floating ice tongues in front of several outlet glaciers in northern Greenland are another glacier-specific factor which could have influenced past glacier dynamics in northern Greenland. Table 2.1 highlights glaciers in the region which still have floating ice tongues and those where they have been lost. Changes in buttressing forces provided by floating ice tongues can influence glacier velocities [Howat *et al.*, 2007; Nick *et al.*, 2009, 2012]. Floating ice shelf collapse led to increased glacier velocities at the Larsen B ice shelf in Antarctica [Scambos *et al.*, 2004] and there is potential for this process to occur at floating ice tongue terminating outlet glaciers in northern Greenland. However, little increase in velocities at Petermann Glacier [Nick *et al.*, 2012; Johannessen *et al.*, 2013] and C. H. Ostenfeld Glacier [Joughin *et al.*, 2010b] were found following ice tongue collapse, suggesting this may not be the case. This is of key consideration in the future, as further ice tongue retreat at northern Greenland outlet glaciers could substantially increase ice velocities, although modulated by ice shelf and fjord specific characteristics.

2.4.3.3 Basal topography

In contrast to most of the rest of the ice sheet [Bamber *et al.*, 2013; Morlighem *et al.*, 2014], a large proportion of northern Greenland rests below sea level and is characterized by deep fjords beneath outlet glaciers (Figure 2.2b). The regions with the greatest areas below sea level are at Nioghalvfjærdsfjorden and Zachariæ Isstrøm, Humboldt, and Petermann Glaciers (Figure 2.2b). At Nioghalvfjærdsfjorden and Zachariæ Isstrøm, the basal trough extends ~ 130 km to the interior of the ice sheet and reaches up to 550 m below sea level (Figure 2.2b). Evidence from Humboldt Glacier also shows that basal topography can have a major impact on glacier retreat and ice velocities [Carr *et al.*, 2015]. Here, retreat and ice velocities are an order of magnitude greater in the northern sector, which is underlain by a deep basal trough (up to 475 m deep) and an inland-sloping bed. The southern section, is comparatively shallow (~ 220 m deep) and slopes upwards inland [Rignot *et al.*, 2001; Carr *et al.*, 2015]. Petermann Glacier also has a deep channel that extends to the interior of the ice sheet [Bamber *et al.*, 2013; Morlighem *et al.*, 2014] which could have a substantial impact on ice dynamics.

At some of the smaller glaciers in northern Greenland, basal topography has also been identified as a potentially important control on dynamics. In particular, contrasting basal topography may have been responsible for the differing rates of retreat at Heilprin and Tracy Glaciers, where a deeper bed beneath Tracy Glacier allows a greater ice area to

be subject to warmer ocean waters and associated increased submarine melt rates [Porter *et al.*, 2014]. Similarly, at Hagen Bræ and Academy Glaciers, deep basal troughs could be susceptible to ocean warming and linked to glacier instability [Morlighem *et al.*, 2014]. However, an alternative explanation for increased flow velocities at Hagen Bræ, may be the loss of resistance as the glacier retreated from being in contact with an island pinning point [Joughin *et al.*, 2010b]. Basal topography is also important at Ryder Glacier, through its impact on water storage and short-term velocity variations [Joughin *et al.*, 1996b; Abdalati *et al.*, 2001]. Thus, basal topography is likely to be an important control on observed glacier retreat and could have important implications for future instability in northern Greenland.

Of further consideration is the nature of the bed, which can have a key influence on ice-sheet dynamics. In particular, beneath the NEGIS, a weak, deforming bed has been suggested responsible for its streaming flow [Joughin *et al.*, 2001; Layberry & Bamber, 2001], similar to that observed at ice streams in Antarctica [e.g., Bindshadler *et al.*, 2001]. More recent work supports this hypothesis that water-saturated till contributes to the flow speed on the NEGIS [Christianson *et al.*, 2014]. However, this, alongside the effect of subglacial geology, remain under-studied in Greenland in contrast to Antarctica [Walter *et al.*, 2014], and deserves further research.

Differences in bed topography, fjord geometry, and the presence of floating ice tongues at outlet glaciers across northern Greenland are likely to partly explain the varying responses in glacier dynamics observed. However, little examination of glacier specific factors on outlet glacier retreat have been conducted in northern Greenland and we therefore identify this as a key area for future research.

2.4.4 Glacier surging

Some changes in northern Greenland glacier dynamics may not be driven by climatic forcing, and instead relate to surge behavior. Whilst the majority of northern Greenland glaciers have retreated over the last two decades, a number have undergone periods of advance (Figure 2.7).

Several glaciers within the study region have been previously identified as surge-type and, based on the evidence presented in this review, we have classified the study glaciers according to their potential surge likelihood (Figure 2.1). i) Glaciers where surge-type cycles have been observed are defined as ‘Likely’; ii) Glaciers which have shown surge characteristics but either have not been referred to as surge-type or have not undergone

a large surge event (e.g. Ryder) are defined as ‘Possibly’, and iii) glaciers at which no evidence has been recorded in the literature about surging are classed as ‘No Evidence’.

Eight of the twenty-one glaciers reviewed have been referred to as surge-type within the literature (Table 2.1: Figure 2.1), although the evidence for surging varies from glacier to glacier. Harald Moltke Bræ, Brikkerne, Storstrømmen and L. Bistrup Bræ have all undergone periods of advance, alongside an order of magnitude increase in glacier velocity [Mock, 1966; Higgins, 1990; Reeh *et al.*, 1994; Seale *et al.*, 2011], and we therefore consider it likely these are true surge-type glaciers, which fit the above definition (Figure 2.1). A potential surge event in northern Greenland that received notable research attention was a ‘mini-surge’ at Ryder Glacier in 1995, during which velocity increased at least three-fold over a seven-week period [Joughin *et al.*, 1996b]. However, as no further or larger surge events have been recorded, we deem it ‘Possibly’ surge-type. We assign the same classification to Hagen Bræ (Figure 2.1). Here, past acceleration has been attributed to surge behavior, but it is unclear whether surging persists today and recent velocity increases may instead be attributed to reduced resistive stresses at the terminus, due to retreat from basal pinning points [Joughin *et al.*, 2010b]. The neighboring Academy Glacier also experienced an order of magnitude increase in ice velocity between 2000 and 2006 [Joughin *et al.*, 2010b], which is suggestive of surge behavior [Rignot & Kanagaratnam, 2006]. However, the glacier continued to retreat during this period, albeit at a reduced rate [Murray *et al.*, 2015].

As previously stated, glacier surges may either be thermally or hydrologically controlled [Murray *et al.*, 2003]. At Ryder Glacier, it is likely the mini-surge was hydrologically induced due to its underlying topography. Two transverse subglacial ridges beneath the glacier were suggested to have allowed water ponding upstream and, once it reached a critical pressure threshold, could have initiated the surge [Joughin *et al.*, 1996b, 1999; Rignot *et al.*, 2001]. However, the drainage of supraglacial lakes and water-filled crevasses may also have been at least partly responsible for the surge event [Joughin *et al.*, 1996b]. Given recent advances in our understanding of GrIS dynamics [Das *et al.*, 2008; Sole *et al.*, 2013; Bougamont *et al.*, 2014], we hypothesize that it is unlikely the ‘mini-surge’ event at Ryder Glacier [Joughin *et al.*, 1996b] satisfies a strict definition [Meier & Post, 1969; Sharp, 1988] of surging. Instead it may reflect a seasonal speed up event, similar to which has been seen on the west coast of Greenland [Palmer *et al.*, 2011; Doyle *et al.*, 2015]. Such acceleration events appear to be followed by an extra slowdown [Meier *et al.*, 1994], which offsets the annual average [Sole *et al.*, 2013]. However, more recent work recorded substantial glacial advance during several years between 2000 and 2010 [Box & Decker, 2011; Murray *et al.*, 2015], which may suggest surging is continuing at Ryder Glacier.

Thus it remains unclear whether these advances were internally or externally controlled and whether Ryder Glacier is of true surge-type requires further study.

Generally, surge-type glaciers have not been systematically identified across Greenland, apart from in eastern Greenland [Jiskoot *et al.*, 2003; Pritchard *et al.*, 2005]. As such, large uncertainties remain as to the nature of surge-type glaciers in northern Greenland, and the possible surge mechanisms have been little-studied. Thus, with several glaciers in northern Greenland having been referred to as ‘surge type’ there is an important need for further research to provide a comprehensive account of surge behavior in northern Greenland and to separate this behavior from changes driven by external forcing.

2.5 Future changes

An important consideration in northern Greenland is the region’s sensitivity to future climate change. During the period 2081-2100, average Arctic air temperatures are expected to be 4.2°C warmer than present under Representative Concentration Pathway (RCP) 4.5 and 8.3°C warmer under RCP8.5 [Collins *et al.*, 2013].

As northern Greenland experiences the lowest accumulation rates across the ice sheet [Goelzer *et al.*, 2013] and warming in these high latitudes is expected to be greatest [Gregory & Huybrechts, 2006], it is likely the northern regions of the ice sheet could be more sensitive to future climate change. However, this will also be dependent on how much additional precipitation may be delivered by a warmer atmosphere. Of particular concern to northern Greenland is that simulations of surface melt show the largest amplification in northern Greenland [Fettweis *et al.*, 2013], due to reduced sea ice cover as a result of increased air temperatures [Mernild *et al.*, 2009; Franco *et al.*, 2011]. Recent work has also shown an exceptional atmospheric ridge led to greater runoff, low albedo, and higher surface temperatures in the northern regions of the GrIS during 2015 [Tedesco *et al.*, 2016]. Goelzer *et al.* [2013] also showed large negative surface mass balance anomalies to occur around the north coast of Greenland between 2091 and 2100 obtained from a positive degree day model relative to 1989-2008 reference period. Recent studies in northern Greenland have also suggested that increased temperatures and subsequent enhanced surface melt have the potential to weaken floating ice tongues [Johannessen *et al.*, 2013]. While several of the glaciers in northern Greenland have shown acceleration and retreat (Figure 2.7), this is not ubiquitous and ambiguity exists as to the velocity response of northern Greenland outlet glaciers to ice tongue loss in the future.

At Petermann Glacier, future projections driven by atmospheric warming (A1B scenario) show the glacier to primarily lose mass by surface melt between 2000 and 2100, which is in contrast to Helheim and Kangerdlugssuaq glaciers, which instead lose mass via dynamic mechanisms [Nick *et al.*, 2013]. Further projections between 2100 and 2200, however, showed dynamic mass losses through increased rates of submarine melt to become far greater at Petermann [Nick *et al.*, 2013]. Few other studies have considered outlet glacier response to future climate change at specific outlets in northern Greenland. Thus, substantial uncertainty remains as to the regions sensitivity to future atmospheric and oceanic temperature changes. We therefore suggest further consideration of terminus changes, particularly the loss of floating ice tongues across the entirety of northern Greenland, their effect on ice dynamics, and their relationship to atmospheric/oceanic temperatures, is necessary to better understand and predict future changes under a warmer climate.

2.6 Conclusions

Northern Greenland is an important region of the GrIS because it consists of large fast-flowing marine-terminating outlet glaciers, draining a significant area of the ice sheet (collectively, around 40% of the ice sheet area is drained by 21 glaciers), of which a large proportion sits below sea level. This paper reviewed previously published work focusing on 21 major outlet glaciers in northern Greenland to provide a synthesis of changes in their dynamics between the late 19th century and 2015, and potential links to changes in the ocean-climate system. A clear conclusion from this analysis is that all glaciers have retreated over the last century and that this retreat has accelerated in the last two decades. Indeed, several glaciers have shown kilometer-scale retreat (> 10 km) over the last two decades, in particular at Petermann, Hagen Bræ, Tracy, Zachariæ Isstrøm and C. H. Ostenfeld Glaciers. The flow velocity of a number of outlets has also accelerated during this period (e.g. Academy and Hagen Bræ). Despite an overall pattern of retreat, however, we also note variability in glacier response, which likely results from differing sensitivity to various forcings (e.g. air versus ocean temperatures) and/or local factors, such as fjord geometry or the presence of floating ice tongues. Indeed, the impact of ice tongue retreat on glacier velocity remains uncertain because some glaciers experienced enhanced velocities (e.g. Hagen Bræ), but others showed only a limited response (Petermann and C. H. Ostenfeld). In addition, dynamic ice discharge in northern Greenland remained relatively constant throughout the 20th century Kjeldsen *et al.* [2015], which suggests that some outlets may have been insensitive to recent retreat. However, the precise links between retreat and dynamic thinning remain poorly understood in the region. There is also some

confusion surrounding the possibility of surge-type glaciers in northern Greenland, which add further complexity when attempting to elucidate the precise drivers of glacier change.

Given the above, large uncertainty surrounding glacier responses to external factors in northern Greenland remain. While several studies have focused on the major calving event at Petermann Glacier in 2010, it remains unclear whether this was exceptional or part of a long-term cyclical trend. Studies of a similar nature, comprising detailed measurements of frontal retreat and ice velocity are needed for surrounding outlet glaciers in northern Greenland to improve our understanding of the factors that are forcing recent outlet glacier retreat in the region. Future work could usefully focus on improving high resolution data, in particular fjord bathymetry and ocean temperatures, alongside assessing the role of glacier specific factors (e.g. through numerical modelling), to better understand the links between climatic-oceanic forcing and local topographic factors. Further work is also required to systematically classify surge-type glaciers in the region, and help distinguish externally-driven retreat from internally-driven surge cycles that may not be related to changes in the ocean-climate system.

Chapter 3

Dynamic changes in outlet glaciers in northern Greenland from 1948 to 2015

3.1 Chapter summary

The Greenland Ice Sheet (GrIS) is losing mass in response to recent climatic and oceanic warming. Since the mid-1990s, tidewater outlet glaciers across the ice sheet have thinned, retreated, and accelerated, but recent changes in northern Greenland have been comparatively understudied. Consequently, the dynamic response (i.e. changes in surface elevation and velocity) of these outlet glaciers to changes at their termini, particularly calving from floating ice tongues, is poorly constrained. The primary motivation for this Chapter was to understand the regional signal of terminus change over long-time scales to assess the exceptional or cyclic nature of recent glacier change in northern Greenland. This Chapter therefore addresses the second objective of this thesis, and uses satellite imagery and historical maps to produce an unprecedented 68-year record of terminus change across 18 major outlet glaciers. These data were then combined with previously published surface elevation and velocity datasets to determine the dynamic glacier response to changes at the terminus. In addition, this chapter analysed the differences in behaviour depending on whether the glacier was grounded or floating at the terminus, and the geometric controls upon glacier sensitivity to terminus change. This Chapter was published as a journal paper in *The Cryosphere* in August 2018 (see reference below), in which I carried out all the analysis, produced all the figures, and wrote the manuscript. Co-authors helped to

develop the research ideas, and provided editorial input.

HILL, E. A., CARR, J. R., STOKES, C. R. & GUDMUNDSSON, G. H. 2018a Dynamic changes in outlet glaciers in northern Greenland from 1948 to 2015. *Cryosphere* **12** (10), 3243–3263

To summarise, recent (1995–2015) retreat rates were higher than at any time in the previous 47 years (since 1948). Despite increased retreat rates from the 1990s, there was distinct variability in dynamic glacier behaviour depending on whether the terminus was grounded or floating. Grounded glaciers accelerated and thinned in response to retreat over the last two decades, while most glaciers terminating in ice tongues appeared dynamically insensitive to recent ice tongue retreat and/or total collapse. We also identify glacier geometry (e.g. fjord width, basal topography, and ice tongue confinement) as an important influence on the dynamic adjustment of glaciers to changes at their termini. Recent grounded-outlet glacier retreat and ice tongue loss across northern Greenland suggests that the region is undergoing rapid change and could soon contribute substantially to sea level rise via the loss of grounded ice.

3.2 Introduction

Mass loss from the Greenland Ice Sheet (GrIS) has accelerated since the early 2000s, compared to the 1970s and 80s [Kjeldsen *et al.*, 2015; Rignot *et al.*, 2008], and could contribute 0.45–0.82 m of sea level rise by the end of the 21st century [Church *et al.*, 2013]. Recent mass loss has been attributed to both a negative surface mass balance and increased ice discharge from marine-terminating glaciers [van den Broeke *et al.*, 2016; Enderlin *et al.*, 2014]. The latter contributed $\sim 40\%$ of total mass loss across the GrIS since 1991 [van den Broeke *et al.*, 2016], and increased mass loss was synchronous with widespread glacier acceleration from 1996 to 2010 [Carr *et al.*, 2017b; Joughin *et al.*, 2010b; Moon *et al.*, 2012; Rignot & Kanagaratnam, 2006]. Coincident with glacier acceleration, dynamic thinning has occurred at elevations < 2000 m on fast flowing marine-terminating outlet glaciers [Abdalati *et al.*, 2001; Krabill *et al.*, 2000], particularly in the south-east and north-west of the GrIS [Csatho *et al.*, 2014; Pritchard *et al.*, 2009]. Alongside thinning and acceleration, terminus retreat has been widespread since the 1990s [e.g., Box & Decker, 2011; Carr *et al.*, 2017b; Jensen *et al.*, 2016; Moon & Joughin, 2008], and several studies have identified terminus retreat as a key control on inland ice flow acceleration and dynamic thinning [Howat *et al.*, 2005; Joughin *et al.*, 2004, 2010b; Nick *et al.*, 2009; Thomas, 2004; Vieli & Nick, 2011].

Ice sheet wide dynamic changes have been linked to 21st century atmospheric/ocean warming, and the loss of sea-ice [e.g., Bevan *et al.*, 2012; Cook *et al.*, 2014; Holland *et al.*, 2008; McFadden *et al.*, 2011; Moon & Joughin, 2008]. However, tidewater glaciers can also behave in a cyclic manner, which is not always directly related to climate forcing [Meier & Post, 1987; Pfeffer, 2007], but instead relates to their fjord geometry [Carr *et al.*, 2013b; Enderlin *et al.*, 2013; Howat *et al.*, 2007; Powell, 1990]. These glacier cycles are characterised by slow periods of advance (up to centuries) followed by rapid unstable retreat [Meier & Post, 1987; Post, 1975; Post *et al.*, 2011]. Once initiated, terminus retreat can initiate dynamic adjustments independent of climate and instead modulated by local outlet glacier geometry and associated resistive stresses. However, differences in the nature of calving and basal/lateral resistive stresses acting at tidewater glaciers with either grounded or floating termini can alter their dynamic response to retreat. Continuous small magnitude calving events and the loss of basal and lateral resistance at grounded-termini, can prolong the dynamic readjustment at the terminus. In contrast to continuous calving, large episodic calving events often occur at floating ice tongues, which can decrease buttressing forces on grounded ice, and also increase driving stress and accelerate ice flow [e.g., MacGregor *et al.*, 2012]. In the case of floating ice tongues, the response of inland ice to large calving events depends on the amount of lateral resistive stress provided by the tongue prior to calving: the loss of portions of ice tongues that are highly fractured and/or have limited contact with the fjord margins are unlikely to substantially influence inland ice dynamics.

Most previous work at tidewater glaciers in Greenland has concentrated on the central-west and south-east regions, and notably at Jakobshavn Isbræ, Helheim, and Kangerdlugssuaq Glaciers [e.g., Howat *et al.*, 2005, 2007; Joughin *et al.*, 2004; Nick *et al.*, 2009]. Observations at all three glaciers showed acceleration and surface thinning following terminus retreat. Dynamic changes at Jakobshavn, have been linked to the gradual collapse of its floating ice tongue [Amundson *et al.*, 2010; Joughin *et al.*, 2008b; Krabill *et al.*, 2004]. In northern Greenland, several glaciers have thinned [Rignot *et al.*, 1997], accelerated [Joughin *et al.*, 2010b], and retreated, losing large sections of their floating ice tongues between 1990 and 2010 [Box & Decker, 2011; Carr *et al.*, 2017b; Jensen *et al.*, 2016; Moon & Joughin, 2008; Murray *et al.*, 2015]. Floating ice tongue retreat does not directly contribute to sea level rise. However, with amplified warming and surface melt forecast in northern Greenland [Fettweis *et al.*, 2013; Franco *et al.*, 2011; Mernild *et al.*, 2009], floating ice tongues across the region could soon collapse entirely. As a consequence, northern Greenland could become a more substantial contributor to dynamic mass loss and sea level rise. However, fewer studies have focused specifically on northern Greenland, with the exception of more detailed work at Petermann and the NEGIS [e.g., Khan *et al.*,

2015; Nick *et al.*, 2012]. As such, few long-term records of frontal positions exist in the region, and their potential impact on inland ice flow remains unclear.

Here we present changes in frontal position, ice velocity and surface elevation over the last 68 years (1948 to 2015) in northern Greenland. We couple a multi-decadal annual terminus position record between 1948 and 2015 with recently published surface elevation and ice velocity datasets. We then use these datasets to evaluate dynamic responses (i.e. acceleration and thinning) to frontal position change and examine disparities in the context of glaciers with floating or grounded termini. Finally, we assess local topographic setting (i.e. fjord width and depth) as a control on glacier behaviour.

3.3 Methods

3.3.1 Study region

We define Northern Greenland as the region of the GrIS located north of 77°N (Figure 3.1). This region drains $\sim 40\%$ of the ice sheet by area [Hill *et al.*, 2017; Rignot & Kanagaratnam, 2006] and includes 18 major marine-terminating outlet glaciers, which emanate from 14 major catchments (Figure 3.1). Aside from at Petermann Glacier and the NEGIS, little work has focused on the other glaciers in northern Greenland, where the presence of floating ice tongues could alter the dynamic response of inland ice to calving events. Here, we use the ice-ocean mask from the Operation IceBridge BedMachine v3 product (nsidc.org/data/IDBMG4) to categorise glaciers in northern Greenland based on either grounded or floating termini [Howat *et al.*, 2014; Morlighem *et al.*, 2017]. We also use the grounding line in this dataset to assess the location of past ice tongues. Currently, five glaciers in northern Greenland terminate in floating ice tongues (Figure 3.1), which range between 0.5 and 70 km long [Hill *et al.*, 2017]. An additional four glaciers have lost their ice tongues entirely over the last two decades (1995 to 2015). The study region includes a further nine outlet glaciers, which are grounded at their termini. We note that Humboldt glacier is classified as grounded as the majority of the ~ 100 km long terminus is grounded, despite a small floating ice tongue in the northern section [Carr *et al.*, 2015].

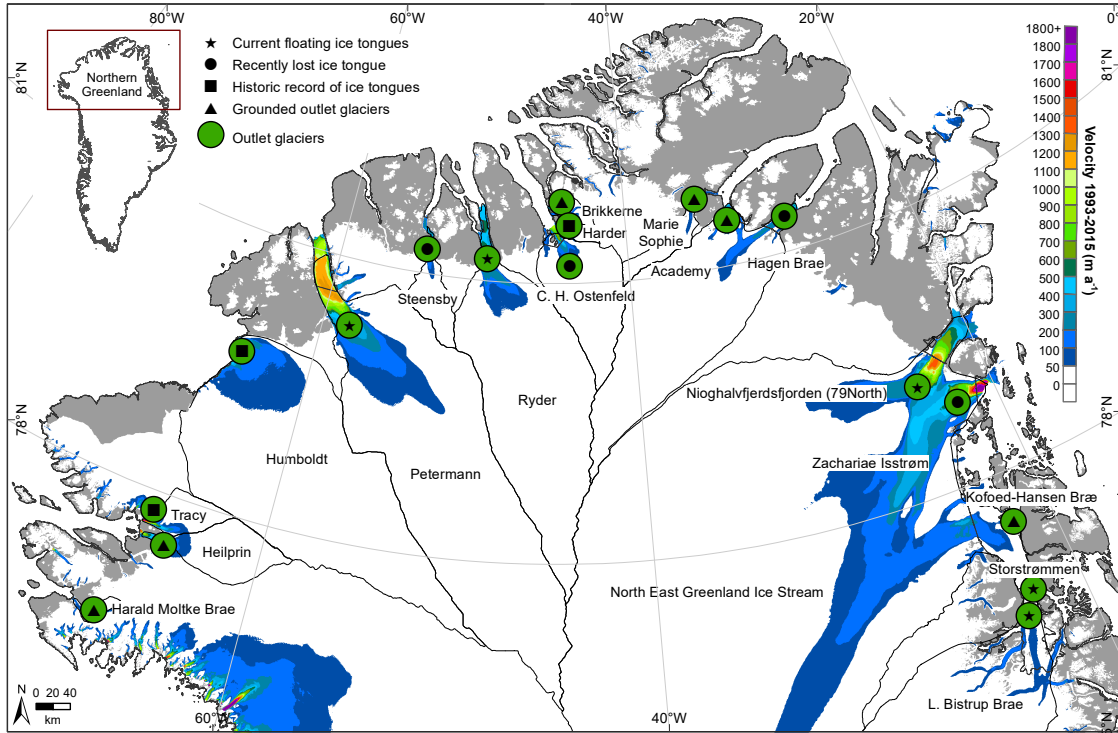


Figure 3.1: Study region of northern Greenland. Green circles show the location of each of 18 northern Greenland study outlet glaciers. Average glacier velocities (m a^{-1}) are shown between 1993 and 2015 derived from the multi-year mosaic dataset [Joughin *et al.*, 2010b]. Black outlines show glacier drainage catchments. Symbols represent the state of the glacier terminus. Stars show glaciers which currently have floating ice tongues, circles represent glaciers which lost their ice tongues (during 1995 to 2015), squares denote glaciers which have some previous literature record of a floating ice tongue, and triangles are glaciers which are grounded at their termini and have been throughout the study record.

3.3.2 Terminus change

3.3.2.1 Data sources

The terminus positions of 18 study glaciers in northern Greenland (Figure 3.1) were manually digitised from a combination of satellite imagery and historical topographic navigational charts between 1948 and 2015 (Table 3.1). From 1975 to 2015 we used Landsat 1-5 MSS (1975-1994), Landsat 7 TM (2000-2013) and Landsat 8 (2013-2015). These scenes were acquired from the United States Geological Survey (USGS) Earth Explorer website (earthexplorer.usgs.gov). To reduce the influence of seasonal changes in terminus position, one scene per year was selected from late summer, and 70% were within one month of the 31st August. Several Landsat MSS images required additional georeferencing and were georeferenced to 2015 Landsat 8 images, as these have the most accurate georeferenc-

ing. Early Landsat scenes (1970-1980s) were supplemented with SPOT-1 imagery from the European Space Agency (ESA) (intelligence-airbusds.com). These scenes covered 8 of 18 study glaciers in 1986/87, and were also selected from late August. SPOT-1 scenes were also georeferenced to 2015 Landsat Imagery. Additionally, we used aerial photographs (2 m resolution), which were provided orthorectified by Korsgaard *et al.* [2016]. These covered all study glaciers between Humboldt east to L. Bistrup Bræ in 1978, and Harald Moltke Bræ, Heilprin and Tracy Glaciers in NW Greenland in 1985 [Korsgaard *et al.*, 2016].

To extend the record of glacier terminus positions further back in time, declassified spy images from the Corona satellite were acquired from the USGS Earth Explorer website (Table 3.1), which covered 5 of 18 glaciers in 1962/63 and Petermann and Ryder Glaciers in 1966. These images were georeferenced to a Landsat 8 scene from 2015, with total RMSE errors of 105 to 360 m. Frontal position changes smaller than this error value were discounted from the assessment. To further assess the historical terminus positions of the glaciers we used navigational map charts from the United States Air Force 1:1,000,000 Operational Navigation Charts from 1968/69 (lib.utexas.edu/maps/onc/). These were made available through the Perry-Castañeda Library, courtesy of the University of Texas Libraries, Austin. Data from 1948 comes from AMS C501 Greenland 1: 250,000 Topographic Series maps distributed by the Polar Geospatial Centre (pgc.umn.edu/data/maps/). All maps were georeferenced to 2015 Landsat 8 imagery using a minimum of 10 ground control points (GCPs), which were tied to recognisable stationary features such as on nunataks and fjord walls. RMSE errors across all glaciers ranged between 150 and 510 m.

3.3.2.2 Front position mapping

Changes in glacier frontal positions were measured using the commonly adopted box method, which accounts for uneven calving front retreat [e.g., Carr *et al.*, 2013b; Howat & Eddy, 2011; Moon & Joughin, 2008]. For each glacier, a rectilinear box was drawn parallel to the direction of glacier flow (Figure 3.2), and extending further inland than the minimum frontal position. Due to Steensby Glacier’s sinuous fjord, a curvilinear box was used [see Lea *et al.*, 2014]. Glacier frontal positions were digitised in sequential images and the difference between successive terminus polygons give area changes over time within the box. Dividing these areas by the width of the reference box derives width-averaged relative glacier front positions.

| Year | Data | Resolution | Source |
|---------------------------------|--|-------------|--|
| Front Position | | | |
| 1948 | AMS C501 Greenland Topographic Series | 1: 250,000 | Polar Geospatial Center |
| 1962-63 | Corona Declassified Spy Satellite | - | USGS Earth Explorer |
| 1968/69 | USAF Operational Navigation Charts | 1:1,000,000 | Perry-Castañeda Library, University of Texas |
| 1975-94 | Landsat 1-5 MSS | 30 m | USGS Earth Explorer |
| 1978 | Aerial Photographs | 2 m | Danish History Museum [Korsgaard <i>et al.</i> , 2016] |
| 1986-87 | SPOT-1 Satellite Imagery | 10 m | European Space Agency |
| 1992-1999 | ERS-1/2 SAR Imagery | - | European Space Agency |
| 2000-2012 | Landsat 7 ETM Panchromatic band (band 8) | 15 m | USGS Earth Explorer |
| 2013-2015 | Landsat 8 Panchromatic band (band 8) | 15 m | USGS Earth Explorer |
| Ice Velocity | | | |
| 1991/92 | ERS 1 winter velocity | 500 m | GrIS CCI project |
| 1995/96 | ERS 2 winter velocity | 500 m | GrIS CCI project |
| 2000/01 | MEaSURES Greenland Annual Ice Velocity from InSAR (Version 2) | 500 m | National Snow and Ice Data Center |
| 2004/05-2009/10 | MEaSURES Greenland Ice Velocity: Selected Glacier Site Velocity Maps from InSAR (TerraSAR-X) | 100 m | National Snow and Ice Data Center |
| 2011-2013 | MEaSURES Greenland Ice Velocity: Selected Glacier Site Velocity Maps from InSAR (TerraSAR-X) | 100 m | National Snow and Ice Data Center |
| 2014-2016 | Sentinel-1 SAR velocity | 500 m | GrIS CCI project |
| Surface Elevation Change | | | |
| 1996-2011 | ERS1, ERS2 and ENVISAT 5-yr means | 5 km | GrIS CCI project |
| 2011-2015 | Cryosat 2 Surface Elevation Change v2 2-yr means | 5 km | GrIS CCI project |
| Topography | | | |
| 1993-2014 (nominal 2007) | Ice surface elevation Ice thickness Bedrock elevation Surface Digital Elevation Model | 150 m | National Snow and Ice Data Center IceBridge Bed Machine |
| 1978 | | 25 m | National Oceanic and Atmosphere Administration |

Table 3.1: List of data sources used in this study. Data is split by usage and shown for each year

Aside from georeferencing errors outlined in the previous section, the main source of error was attributed to manual digitisation [e.g., Carr *et al.*, 2013b; Howat & Eddy, 2011; Moon & Joughin, 2008]. We quantified this by repeatedly digitising a ~ 3 km section of rock coastline 20 times for each image type or map source. The resultant total mean errors were: 3.6 m for Landsat 8, 19 m for Landsat 7 ETM, 17 m for Landsat MSS, 20 m for SPOT-1, 16 m for Orthophotographs, 21 m for Corona, and 27 m for historical maps. Overall, the mean total error associated with manual digitising was 19 m, which is below the pixel resolution of all imagery sources except the 15-m panchromatic Landsat band. The presence of sea ice and highly fractured glacier termini made terminus picking at Steensby, C. H. Ostenfeld and glaciers draining the NEGIS more difficult [Bevan *et al.*, 2012; Howat & Eddy, 2011; Murray *et al.*, 2015]. Re-digitising all 1999-2015 Landsat terminus positions yielded additional errors of $\pm 13\%$ for these glaciers. At these glaciers, similar inaccuracies in identifying the true glacier terminus may have occurred by the authors of the earliest map charts (1948 and 1969), and we therefore consider these to be a broad estimate of the past location of glacier termini rather than exact frontal positions.

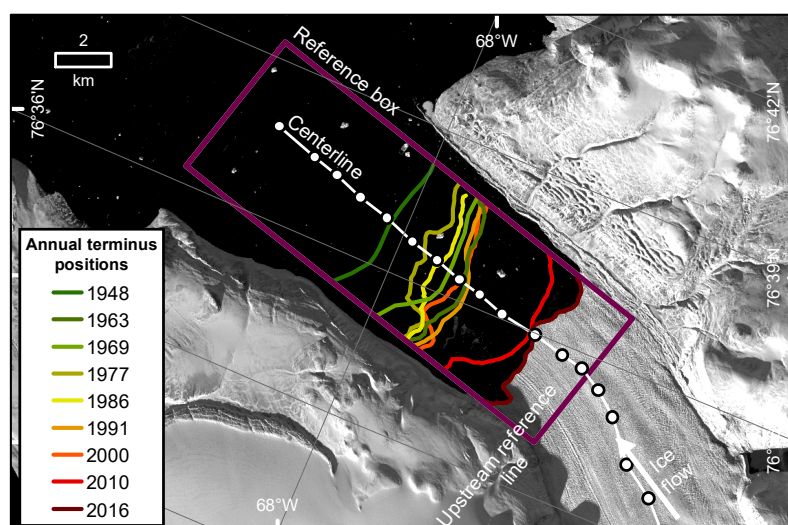


Figure 3.2: Rectilinear box method used to measure glacier terminus positions. An example at Harald Moltke Bræ, NW Greenland. This includes: reference box (pink), and roughly decadal terminus positions (green to red). The glacier centreline profile is shown in white and the location of 500 m sample points (white circles). Background image is Landsat 8 band 8 from the USGS Earth Explorer.

3.3.2.3 Changepoint analysis

‘Changepoint’ analysis can be used to objectively identify significant breaks in time series data at which a statistical property of the data changes suddenly [Bunce *et al.*, 2018; Carr *et al.*, 2017a]. Here we used changepoint analysis to detect statistically significant breaks in the time-series (1948 to 2015) of terminus position change for each of the 18 study glaciers in northern Greenland. We then compare the timing and duration of these breaks to determine if distinct patterns of terminus change behaviour exist based on terminus type (grounded or floating). To do this we use the ‘findchangepts’ function in MATLAB software which employs the methodology of Killick *et al.* [2012] and Lavielle [2005]. This tool allows for automatic detection of when a change point occurs, without giving the algorithm any prior knowledge about when we are expecting a change to occur. It does so by splitting the time series into two at a point and then estimating the statistical property e.g. mean either side of that point. Then at each data point either side of this, the algorithm determines how much the value deviates from the statistic of choice and calculates the residual error. This process is repeated until the minimum total residual error is found, at which point a significant change is identified. Firstly, changepoint analysis requires continuous data, so we filled missing data points using the nearest neighbour method. Similar to Carr *et al.* [2017a] we then chose to determine change points using linear regression. This approach detects significant breaks in the continuous frontal position time where there was a significant change in the mean and regression coefficients (slope and intercept) of the linear regression equation on either side of a data point. In addition, to allow for the fully automatic estimation of the number of changepoints, we included a minimum threshold penalty value, which we set as the mean terminus position for each glacier. This penalty only allows a changepoint to occur when the time-series deviates significantly from the threshold value. Using these automatically-identified changepoints we can determine if statistically different changes in the rate of terminus position change exists for study glaciers in northern Greenland according to their terminus type.

Changepoint analysis lets us identify significant breaks in the frontal position time series for each glacier. Using these breaks and the frontal position data we qualitatively identify distinct patterns of behaviour (see Figure 3.3) that align with the different terminus types. Category 1 displays periods of minimal frontal retreat, or in some cases minimal advance, followed by a period of steady and continuous glacier retreat (average = -150 m a^{-1}). The second category shows that the majority of glacier experienced minimal frontal position change, followed by a switch to a period of short-lived high magnitude rapid retreat (average = -5500 m a^{-1}). To ensure that these categories of terminus behaviour were distinct, we use a two-paired t-test between glacier retreat rates during these

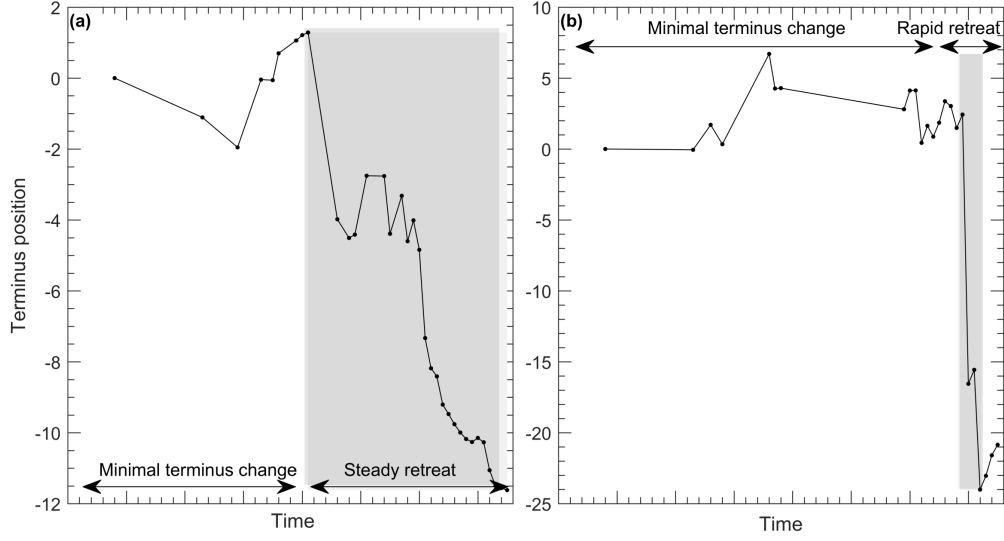


Figure 3.3: Schematic diagram of terminus position behaviour in northern Greenland. Two categories of behaviour determined from changepoint detection, which align to the differences in terminus type. The first (a) is an example of a glacier front position switching from minimal terminus change to a period of steady terminus retreat (grey), the second (b) shows a glacier which undergoes a period of rapid retreat (grey) after minimal terminus change.

respective periods of steady or rapid retreat (categories 1 and 2 respectively). Retreat rates between these categories are significantly different to a 99% confidence level (p -value 0.009), supporting the distinct nature of these models of terminus behaviour.

3.3.3 Ice velocity and surface elevation

Previously published datasets of annual ice velocity and surface elevation change were compiled to assess dynamic glacier changes in northern Greenland. Velocity and surface elevation change datasets are generally only available from 1990 onwards. The earliest velocity maps from winters 1991/92 and 1995/96 were acquired from the European Remote Sensing (ERS) satellites (1 and 2), as part of the ESA GrIS CCI (Climate Change Initiative) project [Nagler *et al.*, 2016]. The earlier (1991/92) covers northern Greenland drainage basins from Humboldt and then east to Hagen Bræ, and the later (1995/96) covers all 18 study glaciers. Using dataset error maps we estimated average errors in velocity magnitude across all northern Greenland drainage basins, which were 2.5 m a^{-1} for 1991/92 and 10 m a^{-1} for 1995/96.

Subsequent velocity datasets were primarily acquired from the NASA MEaSUREs program [Joughin *et al.*, 2010b]. These velocity maps were derived from 500 m resolution

Interferometric Synthetic Aperture Radar (InSAR) pairs from the RADARSAT satellite in winter 2000/01, and then annually from winter 2005/06 to 2009/10 [Joughin *et al.*, 2010b]. Using the dataset error values [Joughin *et al.*, 2010b], we estimate mean velocity errors across all years and study drainage catchments to be 6.3 m a^{-1} . For 7 study glaciers, additional annual velocity data, derived from ERS1, ERS2 and Envisat satellites, were available annually between 1991/92 to 1997/98 and between 2003/04 to 2009/10 from the ESA Greenland CCI project [Nagler *et al.*, 2016]. Winter velocities from these data were calculated from October to April.

For the winters of 2010/11, 2011/12 and 2012/13, glacier velocity maps were also acquired from InSAR (TerraSAR-X image pairs) for 11 of 18 study glaciers [Joughin *et al.*, 2010b]. Despite higher spatial resolution (100 m), these maps are limited to the grounding line and extend 27-56 km inland. Mean error for these data is 23 m a^{-1} across all years [Joughin *et al.*, 2010b]. Winter velocities for 2013/14 were derived from intensity tracking of RADARSAT-2 satellite data, and from offset tracking of Sentinel-1 radar data for 2014/15 and 2015/16, as part of the ESA CCI project [Nagler *et al.*, 2016]. The published mean error of these data from a central section of northern Greenland is 7.3 m a^{-1} [Nagler *et al.*, 2015]. Using the earliest full regional velocity map (1995/96) and the most recent record (2015/16), the rate of annual velocity change was calculated over this 20-year period.

We use surface elevation change data from ERS-1, ERS-2, Envisat, and Cryosat-2 radar altimetry for 1992 to 2015, which were made available by the ESA's GrIS CCI project [Khvorostovsky, 2012; Simonsen & Sørensen, 2017; Sørensen *et al.*, 2015]. Data from 1992 to 2011 were acquired from the ERS-1, ERS-2 and Envisat satellites, using a combination of cross-over and repeat track analysis, which have then been merged to create a continuous dataset across satellites [Khvorostovsky, 2012]. These data are provided in 5-year running means from 1992-1996 to 2007-2011 and at a resolution of 5 km. For the most recent elevation change (2011 to 2015), we used Cryosat-2 satellite elevation change which are provided in 2-year means [Simonsen & Sørensen, 2017]. These data were generated using the Least Mean Squares method, where grid cells were subtracted from the Greenland Ice Mapping Project (GIMP) DEM [Howat *et al.*, 2014] and corrected for backscatter and leading edge width [Simonsen & Sørensen, 2017]. Calculations were made at a 1 km grid resolution and resampled to 5 km to conform with 1992-2011 datasets [Simonsen & Sørensen, 2017]. Using error estimates [Simonsen & Sørensen, 2017], we calculated mean errors across all years and across all northern Greenland drainage basins to be $\pm 0.14 \text{ m a}^{-1}$. Elevation changes from 1992-1996 were compared to elevation changes for 2014-2015 to assess how changes in surface elevation have evolved during the study

period.

Velocity and surface elevation time series were extracted along each glacier centreline, which were drawn following Lea *et al.* [2014]. To draw these centrelines we first calculated euclidean distance between parallel fjord walls that were digitised in 2015 Landsat 8 imagery. The maximum distance line (i.e. centreline) was then traced from the furthest terminus extent back to the inland end of the glacier fjord. Annual average velocities were calculated within 5 km inland of the grounding line of each glacier, and elevation change rates were averaged across the entire centreline profile due to poorer/coarser data resolution (Figure 3.2).

3.3.4 Fjord width and basal topography

To assess the control of fjord geometry on outlet glacier behaviour we calculate fjord width and depth. Fjord width was measured perpendicular to glacier centrelines following Carr *et al.* [2014]. Points were extracted at 500 m intervals along each fjord wall and joined by lines that crossed the fjord. The length of these lines is the width between the fjord walls, and changes along each fjord were fitted with a linear regression model to determine if the fjord widens or narrows with distance inland. To determine the fjord bathymetry of each study glacier in northern Greenland, regional basal topography was taken from the Operation IceBridge BedMachine v3 dataset which is derived from ice thickness and mass conservation [Morlighem *et al.*, 2017]. Basal topography was sampled at 500 m points along glacier centrelines. Using the error map from BedMachine v3 (Figure A.2), we calculated errors along the grounded and non-grounded portions of each glacier centreline profile (Table A.1 in Appendix A). Mean grounded bed topography errors at 14 of 18 study glaciers range between 25 and 87 metres. These glaciers are well constrained by the mass conservation method, which works best for fast flowing areas near the glacier terminus [Morlighem *et al.*, 2014, 2017]. The remaining four glaciers (Storstrømmen, L. Bistrup Bræ, Kofoed-Hansen Bræ, and Brikkerne Glacier) have higher errors (from 112 to 215 m), owing to poor data coverage and kriging interpolation [Morlighem *et al.*, 2017]. Mean errors in bathymetry data are greater at all glaciers, averaging 156 metres and ranging from 15 to 283 m. To assess bed slope direction, we fit each glacier profile from the grounding line to 20 km inland with a linear regression model. These sections of each bed profile and model fit are presented in Figure A.1, while entire bed profiles, and landward/seaward direction are presented in the results. Errors in basal topography do not significantly affect the assessment of bed slope direction, and we only use topography along the grounded portion of the glacier where errors are lowest. We treat basal profiles

in the far east of the study region with caution due to their higher errors. Finally, to estimate drainage catchment areas and the percentage of each catchment below present sea level for each study glacier, surface drainage catchments (Table 3.4) were delineated using the GIMP surface DEM [Howat *et al.*, 2014] and topographic analysis functions within TopoToolbox in MATLAB [Schwanghart & Kuhn, 2010]. We calculated each drainage area using catchments constrained by gradients in the surface DEM.

3.4 Results

3.4.1 Changes in glacier frontal position (1948-2015)

Across northern Greenland, 13 of the 18 study glaciers underwent net retreat between 1948 and 2015, while the remaining five advanced (Figure 3.4). However, long-term frontal retreat rates (1948-2015) varied between glaciers across northern Greenland (Table 3.2), and ranged from -15 m a^{-1} at Marie-Sophie Glacier, to twenty times greater at Petermann Glacier (-311 m a^{-1}). At outlet glaciers in northern Greenland, we expect terminus changes and dynamic response to be different dependent on terminus type (i.e. floating or grounded). Nine outlet glaciers were grounded at their terminus throughout the study period, while at the end of the study period another nine still had ice tongues or lost them during the last two decades (1996 to 2015: Figure 3.1, Table 3.2). Statistical changepoint analysis compared the duration and magnitude of frontal position changes at all study glaciers: this confirms that, in general, there are two different types of frontal position behaviour and dynamic response to calving based on terminus type (grounded or floating).

In addition to the long-term record of frontal position change (1948-2015), we further assess the variability of retreat rates across northern Greenland, by presenting mean retreat rates across five decadal time periods (1976-1985, 1986-1995, 1996-2005, 2006-2015) in Figure 3.5 (a-e), except for the earliest epoch (1948-1975) which spans 27 years due to image availability. We also present mean decadal frontal position change based on terminus type in Table 3.3. During the first epoch (1948 to 1975) small advances and retreats took place across the region ($< 500 \text{ m a}^{-1}$ magnitude). This was followed by a decade (1976-85) dominated by glacier advance, in particular at glaciers with floating ice tongues (Table 3.3), which had high retreat rates when averaged over the entire study period (e.g. Hagen Bræ, Zachariæ Isstrøm, Petermann: Table 3.2). In the subsequent epoch (1986 to 1995), a mixture of advance and retreat occurred and the range of frontal position changes was great, from -780 m a^{-1} retreat at C. H. Ostenfeld to 750 m a^{-1} advance at Storstrømmen

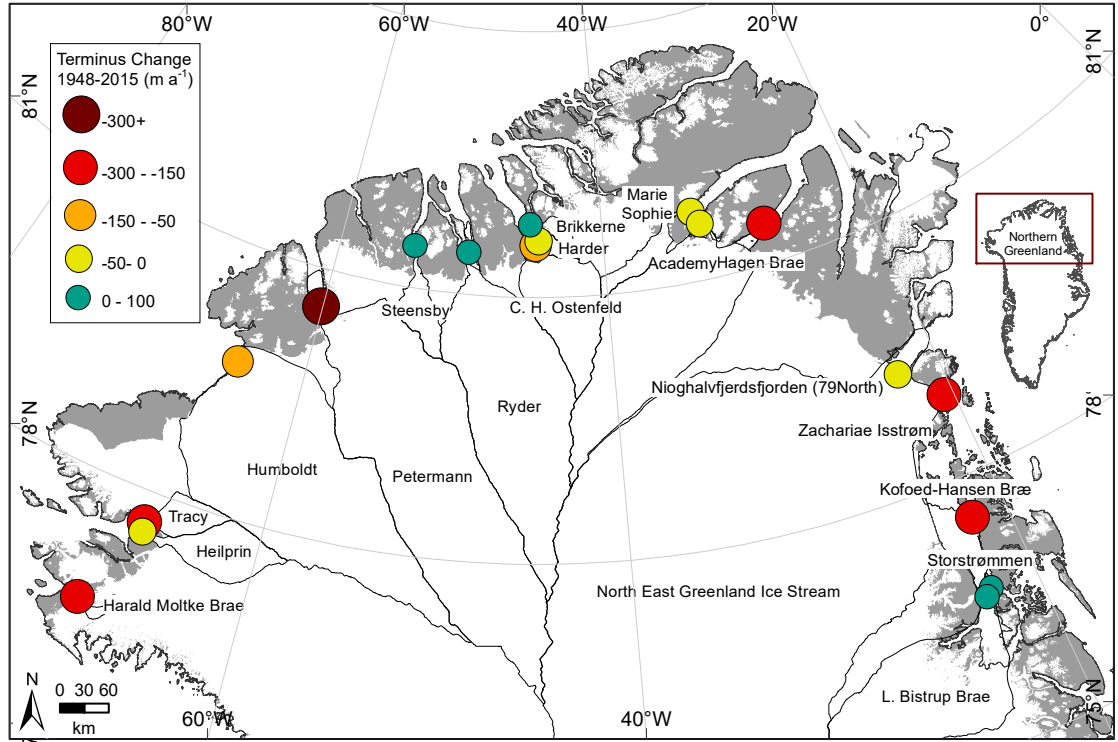


Figure 3.4: Overall mean rate of terminus change (m a^{-1}) at 18 outlet glaciers in northern Greenland from 1948 to 2015. Green circles represent glaciers which have undergone overall advance during the record, while yellow to red circles represent increasing retreat rates from 0 to larger than -300 m a^{-1}

(Figure 3.5c). During the last two decades of the study period (1996 to 2015), retreat rates were substantially higher than in the previous three epochs. However, variability in the magnitude of frontal position change over this period appears to be particularly related to terminus type (grounded or floating). Decadal mean retreat rates at glaciers with ice tongues (-745 to -835 m a^{-1}) were substantially higher than at grounded-outlet glaciers (-99 to 165 m a^{-1} ; Table 3.3). Based on the differences in terminus behaviour observed over the long-term and decadal time series based on terminus type (grounded or floating), we now treat these as separate categories for the remainder of the results, during which we describe short-term trends derived from the changepoint analysis (Figure 3.6).

| North Greenland outlet glaciers | | Terminus change (1948-2015) (m a ⁻¹) | Velocity change (1995/96-2015/16) (m a ⁻¹) | Difference in surface elevation change rates (1992-1996 and 2014-2015) (m a ⁻¹) |
|---------------------------------|-----------------------|--|--|--|
| Grounded terminus | Tracy | -173 | 36.8 | -0.11 |
| | Kofoed-Hansen Bræ | -169 | -0.06 | 0.12 |
| | Harald Moltke Bræ | -156 | 22.6 | |
| | Humboldt | -111 | 0.32 | -0.51 |
| | Heilprin | -45 | 7.16 | -0.15 |
| | Academy | -31 | -4.87 | -0.97 |
| | Harder | -25 | 0.58 | -0.89 |
| | Marie-Sophie | -15 | 1.03 | -0.43 |
| | Brikkerne | 82 | -2.56 | |
| Floating ice tongue | Petermann | -311 | 3.78 | -1.34 |
| | Zachariæ Isstrøm | -282 | 20.3 | -2.98 |
| | Hagen Bræ | -162 | 6.45 | -0.83 |
| | C.H. Ostenfeld | -58 | 2.96 | -1.26 |
| | Nioghalvfjerdsfjorden | -28 | 1.62 | -1.99 |
| | Steensby | 2 | 2.59 | -0.33 |
| | L.Bistrup Bræ | 39 | -3.89 | 0.57 |
| | Storstrømmen | 41 | -1.11 | -0.18 |
| | Ryder | 43 | -0.08 | 0.47 |

Table 3.2: Mean decadal frontal position change for all study outlet glaciers in northern Greenland, and split based on our two glacier categories of terminus type: grounded terminus or terminating in a floating ice tongue.

3.4.2 Frontal position change according to terminus type

Grounded-terminus outlet glaciers

Calving-induced retreat of grounded marine-terminating outlet glaciers, contributes to dynamic mass loss and directly to sea level rise. At grounded outlet glaciers in northern Greenland (nine of the study glaciers: Figure 3.6), retreat rates increased substantially during the last two decades (1996 to 2015) of the study period. At the beginning of the record, grounded outlet glaciers went through an initial period of minimal frontal position change averaging -26 m a^{-1} and ranging from $+24 \text{ m a}^{-1}$ advance at Kofoed-Hansen Bræ to -105 m a^{-1} retreat at Tracy Glacier (Figure 3.6). Frontal position change then switched to a period of higher magnitude retreat at eight glaciers (excluding Brikkerne), which lasted for an average of 26 years. During this period, frontal position change averaged -150 m a^{-1} , and net retreats ranged from -0.6 to 8 km . The greatest total terminus changes took place at Tracy Glacier (8 km retreat: 1981-2015), Harald Moltke Bræ (5 km retreat: 1988-2015), and Kofoed-Hansen Bræ (4.6 km : 1973-2015: Figure 3.7a-c). The timing of this switch from minimal change to steady retreat was not uniform, but most glaciers began steadily retreating from the 1990s to 2000s and continued at the same rate thereafter (Figure 3.6). The exception to this pattern of behaviour is Brikkerne glacier, which instead advanced by

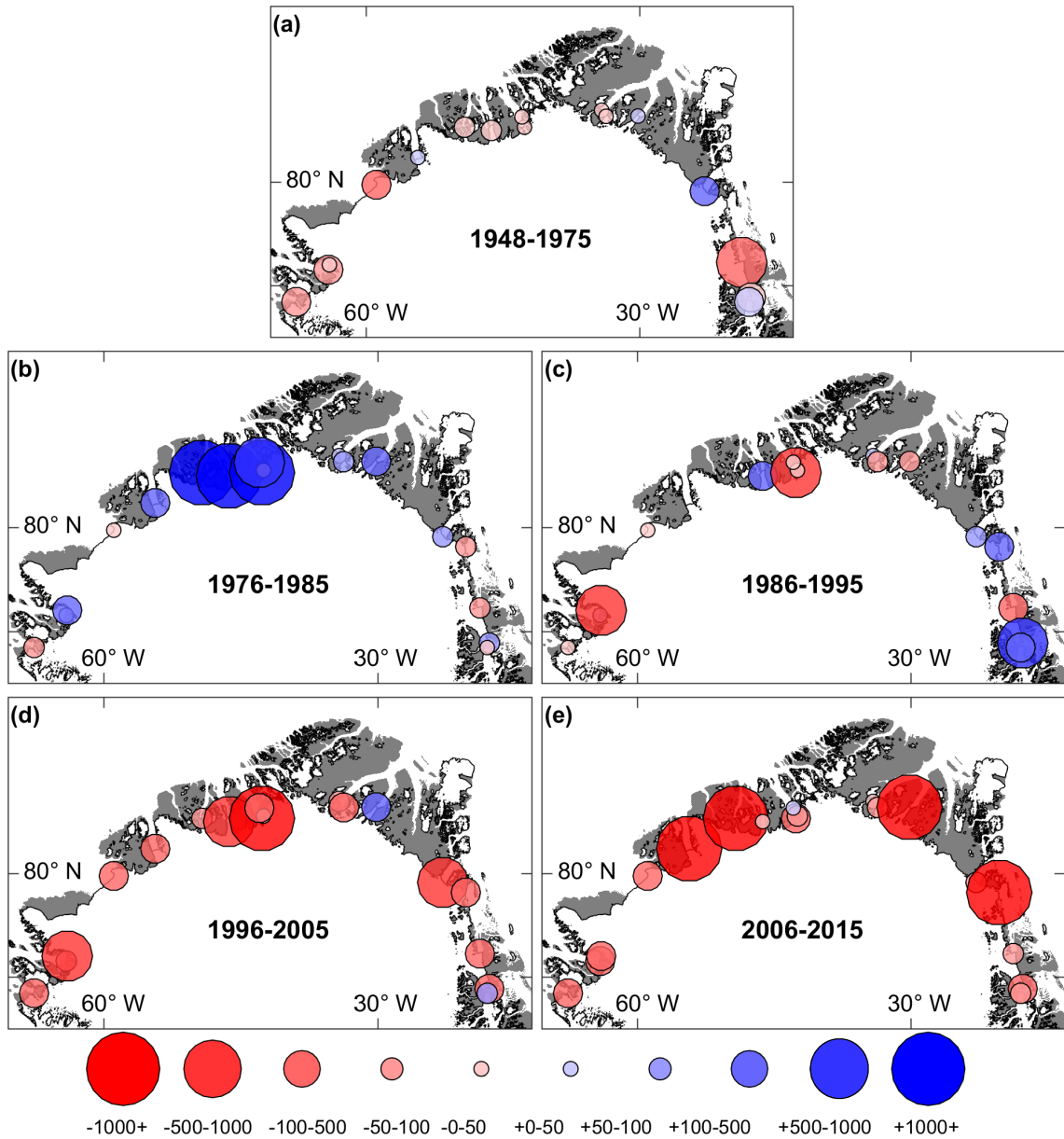


Figure 3.5: Mean decadal rates of terminus change across northern Greenland. These are shown for five epochs between 1948 and 2015. Increasing red circles represent glacier retreat rates between 0 and exceeding -1000 m a^{-1} . Increasing blue circles represent advance rates between 0 and exceeding $+1000 \text{ m a}^{-1}$.

9 km between 1968 and 1978 before returning to minimal terminus change (Figure 3.7i).

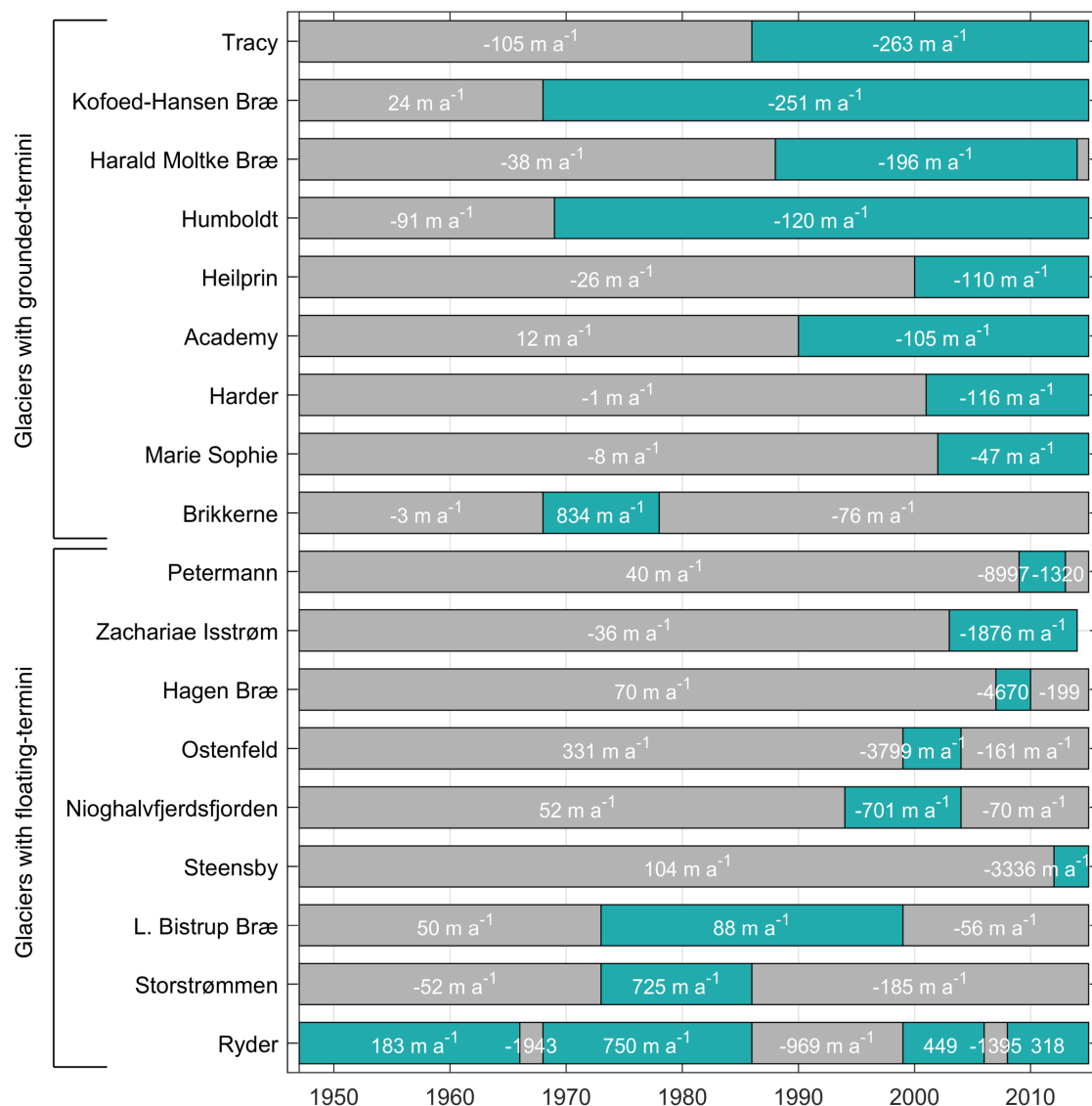


Figure 3.6: Retreat rates during identified periods of either minimal frontal position change or periods of either steady or rapid retreat and displayed by either grounded or floating termini. Glaciers are then ordered based on their overall (1948-2015: Table 3.2) frontal position change rates within each of these categories. Grey bars show their periods of minimal/variable terminus change (in some cases advance) and turquoise bars show the period of higher magnitude frontal position change.

Glaciers with floating ice tongues

The retreat of floating glacier termini can reduce the resistive stresses at the terminus and increase the dynamic glacier response to calving. Rapid retreat in the form of large episodic calving events removed substantial floating ice sections (11.6-26 km net retreat:

| Mean terminus change (m a^{-1}) | 1948–1975 | 1976–1985 | 1986–1995 | 1996–2005 | 2006–2015 |
|--|-----------|-----------|-----------|-----------|-----------|
| All ($n = 18$) | –63.65 | 503.36 | –7.83 | –454.99 | –467.06 |
| Grounded ($n = 9$) | –167.35 | 93.87 | –112.07 | –164.50 | –99.23 |
| Floating ($n = 9$) | 40.05 | 912.84 | 126.19 | –745.49 | –834.88 |

Table 3.3: Mean decadal frontal position change for all study outlet glaciers in northern Greenland, and split based on our two glacier categories of terminus type: grounded terminus or terminating in a floating ice tongue.

Figure 3.8) from several northern Greenland outlet glaciers (Zachariæ Isstrøm, Petermann and Steensby, C. H. Ostensfeld, and Hagen Bræ) between 1995 and 2015. However, frontal position changes at some glaciers with floating ice tongues were instead cyclic. At the beginning of the study period, six of the nine study glaciers with floating ice tongues showed minimal terminus change/advance (93 m a^{-1}), followed by short-lived rapid retreat, lasting less than 6 years on average (Figure 3.6). During the phases of rapid retreat, rates ranged between -700 m a^{-1} at Nioghalvfjerdsfjorden to -8997 m a^{-1} at Petermann Glacier (Figure 3.6), and were on average 40 times greater (-4536 m a^{-1}) than during the steady retreat phases at glaciers grounded at their terminus (-150 m a^{-1}). During this period, large calving events led to complete ice tongue loss at Zachariæ Isstrøm by 2011/12, and at C. H. Ostensfeld, Steensby and Hagen Bræ by 2016 (Figure 3.8). Rapid retreat was often followed by another period of relative minimal terminus change (-437 m a^{-1}) compared to order of magnitude earlier retreat (e.g. Petermann Glacier and Hagen Bræ: Figure 3.6). Similar to glaciers with grounded-termini, the timing of the switch to rapid retreat was not synchronous, but mainly occurred after 1990 (Figure 3.6). At most glaciers, the duration of rapid retreat was short-lived (< 5 years) in comparison to the duration of steady retreat (> 13 years) at grounded-glaciers.

Several glaciers with floating ice tongues (Storstrømmen, L. Bistrup Bræ, and Ryder) have instead shown cyclic periods of advance and retreat between 1948 and 2015 (Figure 3.8g-i). Periods of terminus advance at these glaciers averaged $\sim 420 \text{ m a}^{-1}$ and lasted for an average of 18 years (Figure 3.6). Adjacent glaciers Storstrømmen and L. Bistrup Bræ advanced during a similar period (from 1973 to 1990), and for ~ 13 -17 years. After this, both glaciers underwent relatively limited terminus change from 2000 onwards (Figure 3.6). Despite synchronous advance, their advance rates differed by almost an order of magnitude (89 m a^{-1} at L. Bistrup Bræ, and 725 m a^{-1} at Storstrømmen, Figure 3.6). At Ryder Glacier, there were four main cycles of glacier advance and retreat during the record. These took place between 1948-1966, 1968-1986, 1999-2006, and 2008-2015 and advance rates ranged from 183 to 750 m a^{-1} (Figure 3.6). Periods of advance (7-48 years) were separated by shorter periods (2-13 years) of higher magnitude retreat (ranging from -960 to -1950 m a^{-1}) (Figure 3.6).

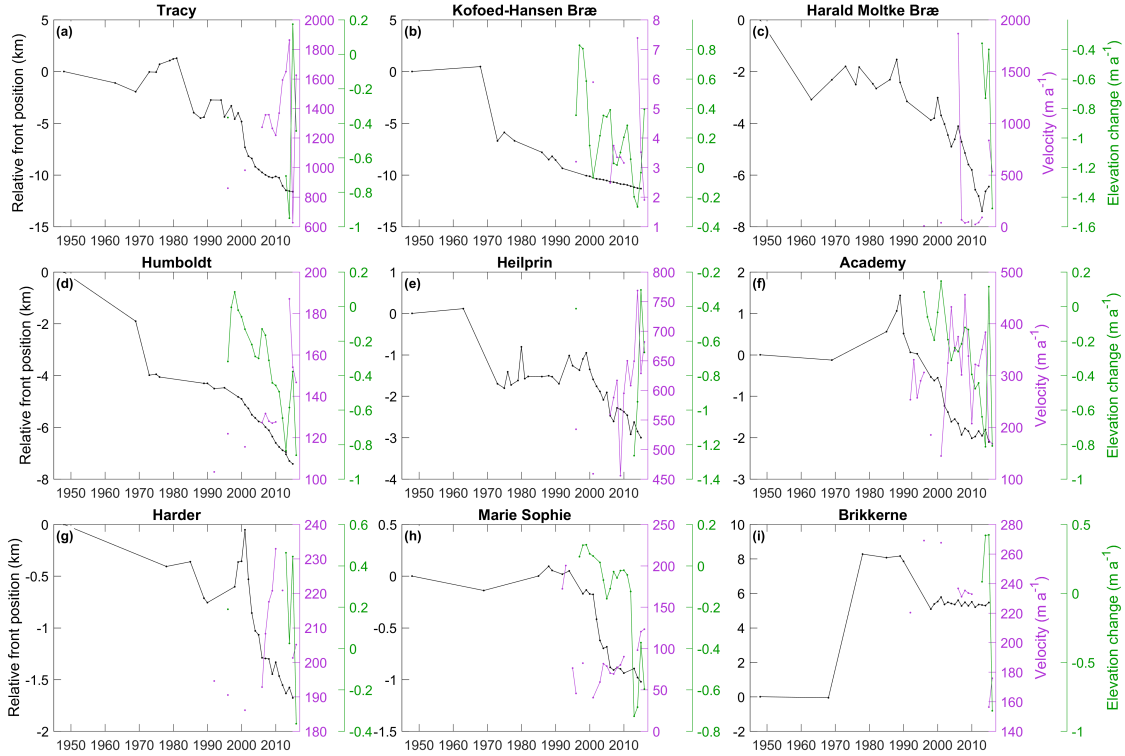


Figure 3.7: Front position, velocity and elevation change at nine outlet glaciers grounded at their terminus in northern Greenland. Left axes show relative front position (black line) between 1948 and 2015 relative to their initial position in 1948. Grounding line velocities (purple) on right axes one between 1996 and 2015. Surface elevation changes averaged across the glacier centreline profile (green) for 1996 to 2015.

3.4.3 Ice velocity change

Grounded-terminus outlet glaciers

Overall, most grounded outlet glaciers in northern Greenland accelerated along their centreline profiles (ranging from 0.32 to 37 m a^{-1}) from 1996 to 2016 (Table 3.2). Acceleration at these glaciers was also greatest (averaging 27%), during periods of steady retreat (Figure 3.6). This was particularly the case in northwest Greenland at Heilprin, Tracy, and Harald Moltke Bræ. At Heilprin Glacier this resulted in a 49% increase (from 458 to 681 m a^{-1}) in grounding line velocity from 2001 to 2016 (Figure 3.7e), during which the glacier retreated at -110 m a^{-1} (Figure 3.6). Substantially greater acceleration (89%) took place at Tracy Glacier from 1996 to 2016 (Figure 3.7a), which was associated with higher magnitude retreat rates (-263 m a^{-1} : Figure 3.6). Harald Moltke Bræ also accelerated between 1990 and 2016 (22 m a^{-1} : Table 3.2), and retreated at -196 m a^{-1} (Figure 3.6). However, it underwent two very large velocity increases ($> 1000 \text{ m a}^{-1}$) between 2001 and

2006 and again during winter 2013/14, both of which coincided with short-lived glacier advance (0.5-0.8 km: Figure 3.7c). Slower flowing grounded outlet glaciers in the region ($< 400 \text{ m a}^{-1}$: Humboldt, Harder, and Marie-Sophie Glaciers) also accelerated by 27-108% during steady retreat (Figure 3.7). By contrast, some grounded-terminus outlet glaciers did not show substantial acceleration following retreat: Kofoed-Hansen Bræ and Academy Glacier had sustained periods of steady retreat, but showed no net trend in velocity and high variability (Figure 3.7b,f), which did not coincide with periods of increased retreat rates (Figure 3.6). Brikkerne Glacier decelerated from 1996 to 2016, while the terminus position changed little (Figure 3.7i).

Glaciers with floating ice tongues

Despite major retreat episodes and ice tongue disintegration, most glaciers in northern Greenland that terminate in floating ice tongues (except Zachariæ Isstrøm) showed minimal net velocity change between 1996 and 2016 (Table 3.2). In contrast to grounded-outlet glaciers, the velocity response to retreat was also more variable between individual glaciers. However, we identify two main patterns in velocity change following periods of rapid retreat: 1) short-lived, minimal glacier acceleration, followed by some deceleration, 2) continuous acceleration following initial terminus retreat. The first pattern of velocity change encompasses seven of nine glaciers with floating ice tongues, the clearest examples of which are at C. H. Ostenfeld, Hagen Bræ, Petermann Glacier and Steensby Glacier. In all cases, rapid ice tongue retreat was followed by short-lived (< 3 year) low magnitude ($< 8\%$ acceleration, but $\sim 25\%$ at Steensby) grounding-line acceleration. After retreat ceased, ice flow decelerated, ranging from 2% at Petermann to 28% at Hagen Bræ. In addition, prior to rapid retreat some glaciers advanced. In the year preceding rapid retreat (2005 to 2006), Hagen Bræ showed higher magnitude acceleration ($\sim 52\%$) alongside some glacier advance. This was also the case at Ryder Glacier, which showed cyclic behaviour, of grounding line acceleration ($\sim 8\%$: $4.7\text{-}5.5 \text{ m a}^{-1}$) during both 7-year periods of terminus advance, followed by deceleration (11%) during high magnitude retreat (~ 2 years) in-between periods of advance. Storstrømmen and L. Bistrup Bræ also show evidence of some acceleration immediately following retreat, later followed by deceleration (Figure 3.8h,i) from 2010 to 2016. However, in contrast to most tidewater glaciers which flow fastest at their terminus, velocities at both glaciers are fastest inland, and decrease with distance towards the terminus (Figure 3.9). Grounding line terminus velocities accelerated by 350% and 150% at Storstrømmen and L. Bistrup Bræ throughout the record (1996 to 2016: Figure 3.8); and velocities $\sim 20\text{-}40 \text{ km}$ inland decelerated by $10\text{-}15 \text{ m a}^{-1}$ ($> 54\%$).

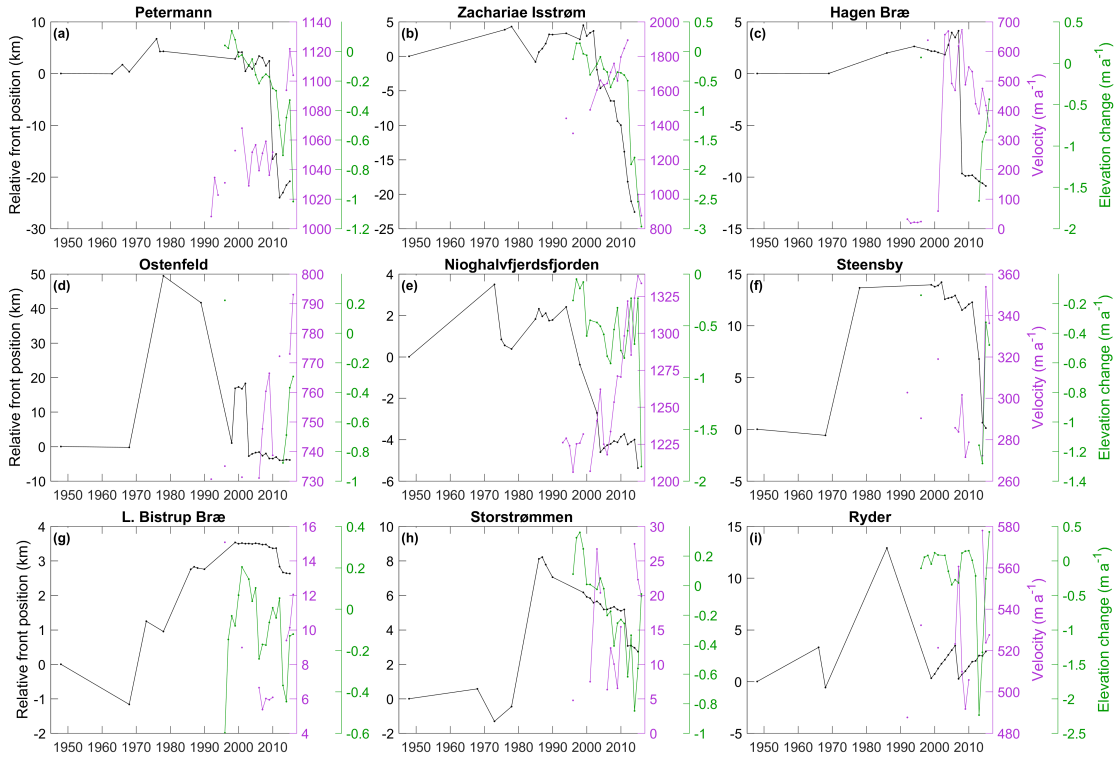


Figure 3.8: Front position, velocity and elevation change at nine outlet glaciers which terminate in floating ice tongues in northern Greenland. Left axes show relative front position (black line) between 1948 and 2015 relative to their initial position in 1948. Grounding line velocities (purple) on right axes one between 1996 and 2015. Surface elevation changes averaged across the glacier centreline profile (green) for 1996 to 2015.

The second pattern of velocity change occurred at both glaciers draining the NEGIS where ice tongue retreat was followed by gradual glacier acceleration in the subsequent decade (2006 to 2016: 43% at Zachariae Isstrøm and 10% at Nioghalvfjærdsfjorden). This prolonged glacier acceleration following retreat, is more similar to patterns observed on grounded termini, rather than the other floating tongues. Further, the removal of the entire ice tongue at Zachariae Isstrøm in 2011/12 was followed by glacier acceleration (125 m a^{-2} : 2012 to 2016, Figure 3.8g), whereas other glaciers (e.g. C. H. Osterfeld and Hagen Bræ) underwent a similar collapse, but changes in velocities were limited. Despite this behaviour in the northeast of the study region, the majority of glaciers in northern Greenland showed negligible acceleration in response to retreat and/or collapse of their floating ice tongues.

3.4.4 Surface elevation change

Grounded-terminus outlet glaciers

Alongside continuous retreat and acceleration at outlet glaciers with grounded-termini, thinning rates increased between 1992-1996 and 2014-2015 (Table 3.2). In most cases, surface lowering was synchronous with the start of their steady retreat (Figure 3.7). Examples of this were at Marie-Sophie and Academy Glaciers, where small increased thinning or reduced thickening rates (1999 to 2000: Figure 3.7f,h), were followed by high retreat rates in the following years at both Marie-Sophie (-130 m a^{-1} : 2001 to 2004) and Academy Glacier (-205 m a^{-1} : 2001 to 2003). Periods of greater retreat (2001 to 2003/04) were followed by dramatically increased thinning rates at both glaciers to -0.3 m a^{-1} (Academy) and -0.16 m a^{-1} (Marie-Sophie: Figure 3.7f,h). Thinning rates similarly increased strongly from -0.19 m a^{-1} to -0.78 m a^{-1} at Humboldt Glacier from 1996-2005 to 2005-2012, which coincided with increased retreat rates (-98 to -160 m a^{-1} : Figure 3.7d). Limited data prevent us from commenting in depth on elevation changes at glaciers in NW Greenland. However, the few years of data available at Harald Moltke Bræ show increased thinning between 2012 and 2015, coincident with retreat (Figure 3.7c). Within this record lies an anomalous year of reduced thinning rates (2013 to 2014), which were coincident with an order of magnitude increase in velocity ($\sim 1000 \text{ m a}^{-1}$) and 0.8 km terminus advance.

Glaciers with floating ice tongues

In general, glaciers with floating ice tongues had higher thinning rates than grounded termini from 1992-1996 to 2014-2015 (Table 3.2), and were characterised by short-lived increases in thinning rates following ice tongue retreat. In several cases (e.g. Petermann, Hagen Bræ, and Zachariæ Isstrøm), slight thickening occurred before ice tongue retreat/collapse, followed by a switch to thinning immediately before large calving events (Figure 3.8). For example, Petermann Glacier switched from negligible thickening in 2008 (0.03 m a^{-1}) to thinning (-0.22 m a^{-1}) in 2009, before the removal of 27 km of floating ice in the following three years (2010 to 2013: Figure 3.8a). At Zachariæ Isstrøm a switch to thinning was synchronous with the onset of rapid retreat in 2003 (Figure 3.8b), although thinning rates were greater once the entire ice tongue was lost (2011 to 2012). During or immediately after floating ice tongue retreat, thinning rates increased from minimal change ($< -0.2 \text{ m a}^{-1}$ thinning) to -0.8 m a^{-1} at Petermann Glacier (2010 to 2013), -1.7 m a^{-1} at Hagen Bræ (2007/11 to 2012/13), and -2 m a^{-1} at Zachariæ Isstrøm (2011/12 to 2012/13: Figure 3.8). This increased thinning was also coincident with acceleration during

the years following ice tongue removal (Figure 3.8). Other glaciers showed more gradual and smaller increases in thinning rates (Figure 3.8). For example, at C. H. Ostenfeld the removal of 21 km of floating ice between 2002 and 2003 was followed by a steady and low magnitude increased thinning rates at a rate of -0.15 m a^{-1} from 2006 to 2014 (Figure 3.8d). In this case, velocity increases alongside increased thinning rates were also gradual, but minimal in comparison to other glaciers. Ryder Glacier also showed increased thinning rates prior to retreat (2005-2006) but was followed by a rapid switch to thickening as ice flow accelerated, and the calving front advanced (Figure 3.8i).

Two glaciers with floating ice tongues in northeast Greenland showed a different pattern of elevation change to the rest of the region: Storstrømmen and L. Bistrup Bræ thinned at the glacier terminus and thickened inland from 1996 to 2015 (Figure 3.9). Periods of glacier advance ($\sim 1970\text{s}-80\text{s}$) at both Storstrømmen and L. Bistrup Bræ preceded the earliest record of elevation change and, following this, their terminus positions underwent minimal change (Figure 3.6). Between 1996 and 2015, inland elevation change was minimal (Figure 3.9), whereas greater thinning took place at the terminus. Large retreat events of 2.1 km at Storstrømmen and 0.7 km at L. Bistrup Bræ between 2011 and 2013 coincided with increased terminus thinning rates of -0.8 m a^{-1} at Storstrømmen (2011 to 2012) and -1.76 m a^{-1} at L. Bistrup Bræ (2011 to 2013; Figure 3.9). These spatial patterns of elevation change were synchronous with velocity variations: deceleration and thickening occurred inland, while acceleration, thinning, and retreat were synchronous at the terminus (Figure 3.9).

3.4.5 Topographic factors

Grounded-terminus outlet glaciers

Distinct variability in glacier geometry exists between individual outlet glaciers in northern Greenland. At many outlet glaciers with grounded termini (Harald Moltke Bræ, Heilprin, Tracy and Humboldt), deep inland sloping beds are associated with higher retreat rates (averaging -121 m a^{-1}), and greater increases in velocity (Table 3.2). These glaciers rest between -33 and -370 m below sea level (Figure 3.10) and appear to have been retreating down steep bed-slopes (Figure A.1) away from topographic ridges at the end of their fjords (Figure 3.10). However, variability in fjord width (widening/narrowing) does not appear to be a main determinant of higher retreat rates (Table 3.4). Additionally, some grounded outlets (Harder, Academy, and Marie-Sophie) have shallower seaward sloping topography which correlated with lower magnitude retreat rates (-24 m a^{-1} ; Table 3.2).

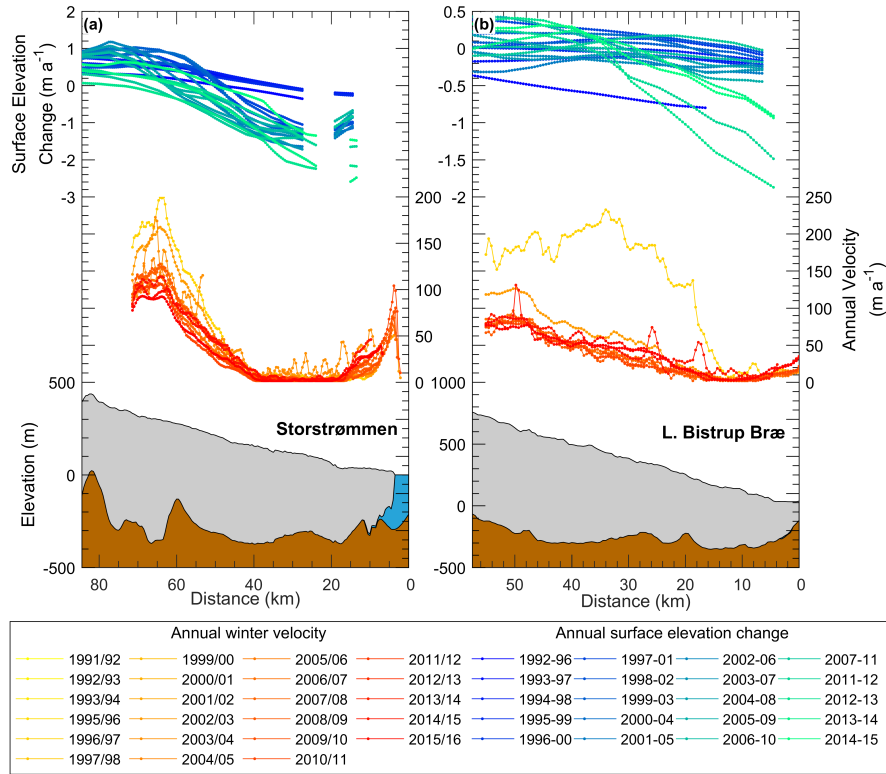


Figure 3.9: Annual surface elevation change, annual velocity and surface/bed topography for two outlet glaciers in northeast Greenland: Storstrømmen (a) and L. Bistrup Bræ (b). Blue to green coloured lines represent annual surface elevation through time (1992-96 to 2014-15) and yellow through to red lines represent annual winter velocity from 1991/92 to 2015/16.

Glaciers with floating ice tongues

Basal topography beneath floating ice tongues does not impact on their dynamic response to retreat. Instead, we examine bed topography inland of the grounding line, which may have implications for grounding line retreat and associated instability once ice tongues collapse. Deeper bed topography (-73 to -1000 m below sea level: Figure 3.11) exists at floating ice tongues, and most (seven of nine) also have inland sloping topography within 20 km of their grounding lines (Table 3.4). Unlike grounded outlet glaciers there is no obvious link to higher retreat rates or fjord widths between these glaciers. However, the current grounding line position along glacier bed profiles appear to be associated with differences in the dynamic response of glaciers to either large calving events or entire ice tongue collapse. Grounding line positions at Petermann, C. H. Ostenfeld and Hagen Bræ, rest on relatively flat topography (Figure 3.11a,c,d), rather than retrograde slopes. In all cases, either large calving events at Petermann Glacier or entire ice tongue collapse at

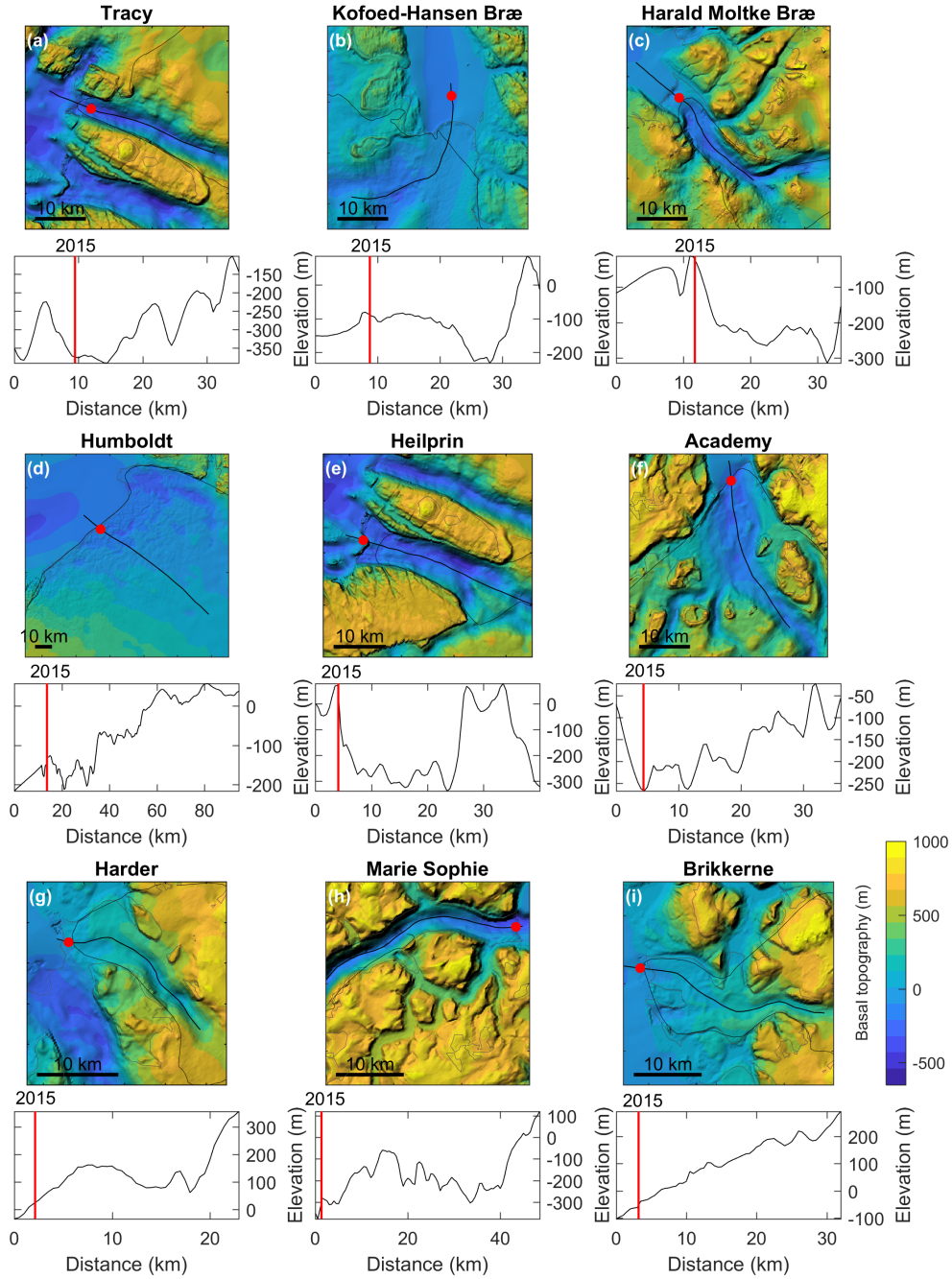


Figure 3.10: Basal topography from Operation IceBridge BedMachine v3 [Morlighem *et al.*, 2017] beneath nine study glaciers with grounded termini in northern Greenland. Red points represent the position of the terminus/grounding line at each glacier from our most recent record of their terminus position (2015). Black lines are glacier centreline profiles. Profile plots show basal elevations along each glacier centreline profile and solid red lines nearest to zero show the terminus location.

C. H. Ostenfeld and Hagen Bræ, coincided with limited glacier acceleration. In contrast, the grounding lines of glaciers draining the NEGIS (Nioghalvfjærdsfjorden and Zachariæ Isstrøm), rest on steeper inland sloping beds (Figure 3.11), which correlates with their gradual ice tongue retreat and prolonged glacier acceleration. Since losing its ice tongue in 2011/12, Zachariæ Isstrøm retreated down its steep basal trough, past the recorded (nominal date of 2007 in BedMachine dataset) grounding line position (Figure 3.11b). A possible exception to this pattern of grounding line instability on retrograde slopes is Ryder Glacier. It too has a deep basal trough (~ 800 m below sea level) 20 km inland of the grounding line, but further inland (~ 50 km from the terminus) it has a steep seaward sloping bed, and a large topographic ridge immediately seaward of the current grounding line position (Figure 3.11c).

3.5 Discussion

3.5.1 Timing of glacier change between 1948 and 2016

Decadal terminus changes at all 18 study glaciers (Figure 3.5), showed a transition from slow low magnitude advance and retreat (averaging $+72 \text{ m a}^{-1}$) between 1948 and 1995 to rapid high magnitude retreat (averaging -445 m a^{-1}) between 1996 and 2015. The latter period included the onset of steady retreat at most grounded outlet glaciers in northern Greenland, and the occurrence of large, rapid retreat events at floating ice tongue glaciers (Figure 3.6). While this switch from minimal terminus change/advance to more rapid retreat is perhaps similar to the cyclic behaviour of tidewater glaciers [Meier & Post, 1987; Pfeffer, 2007], it is unlikely that this pattern of widespread retreat is driven by internal factors alone [e.g., Nick *et al.*, 2007]. Instead, climate-induced dynamic thinning at outlet glacier margins [Khan *et al.*, 2014; Pritchard *et al.*, 2009], may have been the initial forcing for increased glacier retreat rates in northern Greenland. The switch to terminus retreat in the 1990s was coincident with: increased air and ocean temperatures across the GrIS [e.g., Box *et al.*, 2009; Hanna *et al.*, 2008; Luckman *et al.*, 2006], ice marginal thinning (< 2000 m elevation) since the 1990s [Abdalati *et al.*, 2001; van den Broeke *et al.*, 2016; Krabill *et al.*, 2000], and with Arctic-wide increased retreat rates [Carr *et al.*, 2017b; Moon & Joughin, 2008; Jensen *et al.*, 2016]. Previous studies in northern Greenland have suggested that climate-ocean forcing at glacier termini i.e. increased air temperatures, reduced sea ice concentration, and ocean warming induced basal melt, triggered dynamic thinning, retreat, and mass loss from outlet glacier margins [Khan *et al.*, 2014; Reeh *et al.*, 2001; Rignot *et al.*, 2001; Rignot & Steffen, 2008]. Here, we do not assess in detail

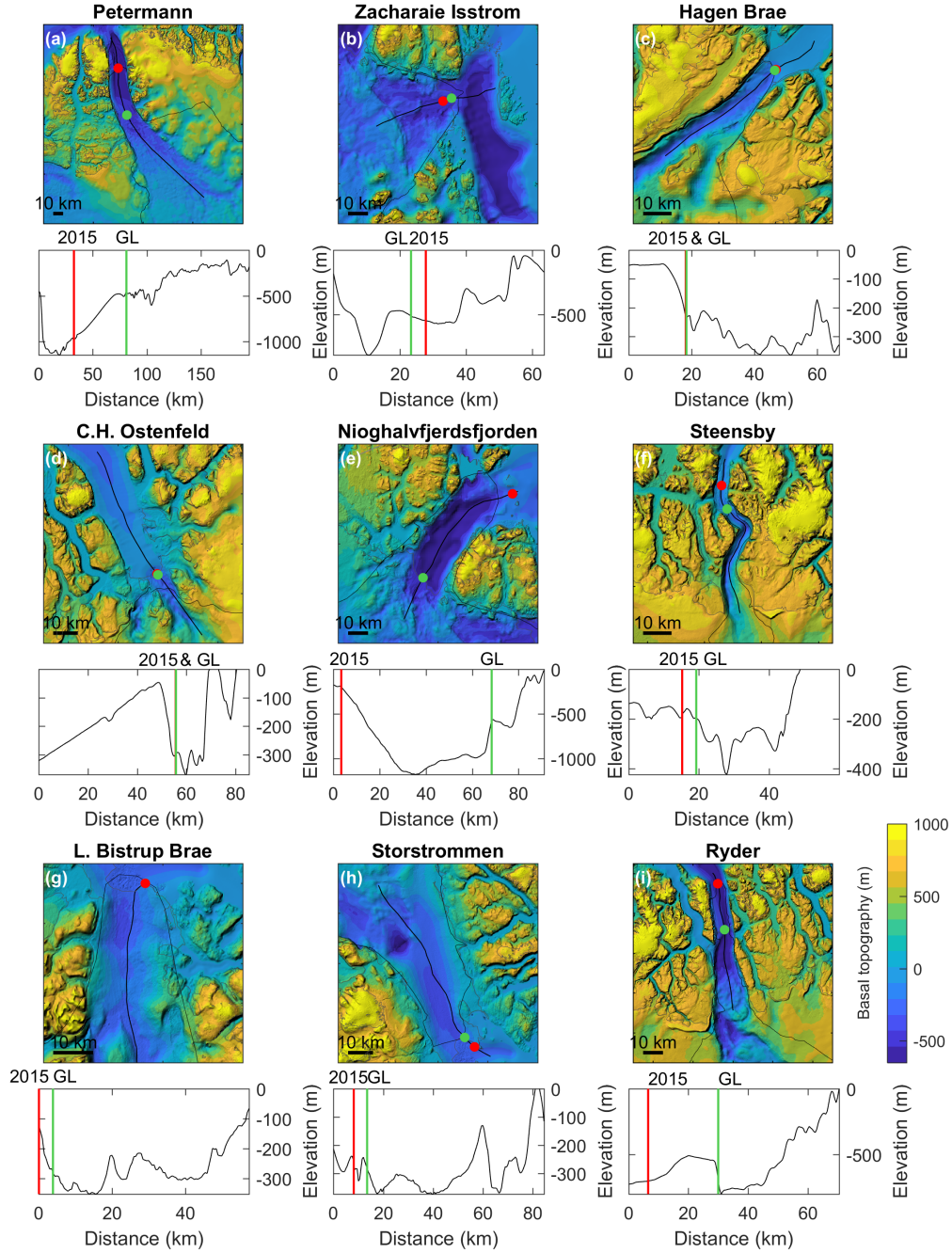


Figure 3.11: Basal topography from Operation IceBridge BedMachine v3 [Morlighem *et al.*, 2017] beneath nine study glaciers which terminate in floating ice tongues in northern Greenland. Red points represent the most recent recorded terminus position (2015) from this study. Green points represent the location of the grounding line along the centreline profile from the GIMP DEM mask [Howat *et al.*, 2014]. Profile plots show basal elevations along each glacier centreline profile, where closest to zero red lines show the terminus locations, and further inland green lines shown the grounding line.

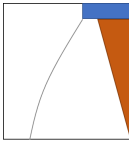
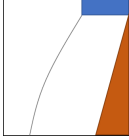
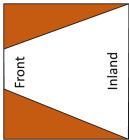
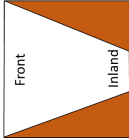
| Northern Greenland outlet glaciers | Drainage basin size (km ²) | Drainage basin below sea level (%) | Inland bed slope | Seaward bed slope | Widening fjord | Narrowing fjord |
|------------------------------------|--|------------------------------------|---|--|---|---|
| | | |  |  |  |  |
| Grounded terminus | | | | | | |
| Tracy | 3176 ^b | 3.6 ^b | X | | | X |
| Kofoed-Hansen Bræ | | | X | | X | |
| Harald Moltke Bræ | 666 | 17 | X | | | X |
| Humboldt | 51 815 | 27 | X | | Does not terminate in fjord | |
| Heilprin | 6593 ^a | 2.9 ^a | X | | | |
| Academy | | | | X | | |
| Harder | 792 | 0.2 | | X | | X |
| Marie-Sophie | 2567 | 6.8 | | X | X | |
| Brikkerne | 929 | 2.3 | | X | | X |
| Floating ice tongue | | | | | | |
| Petermann | 60 093 | 67 | X | | X | |
| Zachariae Isstrøm | 257 542 ^b | 54 | X | | X | |
| Hagen Bræ | 30 250 ^a | 20 | | X | X | |
| C. H. Ostenfeld | 11 013 ^b | 1.5 ^b | X | | | X |
| Nioghalvfjordsfjorden | | | X | | | X |
| Stensby | 3356 | 4.2 | X | | | X |
| L. Bistrup Bræ | 26 660 ^b | 4.4 ^b | X | | X | |
| Storstrømmen | | | X | | X | |
| Ryder | 36 384 | 40 | | X | X | |

Table 3.4: Glacier-specific factors at 18 northern Greenland study glaciers ordered by terminus type and then based on high-low magnitude retreat rates. This includes the size and percentage of each surface drainage basin below sea level, the direction of the bed slope 20 km inland of the grounding line (inland or seaward), and whether the fjord widens or narrows with distance inland. ^aCombined drainage catchment of Hagen Bræ and Academy Glacier. ^bNortheast Greenland Ice Stream (NEGIS) drainage catchment.

the climate-ocean forcing mechanisms that may have influenced recent terminus change behaviour in northern Greenland, partly due to lack of data and partly because the focus of this paper is on glacier dynamics and their interaction with topography. However, we note that surface thinning preceded rapid terminus retreat at many northern Greenland glaciers (Figures 3.7 and 3.8). Therefore, we suggest that dynamic thinning could have been the initial process that accelerated glacier retreat in northern Greenland since the 1990s [cf. Felikson *et al.*, 2017; Nick *et al.*, 2009; Price *et al.*, 2011]. However, in line with tidewater glacier cyclic behaviour, it is likely that after an initial change in dynamics at the terminus triggered by climate forcing, fjord width and depth become more important controls (see Section 3.5.3) on the duration and magnitude of retreat at individual glaciers [Benn *et al.*, 2007; Catania *et al.*, 2018; MacGregor *et al.*, 2012].

3.5.2 Dynamic glacier response to terminus change

Our analysis of termini behaviour shows that the dynamic glacier response (acceleration and thinning) to a frontal position change is highly dependent on whether the terminus is grounded or the glacier terminates in a floating ice tongue [Benn *et al.*, 2007]. Informed by changepoint analysis, we infer two dominant calving behaviours in northern Greenland based on these terminus types: 1) low magnitude continuous calving events/terminus retreat at grounded outlet glaciers, 2) large episodic tabular calving events at glaciers with floating ice tongues. Independent of these styles (continuous vs episodic), calving at both categories of terminus type is influenced by the velocity structure of the glacier, and ice velocity itself is sensitive to changes in terminus position and alterations to the force balance, i.e. decreased basal/lateral resistance and increased driving stress [Benn *et al.*, 2007]. In the previous section, we hypothesised that increased thinning at the glacier terminus (~ 1990 s), may have initiated enhanced retreat and accelerated terminus velocities in the following two decades (1996 to 2015), similar to other regions of the ice sheet [e.g., Luckman *et al.*, 2006; McFadden *et al.*, 2011; Moon & Joughin, 2008]. Such thinning could cause downstream increases in velocity, which stretches the ice, promotes crevasse propagation induced calving, and propagates the dynamic response (i.e. acceleration) up-glacier. However, the coarse resolution of the elevation change datasets limits our ability to deduce the initial cause of accelerated retreat, so instead we focus on the trends in dynamic glacier changes (acceleration and thinning), after the onset of retreat.

Following an assumed initial change in terminus conditions (~ 1990 s), outlet glaciers in northern Greenland that are grounded at their terminus, underwent prolonged periods of steady terminus retreat (on average -150 m a^{-1}), that usually lasted for two to three

decades (Figure 3.6). Like grounded-outlet glaciers elsewhere, e.g. Helheim and Kangerdlugssuaq [Howat *et al.*, 2005, 2007, 2008] and in west Greenland [McFadden *et al.*, 2011], periods of steady and continuous retreat at grounded-terminus outlet glaciers in northern Greenland were accompanied by increased annual ice velocities (27-110%), and dynamic thinning (Figure 3.7). From this dynamic response we suggest that continuous calving and retreat, and the associated reduction in resistive stresses at the terminus, substantially altered the force balance by increasing longitudinal stretching and driving stress. This prolonged stress perturbation at the terminus of most grounded outlet glaciers in northern Greenland, allowed acceleration and thinning to propagate inland and continue for a longer period as most glaciers may have not reached a stable geometry [McFadden *et al.*, 2011; Nick *et al.*, 2009, Section 3.5.3]

In contrast, terminus changes at most glaciers with floating ice tongues were characterised by short-lived (<6 years), significantly higher magnitude retreat events that averaged -4536 m a^{-1} (after ~ 1990 s). These high magnitude retreat events were often due to the calving of large tabular icebergs, initiated by rift propagation [e.g., MacGregor *et al.*, 2012]. However, these large calving events were followed by minimal/and or short-lived increases in annual velocity, and short-term increases in ice surface thinning rates (Figure 3.8). From these velocity records we infer that in most cases large calving events, appeared not to substantially perturb the glacier force balance by neither increasing longitudinal stretching, nor driving stresses on grounded ice, which would lead to annual acceleration (Figure 3.8). This was particularly the case at Petermann, Hagen Bræ and C. H. Ostenfeld, in response to ice tongue collapse or large calving events. This contrasts with the behaviour of ice-tongue terminating glaciers elsewhere in Greenland [e.g., Joughin *et al.*, 2004, 2008*b*] and glaciers draining into Antarctic ice shelves [e.g., Scambos *et al.*, 2004], which instead showed prolonged acceleration and dynamic thinning following the loss of substantial parts of floating ice. At some glaciers short-lived acceleration was followed by reduced retreat, and deceleration (e.g. Hagen Bræ), which represents a rapid re-adjustment at the terminus, and that calving at floating ice tongue glaciers in northern Greenland appear to limit the dynamic glacier response to large calving events. This could be due to limited lateral resistance provided by floating ice tongues (Section 3.5.3).

However, Zachariæ Isstrøm was a notable exception to this pattern. At Zachariæ Isstrøm, sustained annual calving was accompanied by a longer period of glacier acceleration and thinning (Figure 3.8*b*). This is comparable to the behaviour of grounded outlet glaciers in northern Greenland, and ice-tongue terminating glaciers elsewhere [e.g., Jakobshavn Isbræ: Joughin *et al.*, 2004, 2008*b*]. In this case, continuous retreat is likely to have gradually reduced resistive forces (i.e. backstress) acting on inland grounded ice,

causing higher magnitude and prolonged flow acceleration. Apart from Zachariæ Isstrøm, the data shows that outlet glaciers in northern Greenland have been largely insensitive to either entire ice tongue loss (C. H. Ostenfeld, Steensby and Hagen Bræ), or large ice-berg calving events (Petermann, Nioghalvfjærdsfjorden). Thus, despite some similarities (e.g. Zachariæ Isstrøm to grounded-behaviour), region wide glacier behaviour in northern Greenland appears dependent on whether the terminus is grounded or floating, due to their calving nature and dynamic response to perturbations of their termini. This highlights the need to consider terminus type when assessing the long-term response of outlet glaciers to changes at their terminus.

3.5.3 Influence of glacier geometry

While climate-ocean forcing may have triggered a change in glacier dynamics at the terminus of outlet glaciers in northern Greenland [e.g., Khan *et al.*, 2014; Reeh *et al.*, 2001], glacier geometry (e.g. width and depth of fjords) may have determined the duration and extent of the resultant retreat. Indeed, variations in basal topography and fjord width have been previously identified as an important control on the dynamic response of glaciers in many regions of the GrIS [e.g., Carr *et al.*, 2013*b*, 2017*b*; Howat & Eddy, 2011; McFadden *et al.*, 2011; Millan *et al.*, 2018; Thomas *et al.*, 2009]. Collectively these factors could explain differences between grounded-terminus and floating ice-tongue glaciers [McFadden *et al.*, 2011], as well as individual glacier variability.

Calving from grounded outlet margins is controlled by both basal and lateral drag, and both reduce as a glacier retreats into a deeper and wider fjord [Benn *et al.*, 2007]. At grounded outlet glaciers in northern Greenland, prolonged acceleration and thinning following retreat suggests that these glaciers were still adjusting to terminus change by the end of the study period in 2015. This is likely due to deep basal topography (> 200 m below sea level), and retrograde bed slopes (~ 20 km of their grounding zones) beneath most grounded-terminus glaciers (Figure 3.10). We suggest grounded-terminus retreat into deeper water contributed to: (i) buoyancy driven feedbacks, as the ice thinned to flotation [van der Veen, 1996], (ii) the penetration of basal crevasses through the full ice thickness [van der Veen, 1998, 2007], and (iii) subsequent enhanced rates of calving and continued retreat [e.g., Joughin *et al.*, 2008*b*]. Our results showed grounded-outlet glaciers which retreated into deeper fjords, had higher retreat rates (e.g. Tracy, Harald Moltke Bræ, and Heilprin), than those with shallower basal troughs (e.g. Academy and Marie-Sophie). The former three glaciers also appear to be retreating downslope from topographic highs at the edge of their fjords (Figure 3.10a,c,e).

Unlike grounded-termini, floating ice tongues predominantly provide resistive stresses through their contact with the lateral fjord margins. Consequently, lateral resistive stresses are the main control on the glacier force balance and driving stresses, and hence the impact of terminus retreat on inland ice dynamics. Our data have shown variability in glacier response to ice tongue loss (Figure 3.8), and we suggest that this could be due to differences in the lateral resistance the floating ice tongue provides when it is in place. Once the ice tongue has entirely collapsed, the terminus becomes grounded, at which point basal drag becomes an important control, and basal topography at and immediately inland of the grounding line becomes more significant.

At most glaciers with floating ice tongues in northern Greenland, the minimal dynamic response to ice tongue retreat and/or collapse (Figure 3.8), may be due to limited lateral resistance provided by their floating ice tongues. In particular, C. H. Ostenfeld and Hagen Bræ, have heavy rifting along their shear margins, appear relatively un-confined by their fjord walls, and weakly attached to the grounded terminus (Figure 3.12b,c). Indeed, both glaciers showed no significant increase in flow speeds following large calving events. This suggests that, in both cases, the buttressing provided by the tongues was minimal, and large ice tongue retreats caused a limited change in the inland force balance. By contrast, Steensby Glacier showed some acceleration ($\sim 25\%$) following ice tongue retreat, which could be due to both a greater loss of lateral resistive stresses from a well-confined ice tongue, and retreat past a narrower sinuous section of the fjord (Figure 3.12a).

As well as the lack of resistive stress provided by their ice tongues, the limited response of Hagen Bræ and C. H. Ostenfeld to terminus retreat (Figure 3.8) may result from their

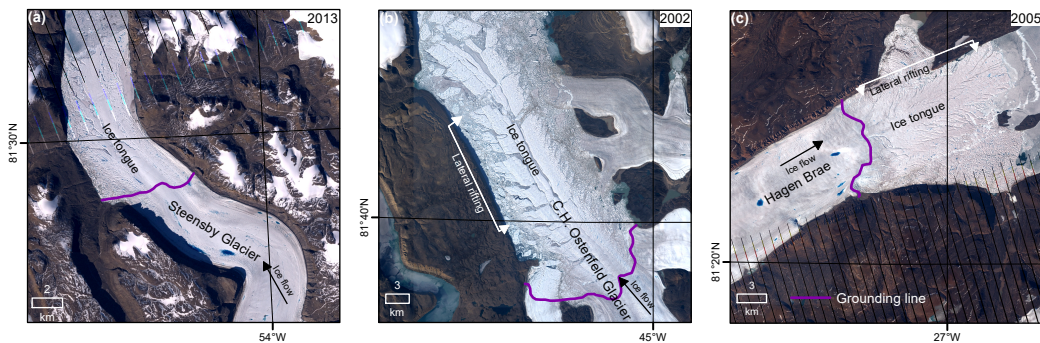


Figure 3.12: Landsat imagery of three glaciers which terminate in floating ice tongues in northern Greenland before their ice tongue collapse. (a) Steensby Glacier in 2013, (b) C. H. Ostenfeld Glacier in 2002, (c) Hagen Bræ in 2005. Purple lines denote the location of the grounding line.

basal topography: following retreat, both grounding lines retreated into shallow water (Figure 3.11). This may have suppressed retreat rates, as it reduces grounding line thickness and therefore discharge. In turn, this would reduce the impact on inland ice velocities and surface thinning rates [Vieli & Nick, 2011]. The flat sections of basal topography beneath the grounding lines of Petermann Glacier and Nioghalvfjærdsfjorden may also control their future response to ice tongue collapse, as their grounding lines would need to retreat ~ 20 km inland to sit on a retrograde slope (Figure 3.9b, g). In contrast, ice tongue collapse at Zachariæ Isstrøm, was followed by continued acceleration, retreat, and more dramatic thinning (Figure 3.8b). Here, the deep retrograde bed-slope that extends ~ 20 km inland of the grounding line, is likely responsible for continued retreat [Khan *et al.*, 2014; Mouginot *et al.*, 2015]. Retreat into deeper water, gradually reduced buttressing forces, and caused continuous glacier acceleration and surface thinning following ice tongue collapse, similar to Jakobshavn Isbræ [Vieli & Nick, 2011].

3.5.4 Glacier surging

Surge-type behaviour has been previously documented at several outlet glaciers in northern Greenland [e.g., Hill *et al.*, 2017; Rignot *et al.*, 2001; Weidick *et al.*, 1994], but detailed evidence for surging is rare. Here we briefly discuss how the surge-nature of several glaciers in northern Greenland may have altered their dynamic behaviour independent of their terminus type.

Our results provide further evidence for the presence of three surge-type glaciers in northern Greenland (Storstrømmen, L. Bistrup Bræ, and Harald Moltke Bræ). This is based on the following characteristics: 1) substantial periods of glacier advance (> 90 m a^{-1}) followed by retreat during the study period, 2) accelerated ice flow coincident with periods of advance, and 3) surface thickening inland and thinning at the terminus position indicative of a quiescent surge-phase. Both Storstrømmen and L. Bistrup Bræ have floating ice tongues which began advancing in the 1970s [Reeh *et al.*, 1999], and continued until 1985 at Storstrømmen, and 1998 at L. Bistrup Bræ (Figure 3.6). While velocity and surface elevation change datasets do not cover this period, dynamic changes later on (1992 to 2016: Figure 3.9) were indicative of quiescence [Abdalati *et al.*, 2001; Csatho *et al.*, 2014; Thomas *et al.*, 2009]. In this respect, these glaciers have behaved differently to the majority of glaciers in the region with floating ice tongues i.e. thickening and deceleration inland, and thinning and acceleration at the terminus (Figure 3.9). In northwest Greenland, Harald Moltke Bræ has been previously considered surge-type. Here we record an additional surge event from 2013 to 2014, based on high magnitude acceleration (~ 1000 m a^{-1}) and glacier

advance (0.8 km: Figure 3.7c). This glacier fits the conventional definition of surging, i.e. a short active phase, which included an order of magnitude increase in velocity. However, it has a short surge-cycle (< 10 years) compared to most other glaciers in the Arctic, and underwent overall retreat from the late 1980s to 2015 (Figure 3.6). This suggests that despite short-lived surge events, recent climate-ocean forcing may be altering its cyclical behaviour.

Finally, we draw attention to Ryder Glacier as it appears to be behaving dissimilarly to the rest of the study glaciers in northern Greenland. It too has been referred to as surge-type in the past [Joughin *et al.*, 1996b, 1999; Rignot *et al.*, 2001], and has shown some surge-like behaviour during the study period (1948–2015): several cycles of advance (~ 7 -years) and retreat (2-years), and some acceleration during advance. Additionally, previous studies also identified near-terminus thinning ($2\text{--}4\text{ m a}^{-1}$: 1997 to 1999) and, at ~ 50 km inland, a similar magnitude of thickening [Abdalati *et al.*, 2001], which is indicative of the quiescent phase of surge-type glaciers [Kamb *et al.*, 1985; Meier & Post, 1969; Sharp, 1988]. However, the behaviour of Ryder Glacier appears to be more characteristic of a tidewater glacier cycle, which may be controlled by basal topography. In contrast to the role of basal topography at most other outlet glaciers in northern Greenland (i.e. unstable retreat down inland sloping beds), a large basal ridge (Figure 3.11i) or terminal moraine/moraine shoal at Ryder Glacier may have promoted periods of glacier advance [Alley, 1991; Nick *et al.*, 2007; Powell, 1990]. Nevertheless, further investigation on the cyclic nature and precise controls on Ryder Glaciers' dynamic behaviour is needed.

3.6 Conclusions

Outlet glaciers in northern Greenland drain $\sim 40\%$ of the ice sheet by area but remain understudied compared to other regions of the ice sheet. We have analysed the dynamics of 18 major marine-terminating outlet glaciers in northern Greenland between 1948 and 2015. Overall, long-term glacier retreat rates ranged from -15 to -311 m a^{-1} over the entire study period. Between 1948 and 1995 glaciers exhibited generally low magnitude advance and retreat, with an average frontal position change of $+72\text{ m a}^{-1}$ (advance) across the 18 study glaciers. Following this, there was a regional transition to more rapid and widespread retreat, when average frontal position change was -445 m a^{-1} (1995 to 2015). This was coincident with accelerated retreat in other regions of the ice sheet [Carr *et al.*, 2013b; Howat *et al.*, 2008; Howat & Eddy, 2011]. From 1996 to 2015, most glaciers also experienced accelerated ice flow and increased dynamic thinning.

While increased retreat rates from the mid-1990s were near-ubiquitous, we observe distinct differences in glacier behaviour depending on whether the terminus is grounded or floating. Three factors play a role in the dynamic behaviour of these two types of glacier; i) different methods of calving (i.e. continuous small magnitude calving vs large episodic calving); ii) differences in resistive stresses at the terminus; iii) glacier geometry. Continuous retreat into deep fjords at grounded-terminus glaciers led to a greater reduction in basal/lateral resistive stresses, and caused high magnitude acceleration and dynamic thinning. In contrast, large episodic calving events, from unconfined ice tongues that provided little lateral resistance meant that most glaciers with floating ice tongues appear dynamically insensitive to the retreat of their terminus. We note there are exceptions; continuous ice tongue retreat at Zachariæ Isstrøm caused prolonged acceleration and thinning, and several glaciers with ice tongues went through cycles of advance and retreat during the study record (e.g. Ryder Glacier). At Zachariæ Isstrøm this can be explained by the method of glacier calving (continuous rather than episodic), and a deep wide fjord that promoted unstable retreat. Glacier advance can be explained by surging, or topographic controls which allow cyclic advance and retreat. We provide further evidence for surging at three glaciers (Harald Moltke Bræ, Storstrømmen and L. Bistrup Bræ) in northern Greenland, and an explanation for the cyclic behaviour of Ryder Glacier, which is likely related to topographic controls (e.g. moraine shoal), that allowed the re-advance of the terminus. While we have shown that northern Greenland has begun to undergo rapid dynamic change over the last two decades (1996 to 2015), we highlight variability between individual glaciers and the importance of considering terminus type and glacier geometry (basal topography, fjord width and ice tongue confinement) when considering future glacier response to climate change across this region of the ice sheet. Currently, ice tongue retreat does not appear to substantially affect inland ice dynamics. However, once these glaciers become grounded, they may accelerate, thin, and increase the volume of grounded ice discharge into the ocean.

Chapter 4

Velocity response of Petermann Glacier, northwest Greenland to past and future calving events

4.1 Chapter summary

Dynamic ice discharge from outlet glaciers across the Greenland ice sheet (GrIS) has increased since the beginning of the 21st century. Calving from floating ice tongues that buttress these outlets can accelerate ice flow and discharge of grounded ice. However, little is known about the dynamic impact of ice tongue loss in Greenland compared to ice shelf collapse in Antarctica. The rapidly flowing ($\sim 1000 \text{ m a}^{-1}$) Petermann Glacier in north-west Greenland has one of the ice sheet's last remaining ice tongues, but it lost $\sim 50\text{-}60\%$ ($\sim 40 \text{ km}$ in length) of this tongue via two large calving events in 2010 and 2012. The glacier showed a limited velocity response to these calving events, but it is unclear how sensitive it is to future ice tongue loss. This chapter addresses the third objective of this thesis and the primary motivation was to assess the sensitivity of a large outlet glacier in northern Greenland (Petermann Glacier) to changes in the extent of its floating ice tongue. To assess this sensitivity, I use an ice flow model ($\dot{U}a$) to perform a series of numerical modelling experiments that instantaneously removed large sections of the tongue and calculated the velocity change, due to a loss of buttressing. This chapter was published as a journal paper in *The Cryosphere* in December 2018 (see reference below), in which I carried out all the analysis, produced all the figures, and wrote the manuscript.

Co-authors helped to develop the research ideas, and provided editorial input.

HILL, E. A., GUDMUNDSSON, G. H., CARR, J. R. & STOKES, C. R. 2018*b* Velocity response of Petermann Glacier, northwest Greenland, to past and future calving events. *Cryosphere* **12** (12), 3907–3921

The results of these experiments confirm that the glacier was dynamically insensitive to large calving events in 2010 and 2012 ($<10\%$ annual acceleration). We then simulate the future loss of similar sized sections to the 2012 calving event (~ 8 km long) of the ice tongue back to the grounding line. We conclude that thin soft sections of the ice tongue >12 km away from the grounding line, provide little frontal buttressing, and removing them is unlikely to significantly increase ice velocity or discharge. However, once calving removes ice within 12 km of the grounding line, loss of these thicker and stiffer sections of ice tongue could perturb stresses at the grounding line enough to substantially increase inland flow speeds (~ 900 m a^{-1}), grounded ice discharge, and Petermann Glacier’s contribution to global sea level rise.

4.2 Introduction

Dynamic ice discharge from marine-terminating outlet glaciers is an important component of recent mass loss from the Greenland Ice Sheet (GrIS) [van den Broeke *et al.*, 2016; Enderlin *et al.*, 2014]. Since the 1990s, tidewater outlet glaciers in Greenland have been thinning [Pritchard *et al.*, 2009; Krabill *et al.*, 2000], retreating [e.g. Carr *et al.*, 2017*b*; Jensen *et al.*, 2016; Moon & Joughin, 2008], and accelerating [Joughin *et al.*, 2010*b*; Moon *et al.*, 2012], in response to climate-ocean forcing. Marine-terminating glaciers are influenced by ocean warming [e.g. Holland *et al.*, 2008; Mouginot *et al.*, 2015; Straneo *et al.*, 2013], increased surface air temperatures [Moon & Joughin, 2008], and reduced sea ice concentration in the fjords [Amundson *et al.*, 2010; Shroyer *et al.*, 2017; Reeh *et al.*, 2001]. However, glacier response to ocean-climate forcing is highly variable between regions and between individual glaciers, due to differences in glacier topography and fjord geometry [e.g. Bunce *et al.*, 2018; Carr *et al.*, 2013*b*; Porter *et al.*, 2014]. Moreover, changes at the terminus of these glaciers (i.e. calving or thinning), can reduce basal and lateral resistance which alters the force balance at the terminus, and causes inland ice flow to accelerate. Indeed, 21st century retreat at two large outlet glaciers in south-east Greenland (Heilheim and Kangerdlugssuaq) was followed by acceleration and ice surface thinning [Howat *et al.*, 2005, 2007; Nick *et al.*, 2009].

Floating ice shelves or tongues that extend out from outlet glacier grounding lines can also control a glacier’s response to calving events [Schoof *et al.*, 2017]. Floating ice adjacent to the glacier grounding line can buttress inland ice, depending on the amount of shear and lateral resistance provided along the ice shelf margins [Pegler, 2016; Pegler *et al.*, 2013; Haseloff & Sergienko, 2018]. Consequently, thinning and retreat of ice shelves can reduce backstress, which can perturb the stresses at the grounding line and propagate increases in driving stress inland causing accelerated ice flow. Understanding how glaciers may respond to ice shelf loss is therefore important for estimating future flow speeds and, ultimately, their increased contributions to grounded ice discharge and global sea level rise. Considerable work has focused on the role of buttressing ice shelves on grounded ice dynamics in Antarctica [e.g. Schoof, 2007; Gudmundsson *et al.*, 2012; Goldberg *et al.*, 2009; Reese *et al.*, 2018b], but less work has been done on floating ice tongues in Greenland, where large calving events have recently taken place [Hill *et al.*, 2017; Box & Decker, 2011; Rignot *et al.*, 2001].

One of the last remaining ice tongues in Greenland is at Petermann Glacier, northwest Greenland. Petermann Glacier is fast flowing ($\sim 1000 \text{ m a}^{-1}$; Figure 4.1), and drains approximately 4% of the GrIS by area [Rignot & Kanagaratnam, 2006; Hill *et al.*, 2017]. Mass loss is predominantly via high melt rates ($10\text{-}50 \text{ m a}^{-1}$) beneath the ice tongue [Rignot & Steffen, 2008; Wilson *et al.*, 2017], and also occurs via large episodic calving events [Johannessen *et al.*, 2013]. Formerly the glacier terminated in a 70 km long floating ice tongue, but two well-documented large calving events in 2010 and 2012 removed ~ 40 km of the tongue [Johannessen *et al.*, 2013; Nick *et al.*, 2012; Falkner *et al.*, 2011; Münchow *et al.*, 2014]. Contrary to the behavior of glaciers terminating in floating ice elsewhere, large calving events at Petermann Glacier were noted to be followed by minimal glacier acceleration ($< 100 \text{ m a}^{-1}$) [Nick *et al.*, 2012; Münchow *et al.*, 2014, 2016; Ahlstrøm *et al.*, 2013], suggesting that calving from the seaward parts of the ice tongue appear to have limited impact on flow upstream of the grounding line.

Several ice tongues have been lost from neighboring glaciers in northern Greenland since the early 2000s (C. H. Ostenfeld, Zachariæ Isstrøm, Hagen Bræ: Rignot *et al.* 2001; Hill *et al.* 2017; Mouginot *et al.* 2015), and with Arctic air and ocean temperatures predicted to increase in a warming climate [Gregory *et al.*, 2004], the question remains: at what point will Petermann Glacier lose its ice tongue and how might its complete removal impact on ice dynamics? Petermann’s tongue has been retreating from the end of the fjord (~ 90 km from the present grounding line) since the beginning of the Holocene [Jakobsson *et al.*, 2018] and currently resides at its most retreated position in recent history [Jakobsson *et al.*, 2018; Falkner *et al.*, 2011; Hill *et al.*, 2018a]. More recently (2016), another large

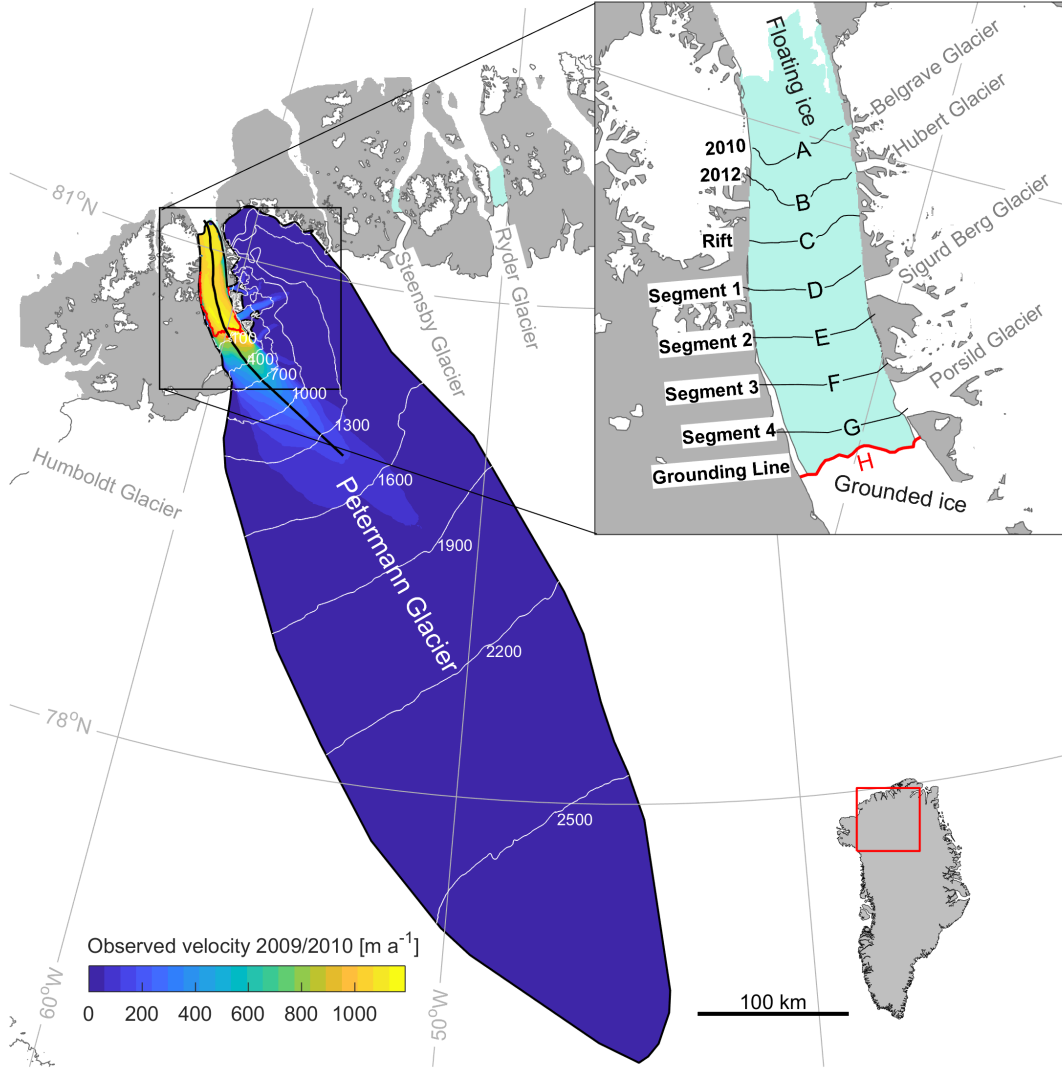


Figure 4.1: Study location, Petermann Glacier, northwest Greenland. Observed ice speeds from the MEaSUREs program (winter 2009/10: Joughin *et al.* 2010b) across the Petermann Glacier catchment, which corresponds with the model domain. White lines show 300 m ice surface contours across the catchment. The thick black line is the glacier centerline and the thick red line is the glacier grounding line. Inset shows the location of newly prescribed terminus positions for each diagnostic perturbation experiment (A-H). Light green shows floating ice, and white is grounded ice.

rift formed across the ice tongue [Münchow *et al.*, 2016], suggesting another large calving event is imminent. As Petermann Glacier is fast flowing and drains a large area of the GrIS ($\sim 4\%$), it has the potential to contribute to increased ice discharge and ultimately sea level rise, once it becomes grounded. Here, we attempt to answer the question: at what point do large calving events from the Petermann ice tongue cause substantial acceleration (i.e.

$> 100 \text{ m a}^{-1}$ that propagates inland of the grounding line) and increased ice discharge? To do this we use the community finite-element ice flow model $\dot{U}a$ [Gudmundsson *et al.*, 2012] to:

- i). Infer the stress conditions beneath the glacier catchment and along the ice tongue walls
- ii). Test whether the recent small changes in velocity following calving events in 2010 and 2012 can be replicated
- iii). Assess the future response (acceleration and ice discharge) of Petermann Glacier to further calving events, and eventual entire loss of the remainder of the ice tongue (Figure 4.1)

First, we initialize the model using observational datasets of surface and basal topography. We then invert observed ice velocities prior to the 2010 calving event to determine the initial basal conditions (slipperiness and rheology of the ice). Finally, we perform a series of diagnostic perturbation experiments where we remove sections of the Petermann Glacier ice tongue and assess the instantaneous glacier acceleration and increase in grounding line ice flux.

4.3 Methodology

4.3.1 Data Input

To initialize the model, we used several observational datasets of glacier geometry and ice velocity. Ice surface topography of Petermann Glacier was taken from the GrIS Mapping Project (GIMP) Digital Elevation Model (DEM) [Howat *et al.*, 2014]. The surface topography was also used to calculate the surface drainage catchment, using flow routing hydrological analysis in the MATLAB TopoToolbox [Schwanghart & Kuhn, 2010]. The defined catchment is $\sim 85,000 \text{ km}^2$, extends approximately 550 km inland of the grounding line, and encompasses the tributary glaciers flowing into the east side of the Petermann Glacier ice tongue (Figure 4.1). Ice thickness and basal topography were taken from the Operation IceBridge BedMachine v3 dataset [Morlighem *et al.*, 2017]. These data were generated from radar ice thicknesses, ice motion, and the mass conservation method, to resolve the basal topography and ice thickness of the GrIS [Morlighem *et al.*, 2017]. This

version also includes high resolution bathymetry of Petermann Glacier fjord seaward of the ice tongue [Jakobsson *et al.*, 2018; Morlighem *et al.*, 2017]. All three topographic datasets have a resolution of 150 m, and a nominal date of 2007, which precedes the large calving event in 2010.

Firstly, to initialize the model via inversion (see Section 4.3.3), we required annual ice velocities prior to the first experiment, which is the calving event in 2010 (Table 4.1). These were taken from winter 2009/10 from the Greenland MEaSUREs dataset (Table 4.1: Joughin *et al.* 2010b). This dataset has a resolution of 500 m, and an average error of 8 m a^{-1} across the entire Petermann catchment, which increases to 18 m a^{-1} along the floating ice tongue (Table 4.1). To validate the modeled velocity changes in response to calving events in both 2010 and 2012, we required observed velocities from the years preceding and succeeding these events. Velocities from winter 2009/10 (used for inversion), also acted as the baseline velocities that we compared with observed velocities after each calving event. However, Greenland wide velocities for the winter following the 2010 calving event (2010/11) were not readily available. Instead a series of datasets exist that cover select regions of the ice sheet, derived from feature- or intensity-tracking of optical Landsat imagery [Howat, 2017; Rosenau *et al.*, 2015], or synthetic aperture radar (SAR) imagery [Joughin *et al.*, 2010b]. We do not use optical Landsat 7 ETM+ derived velocities, because their coverage is restricted to mid-summer, which may reflect seasonal speedups rather than the inter-annual impact of large calving events on ice velocity. Additionally, Landsat derived velocities may have errors associated with cloud cover and or the scanning line correction image banding from May 2003 onwards. Instead, we used a combination of SAR derived velocities (TSX and PALSAR) which are not limited to the summer months, and benefit from higher resolution, and more frequent repeat pass imagery (Table 4.1). High resolution TSX imagery (100 m) was acquired from the MEaSUREs program [Joughin *et al.*, 2010b], but is limited to 11-45 km inland of the grounding line at Petermann Glacier. To supplement this we also used PALSAR derived velocities (Table 4.1: Nagler *et al.* 2016), which provided additional coverage along the western half of the floating ice tongue. Average errors across the catchment are 4 m a^{-1} and 16 m a^{-1} for TSX and PALSAR respectively (Table 4.1). Greenland wide, winter 2012/13 (post-2012 calving event) velocities were also acquired from the MEaSUREs program (Table 4.1: Joughin *et al.* 2010b).

To determine observed velocity change, we differenced velocity fields after each calving event (2010/11 and 2012/13) from initial baseline velocities (2009/10) (Figure 4.2). For 2009/10 to 2010/11 speedup along the ice tongue averaged 29 m a^{-1} , but further inland of the grounding line, noisy and unphysical velocity differences (Figure 4.2) indicate that

| Dataset | Year | Sensor(s) | Resolution (m) | Catchment Error (m) | Use |
|--|---------|--------------------------------------|----------------|----------------------|--|
| MEaSURES Greenland wide winter velocity NSIDC ^a | 2009/10 | ALOS TerraSAR-X | 500 | 8 m a ⁻¹ | Model inversion Baseline initial velocities |
| MEaSURES Greenland Ice Velocity: Selected Glacier Site Velocity Maps from NSIDC ^a | 2010/11 | TerraSAR-X | 100 | 4 m a ⁻¹ | Validate modeled change post-2010 calving |
| ESA GrIS CCI project IV Greenland margin winter velocities ^b | 2010/11 | PALSAR | 500 | 16 m a ⁻¹ | Validate modeled change post-2010 calving |
| MEaSURES Greenland wide winter velocity NSIDC ^a | 2012/13 | RADARSAT-1 TerraSAR-X TanDEM-X | 500 | 3 m a ⁻¹ | Validate modeled change post-2012 calving |

Table 4.1: Velocity data sources for Petermann Glacier. ^a is from [Joughin *et al.*, 2010b] and ^b is from [Nagler *et al.*, 2016]

there was no coherent velocity change, and it is unlikely velocity changes propagated far inland. For clarity we present centerline velocity profiles in Figure 4.3, which show that increases in speed were limited to the lower portions of the ice tongue. Observed velocity estimates presented here after the calving event in 2010, are within the range of previous studies, which showed a 30-125 m a⁻¹ speed increase along the ice tongue [Johannessen *et al.*, 2013; Nick *et al.*, 2012; Münchow *et al.*, 2016], and limited change further inland [Nick *et al.*, 2012]. After the calving event in 2012, velocity increases averaged 79 m a⁻¹ along the ice tongue, and propagated further towards the grounding line (Figures 4.2 and 4.3).

4.3.2 Model Initialization

To model the response of Petermann Glacier to ice tongue loss we used the finite-element model $\dot{U}a$ [Gudmundsson *et al.*, 2012]. $\dot{U}a$ solves equations of ice dynamics using the shallow ice-stream approximation (SSA) [MacAyeal, 1989; Morland, 1987], a Weertman-sliding law, and Glen’s flow law. The momentum equation of the vertically integrated SSA can be written in the form

$$\nabla_{xy} \cdot (h\mathbf{T}) - \tau_{bh} = \rho_i g h \nabla_{xy} s + \frac{1}{2} g h^2 \nabla_{xy} \rho_i, \quad (4.1)$$

where

$$\nabla_{xy} = (\partial_x, \partial_y)^T, \quad (4.2)$$

and \mathbf{T} is the resistive stress tensor defined as

$$\mathbf{T} = \begin{pmatrix} 2\tau_{xx} + \tau_{yy} & \tau_{xy} \\ \tau_{xy} & \tau_{xx} + 2\tau_{yy} \end{pmatrix}. \quad (4.3)$$

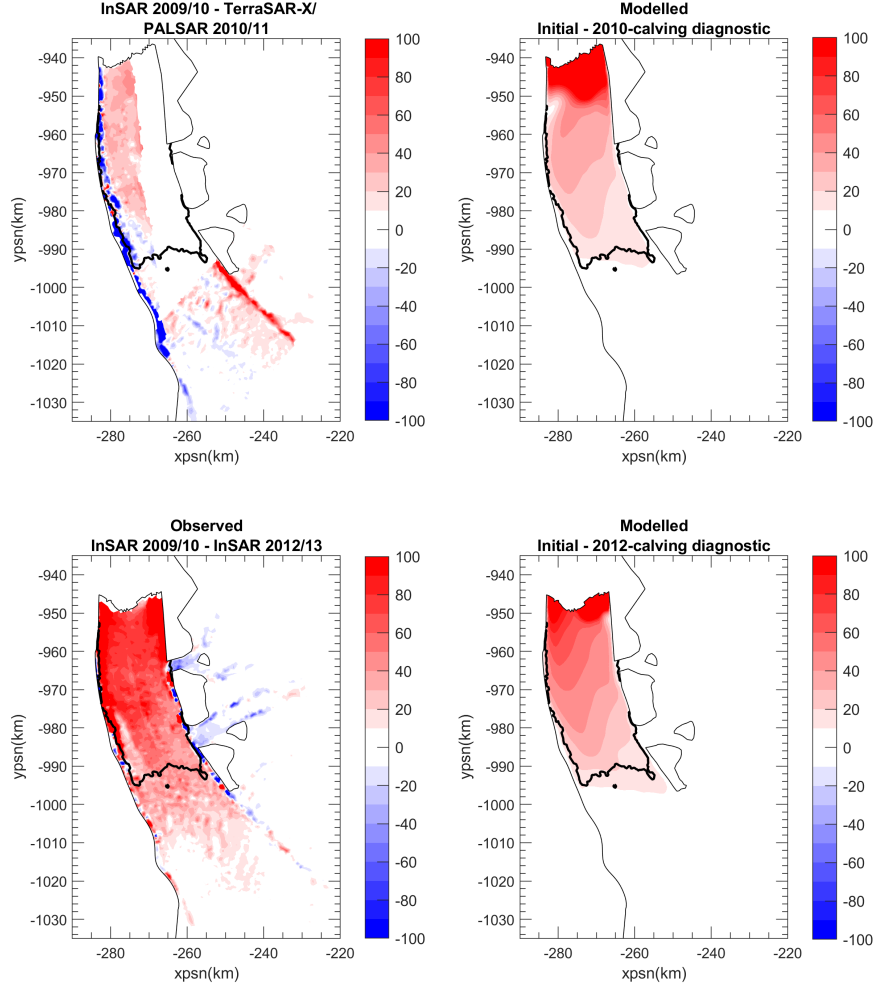


Figure 4.2: Spatial distribution of observed and modeled changes in flow speeds across the Petermann Glacier ice tongue after calving events in 2010 and 2012. Left two plots show the observed changes in speed between initial pre-calving observed speed (winter 2009/10, MEaSUREs Joughin *et al.* [2010b]) and observed speeds after the 2010 calving event (top) and 2012 calving event (bottom). Right hand plots show the corresponding modeled change in speed between initial modeled flow speeds and speeds after removing sections of the ice tongue in 2010 (top) and 2012 (bottom). xpsn and yposn are x and y kms in polar stereographic north projection, respectively

In the above equation s is the surface topography, h is the ice thickness, p_i is vertically averaged ice density, g is the gravitational acceleration, and τ_{bh} is the horizontal part of the bed-tangential basal traction τ_b .

$\dot{U}a$ has been previously used to understand glacier behavior following ice shelf loss in Antarctica [De Rydt *et al.*, 2015], and ice tongue collapse at the NEGIS [Rathmann *et al.*, 2017]. It has also been used to assess the impact of buttressing ice shelves around

Antarctica [Reese *et al.*, 2018a]. Previous modeling studies at Petermann Glacier have been conducted using a one-dimensional flowline approach [Nick *et al.*, 2012]. Here we aim to expand on earlier work at Petermann to assess if $\dot{U}a$, a two horizontal dimensional, vertically integrated approach, can also replicate the observed velocity response to calving events in 2010 and 2012, and then be used to estimate the impact of future calving events on ice flow and discharge. This model is advantageous over a flowline approach, as it allows us to account for stresses in both horizontal dimensions, which can better assess the impact of ice shelf changes on the force balance at the glacier grounding line [Gudmundsson, 2013].

To set-up the model, we used the surface velocity catchment (Figure 4.1) as the outer computational boundary, and imposed Dirichlet (essential) boundary conditions by fixing velocities to zero inland of the ice divide. Nunataks and rock outcrops along the east side

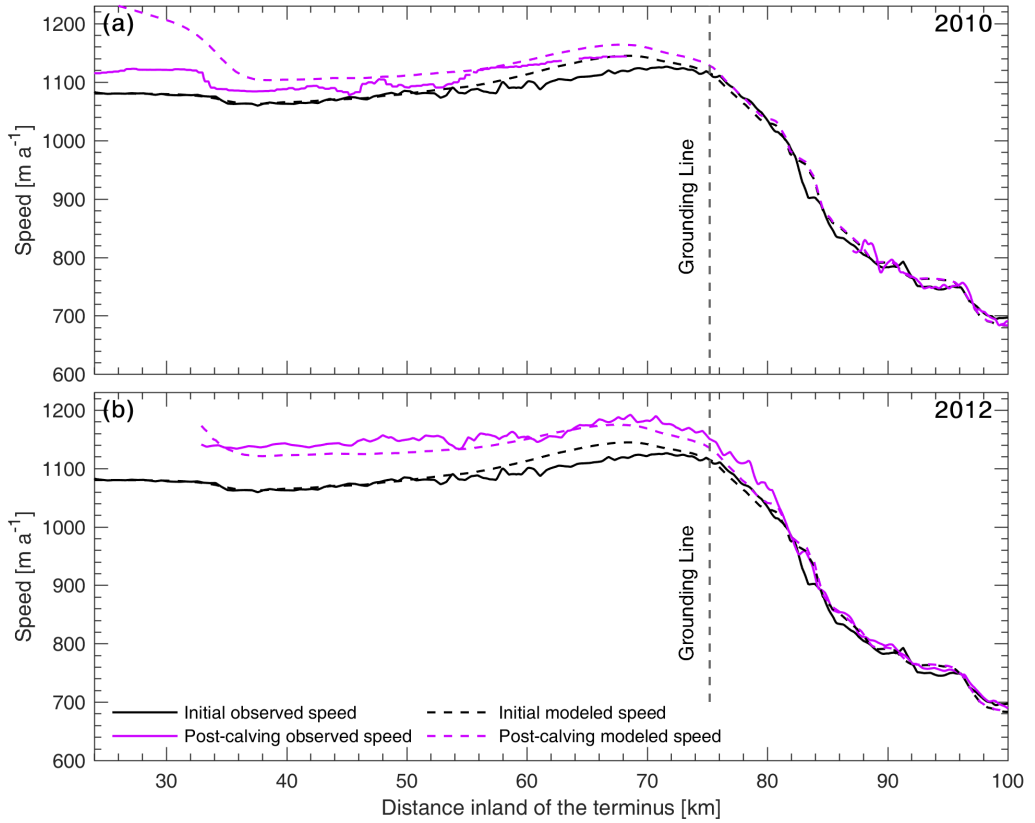


Figure 4.3: Observed and modeled velocities along the Petermann Glacier centerline before and after calving events in 2010 **a)** and 2012 **b)**. Observed initial speed (MEaSURES InSAR winter 2009/10) is shown with a solid black line. Observed post-calving speeds after the 2010 calving event (PALSAR and TerraSAR-X winter 2010/11) and the 2012 calving event (MEaSURES InSAR winter 2012/13) are shown with solid purple lines. Modeled initial speeds are shown in dashed black, and speeds after each respective modeled calving event are shown in dashed purple. Note the small change in both observed and modeled velocities, particularly inland of the grounding line.

of the ice tongue were digitized using Landsat 8 imagery and treated as holes within the mesh. Ice velocities along the nunataks' boundaries were set to zero, i.e. no-slip boundary condition. Initially, it was less clear what type of boundary condition to impose along the margins of the ice-shelf where it is in contact with the side walls. We began by imposing a free-slip boundary condition along the ice tongue margins, but conducted further runs with no-slip boundary conditions along the side walls to determine which boundary conditions were most appropriate (see Section 4.3.4).

The initial calving front boundary was the location of the terminus in 2009, digitized from Landsat 7 ETM+ imagery, and in all cases a Neumann (natural) boundary condition was imposed along the terminus. Using this computational domain, and the finite element mesh generator *Gmsh* [Geuzaine & Remacle, 2009], we generated a high resolution mesh, with 58,000 linear (3-node) elements, and $\sim 30,000$ nodes (Figure 4.4). The unstructured mesh capabilities of *Úa* allowed us to refine the mesh based on the observed velocity field. Where ice speeds are fastest ($> 500 \text{ m a}^{-1}$), primarily along the ice tongue, element sizes are 0.75 km, whereas element sizes inland have a maximum size of 2.7 km. Overall the mean element size is 1.52 km, with a median of 1.4 km. We also increased the mesh resolution of the slower flowing ($< 500 \text{ m a}^{-1}$) tributary glaciers to the east of the Petermann Glacier ice tongue to 0.75 km. Topographic datasets (surface, bed, and ice thickness), and pre-calving observed ice velocities (winter 2009/10) were mapped onto this mesh using linear interpolation.

4.3.3 Model Inversion

Before modeling changes in the flow speed of Petermann Glacier due to perturbations in the calving front position, we must first estimate the prior stress conditions. We used *Úa* to invert the known velocity field (winter 2009/10) before the calving event to estimate the basal slipperiness (C) and ice rate factor (A) across the catchment. We simultaneously invert for parameters of C and A . To estimate these parameters, *Úa* uses a standard methodology whereby a cost function involving a misfit term and a regularization term is minimized. The gradients of the cost function with respect to A and C are determined in a computationally efficient way using the adjoint method. Here we used Tikhonov regularization involving both amplitude and spatial gradients of A and C . Values of regularization parameters were varied by orders of magnitude between 1 and 10,000, and then within range. We also experimented with different sliding law exponent values of m (1,2,3,4,5,7,9) and found the results of the diagnostic experiments to be insensitive to the value of m (see Figure B.1). We set the stress exponent in Glen's Flow law to $n = 3$.

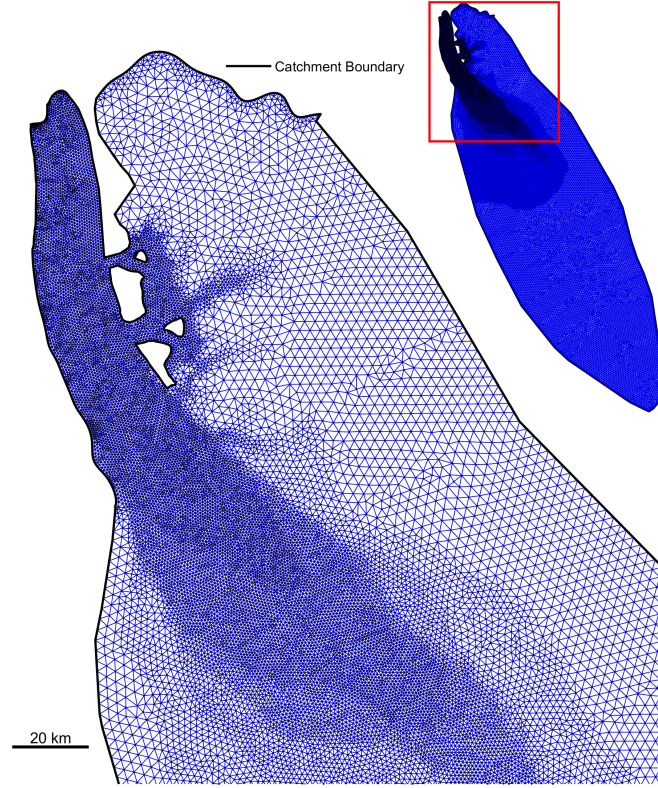


Figure 4.4: Finite element mesh for Petermann Glacier. The inset shows the mesh across the entire Petermann catchment and the red square highlights the areas shown in the main figure. Element sizes are smallest in the areas of fastest flow (see Figure 4.1), and larger towards the slower flowing inland regions of the glacier catchment. The thick black line is the model domain.

To begin with, we inverted the model using a fixed zero velocity condition along the outer catchment boundary only, and we allowed the Petermann Glacier ice tongue to have free-slip boundary conditions (Section 4.3.2). In the following section we discuss two additional inversion experiments where we varied the boundary conditions along the ice tongue. The model was inverted until the misfit converged which was after 120 iterations. Resultant model velocities (U_{mod}) are in good agreement with observations (U_{obs}) as shown in Figure 4.5. The mean percentage difference between observed and modeled velocities is 26%, which equates to an absolute difference of 11 m a^{-1} (Table 4.2). Absolute mean velocity difference increases to 28 m a^{-1} in areas flowing faster than 300 m a^{-1} and to 66 m a^{-1} along the floating ice tongue, which is only 7% of the average ice tongue speed (967 m a^{-1}). Flow velocities are not well resolved along the far north-eastern tributary glacier which is due to thin ice thicknesses and poorly resolved bed topography from interpolation (errors of $\sim 150 \text{ m}$).

By inverting the known velocity field (winter 2009/10), we can infer the basal con-

ditions beneath Petermann Glacier. To our knowledge, a catchment scale assessment of the basal slipperiness and ice stiffness has not been previously documented for this region. Some studies have examined the basal thermal state [MacGregor *et al.*, 2016; Chu *et al.*, 2018], or provided Greenland wide slipperiness estimates [Lee *et al.*, 2015]. However aside from these, little is known on the stress conditions of Petermann Glacier. Here, we provide a new record of the basal conditions beneath Petermann Glacier, which are important for understanding dynamic glacier behavior. For the initial inversion, the distribution of basal slipperiness (C), ice rate factor (A), and the misfit between observed and modeled velocities are shown in the first line of Figure 4.6. Basal slipperiness was on average two orders of magnitude greater within 10 km of the grounding line ($C \approx 7.2 \times 10^{-2} \text{ m a}^{-1} \text{ kPa}^{-3}$) than the rest of the grounded glacier catchment (mean $C \approx 1.47 \times 10^{-4} \text{ m a}^{-1} \text{ kPa}^{-3}$; Figure 4.6). Grounded ice across the Petermann catchment is on average stiffer ($A \approx 1.2 \times 10^{-8} \text{ a}^{-1} \text{ kPa}^{-3}$) than along the ice tongue ($A \approx 7.4 \times 10^{-8} \text{ a}^{-1} \text{ kPa}^{-3}$). However, the misfit between observed and modeled velocities is highest along the ice tongue (Figure 4.6g), which suggests that ice rheology parameter (A) may not reflect the true stress conditions along the ice tongue. The distribution of basal slipperiness and ice rheology parameter (A) for the initial inversion are discussed in more detail in the following section.

4.3.4 Boundary Conditions

In an attempt to improve the misfit between observed and modeled velocities, and accurately replicate the lateral resistive stresses along the ice tongue margins, we conducted

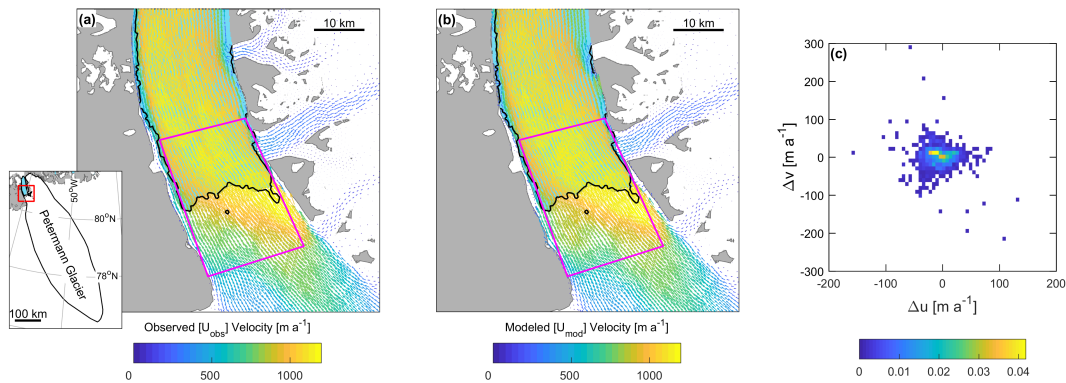


Figure 4.5: Observed (U_{obs}) winter velocities 2009/10 (a) in the proximity of the grounding line, (b) Modeled (U_{mod}) velocities. (c) shows a normalized bivariate histogram of the velocity residuals which are the difference between modeled and observed velocities in the vicinity of the grounding line (magenta). $\Delta u = u_{\text{mod}} - u_{\text{obs}}$ and $\Delta v = v_{\text{mod}} - v_{\text{obs}}$. u and v are x and y components of the velocity vectors, respectively.

| Boundary Condition Scenario | Mean percentage difference (%) | Mean velocity difference (m a ⁻¹) | Mean velocity difference (>300 m a ⁻¹) | Mean velocity difference ice tongue (m a ⁻¹) |
|--|---|--|---|--|
| 1. Natural ice tongue boundary | 26 | 11 | 28 | 66 |
| 2. Fixed west ice tongue margin to zero | 24 | 12 | 34 | 77 |
| 3. Fixed both ice tongue margins to zero | 20 | 9.4 | 25 | 51 |

Table 4.2: Misfit between observed and modeled velocity for each boundary condition scenario

runs with both no-slip and free-slip boundary conditions along the side walls. We then tested which produced the best fit to observed velocities. Alongside the additional inversion (Scenario 1), where no velocity condition was imposed along the ice tongue margins, we inverted the model using two further sets of boundary conditions. These are: Scenario 2) fixed velocities along the western margin of the ice tongue to zero (no-slip) and leave the east margin as free-slip, Scenario 3) fixed velocities to zero (no-slip) along both margins of the floating ice tongue. We then based the assessment of these boundary condition scenarios on three criteria: i) the misfit between observed and modeled velocities, ii) observations of the confinement and attachment of the ice tongue to the fjord walls in satellite imagery (i.e. heavy rifting or not), iii) the ability of each set of boundary conditions to replicate the observed velocity response following the 2010 calving event. The former two criteria are discussed in this section, and the third criterion is discussed alongside the model experiments in the following section (Section 4.3.5). As before, we perform each inversion for 120 iterations until the misfit has converged, and use the same values of: m , n , and regularization parameters for each scenario. The slipperiness (C), ice rate factor (A) and misfit distributions ($|U_{\text{obs}}| - |U_{\text{mod}}|$) are shown for each boundary condition scenario in Figure 4.6. Mean misfits between observed and modeled velocities for each scenario are in Table 4.2.

Slipperiness values showed a similar spatial distribution across all boundary condition scenarios, i.e. increasing towards the grounding line and decreasing further inland (Figure 4.6 a-c), and do not vary substantially within 10 km of the grounding line (range: $(3.8 - 7.2) \times 10^{-2} \text{ m a}^{-1} \text{ kPa}^{-3}$) or across the entire grounded catchment (range: $(1.47 - 2.18) \times 10^{-4} \text{ m a}^{-1} \text{ kPa}^{-3}$). In contrast, spatial variations in ice stiffness (A) were more obvious between each scenario, which corresponds to differences in the misfit distributions (Figure 4.6). Average A values along the ice tongue varied by three orders of magnitude between scenarios 1 ($A \approx 7.4 \times 10^{-8} \text{ a}^{-1} \text{ kPa}^{-3}$) and 3 ($A \approx 1.4 \times 10^{-5} \text{ a}^{-1} \text{ kPa}^{-3}$). Scenarios 1 and 2 show stiff ice across the entire ice tongue, which does not reflect the stiff ice tongue center and weaker margins we would expect from lateral reductions in longitudinal strain rates and ice velocity associated with shearing along the fjord walls [Raymond, 1996]. In

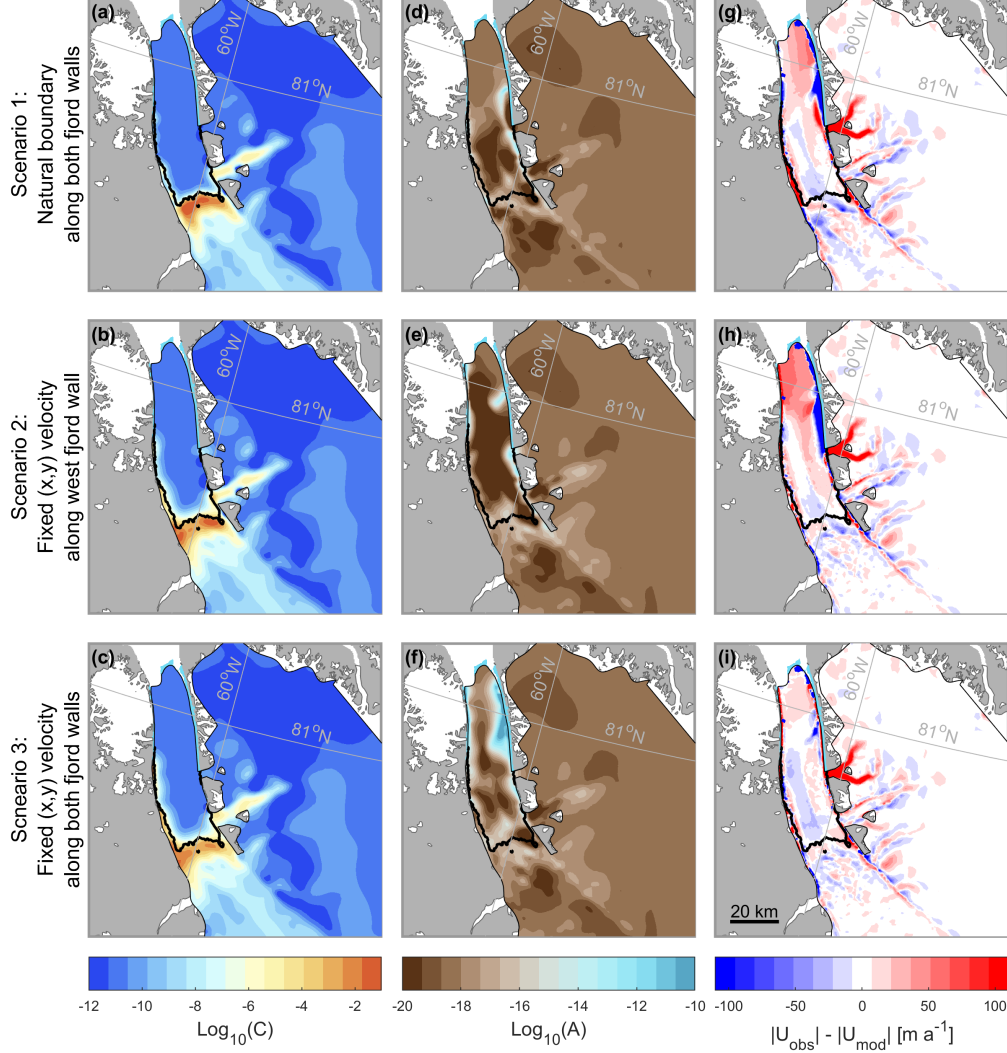


Figure 4.6: Inversion experiments using three sets of boundary conditions along the floating ice tongue. **a-c** show logarithmic calculated basal slipperiness (C) for boundary condition Scenarios 1 to 3 respectively, where orange represents highly slippery areas. Glen's flow law rate factor A (**d-f**), where light blue represents soft ice, and brown is stiff ice. The final column (**g-i**) is the absolute difference between observed (U_{obs}) and modeled velocities (U_{mod}) after inversion using each set of boundary conditions.

both cases, velocities do not well reproduce observations along the lateral margins and lower portion of the ice tongue (criterion i: Figure 4.6 g-h).

In contrast, areas of softer ice ($A \approx 4.6 \times 10^{-5} \text{ a}^{-1} \text{ kPa}^{-3}$) exist along the lateral margins of the lower portion of the ice tongue (Figure 4.6f) when we used a no-slip boundary condition along both ice tongue margins during inversion (Scenario 3). In accordance with previous studies [Nick *et al.*, 2012] and our own observations of satellite imagery, this repli-

cates the apparent weak attachment of floating ice to the fjord walls in the lower/eastern parts of the tongue prior to the 2010 calving event (criterion ii). In Scenario 3, overall mean percentage difference between U_{obs} and U_{mod} was also improved by 6% and absolute difference reduced by 15 m a^{-1} along the ice tongue (Table 4.2). We found that by imposing a no-slip boundary condition along both side-walls of the ice tongue (Scenario 3) allowed the inversion procedure to automatically resolve the weak margins of the tongue. Based on criteria i and ii, this Scenario (3) therefore provides the most realistic distribution of ice softness along the ice tongue (criterion ii) and the best model fit to observed velocities (criterion i). These experiments have shown the importance of considering boundary conditions, particularly along floating ice margins in this study, for accurately determining lateral resistive stresses and replicating the observed velocity field.

4.3.5 Model Experiments

Following model initialization and inversion, we performed a series of diagnostic experiments (Figure 4.1) that perturb the calving front position to replicate previous large calving events and potential future loss from the Petermann Glacier ice tongue. We then examine the instantaneous velocity change with respect to the initial modeled velocities. As the focus of this paper is the impact of large calving events on glacier velocity, we do not incorporate ice loss via surface and/or basal melting. For each perturbation experiment, we removed all elements from the mesh downstream of the new calving front position, and mapped all topographic datasets onto the new mesh. We then performed a forward-diagnostic model run, which solves the shallow ice-stream equations (see Eq. 4.1) independent of time. In each case, the model is restarted from the previous experiment set up. During all experiments, grounding line position, boundary conditions, and ice thickness remained fixed. We also use initially inverted parameters of basal slipperiness and ice rheology as inputs to all experiments. We acknowledge that in reality there is likely to be a period of relaxation and geometric adjustment after each individual calving event. Thus, by performing these sequential calving experiments in a diagnostic time-independent mode, we are modeling the immediate velocity change in response to a perturbation in buttressing at the terminus. We therefore do not allow any relaxation/adjustment or deviation from initial stress conditions (slipperiness or rheology) in between subsequent events. It is therefore possible that these estimates of ice flow and discharge may be higher than the transient glacier response over longer timescales.

We started by removing sections of the ice tongue that calved in 2010 and 2012 (Figure 4.1), for which the new terminus positions were digitized from Landsat ETM+ imagery

from 31st August and 21st July respectively. We then assumed that the next iceberg to calve from the tongue will follow the path of the rift that formed in 2016. Then, we estimated the glacier response to future calving events, following two assumptions: i) Petermann Glacier will continue to calve episodically, via rift propagation, back to the grounding line, ii) that future icebergs will be similar sized to previous calving events (~ 8 km long: Figure 4.1). Each segment along the ice tongue acted as the new prescribed terminus position, which has a natural boundary condition. In reality, the size and nature of future calving events may vary (e.g. may be a series of small icebergs), but we conduct these experiments to assess the impact of future events similar in magnitude to previous calving. After each diagnostic experiment we calculated the vertically and horizontally integrated flux across the grounding line in Gt a^{-1} with respect to pre-calving flux. We then convert to sea level equivalent (mm) by dividing by the volume of ice needed to raise global sea levels by 1 mm (361.8 Gt).

For the first diagnostic experiment, we used all three sets of boundary conditions (Scenarios 1-3) proposed in Section 4.3.4 to fulfill the third criterion (iii) of which scenario best replicates the small increase in velocity observed after the 2010 calving event (Figure 4.7). Basal slipperiness (C), ice rate factor (A), and boundary conditions for each scenario were input into this first experiment (2010 calving) and the instantaneous increase in speed presented in Figure 4.7. We found that the differences in modeled velocity changes due to calving, using different sets of boundary conditions, were relatively small. Hence, our results are insensitive to the type of boundary condition applied (see also Section 4.3.4). This insensitivity to the type of side-wall boundary conditions can be understood to be related to the inverse methodology (see Section 4.3.3), where A is inferred from measured velocities. In all cases the inversion was able to converge and provide a good fit to observations. Despite this, applying no resistance along the ice tongue margins (Scenario 1: free slip), produces no change in velocity along the tongue, which does not reflect observations (Figure 4.3). However, when applying no-slip side-wall boundary conditions, modeled speed increases along the ice tongue (Scenarios 2 and 3) were closer to observed changes i.e. acceleration at the terminus that did not propagate far inland, and average 45 and 37 m a^{-1} respectively. While both Scenarios 2 and 3 appear to adequately reproduce the observed velocity response after the 2010 calving event, we discount Scenario 2 due to the high misfit between modeled and observed velocities (Table 4.2), and unrealistic ice stiffness along the tongue (Figure 4.6). Thus, boundary conditions and parameters of basal slipperiness (C) and ice rate factor (A) calculated in Scenario 3 are input into the subsequent diagnostic experiments post-2010.

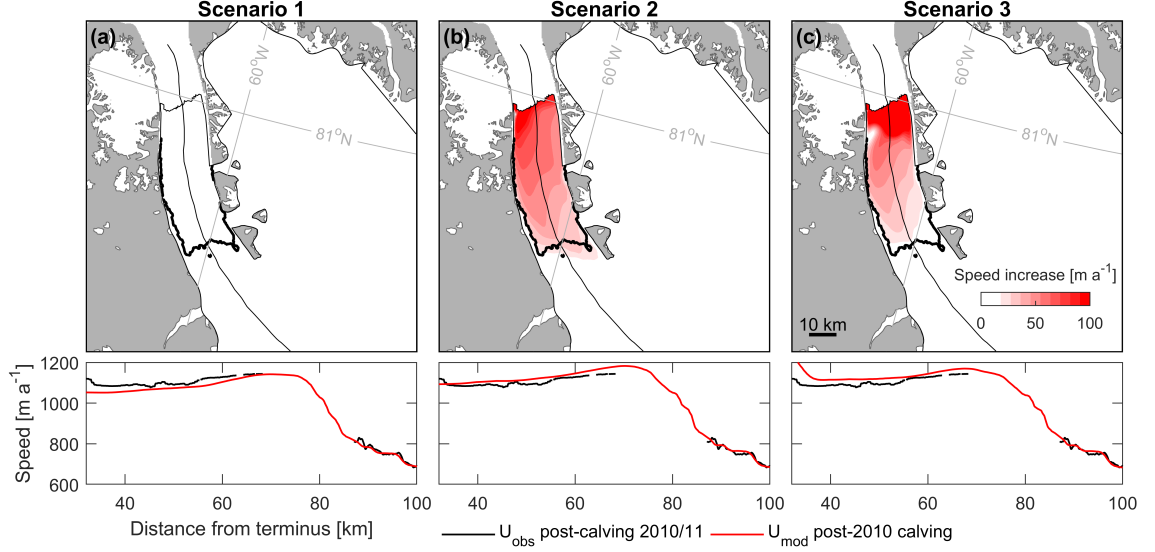


Figure 4.7: Diagnostic perturbation experiments for the 2010 calving event, using three scenarios of boundary conditions applied along the floating ice tongue (a-c). Graduated white to red shows speed increase between initial modeled velocities (U_{initial}) and modeled velocities post-2010 calving (U_{calving}). Bottom plots show observed velocities (U_{obs}) post-calving (winter 2010/11), and modeled velocities (U_{mod}) post-2010 calving along the glacier centerline.

4.4 Results

4.4.1 Response to 2010 and 2012 calving

We have shown that the 2-HD model $\hat{U}a$ can reproduce the flow of Petermann Glacier before the large calving event in 2010. Following this we removed sections of the ice tongue, to replicate large calving events in 2010 and 2012, and compare the model results with observed changes in flow speeds (Figure 4.8a and b).

The iceberg that calved away from Petermann Glacier in 2010 was $\sim 214 \text{ km}^2$ and on average 83 m thick (Figure 4.8). Inverted ice rate factor A reveals that this section of the tongue is softer ($A \approx 2.1 \times 10^{-5} \text{ a}^{-1} \text{ kPa}^{-3}$) by three orders of magnitude than the rest of the ice tongue (Figure 4.9b) or grounded glacier catchment ($A \approx 1.2 \times 10^{-8} \text{ a}^{-1} \text{ kPa}^{-3}$). Model results show that removing this section of the tongue was followed by a slight instantaneous increase in speed, ranging from $\sim 65 \text{ m a}^{-1}$ (6% increase of tongue speed) at the terminus, to $< 20 \text{ m a}^{-1}$ between 60 and 80 km along the centerline (Figure 4.8a). These modeled velocity changes are in very good agreement with observed velocities presented here (Figure 4.3), and documented in previous studies [Nick *et al.*, 2012; Münchow *et al.*, 2016]. After the 2010 calving event increases in speed across the entire ice tongue averaged

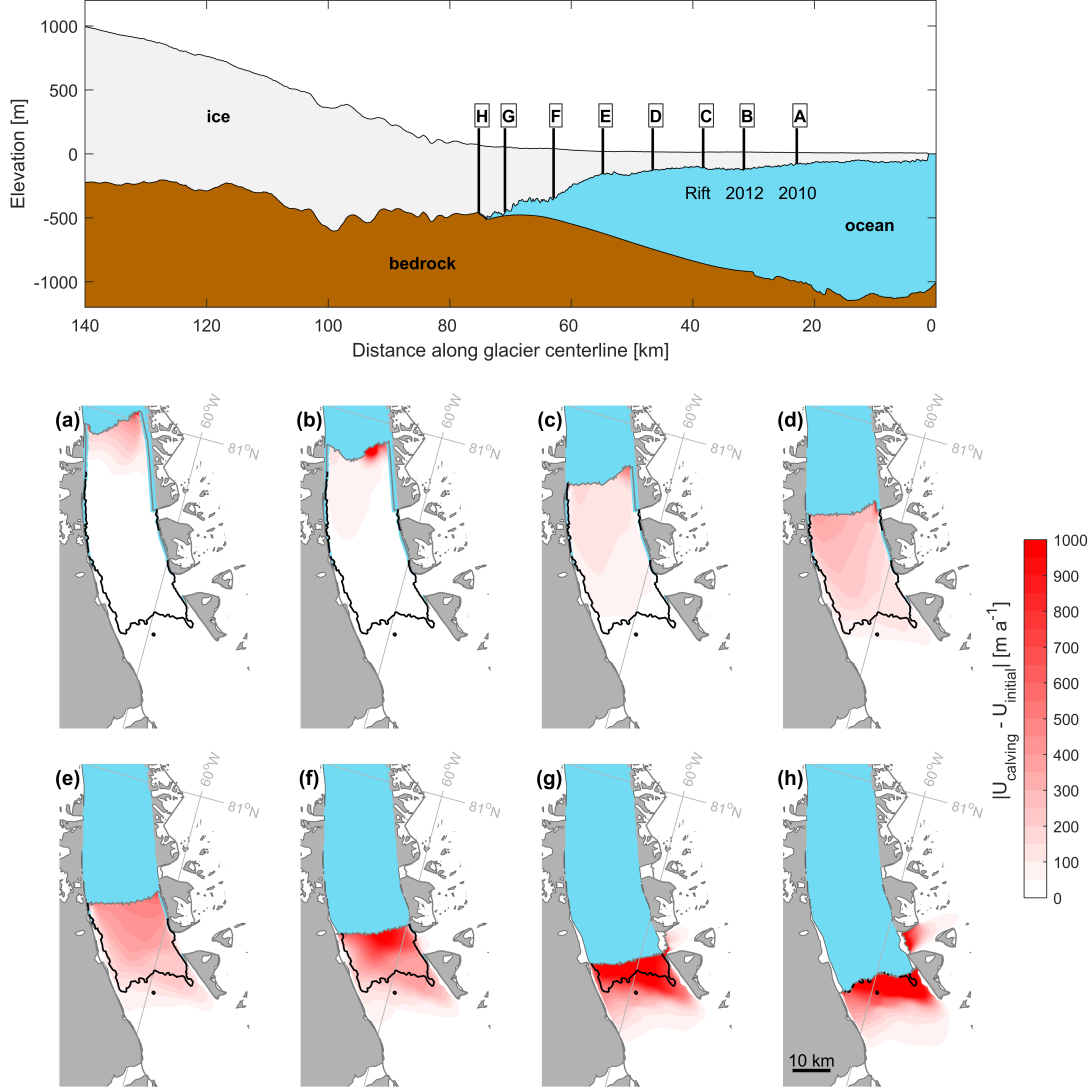


Figure 4.8: Diagnostic perturbation experiments at Petermann Glacier. Top panel shows a cross-sectional centerline profile of Petermann Glacier from the BedMachine v3 dataset [Morlighem *et al.*, 2017]. Letters A to H represent the points along the glacier centerline at which sections of the terminus were removed for each experiment. A is the 2010 calving event, B is the 2012 calving event, and C is the location of a large rift that formed in 2016. D to G are successive 8 km splices and H is the current grounding line location. Bottom panels (a-h) show the modeled instantaneous increase in speed after each experiment with respect to initial pre-calving (before 2010) speeds.

29 m a⁻¹ and 37 m a⁻¹ in observed and modeled velocities respectively (Figure 4.3). Modeled perturbations in flow speeds did not propagate far inland and averaged only +6 m a⁻¹ inland of the grounding line, which is below the average misfit between observed and modeled velocities (9.4 m a⁻¹: Table 4.2) and therefore indistinguishable from errors.

Prior to the calving event, the modeled grounding line flux of 10.12 Gt a^{-1} was within the range of previous estimates by Rignot & Steffen [2008] ($12 \pm 1 \text{ Gt a}^{-1}$) and Wilson *et al.* [2017] ($10.8 \pm 0.52 \text{ Gt a}^{-1}$). Limited changes in speed following the 2010 calving event were accompanied by little change in modeled grounding line flux ($+0.14 \text{ Gt a}^{-1}$) and a negligible increase in sea level rise contribution (Figure 4.9b).

In the next experiment, we removed a 96 km^2 section of the ice tongue to replicate a subsequent large calving event in July 2012. Importantly this calving event removed a thicker section of the ice tongue that averaged 111 m (Figure 4.9a). Similar to the modeled dynamic response after 2010, ice flow speeds increased along the ice tongue after the 2012 calving event, and did not propagate far inland of the grounding line (Figure 4.8b). These modeled velocity changes are consistent with observed velocities in 2012/13 (Figures 4.2 and 4.3). Both modeled and observed speeds increased within the range of 3-5% at the terminus, and showed limited change inland of the grounding line (Figure 4.3). The 2012 calving event was <50% of the 2010 iceberg area, and almost four times softer ($A \approx 9.7 \times 10^{-5} \text{ a}^{-1} \text{ kPa}^{-3}$), suggesting it should provide less resistive stress. However, speed increases were 46% greater along the ice tongue than in 2010 (averaging 59 m a^{-1}) and propagated further towards the grounding line. Despite some acceleration, the 2012 calving event had a limited impact on grounding line flux, increasing it by only 0.35 Gt a^{-1} (3.4%) compared to initial ice flux, and increased sea level rise contribution to 0.029 mm a^{-1} (Figure 4.9b).

4.4.2 Response to future calving events

Calving events in 2010 and 2012 had a limited dynamic impact on the ice flow of Petermann Glacier and were followed by <10% acceleration along the ice tongue, and <2% at the grounding line (Figure 4.3). These modeled findings are consistent with observed velocity change (Figure 4.3) and previous modeling of the 2010 calving event [Nick *et al.*, 2012]. After accurately replicating the observed velocity response to large calving events in 2010 and 2012, we were confident in the model's ability to estimate the instantaneous velocity response of Petermann Glacier to a change in stress conditions at the grounding line associated with removing large sections of the ice tongue.

We conducted six further experiments to analyze the glacier dynamic response (instantaneous change in flow speeds) and grounding line flux, to large calving events. Each of the new calving front positions were approximately 8 km apart along the tongue, and ice loss area averages 125 km^2 (Figure 4.9a). First, we assume that the next calving event

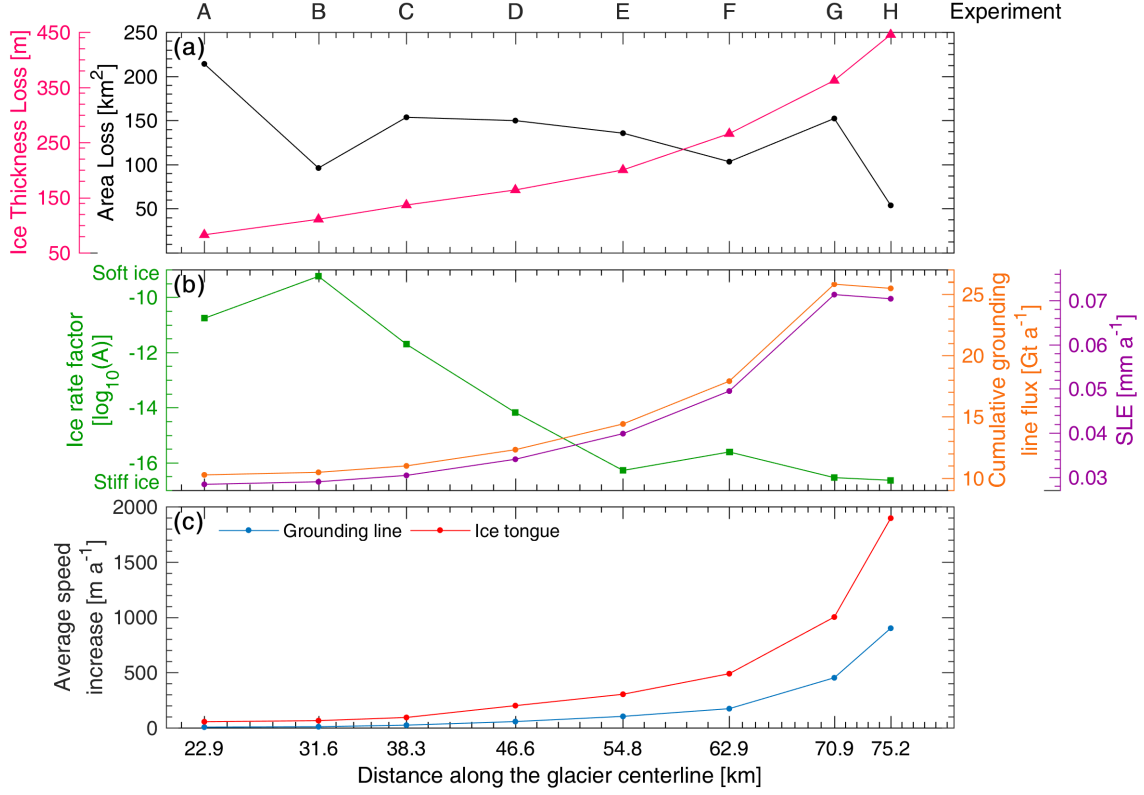


Figure 4.9: Modeled experiment parameters for Petermann Glacier, for each diagnostic experiment (A-H), also shown in Figure 4.8. **(a)** Black line shows iceberg area lost between each experiment [km^2] and magenta is the average ice thickness [m] of each section of ice removed. **(b)** green is the average ice rate factor [$\log_{10} A$] across the section of ice removed in each diagnostic experiment. Orange and purple lines represent the cumulative grounding line flux with respect to an initial ice flux of 10.12 Gt a^{-1} and sea level equivalent contribution after the removal of each section of ice. **(c)** Average increases in ice speed across the entire ice tongue (red) and average ice speed within 10 km inland of the grounding line (blue) after each diagnostic experiment.

from Petermann Glacier will fracture along the path of a large rift that formed in 2016, removing a $\sim 154 \text{ km}^2$ section of the ice tongue (Experiment C: Figure 4.8). This segment is also on average 35 m thicker and sturdier ($A \approx 8.3 \times 10^{-6} \text{ a}^{-1} \text{ kPa}^{-3}$) than the downstream section of the tongue that collapsed in 2010 and 2012 (Figure 4.9b). In this case, average increases in speed along the ice tongue were greater (94 m a^{-1}) and propagated further ($\sim 30 \text{ km}$ from the terminus) towards the grounding line than after previous calving events (Figure 4.8). Acceleration 10 km inland of the grounding line more than doubled to 24 m a^{-1} compared to acceleration after the 2012 calving event (10 m a^{-1}). Despite this, acceleration inland of the grounding line remained 75% smaller than increases along the ice tongue (Figure 4.9c), and did not propagate far into the glacier catchment (Figure 4.8c). After this experiment grounding line flux increased to 11 Gt a^{-1} ($+0.87 \text{ Gt a}^{-1}$) and sea level equivalent rose to 0.03 mm a^{-1} (Figure 4.9b).

Over the subsequent diagnostic calving experiments (D-H), there was a linear increase in average speed change across the ice tongue, as well as a near doubling of average speed increases immediately inland of the grounding line (within 10 km) between each experiment (Figure 4.9). After removing the 164 m thick section D from the tongue, average ice tongue speeds increased by 21% compared to initial velocities ($\sim 954 \text{ m a}^{-1}$), but increases inland of the grounding line (within 10 km) remained small in comparison ($\sim +57 \text{ m a}^{-1}$). During the following three experiments (E-G), instantaneous average velocity increases across the tongue were more substantial than after previous calving events ranging from 304 m a^{-1} after removing segment E, to increasing by $+1000 \text{ m a}^{-1}$ ($> 100\%$ of initial flow speeds) across the small remaining section of the ice tongue after experiment G. Throughout these experiments, higher magnitude increases in speed propagated further into the catchment ($\sim 10\text{-}15 \text{ km}$ inland of the grounding line) than after previous calving events (Figure 4.8). Simultaneous to increases along the ice tongue, average speed increases inland of the grounding line (10 km) went from 103 m a^{-1} (experiment E) to 453 m a^{-1} (experiment G: Figure 4.9). Once the last remaining section of the ice tongue was removed (54 km^2 : H), speed increases were double that of experiment G, reaching $+900 \text{ m a}^{-1}$ immediately inland of the grounding line (10 km). Removing the entire ice tongue, and consequently detaching it from any tributary glaciers also led to a $\sim 530 \text{ m a}^{-1}$ speed up at the terminus of Porsild Glacier (Figure 4.8h).

Alongside linear increases in speed after large calving events, we also note positive trends in the thickness of each calved iceberg, grounding line discharge, and sea level equivalent (Figure 4.9). Ice thickness along the Petermann Glacier tongue increases from $\sim 50 \text{ m}$ towards the terminus to $\sim 500 \text{ m}$ at the grounding line (Figure 4.8: Münchow *et al.* 2014). In our experiments, the ice thickness of each segment increased by an average of 221 m (Figure 4.9a). At the same time, grounding line discharge increased by an average of $+2.17 \text{ Gt a}^{-1}$ after each experiment and once the entire ice tongue was removed, cumulative grounding line flux reached 25 Gt a^{-1} and the glacier contribution to sea level rise increased to approximately 0.07 mm per year (Figure 4.9b). As well as increases in ice thickness along the ice tongue, there is also a general increase in the stiffness of the ice back towards the grounding line. The ice is generally soft in the lower $\sim 40 \text{ km}$ of the tongue (Figure 4.6f) before ice rate factor (A) values decrease by 1-2 orders of magnitude during the last five experiments (E-H: Figure 4.9b). Importantly grounded ice immediately inland of the grounding line (within 10km) is stiffer than the entire ice tongue.

4.5 Discussion and Conclusions

Here, we expand on previous work and provide new insight into the velocity response of Petermann Glacier to past and future large calving events, and eventual ice tongue collapse. In contrast to the removal of buttressing ice shelves elsewhere in Greenland (e.g. Jakobshavn Isbræ: Joughin *et al.* 2008b; Zachariæ Isstrøm: Mouginot *et al.* 2015) and from the Antarctic Peninsula (e.g. Larsen B: De Rydt *et al.* 2015; Scambos *et al.* 2004), we show that Petermann Glacier was dynamically insensitive to the removal of $\sim 310 \text{ km}^2$ of the ice tongue via calving events in 2010 and 2012 (Figure 4.8). After both calving events there was a limited increase in speed ($< 10\%$ of initial flow speeds: Figure 4.3), that remained below the $\sim 22\text{-}25\%$ seasonal variability in flow speeds observed between 2006 and 2017 [Nick *et al.*, 2012; Lemos *et al.*, 2018]. This insensitivity of ice velocities to large calving events can be explained by weak resistance provided by the lower portion of the ice tongue along its lateral margins (Figure 4.6f: Nick *et al.* 2012). From this, we can conclude that the section of the ice tongue that calved away in 2010 and 2012 provided little frontal buttressing on grounded ice.

Given that several floating ice tongues have been lost from neighboring glaciers in northern Greenland [Hill *et al.*, 2018a], and the rapid nature of Petermann Glacier’s Holocene retreat from the fjord mouth [Jakobsson *et al.*, 2018], it is possible that the ice tongue will continue to calve episodically, and in the not too distant future collapse entirely. We set out to determine at what point future calving events at Petermann Glacier (similar in magnitude to past calving) will cause substantial acceleration and increased ice discharge. The key conclusion of this work is that future calving events (C-E) from the lower portions of the ice tongue ($> 12 \text{ km}$ from the grounding line) appear to be passive. We attribute the small modeled velocity response ($< 100 \text{ m a}^{-1}$ increase at the grounding line) to calving events from this lower portion of the tongue to be due to thinner ($< 200 \text{ m}$) and an order of magnitude softer ice, which provides limited buttressing on grounded ice. Indeed, if the next calving event takes the path of the 2016 rift formation, it is unlikely to substantially accelerate ice flow (Figure 4.8c), or increase the glacier contribution to grounded ice discharge and sea level rise (Figure 4.9). However, we find that removing sections of the ice tongue within 12 km of the grounding line (F-H) has a larger impact on ice flow speeds, increasing them by an average of 900 m a^{-1} (96%) after the entire ice tongue is removed (Figure 4.8h). Alongside this, cumulative ice flux across the grounding line increases from 11 Gt a^{-1} (Experiment C) to 25 Gt a^{-1} (H: Figure 4.9b) and cumulative sea level rise could reach 0.07 mm a^{-1} (for event H). Importantly, within 12 km of the grounding line, the thickness and stiffness of the ice tongue increase dramatically (Figure 4.9). As such, this part of the ice tongue provides greater lateral resistance along the fjord

walls and is therefore more effective at buttressing grounded ice. Removing these sections of ice is thus likely to alter the resistive stresses at the grounding line enough to cause a greater increase in flow speeds that propagate further inland.

Overall, our findings show that Petermann Glacier has not responded dynamically to previous calving events in 2010 and 2012, and is unlikely to accelerate substantially after imminent future calving events (Figure 4.8c). However, future large episodic calving events closer to the grounding line have the potential to perturb the stresses acting on grounded ice, and substantially increase flow speeds and ice discharge (Figure 4.9). Despite substantial increases in speed forecast after the ice tongue is removed, the question remains as to whether acceleration will be short-lived, and the glacier will re-stabilize at the current grounding line position or retreat inland. Similar to when the glacier was buttressed by an ice shelf at the end of the fjord [Jakobsson *et al.*, 2018], it may be that the current ice tongue has allowed grounding line stability, and its collapse will similarly lead to unstable grounding line retreat. Indeed, the eastern portion of the current grounding line lies within a deep bedrock canyon [Bamber *et al.*, 2013; Morlighem *et al.*, 2017], which may allow for marine ice sheet instability. However, we cannot discount the possibility that an ice tongue may regrow in the future [Nick *et al.*, 2012]. Here, we have estimated the instantaneous response of Petermann Glacier’s ice flow to the immediate removal of sections of the ice tongue. Importantly, future work incorporating the transient evolution of the glacier geometry and grounding line position in between these large calving events is needed to assess the long-term response of Petermann Glacier to future ice tongue loss.

Chapter 5

Grounding line stability limits 21st century sea level rise from Petermann Glacier in response to ice tongue loss

5.1 Chapter summary

Ice shelves restrain flow from the Greenland and Antarctic ice sheets. Climate-ocean warming could force thinning or collapse of floating ice shelves, and subsequently accelerate flow, increase ice discharge, and raise global sea levels. Petermann Glacier recently lost large sections of the tongue, but its response to future collapse remains uncertain. This chapter also addresses the third objective of this thesis and follows on from the previous Chapter by conducting additional numerical modelling experiments on Petermann Glacier. The main motivation for this follow-on-work was to assess the long-term (100 yr) response of Petermann Glacier to changes in ice tongue extent, and to estimate potential mass loss and sea level rise contribution. These experiments are therefore transient, and allow the geometry of the glacier to evolve through time in response to ice tongue loss. This chapter has been written in short-format for pending submission to *Geophysical Research Letters*. However, for the purposes of this thesis the supplementary information has been incorporated into the main body of the text. Our results suggest that under enhanced basal melt and episodic calving, Petermann Glacier will contribute to only 0.87 mm of

global sea level rise over the next 100-years. Grounded ice loss was limited by grounding line stability at a topographic high approximately 12 km inland. Further inland, the absence of a widening and deepening fjord suggests that Petermann Glacier will remain insensitive to terminus changes in the future.

5.2 Introduction

Fast-flowing outlet glaciers draining the GrIS, are dynamically coupled to changes at their terminus [Nick *et al.*, 2009]. Many outlet glaciers have thinned and accelerated [e.g., Howat *et al.*, 2007; Joughin *et al.*, 2008b; Moon *et al.*, 2012] in response to 21st century terminus retreat. Laterally confined ice shelves at marine termini can provide strong backstress (i.e. buttressing) on grounded ice [Schoof *et al.*, 2017; Haseloff & Sergienko, 2018]. However, floating ice shelves could be destabilised under future climate-ocean warming, reducing resistive stress at the terminus that accelerates ice flow, increases ice discharge, and ultimately raises global sea level. Ice shelf buttressing has been the focus of recent work on ice shelf collapse/stability in Antarctica [e.g., Reese *et al.*, 2018a; De Rydt *et al.*, 2015; Paolo *et al.*, 2015], but has received limited attention in Greenland, largely because there are so few floating tongues.

Petermann Glacier is a fast flowing ($\sim 1 \text{ km yr}^{-1}$) outlet glacier in northwest Greenland that drains approximately 4% of the ice sheet [Münchow *et al.*, 2014]. The catchment contains $1.6 \times 10^5 \text{ km}^3$ of ice volume above flotation (VAF), equivalent to 0.41 m of global sea level rise. Petermann Glacier terminates in one of the last remaining ice tongues in Greenland (hereafter PGIT), that has been retreating since the early Holocene [Jakobsson *et al.*, 2018]. More recently, two large well-documented calving events in 2010 and 2012 [Johannessen *et al.*, 2013; Münchow *et al.*, 2014; Nick *et al.*, 2012], shortened the ice tongue from $\sim 70 \text{ km}$ to 46 km . Petermann Glacier was in steady state prior to these calving events [Rignot & Steffen, 2008], but speeds increased by $\sim 12\%$ after 2012 [Münchow *et al.*, 2016; Rückamp *et al.*, 2019]. Alongside episodic calving, PGIT is controlled by ice-ocean interactions that force high basal melt rates ($\sim 35 \text{ m yr}^{-1}$) beneath the tongue [Rignot & Steffen, 2008]. Recent $\sim 0.2^\circ\text{C}$ warming of Atlantic water (2002 to 2016) [Washam *et al.*, 2018; Münchow *et al.*, 2011], accompanied by stronger ocean circulation and the break up of sea ice, are likely to have promoted warm water transport into the Petermann fjord and beneath the ice tongue [Washam *et al.*, 2018; Shroyer *et al.*, 2017; Johnson *et al.*, 2011]. In response to recent ocean warming and increased subglacial discharge, basal melt rates are estimated to have increased by $+8.1 \text{ m yr}^{-1}$ from the 1990s to early 2000s [Cai *et al.*, 2017]. The most recent estimates revealed -50 m yr^{-1} of basal melt at the grounding line

between 2011 and 2015 [Wilson *et al.*, 2017].

Thinning and calving of the PGIT could reduce buttressing forces at the grounding line and accelerate ice flow, as observed on the Antarctic Peninsula [Scambos *et al.*, 2004; De Rydt *et al.*, 2015]. It is therefore important to quantify the impact of losing the PGIT on future ice discharge and sea level rise. Previous work used a flowline model at Petermann Glacier to examine both the short term response to ice tongue collapse [Nick *et al.*, 2012], and the long-term sea level rise contribution under scenarios of future climate change [Nick *et al.*, 2013]. However, one horizontal dimensional (1HD) models do not account for lateral stresses and buttressing in both horizontal directions which limits the accuracy of sea level rise projections [Bondzio *et al.*, 2017; Gudmundsson, 2013]. More recently, Hill *et al.* [2018b] used a 2-horizontal dimensional (2HD) model $\dot{U}a$ [Gudmundsson *et al.*, 2012], to examine the time-independent response of Petermann Glacier to large calving events. While this showed ice tongue collapse could cause a 96% instantaneous speed-up, it did not examine the transient response of Petermann Glacier to a loss of ice-tongue buttressing. Thus, no study has yet assessed the impact of ice tongue thinning/collapse on Petermann Glacier’s future contribution to sea level rise, using a 2HD vertically integrated approach.

Here, we use an ice flow model ($\dot{U}a$) to assess the long-term dynamic response and sea level contribution of Petermann Glacier (100-yrs) to changes in ice tongue extent. To investigate the importance of basal melting and/or iceberg calving we performed three forward-in-time experiments: 1) enhanced basal melt rates from steady state conditions [Rignot & Steffen, 2008] to those of recent observations [Wilson *et al.*, 2017], but left the terminus position fixed; 2) immediately removed the entire $\sim 885 \text{ km}^2$ ice tongue at the start of the experiment; and 3) enhanced basal melt rates and episodically removed the ice tongue over the first 25 years. These experiments were designed to assess the sensitivity of Petermann Glacier to changes downstream of the grounding line, and to bracket potential future mass loss.

5.3 Methods

5.3.1 Model set-up

$\dot{U}a$ is a vertically integrated ice flow model that solves the ice dynamics equations using the shallow ice-stream approximation [MacAyeal, 1989; Morland, 1987], a Weertman-sliding law, and Glen’s flow law. The model has been used to understand grounding line dynamics

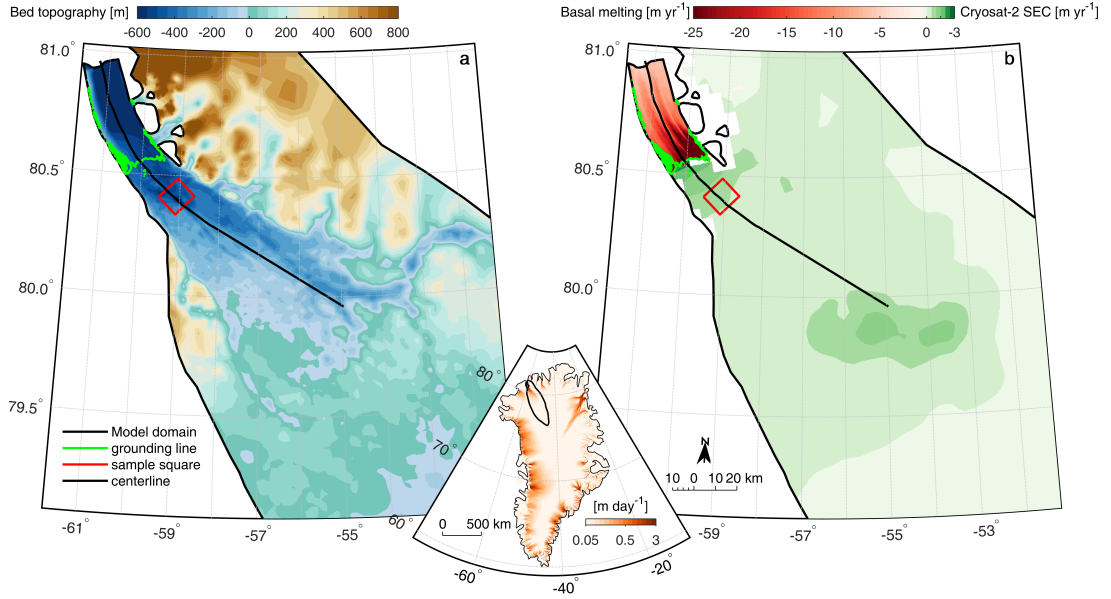


Figure 5.1: a) Bed topography [m] across the lower portion of the Petermann Glacier catchment, b) is initially perscribed steady-state melt rates beneath the ice tongue (red) and green is observed surface elevation change (SEC) from Cryosat-2 between 2011 and 2016, both of which are in m yr⁻¹. Inset map shows Greenland ice flow speed [m day⁻¹] in orange and the Petermann catchment outlined in black.

[Pattyn *et al.*, 2012; Gudmundsson *et al.*, 2012] and the impact of ice shelf buttressing and collapse on outlet glacier dynamics in both Antarctica [Reese *et al.*, 2018a; De Rydt *et al.*, 2015] and Greenland [e.g., Hill *et al.*, 2018b].

To set-up the model we use 150m resolution bedrock geometry, fjord bathymetry, ice thickness, and surface topography from the Operation IceBridge BedMachine v3 dataset [Morlighem *et al.*, 2017]. The model domain extends from the ice tongue front in 2016 across the ice surface drainage catchment of Petermann Glacier ($\sim 85,000$ km²: Figure 5.1). We used the *Mesh2D* Delaunay-based unstructured mesh-generator [Engwirda, 2014] to create a linear triangular finite-element mesh with 111391 elements and 56340 nodes (Figure 5.2). The mesh was refined anisotropically based on three criteria: i) flotation mask, ii) surface elevation, and iii) measured flow speeds. Element sizes range from ~ 0.3 km across the ice tongue, where flow speeds are >250 m a⁻¹, and surface elevation is <750 m, to a maximum of 15 km inland, where flow speeds are <10 m a⁻¹ and surface elevation exceeds 1.2 km (Figure 5.2). Nunataks on the eastern side of PGIT were digitized in 2016 Landsat-8 imagery and treated as holes within the mesh. Topographic parameters were linearly interpolated onto this mesh. A free-slip natural boundary condition was applied along the terminus. Along the inland catchment boundary we use a fixed (no-slip) zero velocity condition to avoid unrealistic gradients in flow out of the domain. Velocities were

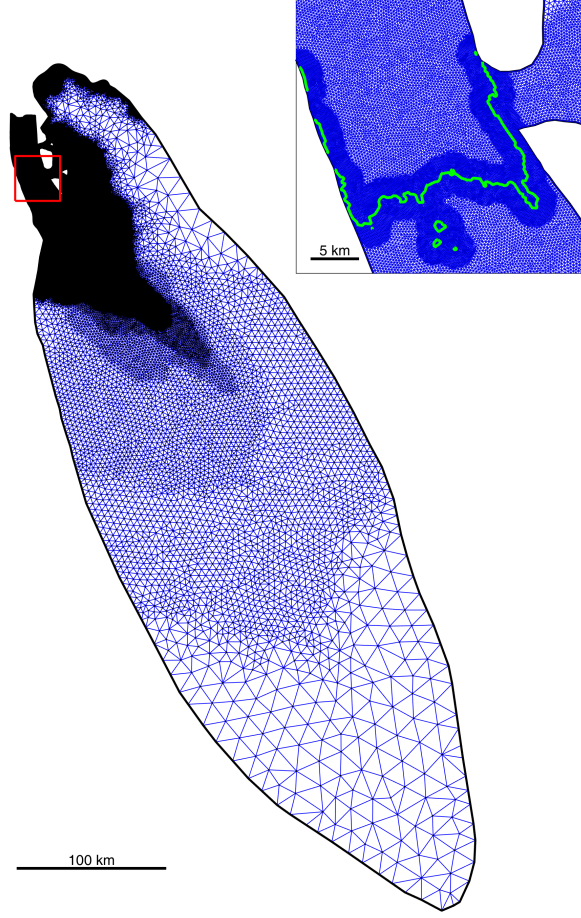


Figure 5.2: Initial finite linear-element mesh across the Petermann Glacier catchment (black line) which acts as our model domain. This mesh has 111391 elements, and 56340 nodes, and is refined in areas of low elevation, along the floating ice tongue, and where the ice is flowing fastest. Inset shows the mesh refinement along the ice tongue (300 m element size) and around the grounding line (100 m element size) shown in green.

also fixed to zero along the lateral ice tongue margins as this optimally replicates lateral stresses and ice flow along the PGIT [see Hill *et al.*, 2018b].

We used inverse methodology to initialize the model. Initial observed velocities were taken from the most recent 2016/17 MEaSURES Greenland annual ice sheet velocity mosaic [Joughin *et al.*, 2010b] derived from both optical (Landsat-8) and synthetic aperture radar data (TerraSAR-X, TanDEM-X, Sentinel-1A and 1B). These data have an average error of 0.62 m yr^{-1} across the Petermann Glacier catchment. We invert observed velocities to estimate parameters of basal slipperiness (C) and an ice rheology parameter (A) using $n = 3$ and $m = 3$ (Figure 5.3). We also performed experiments using different values of m (2,3,4) and found our results are insensitive to the value of m (see Appendix B). Inversion was done by minimizing the cost function of a misfit and regularization term

using the commonly-adopted adjoint method and Tikhonov regularization. We tested a series of regularization parameter values and selected final values based on an L -curve analysis. Our resultant model velocities provide a good fit to observations (see Figure 5.3 top right) and after a total of 900 iterations, the mean difference between modeled and observed velocities was 9.5 m yr^{-1} (15%). This increased to 14 m yr^{-1} where speeds are $>300 \text{ m yr}^{-1}$ and to 23 m yr^{-1} along the PGIT.

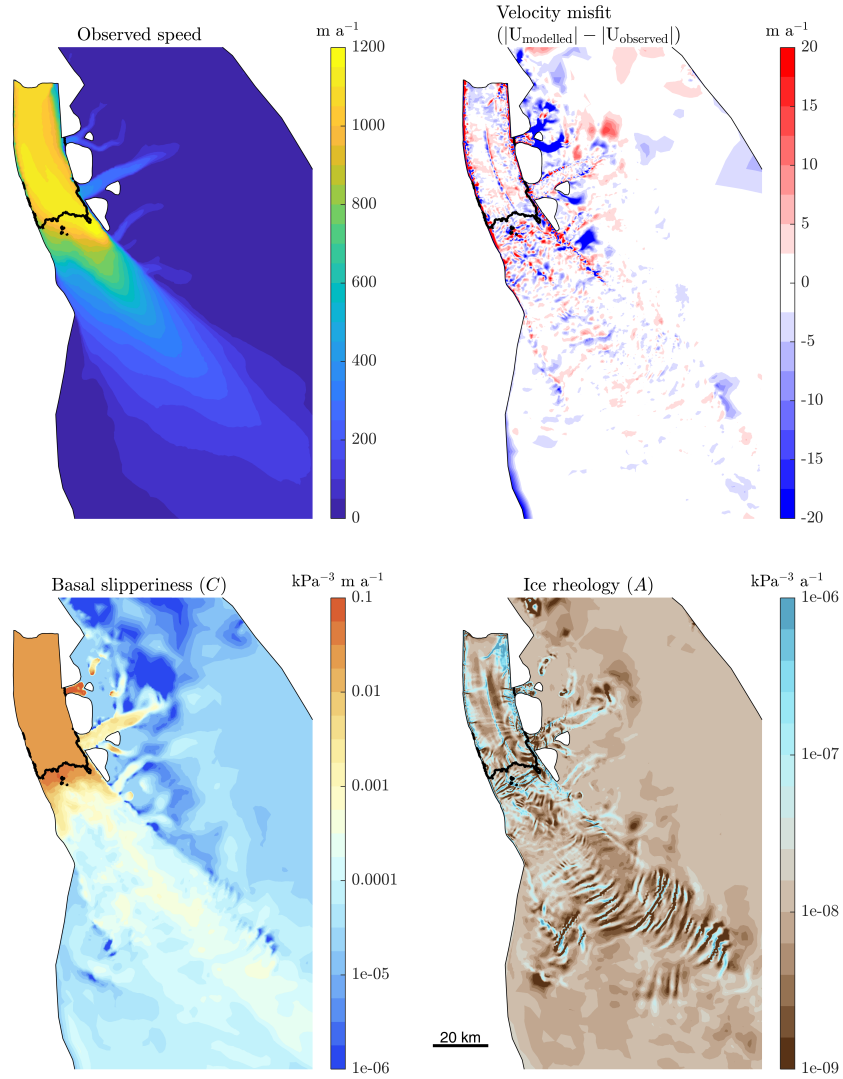


Figure 5.3: Results from model inversion. Top left panel shows observed ice flow speeds, where flow speeds reach up to 1200 m a^{-1} along the ice tongue. Top right panel shows the misfit between observed and modeled ice flow speeds after inversion. The bottom left panel shows basal slipperiness (C) using $m=3$. Light blue through to light and dark orange show areas of slipperiest ice. Note the slippery bed within $\sim 10 \text{ km}$ inland of the grounding line. Bottom right panel shows ice rheology parameter (A) from Glen's flow law using $n=3$. Areas of light to dark turquoise represent the softest ice, while dark brown is the areas of stiffest ice.

Estimates of basal slipperiness (C) and ice rheology (A) are shown in the bottom plots of Figure 5.3. Note we set slipperiness values below the ice tongue to be the same as the average C value within 10 km inland of the grounding line. In the case of grounding line advance during our experiments, this prevents advance into unrealistically stiff bed conditions. Within 10 km inland of the grounding line slipperiness values are three orders of magnitude greater (averaging $C \approx 1.8 \times 10^{-2} \text{ kPa}^{-3} \text{ m a}^{-1}$) than across the rest of the Petermann Glacier catchment. Further inland, areas of streaming fast flow (between 300 and 700 m a^{-1}) are also slippery and average $C \approx 4.7 \times 10^{-3} \text{ kPa}^{-3} \text{ m a}^{-1}$. Ice rheology (A) reveals areas of weak ice in the downstream section of the ice tongue and along the lateral margins, which is consistent with observations of satellite imagery [Nick *et al.*, 2012; Hill *et al.*, 2018a]. Here, ice is an order of magnitude softer ($A \approx 1 \times 10^{-7} \text{ a}^{-1} \text{ kPa}^{-3}$) than ice in the central parts of the tongue ($A \approx 7.4 \times 10^{-8} \text{ a}^{-1} \text{ kPa}^{-3}$). We also note that our inversion procedure has picked out weak ice along the very centre of the ice tongue which represents the location of a persistent supraglacial stream [Macdonald *et al.*, 2018; Münchow *et al.*, 2016]. Further inland of the grounding line our inverted ice rheology also reproduces a complex pattern of frozen and thawed ice identified in earlier studies [Chu *et al.*, 2018; MacGregor *et al.*, 2016]. These results demonstrate that we are able to get high levels of detail on ice conditions from inverting the observed velocity field over a high resolution mesh.

Annual surface mass balance (SMB) for all of our experiments was incorporated from the RACMO2.3 downscaled 1-km product [Noël *et al.*, 2016], averaged over the 5-year period 2011 to 2016, to reflect current mass balance conditions (Figure 5.1). Basal melt rates beneath the PGIT are known to be correlated with ice thickness and enhanced either side of basal channels [Wilson *et al.*, 2017; Rignot & Steffen, 2008]. Initial basal melt rates were prescribed as a linear-function of ice thickness and are consistent with steady-state melt values in previous studies [Rignot & Steffen, 2008; Cai *et al.*, 2017]. Melt rates were highest at the grounding line (-37 m yr^{-1}) and either side of basal channels, decreasing to -1 m yr^{-1} at the minimum ice tongue thickness of 1 m near the terminus (Figure 5.1).

5.3.2 Model initialization and control run

For forward transient experiments, $\dot{U}a$ allows for a fully implicit time integration, where, at each time-step, changes in geometry, grounding line position and velocity are calculated implicitly. During each forward run, we incorporated automated adaptive time-stepping and automated time-dependent mesh refinement around the grounding line, which is known to improve estimates of stress distributions and migration rates of the grounding line [Schoof

et al., 2017; Goldberg *et al.*, 2009; Durand *et al.*, 2009; Pattyn *et al.*, 2012]. Within 2 km of the grounding line, we locally refined element sizes to 100 m.

Using initially input SMB, basal melt rates, and estimates of slipperiness and ice rheology, we performed a reference run (hereby ‘control run’) forward in time for 100 years. This was designed to reflect current non-steady state conditions [Münchow *et al.*, 2016], i.e. small amounts of thinning (Figure 5.1) inland of the grounding line, but with no perturbation in melt rates or ice tongue extent. Thus we prescribe near balance melt rates that bring the mass balance close to 0, but remains slightly negative to reflect the current negative mass balance. We calculate the approximate total mass balance (M_{total}) at the beginning of this run, based on the total melt flux (M_{basal} and M_{surface}) minus the approximate calving flux (M_{calving}) based on width \times height \times velocity at the glacier terminus (equation 5.1).

$$M_{\text{total}} = M_{\text{basal}} + M_{\text{surface}} - M_{\text{calving}} \quad (5.1)$$

At time=0 our estimated calving flux is 0.99 Gt a^{-1} , total melt flux is -3.2 Gt a^{-1} and total mass balance is therefore -4.19 Gt a^{-1} . The ice flux across the grounding line was 9.48 Gt a^{-1} which is similar to previous measurements [Wilson *et al.*, 2017]. Thinning rates were similarly distributed to Cryosat 2.2 elevation changes from 2011 to 2016, but were slightly lower due to imposing steady-state melt rates (see Figure 5.4). Over the entire control run (0-110 years) there is almost no change from our initial mass balance (on average $4.79 \cdot 10^{-4} \%$: Figure 5.5). However, there were some small changes in mass balance within the first 10-years of our experiment (Figure 5.5). As a result we allowed for a short period of model relaxation, as experience has shown that transient runs tend to exhibit a short period of anonymously high rates-of-change following initialization. We found that after 10-years values stabilized and this was the starting point (time=0) for all further experiments. However, our final results are not sensitive to the selected duration of this initial relaxation period as a) our total modelling time is several times larger, and b) all our main results are based on calculated differences with respect to the control run, and the impact of the initial relaxation period cancels out. During this control run, the grounding line position was stable, thinning rates remained small (-0.17 m a^{-1}), acceleration was limited (0.26 m a^{-2} : Figures 5.7 and 5.8), and the total contribution to sea level rise over 100 years was only 0.43 mm (Figure 5.9).

To test the robustness of our Control run results with respect to mesh resolution around the grounding line, we repeat the experiment with a series of different element sizes around the grounding line. We do this for 50 m, 100 m (our initial element size), 150 m, 200 m, 250 m and 300 m. As element sizes were refined to 300 m across the ice tongue

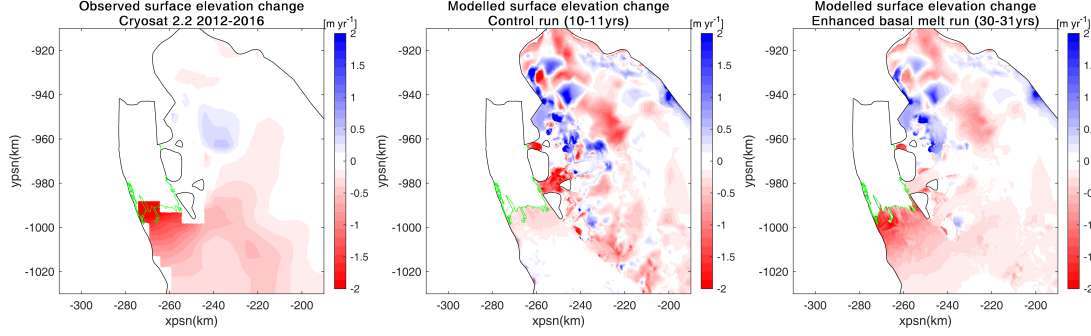


Figure 5.4: Observed and modelled thinning rates of elevation change. Left plot is observed surface elevation change from the Cryosat 2.2 satellite averaged between 2012-2016, which is similar to the date range of our input SMB from RACMO (2011-2016). Middle plot shows modelled surface elevation change at the beginning of our control run (10-11 yrs). As expected, due to prescribing lower basal melt rates than observed during 2012-2016 [Wilson *et al.*, 2017], our thinning rates underestimate observations. As way of comparison, the right hand plot shows thinning rates during our enhanced basal melt rates (at the point at which the glacier begins to respond dynamically to higher melt rates: 30yrs), which show a better fit to observed elevation changes.

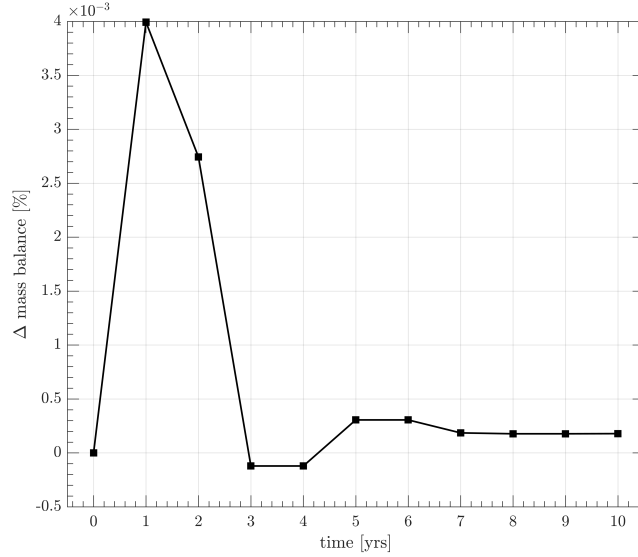


Figure 5.5: Percentage change (10^{-3} %) in total mass balance relative to initial conditions (time=0) during the model relaxation period of 10-years.

any further increases in grounding line element size (>300) would no longer be refining elements around the grounding line. Figure 5.6 shows the change in ice volume above flotation (VAF) in Gt between time=0 and time=100 for each mesh size refinement. This shows that there is little variability between ice volume loss based on the refinement of the mesh size around the grounding line. VAF for all mesh size experiments were within the range of ± 2.2 Gt, which is only 1.4% of the mean ice loss for all experiments (-155.7 Gt). This demonstrates that our transient experiments were insensitive to the size of the

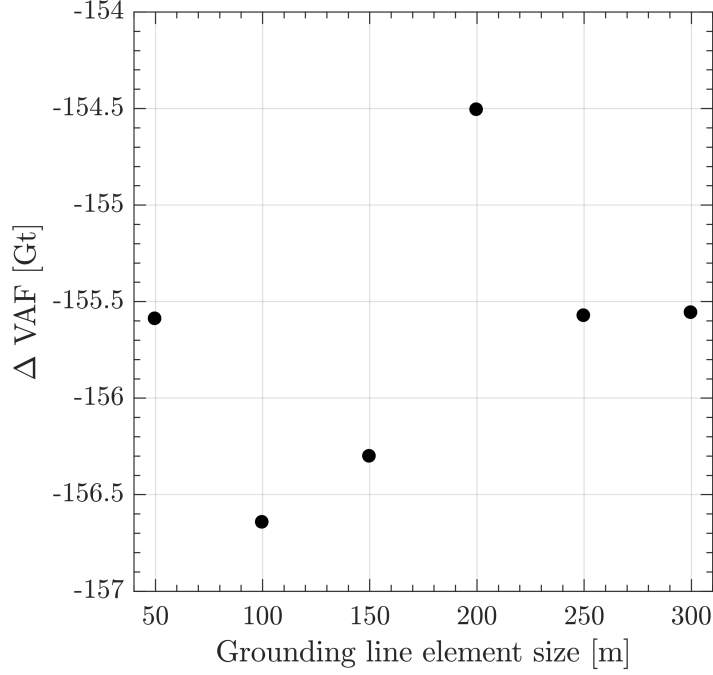


Figure 5.6: Change in ice volume above flotation (VAF) over 100 yrs in Gt for control runs executed using different sized elements within 2 km of the grounding line.

grounding line mesh refinement. Finally, in a post-processing step, and for illustrative purposes, annual width-averaged grounding line retreat was then calculated using the commonly adopted box method.

5.4 Results

Our first experiment raised basal melt rates beneath the PGIT by a factor of 1.5 from steady-state conditions [Rignot & Steffen, 2008] to values similar to recent estimates [Wilson *et al.*, 2017]. These ranged from -50 m yr^{-1} at the grounding line to $\sim -5 \text{ m yr}^{-1}$ near the terminus. It is possible that ocean warming may enhance melt rates further, but given the uncertainties associated with projecting future basal melt rates, we merely assess the impact of current melt conditions over the next 100-years. As a result, these estimates may well be the low-end member response of Petermann Glacier to future ice tongue melt. Nevertheless, under these higher melt conditions, the ice tongue thinned by ~ 100 to 300 m (Figure 5.7c), accelerated by 300 m yr^{-1} (Figure 5.7h), and thinning rates were greatest close to the grounding line (approx. 2 m yr^{-1}) and either side of streamlined basal channels (Figure 5.7m). Greater basal melt induced thinning of the tongue resulted in a 48% increase in ice volume loss above flotation (VAF) after 100 years (-233 Gt) compared

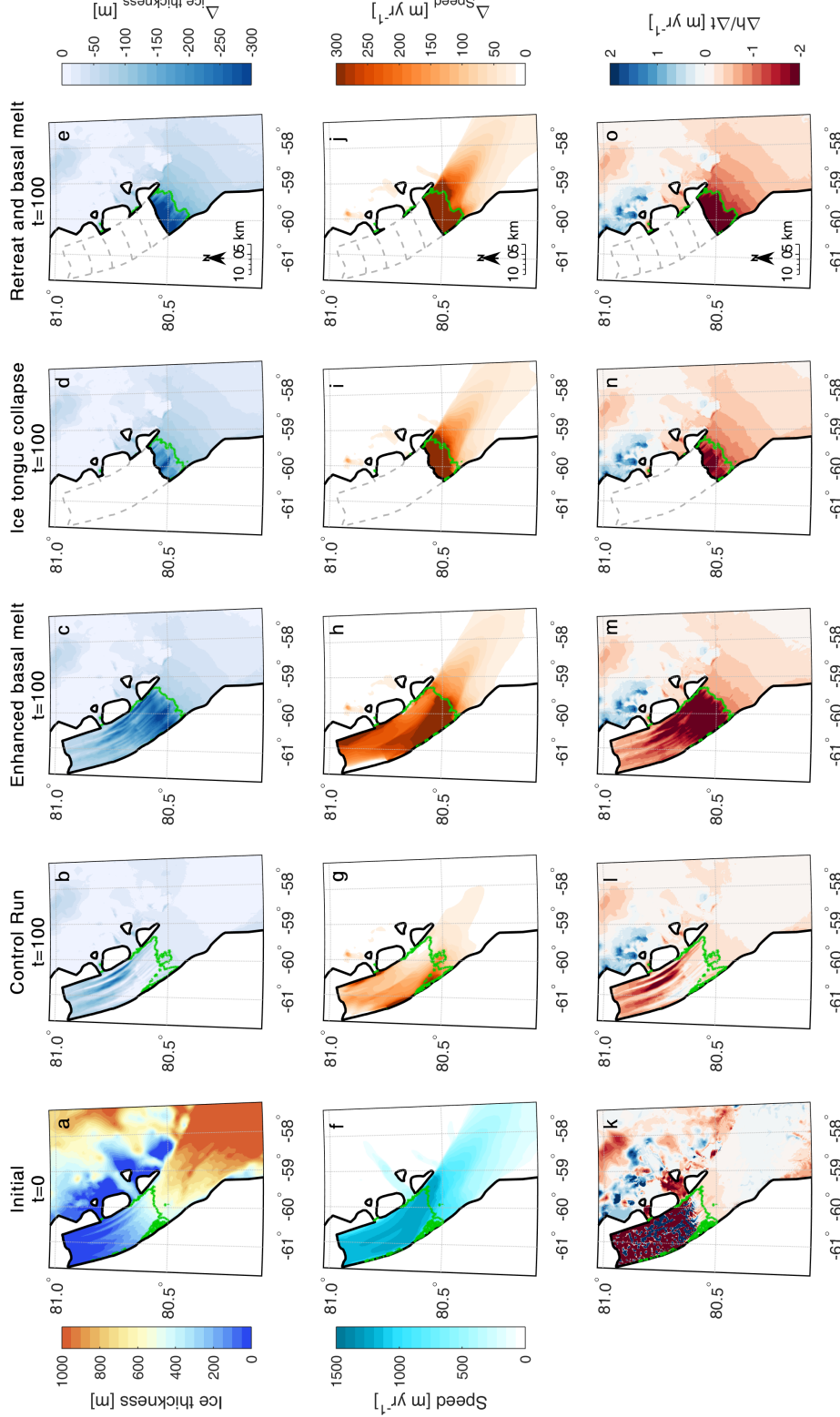


Figure 5.7: Top line shows initial ice thickness [m] at time = 0 (a) and plots b-e show the change in ice thickness [m] after 100 years for each of our experiments. The middle line of plots shows initial ice speed (f) in m yr⁻¹ and plots g-j show change in speed [m yr⁻¹] after 100 years. The final line shows initial thinning rates (k) in m yr⁻¹ where red is thinning and blue is thickening, and plots l-o show thinning rates at 100 years [m yr⁻¹]. In plots a, f and k, the green line represents the initial grounding line position. In all other plots the green line is the position of the grounding line after 100-years for each experiment. The dotted grey line in d,i and n is the previous PGIT extent removed at the beginning of the experiment. In e,j and o, the dotted lines represent calved icebergs at 5-year intervals between 5 and 25 years.

Table 5.1: dhdt, speed and acceleration calculated within a square upstream of the grounding line. Acceleration is relative to initial velocities after 10-year relaxation period (after 0-10 CtrlRun). Flux is average GL flux for 0-100 yrs. Total mass loss is the volume of ice above flotation lost by the end of the 100 year period.

| | dh/dt [m yr ⁻¹] 0-100 yrs | Speed [m yr ⁻¹] 0-100 yrs | Acceleration [m yr ⁻²] 0-100 yrs | Flux [Gt yr ⁻¹] 0-100 yrs | Total VAF mass loss [Gt] | Total SLR [mm] |
|----------------------|---|---|--|---|--------------------------------|----------------------|
| Control run | -0.17 | 691 | 0.26 | 9.845 | 157 | 0.43 |
| Enhanced basal melt | -0.54 | 763 | 1.03 | 10.86 | 233 | 0.65 |
| Ice tongue collapse | -0.70 | 831 | 1.22 | 11.17 | 293 | 0.81 |
| Retreat & basal melt | -0.89 | 841 | 1.71 | 11.64 | 313 | 0.87 |

to our control run (Table 5.1). But overall the impact on global sea level rise was limited to only +0.65 mm (Figure 5.9, Table 5.1).

During the first 20-years there was limited inland surface lowering or acceleration. However, some grounded ice loss (24 km²) and 0.2 km of grounding line retreat (Figure 5.9), initiated positive feedbacks (e.g. acceleration, thinning and retreat) over the following 20-years. Un-grounding of ice increased the area afloat and thus subject to melt, which led to greater thinning closer to the grounding line (188 m between 20 and 40 years) compared to our control run (Figure 5.8b). Crucially, this thinning decreased buttressing at the grounding line, causing it to retreat rapidly (6.8 km), and propagate reductions in longitudinal stresses inland. This led to a 13% increase in flow speeds and greater thinning (to -1 m yr⁻¹). With it there was a 16% increase in the ice flux across the grounding line and 134 km² of grounded ice loss (Figure 5.9). However, acceleration and thinning were only confined to ~10 km inland of the initial grounding line (Figures 5.7 and 5.8). Between 60 and 100 years acceleration and thinning rates decreased, and the grounding line appeared to stabilise ~9 km inland (Figure 5.9). Thus, with no further perturbation of the ice tongue i.e. no further increase in basal melt rates or fracture driven calving, Petermann Glacier approached stable conditions after 60-years.

Since the early 2000s, several floating ice shelves have collapsed, across both Antarctica [e.g., Scambos *et al.*, 2004] and Greenland [Hill *et al.*, 2018a]. At Petermann Glacier, Washam *et al.* [2018] highlight an incised channel close to the grounding line (Figure 5.8c), where thinning could cause the PGIT to fracture, removing it entirely. Our second experiment showed that if the PGIT were to instantly collapse from its current state in 2016, Petermann Glacier would experience some increased thinning and acceleration (Figure 5.7d, i, and n) but the global impact of ice tongue collapse would be quite limited. The glacier would lose about 293 Gt of ice after 100-years in response to a sudden and complete ice-tongue loss (Table 5.1). While this is nearly double the ice loss from our

control run, and greater than our basal melt experiment, it is equivalent to a global sea level rise of only 0.81 mm (Figure 5.9a, Table 5.1).

As expected, removing the entire ice tongue in contact with the grounding line, caused a greater instant loss of buttressing and force imbalance than gradual sub-tongue thinning. In 5-years the grounding line retreated 7.7 km (Figure 5.9c), and with it there was a 63% increase in ice flux that transported an additional 1.5 Gt yr^{-2} across the grounding line (Figure 5.9d). This loss of back-stress also led to substantial ice thinning (18 m yr^{-2}) and a 114% ($+1715 \text{ m yr}^{-1}$) increase in flow speeds at the terminus, that reached a peak of $\sim 2900 \text{ m yr}^{-1}$ after 3-years (Figure 5.8c). Stress imbalances at the terminus diffused inland, where thinning rates increased 5 fold (averaging -5.5 m yr^{-1}) and speeds increased by 31% over the first 5-years. However, our results show that the dynamic glacier response was short-lived and after ~ 10 -years Petermann Glacier appeared to have re-adjusted to the loss of buttressing. After initial acceleration, flow speeds at the terminus rapidly decelerated at 91 m yr^{-2} from 3 to 7 years. Thereafter speeds remained high ($>2000 \text{ m yr}$) but relatively constant (Figure 5.8c). As the terminus region decelerated, grounding line retreat slowed (by 1.5 km yr^{-1}), and after 30-years it stabilized to within 1 km of its position after 100 years in our basal melt experiment (Figure 5.9c). Importantly, terminus deceleration and grounding line stability reduced the driving forces acting on Petermann Glacier. This caused inland flow speeds to decelerate (0.86 m yr^{-2} from 10-100 yrs), thinning rates to subside (averaging -0.32 m yr^{-1} during 10-100 yrs) and a reduction in ice discharge to below our basal melt experiment (Figure 5.9).

In our final experiment we applied increased basal melt rates from experiment one, and we removed five large sections of the ice tongue ($\sim 180 \text{ km}^2$) at 5-year intervals from 5-25 years (Figures 5.7e and 5.8d). This assumes that Petermann Glacier will continue to lose its ice tongue via episodic calving, similar in size to large calving events in 2010 and 2012 [Münchow *et al.*, 2014]. Indeed, a large a rift formed in 2016 suggesting calving is imminent [Münchow *et al.*, 2016]. Here, gradual loss of buttressing associated with both staggered ice tongue collapse and enhanced ice tongue thinning caused a larger stress perturbation at the grounding line than either of our previous experiments. This led to greater inland thinning and acceleration (Figure 5.7j and o) and a total ice volume loss of 313 Gt (Table 5.1). Despite greater ice loss, the impact on global sea level was still limited to $<1 \text{ mm}$ of increase after 100 years (Figure 5.9a).

Consistent with earlier work [Hill *et al.*, 2018b; Nick *et al.*, 2012], our results show that the glacier response to calving differs between removing the lower or upper portions of the PGIT. After removing the first three sections of the ice tongue (at 5, 10, and 15 years), ice flow at the terminus accelerated by only 5-10% in the 5-years between each calving event

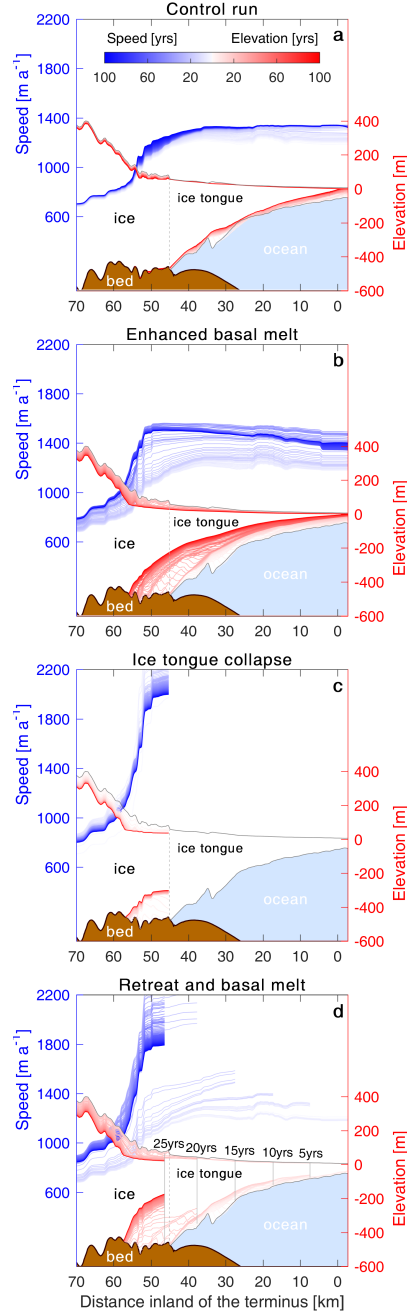


Figure 5.8: Annual speed (blue) and elevation change (red) along the Petermann Glacier centerline (sampled at 100 m intervals) for each of our model experiments (a-d). Pale to dark blue and pale to dark red represent each year between 0 and 100 for speed and elevation respectively. The dotted grey line represents the initial grounding line position and the ice ocean and bed extents are from the Operation IceBridge BedMachine v3 dataset [Morlighem *et al.*, 2017]. In plot d, the grey lines are sections of the PGIT removed at 5 year intervals between 5 and 25 years.

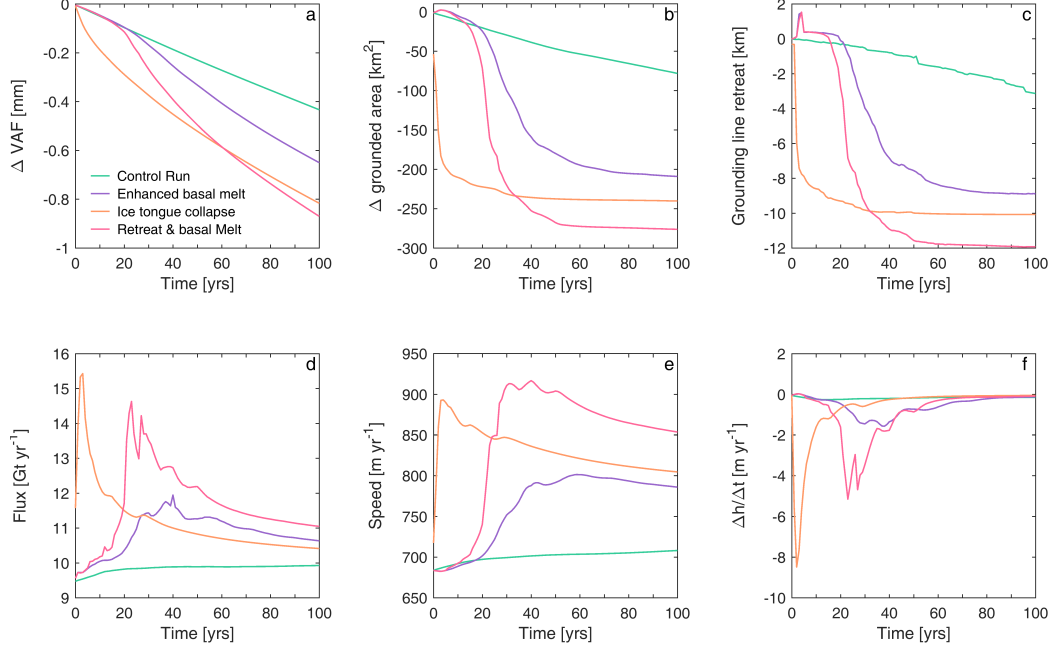


Figure 5.9: Model results for each of our experiments; control run (green), enhanced basal melt (purple), ice tongue collapse (orange) and retreat and enhanced basal melt (pink). a) change in volume above flotation (VAF) in mm of global sea level equivalent. b) change in grounded area [km²]. c) width-averaged grounding line retreat [km], note some advance associated with re-grounding downstream of the main grounding line position. d) annual ice flux [Gt yr⁻¹] across the grounding line. e) average annual ice flow speeds [m yr⁻¹] within a 134 km² square ~ 17 km inland of the grounding line (Figure 5.1). f) average annual thinning rates (change in thickness (h) over time (t)) in m yr⁻¹ within our sample square.

(Figure 5.8d). The grounding line simultaneously retreated at 60 m yr⁻¹ (total of 1.2 km), which is similar to retreat in the early stages of our basal melt experiment (Figure 5.9c). With it there was 46 km² of grounded ice loss, equivalent to only 0.1 mm of sea level rise. Perturbations in stresses at the grounding line did not propagate far inland, with only 6% flow acceleration and 0.05 m yr⁻² increase in thinning rates (Figure 5.9). This indicates that the glacier force balance was not significantly altered by removing these sections of the tongue. In addition, the lower ice tongue includes the large fracture that formed in 2016 [Münchow *et al.*, 2016], which is likely to have already de-coupled the lower PGIT from altering the stress balance at the grounding line [Borstad *et al.*, 2013; Rückamp *et al.*, 2019].

However, removing thicker (Figure 5.8) and stiffer (Figure 5.3) sections of the PGIT closer to the grounding line, caused greater loss of contact with the side-walls, and thus a larger reduction in lateral resistive stress acting on grounded ice. Removing the fourth

section of the tongue led to terminus acceleration of 41%, which was four-fold the acceleration after previous calving events. Some terminus deceleration occurred from 23-25 years, but speeds remained high further inland (Figure 5.9e), and increased by a further 330 m yr^{-1} at the terminus after the final calving event. Crucially, losing these upper sections of the tongue caused the grounding line to retreat a further ~ 8 km by 30-years (Figure 5.9c). This increased driving forces further inland, leading to a 240% increase in thinning rates, 25% flow acceleration and a 31% increase in ice flux during 19-30 years (Figures 5.7 and 5.9). Importantly, this period of dynamic readjustment (inland acceleration, thinning, and grounding line retreat) lasted ~ 10 years longer than under basal melting alone (Figure 5.9). However, after 70-years, Petermann Glacier appeared to have reached a new stable state, indicated by slow deceleration (-0.67 m yr^{-2}), thinning rates returning to initial levels (-0.12 m yr^{-1}), and the grounding line stabilizing at only 3 km further inland of our previous experiments (Figure 5.9c).

5.5 Discussion

Here, our modelling experiments show that future changes in the extent of PGIT (via melt, collapse, or calving) can alter the glaciers force balance, and double the sea level rise contribution from 0.43 mm under control conditions to up to 0.87 mm after 100 years (Table 5.1). In all cases, acceleration and thinning propagated inland and the grounding line retreated (Figure 5.7). Immediate ice tongue removal caused the greatest initial response which is consistent with observed inland thinning and acceleration of Jakobshavn Isbræ [Thomas, 2004; Joughin *et al.*, 2004], and glacier acceleration following the Larsen B ice shelf collapse [Scambos *et al.*, 2004; De Rydt *et al.*, 2015]. However, Petermann Glacier rapidly re-adjusted to the instant loss of buttressing, and without an increase in calving after collapse, the glacier tongue may regrow [Nick *et al.*, 2012]. We do not assess that here, but suggest it warrants further investigation. Alternatively, experiments one and three, that incorporated enhanced basal melt and therefore gradual ice tongue thinning, perturbed the glacier dynamic response for up to 60-70 years. The response to basal melt alone was relatively muted, primarily due to leaving the calving front position fixed, where in reality sub-tongue thinning is likely to act as a precursor to calving [Münchow *et al.*, 2014]. Therefore, calving of the PGIT (particularly closer to the grounding line) in combination with sub-tongue thinning, caused the greatest loss of buttressing and extended the duration of Petermann Glacier’s dynamic imbalance.

Despite some dynamic change at Petermann Glacier, the global impact on sea level rise remains limited. Hence, the key conclusion from these experiments is that in all

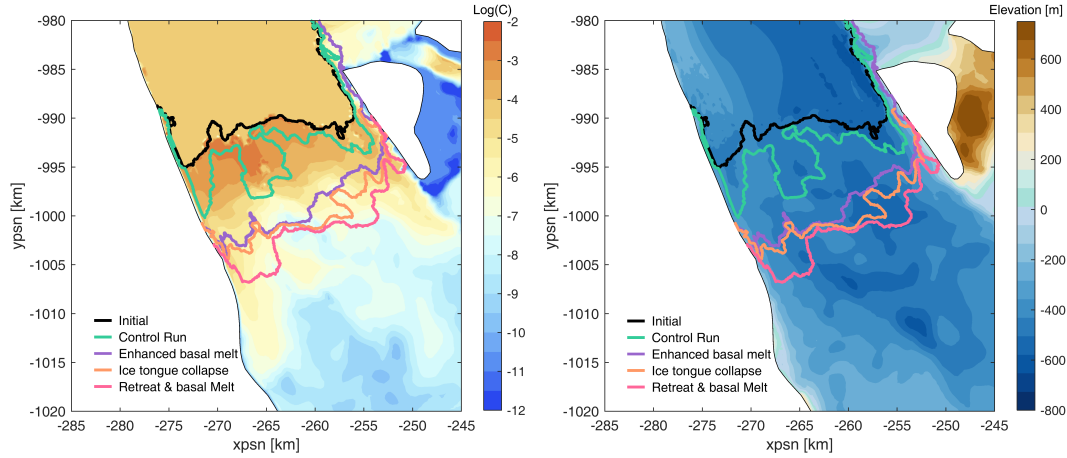


Figure 5.10: Left panel shows the basal slipperiness from our inversion (C), where orange represents high basal slipperiness, and blue is low basal slipperiness. The right panel shows the bed topography from the Operation IceBridge BedMachine v3 dataset [Morlighem *et al.*, 2017], where blue is elevation below sea level and green-brown is above sea level. The initial grounding line position at time=0 is shown in black. Grounding line positions after 100 years for each model run are: control run (green), enhanced basal melt (purple), ice tongue collapse (orange), and retreat and enhanced basal melt (pink).

cases ice tongue perturbations were unable to force long-term instability of Petermann Glacier, i.e irreversible thinning, acceleration, and grounding line retreat. We attribute this insensitivity primarily to a stabilization of the grounding line. In all experiments the grounding line position retreated to within 3 km of each other (Figures 5.9c and 5.10). Crucially, this stabilization limits the sea level rise contribution of Petermann Glacier to <1 mm over the next 100-years. This is three times smaller than projections from Jakobshavn Isbræ (2.77 mm) by 2100 [Bondzio *et al.*, 2017] and similar to the lowest emissions scenario (A1B) projections at Petermann and Kangerdlugssuaq (~ 1 mm: Nick *et al.*, 2013]. We discuss two controls that could have allowed the grounding line to become stable, and thus limit further ice loss. These are: i) bed topography and ii) lateral confinement/fjord width.

Bed slope is known to control stable positions of glacier grounding lines [Schoof, 2007; Choi *et al.*, 2017] in the absense of additional buttressing [Haseloff & Sergienko, 2018; Gudmundsson *et al.*, 2012]. Initial retreat of Petermann Glacier’s grounding line was over a shallow retrograde slope 5 km inland (-0.15°). However, the final grounding line positions rest on a steeper ($+0.33^\circ$) seaward sloping portion of the bed (~ 57 km inland of the current grounding line: Figure 5.8). This suggests that both retreat into shallower water, and the prograde slope further inland, forced the grounding line to stabilise at this position. This is consistent with the observed stability of grounding lines on prograde

bed slopes in west Greenland [Catania *et al.*, 2018], and previous suggestions that seaward sloping bed topography at Petermann Glacier limited past [Hogg *et al.*, 2016] and potential future grounding line retreat [Nick *et al.*, 2013]. Elsewhere in north Greenland, Choi *et al.* [2017] showed that Nioghalvfjærdsfjorden’s grounding line retreat and thus sea level rise contribution (1.12 mm by 2100) was similarly limited by a step in bed topography. Alongside slope, the slipperiness of the bed can also be sensitive to ice shelf buttressing [Gudmundsson, 2003; Schoof, 2007]. We acknowledge that our inversion method means our slipperiness estimate is fixed in time and consequently does not allow for regions of low basal drag to migrate inland. However, we have shown that mass loss is not dependent on slipperiness distribution (Appendix B) and is therefore expected to be a lesser control than a retrograde bed-slope, that would ultimately have promoted rapid and unstable retreat.

In addition to the role of bed topography, channel width can also modulate grounding line retreat [Jamieson *et al.*, 2012; Åkesson *et al.*, 2018], and has been identified as a key control on the retreat of numerous glaciers [e.g., Steiger *et al.*, 2018; Catania *et al.*, 2018]. PGIT is well-confined within its narrow fjord, and hence, its collapse leads to a loss of lateral resistive forces and buttressing. Indeed, the modelled response of Petermann Glacier to ice tongue collapse here, is greater than observations at glaciers (Hagen Bræ and C.H. Ostenfeld) with laterally unconfined ice tongues elsewhere in northern Greenland [Hill *et al.*, 2018a]. However, after an initial inland push of the grounding line in response to an ice tongue perturbation, the fjord width further inland does not vary substantially (< 2 km: Figure 5.10). Hence, there was no significant reduction in lateral drag as the grounding line retreats, nor an increase in the area subject to basal melt [Åkesson *et al.*, 2018], to promote a positive feedback of continued grounding line retreat.

Our results have shown that glacier geometry prevented Petermann Glacier from unstable rapid retreat or a substantial contribution to global sea level rise in response to the loss of its ice tongue. We acknowledge that we do not consider the indirect impact of losing the ice tongue, i.e. once the tongue is lost, what is the response to calving at a grounded terminus? However, unlike Zachariæ Isstrøm, where a deep retrograde bed and widening fjord allowed for sustained retreat once the terminus became grounded [Mouginot *et al.*, 2015; Choi *et al.*, 2017], Petermann Glacier’s inland geometry, (steepening seaward bed and narrow fjord) does not suggest that grounded ice calving will force rapid unstable retreat.

5.6 Conclusions

Here, we present the results of three modelling experiments that perturb the extent of the Petermann Glacier ice tongue to assess the dynamic response and potential sea level rise contribution over the next 100-years. Our findings show that under the most likely scenario, in which the tongue is removed via both enhanced basal melt and episodic calving, Petermann Glacier will lose approximately 313 Gt of ice above flotation. However the global impact is limited to a sea level rise of only 0.87 mm. Irreversible retreat and further ice loss was limited by a stabilization of the grounding line at a rise in bed topography ~ 12 km inland of its current position. Further inland the bed steepens in a seaward direction, and the channel remains narrow, suggesting that Petermann Glacier is geometrically constrained from becoming sensitive to calving in the future.

Chapter 6

Discussion

6.1 Recent retreat of glaciers in northern Greenland and the role of ocean-climate forcing

Future changes in outlet glacier dynamics are likely to increase northern Greenland's contribution to sea level rise [Mouginot *et al.*, 2019]. Despite this, Chapter 2 highlighted that records of outlet glacier change in northern Greenland are sparse, particularly prior to the 1990s. This currently limits our ability to assess recent outlet glacier change or potential glacier sensitivity to future ocean-climate warming. To address the limited number of records of outlet glacier behaviour pre-1990s, one of the aims of this thesis was to quantify outlet glacier change across northern Greenland over multidecadal timescales (1948-2015) and to determine if recent change (predominantly retreat) is part of a tidewater glacier cycle, or is exceptional (Chapter 3). One of the key findings is that in the mid-1990s there was a region-wide switch from variable advance and retreat (during 1948 to 1995) to predominantly high magnitude retreat (Figure 3.5, and Table 3.3). These high retreat rates during the last two decades (1995 to 2015) were primarily due to large calving events from floating ice tongues [Rignot *et al.*, 2001; Box & Decker, 2011; Hill *et al.*, 2018a]. This strongly suggests that recent retreat is exceptional in nature, and that ice tongues or grounded outlet glaciers are unlikely to advance back to their former extents.

The timing of the switch to high magnitude retreat in the 1990s was coincident with increased retreat rates across the Arctic [Carr *et al.*, 2017b; Cook *et al.*, 2019], including acceleration and retreat in south-east Greenland [Howat *et al.*, 2008; Seale *et al.*, 2011], and northwest Greenland [e.g., Carr *et al.*, 2013b; Moon *et al.*, 2012]. This suggests that

either ocean or climate warming forced a change in conditions at glacier margins that initiated recent retreat. However, the relative contribution of these forcing factors differs between regions of the GrIS and elsewhere in the Arctic. Indeed, regional studies in Greenland have previously determined increased air temperatures [Thomas *et al.*, 2011; Luckman *et al.*, 2006], ocean warming [Khan *et al.*, 2014; Wood *et al.*, 2018; Straneo *et al.*, 2013], or a reduction in sea ice concentration [Moon *et al.*, 2015; Carr *et al.*, 2013b; Khan *et al.*, 2014] to be the dominant driver of glacier retreat. Unfortunately, ocean-climate data in northern Greenland is limited and so has not been analysed in detail in this thesis. Nevertheless, it is now worth considering some proposed mechanisms, and which factors may have been important for accelerating retreat in northern Greenland. The final section of this Chapter (Section 6.4) also presents some directions for future research to better determine the precise drivers of recent retreat in the region.

Recent increased air temperatures across the GrIS [Mernild *et al.*, 2009; Box *et al.*, 2009; Cappelen *et al.*, 2010] could have caused thinning close to glacier termini, subsequently steepening the ice surface slope, increasing the driving stress, and accelerating ice mass loss. Indeed, increased thinning has taken place in the ablation areas (< 2000 m elevation: Figure 1.2) around the GrIS since the 1990s [Abdalati *et al.*, 2001; van den Broeke *et al.*, 2016; Pritchard *et al.*, 2009; Krabill *et al.*, 2000]. At several glaciers (e.g. Jakobshavn [Thomas *et al.*, 2011], Helheim, and Kangerdlugssuaq [Howat *et al.*, 2008; Luckman *et al.*, 2006]), linearly increasing air temperatures after the 1990s were linked to thinning in the ablation zone that instigated terminus retreat. Elsewhere in the Arctic, Cook *et al.* [2019] also showed that greater surface melt and runoff due to increased air temperatures, was the main driver of glacier retreat in the Canadian Arctic. In Chapter 3, it was suggested that such ice marginal thinning may also have been the initial forcing for widespread retreat across northern Greenland, based on observations from surface elevation change datasets. Using changepoint analysis (similar to as described in Chapter 3 Section 3.3.2.3) Figure 6.1 shows that there was a significant change in mean annual air temperatures ca. 2000 at weather stations in northwest and northeast Greenland, which had already begun to increase from 1990 onwards. This follows some initial thinning at glacier termini (Figures 3.7 and 3.8) and was coincident with the onset of region-wide increased glacier retreat. Overall, this suggests that warmer air temperatures across northern Greenland are likely to have played an important role in forcing thinning at glacier termini, which in turn may have triggered initial terminus retreats.

In addition to thinning in the terminus region, increased air temperatures may also have promoted increased calving in northern Greenland via increased surface melt and runoff [Phillips *et al.*, 2010; van der Veen *et al.*, 2011] and the feedbacks between subglacial

discharge and submarine melt rates [Motyka *et al.*, 2003, 2013; Schild & Hamilton, 2013]. Firstly, increased surface melt and runoff could have promoted fracture penetration to the bed, either via water filled crevasses [Benn *et al.*, 2007; Nick *et al.*, 2010; van der Veen *et al.*, 2011] or supraglacial lake drainages [Banwell *et al.*, 2013; Carr *et al.*, 2015]. This can both increase calving and lubricate the bed, thereby accelerating ice flow, increasing the driving stress, and increasing mass loss. In northern Greenland, satellite imagery observed in this thesis revealed water-filled crevasses along ice tongues at Zachariæ Isstrøm and C. H. Ostenfeld, and supraglacial lakes close to the terminus at Humboldt Glacier [see also: Carr *et al.*, 2015], which are likely to have pre-conditioned these glaciers for retreat. However, this was not the case at Petermann Glacier, where supraglacial lakes on the ice tongue had a limited impact on instability due to rapid water evacuation by a large supraglacial river [Macdonald *et al.*, 2018]. Thus, the role of water-filled crevasses and supraglacial lake drainages is likely to vary on an individual glacier basis across northern Greenland. Hence, further work is needed to assess the importance of supraglacial lake drainages, and water filled crevasses for forcing calving at outlets in northern Greenland.

Secondly, subglacial discharge, in the form of buoyant meltwater plumes mixes with fjord water, and enhances melt at the glacier front [Jenkins, 2011; Straneo *et al.*, 2013; Xu *et al.*, 2012]. Under warmer conditions, increased volumes of surface melt and thus subglacial discharge can force greater rates of submarine melt [Jenkins, 2011; Xu *et al.*, 2012; Motyka *et al.*, 2013]. While this thesis has not considered this, previous work at Humboldt Glacier linked subglacial plumes to enhanced calving and retreat [Carr *et al.*, 2015]. This could also be important beneath floating ice tongues, where Cai *et al.* [2017] recently found that increased subglacial runoff at Petermann Glacier contributed to a 24% increase in submarine melt. To summarise, alongside thinning at the terminus, increases in surface runoff and subglacial discharge (due to increased air temperatures), are likely to have also forced recent retreat in northern Greenland. This is likely to have been the primary driver of submarine melt and retreat in the far northern regions, as they are not subject to warm ocean waters. With increased air temperatures in the future, this effect could become more profound, with the potential to force further regional retreat.

Alongside increased air temperatures, ocean warming could have also forced recent dynamic change in northern Greenland. Elsewhere in Greenland, increased ocean temperatures have coincided with glacier retreat, thinning, and acceleration [Moon & Joughin, 2008; Straneo *et al.*, 2013; Holland *et al.*, 2008; Christoffersen *et al.*, 2011; Wood *et al.*, 2018; Walsh *et al.*, 2012; Straneo *et al.*, 2013]. Despite not being exposed to warm subtropical waters (e.g. east Greenland Seale *et al.* [2011]), relatively warm ocean waters around the northern margins of the GrIS have the potential to increase submarine melt rates at

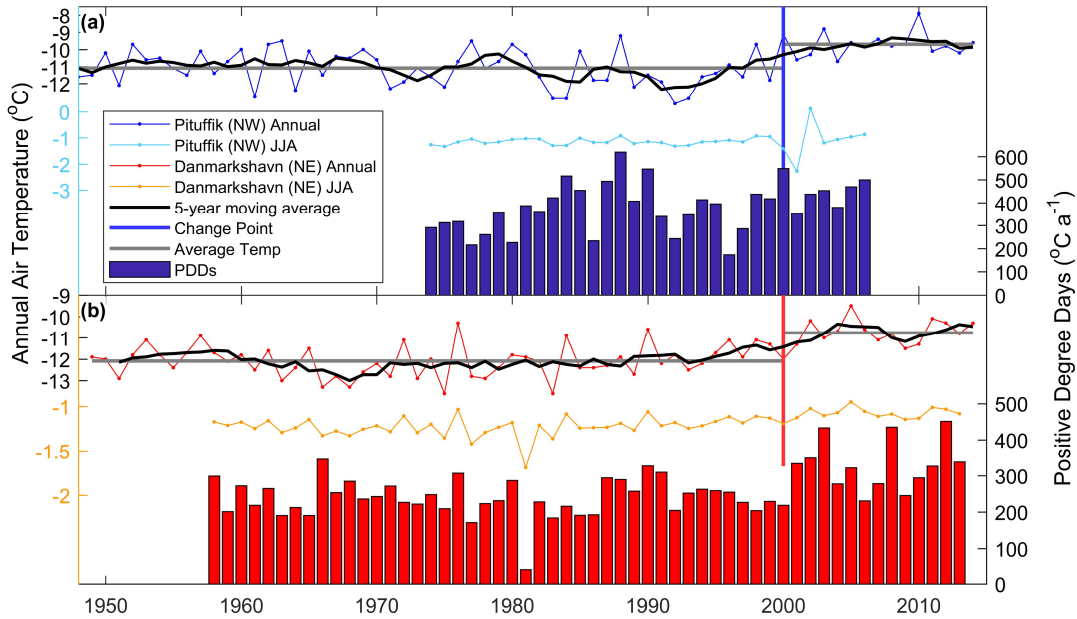


Figure 6.1: Climate data for northern Greenland provided by the Danish Meteorological Institute. A) Annual (dark blue) and summer June July August (light blue) air temperatures from the Pituffik (PK) ($76^{\circ}32'N$, $68^{\circ}45'W$) automatic weather station in northwest Greenland. B) Annual (dark blue) and summer June July August (light blue) air temperatures from the Danmarkshavn (DK) ($76^{\circ}46'N$, $18^{\circ}40'W$) automatic weather station, in northeast Greenland. For both plots the black line represents the 5-year moving average of air temperature time series and solid vertical lines (blue and red) represent a statistically significant change point between the mean air temperature either side (shown in grey). Blue and red bars represent positive degree days from available daily air temperatures from both weather stations.

grounded glacier fronts [Rignot *et al.*, 2010; Straneo *et al.*, 2013; Joughin *et al.*, 2012a] or along the underside of floating ice tongues [Mouginot *et al.*, 2015; Reeh *et al.*, 1999; Rignot *et al.*, 2001, 1997; Motyka *et al.*, 2011]. Ultimately, increased rates of submarine melt can promote undercutting at the grounding line or calving front, which enhances rates of retreat and calving [O’Leary & Christoffersen, 2013; Box & Colgan, 2013; Rignot *et al.*, 2015].

Submarine melting along the base of floating ice tongues is an important component of mass loss in northern Greenland [Rignot & Steffen, 2008; Wilson *et al.*, 2017]. Thinning of the ice shelf/tongue increases the glacier driving stress, and accelerates grounded ice discharge. Indeed, this has occurred at ice shelves in Antarctica, which have thinned and undergone accelerated mass loss due to enhanced submarine melt, primarily related to ocean warming [Paolo *et al.*, 2015; Jenkins *et al.*, 2018; Liu *et al.*, 2015; Pritchard *et al.*, 2012; Rignot *et al.*, 2013]. However, the role of ocean temperature induced melt beneath floating ice tongues in Greenland has not received much attention [Joughin *et al.*, 2012a].

Wilson *et al.* [2017] recently inferred melt rates beneath the three remaining ice tongues in northern Greenland (Nioghalvfjærdsfjorden, Petermann and Ryder) using a flux divergence approach. This revealed high melt rates of up to $\sim 50 \text{ m a}^{-1}$, that accounted for 80% of the total melt flux [Wilson *et al.*, 2017]. These estimates are greater than previous values at Petermann Glacier [Rignot & Steffen, 2008], suggesting that submarine melt rates in northern Greenland have increased. Submarine melting could therefore become a more important source of mass loss across the remaining ice tongues if warming continues.

In addition to inferred melt rates beneath the remaining ice tongues, some *in-situ* measurements of ocean conditions also exist in northern Greenland. Data from Petermann Glacier from 2002 to 2016 recorded $\sim 0.2^\circ\text{C}$ Atlantic ocean warming which, alongside stronger circulation, is likely to have promoted warm water circulation beneath the ice tongue [Washam *et al.*, 2018; Münchow *et al.*, 2011; Shroyer *et al.*, 2017], enhancing basal melt rates, and preconditioning the glacier for calving. In northeast Greenland, observations at Nioghalvfjærdsfjorden show the presence of warm (1°C) Atlantic water [Mayer *et al.*, 2000; Wilson & Straneo, 2015], which is likely to have forced recent retreat at the neighbouring Zachariæ Isstrøm [Mouginot *et al.*, 2015]. Alongside ocean-induced melt of floating ice tongues, a number of grounded terminus glaciers have been subject to ocean warming/submarine melt, driving recent retreat in northwest Greenland [Wood *et al.*, 2018; Willis *et al.*, 2018]. In the study region of this thesis, warm water intrusion at Tracy and Helprin Glaciers promoted thinning at the terminus, followed by retreat [Willis *et al.*, 2018], but these rates differed between the two glaciers due to their contrasting bed depth/topography [see Section 6.3: Porter *et al.*, 2014; Willis *et al.*, 2018]. Ocean warming is likely to be the most important driver of recent glacier change in the northwest and northeast regions of Greenland [Rignot & Mouginot, 2012; Wood *et al.*, 2018; Khan *et al.*, 2014], primarily as they are subject to warm ocean water that reaches the fjords. Instead, at glaciers in the far north that are not subject to warm North Atlantic water (e.g. Petermann), it may be that submarine melt is driven primarily by subglacial discharge, related to air temperature induced surface melt [Cai *et al.*, 2017]. Warming of North Atlantic deep water in the future could enhance melt at grounded glacier fronts and beneath floating ice tongues, and ultimately lead to further glacier retreat. Improved measurements of ocean temperatures e.g. via submarines, are needed in the future to quantify the effect of warming water on glacier melt and retreat.

Another key impact of warmer air/ocean temperatures across northern Greenland is the removal of sea ice from the fjords. Sea-ice buttressing has been identified as an important control on glacier calving rates both in northern Greenland [Higgins, 1990; Johannessen *et al.*, 2013; Khan *et al.*, 2014; Reeh *et al.*, 2001, see Section 2.4.2] and elsewhere

[Miles *et al.*, 2016, 2018; Moon *et al.*, 2012, 2015; Amundson *et al.*, 2010]. For example, sea ice stiffened the ice mélange at Jakobshavn Isbæ and held it in place against grounded ice. Crucially, sea ice retreat then weakened the ice mélange, which reduced terminus backstress and promoted calving [Amundson *et al.*, 2010]. Glaciers in northern Greenland are susceptible to a similar process under future warming and decreasing concentrations of sea-ice. Indeed, early work by Reeh *et al.* [2001] suggested that the retreat of fast-ice in northeast Greenland, promoted calving at Nioghalvfjærdsfjorden, which was supported by later work using improved satellite derived sea ice concentrations [Khan *et al.*, 2014]. Sea-ice retreat has also been identified as a key driver of retreat and glacier acceleration in northwest Greenland [Moon *et al.*, 2015; Carr *et al.*, 2013b]. These data suggest that the loss of backstress associated with sea ice retreat is likely to be an important control on northern Greenland outlet glaciers. Arctic sea ice concentrations have shown a negative trend since 1978 [Serreze & Meier, 2019], and if this continues in the future an increase in sea-ice free days may allow for more calving and retreat to occur across the region.

This thesis has identified an important increase in the retreat, acceleration, and thinning of outlet glaciers in northern Greenland which appears synchronous with recent ocean-climate warming around other parts of the GrIS. Importantly, the precise ocean-climate drivers of retreat may differ between sectors of northern Greenland. It is likely that the northwest and northeast parts of the study region are subject to warmer ocean waters, that propagate northward via the North Atlantic and Irminger currents. Such increases in ocean heat, are likely to have promoted submarine melt at grounded calving fronts or beneath the ice tongues at glaciers draining the NEGIS. However, the far northern regions of the ice sheet are not subject to warm deep water, and here it is more likely that warmer air temperatures were the main driver of: thinning, fracture-driven calving, submarine melting (due to increases in subglacial discharge rather than ocean heat), and sea ice retreat. Overall, these results show that like other regions of the ice sheet, northern Greenland has begun a period of rapid glacier retreat that is likely to continue as air and ocean temperatures are forecast to increase in the future.

6.2 Glacier sensitivity to ice tongue loss

Although recent outlet glacier retreat across northern Greenland can be considered exceptional on decadal timescales, Chapter 3 identified that variability exists between the calving nature and magnitude of retreat between individual glaciers. The main aim of this thesis was to quantify the role of ice tongues in modulating outlet glacier response to changes at the terminus. To do this, the temporal pattern of retreat, acceleration,

and thinning of glaciers with grounded termini was compared to those that terminate in floating ice tongues (Chapter 3). The key finding of this work is that the termini of outlet glaciers with floating portions behaved significantly differently to those that are grounded, which led to differences in their dynamic response to terminus perturbations. However, there was also variability in behaviour within these two categories of terminus type (grounded vs floating). For example, some glaciers appeared more sensitive than others to the loss of their floating ice tongues.

Firstly, grounded outlets were characterised by sustained but lower magnitude retreat, owing to gradual calving, followed by acceleration and thinning over approximately two decades. In contrast, glaciers with floating ice tongues exhibited high magnitude episodic calving and/or ice tongue collapse due to rift propagation, which either forced some short-lived acceleration and thinning, or did not cause a change in stresses inland (see discussion in Chapter 3, Section 3.5.2). Therefore, although glaciers with floating ice tongues showed higher magnitude retreat, they generally appeared insensitive to calving in comparison to grounded termini. This is consistent with knowledge of resistive stresses acting on grounded ice [Cuffey & Paterson, 2010]. Grounded ice retreat causes a loss of both basal and lateral resistance which can cause a greater perturbation than in the case of calving or removing an ice shelf, which only restrains flow via lateral resistance [McFadden *et al.*, 2011]. It appears that the collapse of several ice tongues in northern Greenland did not substantially affect inland ice dynamics (e.g. at C. H. Ostenfeld and Hagen Bræ), but calving from their now grounded termini could become more important in the future. Due to the key differences presented in this thesis it is important to consider the role of terminus type in modulating the glacier response when quantifying outlet glacier change in other regions of the Arctic and Antarctic.

This thesis has identified key differences between the dynamic behaviour of glaciers with either grounded or floating termini. In addition to this, observations of ice tongue extent and glacier dynamics presented in Chapter 3, and sensitivity experiments conducted on Petermann Glacier (in Chapters 4 and 5) were used to further assess the role of ice tongues in modulating glacier behaviour. These results revealed that there are distinct differences between the sensitivity of individual glaciers to ice tongue loss in northern Greenland.

Ice tongue buttressing is primarily controlled by the amount of lateral resistance provided by ice shearing along the glacier side-walls [Cuffey & Paterson, 2010; Haseloff & Sergienko, 2018; Pegler *et al.*, 2013]. Observations within Chapter 3 showed that a number of glaciers in northern Greenland (e.g. C. H. Ostenfeld and Hagen Bræ) were insensitive to recent ice tongue collapse. Fragmented, unconfined ice tongues at these glaciers (Figure

3.12) provided limited lateral resistance and as a result were probably already decoupled from grounded ice prior to collapse. This means that they were largely passive, providing little backstress, which was indicated by little to no acceleration or inland propagation of surface thinning in the years following ice tongue loss. This insensitivity to ice tongue retreat could also explain why, despite high magnitude ice tongue retreat in the last two decades, Kjeldsen *et al.* [2015] found limited increase in dynamic ice discharge from the far north. Unlike large ice shelves in Antarctica [Paolo *et al.*, 2015; Fürst *et al.*, 2016; Reese *et al.*, 2018a], this suggests that most ice tongues recently lost from northern Greenland provided limited buttressing on inland ice, and their collapse did not lead to substantial increases in ice discharge.

However, some glaciers in northern Greenland still possess ice tongues (Nioghalvfjærdsfjorden and Petermann) and uncertainty remains as to their response to future ice tongue collapse. As both of these ice tongues are laterally confined their collapse could cause a greater stress perturbation on grounded ice [Jamieson *et al.*, 2012; Haseloff & Sergienko, 2018; Åkesson *et al.*, 2018; Goldberg *et al.*, 2009]. Indeed, this was the case at Zachariæ Isstrøm, which unlike most glaciers with ice tongues in northern Greenland was dynamically sensitive to ice tongue loss. In this sense the glacier behaved similarly to grounded outlets i.e. gradual calving accompanied by prolonged acceleration and thinning. This behaviour is also consistent with the response to laterally confined ice shelf collapse of Jakobshavn Isbræ [Joughin *et al.*, 2004; van der Veen *et al.*, 2011; Steiger *et al.*, 2018], and the glaciers draining into the Larsen ice shelves [Rott *et al.*, 2002; Scambos *et al.*, 2004; Rignot *et al.*, 2004; De Rydt *et al.*, 2015].

To support this further, both diagnostic and transient simulations at Petermann Glacier (Chapters 4 and 4) showed that lateral confinement was a primary control on the glaciers future response to ice tongue loss. In a similar way to the recent calving event from the Larsen C Ice Shelf [Hogg & Gudmundsson, 2017], the lower portions of Petermann Glacier’s ice tongue can be considered passive, providing little resistance to inland flow [Nick *et al.*, 2012; Hill *et al.*, 2018b]. However, calving from thicker and more laterally confined sections of the tongue in the future are likely to cause a greater increase in inland velocity and surface thinning rates. This is in contrast to the observed response to unconfined ice tongue loss elsewhere in northern Greenland (e.g. C. H. Ostenfeld and Hagen Bræ). This highlights the non-linearity of ice tongue calving on glacier dynamics, and disparity between individual glaciers depending on the geometry of the ice tongue/shelf. It could be that similar to Petermann Glacier, calving closer to the grounding line at Larsen C could cause increased ice loss [Hogg & Gudmundsson, 2017], but this requires further investigation. Due to the important role of lateral resistive stresses on restraining

grounded ice flow, it is important that more model studies are conducted in the future on individual outlet glaciers using 2-horizontal dimensions as a minimum. Such models will be able to capture the important role of spatially variable lateral resistive stress on ice shelf buttressing that is often not fully captured in more simplistic flowline models [Nick *et al.*, 2009; Åkesson *et al.*, 2018]. Overall, at glaciers with ice tongues elsewhere in the Arctic, and that drain into ice shelves in Antarctica, it is important to consider both their individual glacier response to a loss of buttressing at the grounding line, and their potential response once they begin to calve grounded ice directly into the ocean. Both of these factors have important implications for accurately projecting mass loss from marine-terminating outlet glaciers both in the Arctic and the Antarctic.

6.3 Role of bed geometry in modulating glacier dynamics

The previous section discussed the role that ice tongues play in modulating the dynamic response to glacier terminus changes, which is primarily related to varying levels of lateral resistance provided by the ice tongues. Alongside this, glacier sensitivity to grounded ice retreat or ice tongue collapse can be controlled by the glaciers bed topography, which can either limit or promote terminus perturbations to propagate inland [Felixson *et al.*, 2017; Enderlin *et al.*, 2013]. This was the motivation for assessing the role of glacier geometry on northern Greenland outlet glacier behaviour in this thesis. The results of Chapter 3 identified that bed topography modulated the magnitude of retreat at grounded termini, and had the potential to limit or enhance grounding line retreat before and after ice tongue collapse. This was further supported by future transient experiments of the future dynamics of Petermann Glacier (Chapter 5), which showed bed topography was a key limiting factor for unstable rapid downslope retreat.

Calving from grounded termini removes ice in contact with the bed, and causes a loss of basal resistance, which subsequently increases the glacier driving force [Cuffey & Paterson, 2010; McFadden *et al.*, 2011]. In the case that calving/terminus retreat occurs down a deepening bed, grounding line discharge increases as the ice rapidly thins to flotation [Schoof, 2007]. This allows a positive feedback to initiate, further increasing driving stress, acceleration, and ice discharge. A number of studies have shown this occurs in Greenland, for example at Helheim Glacier which rapidly retreated into a bedrock depression [Howat *et al.*, 2007; Nick *et al.*, 2009], and via sensitivity experiments based on the geometry of Helheim Glacier, Kangerdlugssuaq Glacier, and Jakobshavn Isbræ [Enderlin *et al.*, 2013].

In northern Greenland, the four grounded outlet glaciers with the highest rates of

terminus change all retreated down retrograde bed slopes (see Table 3.4). In general, these glaciers also showed the greatest acceleration during periods of retreat (Table 3.2), suggesting a greater perturbation on inland ice. This is consistent with significantly higher magnitude retreat rates over retrograde bed slopes in northwest [Carr *et al.*, 2013b; Porter *et al.*, 2014], southeast [Bunce *et al.*, 2018], and central west Greenland [Catania *et al.*, 2018]. For example, within the same fjord in northwest Greenland there were notable differences in the magnitude of retreat and thinning at neighbouring Tracy and Heilprin Glaciers (Figure 3.6), which is primarily related to bed depth [Bunce *et al.*, 2018; Porter *et al.*, 2014; Willis *et al.*, 2018]. Retreat down a deeper and steeper bed at Tracy Glacier is likely to not only have increased the glacier driving stress due to increases in ice thickness, but also have allowed more ocean water to access and thus melt the calving face [Porter *et al.*, 2014]. In the future, these factors could promote further terminus retreat at Tracy and Heilprin Glaciers, and also at glaciers with deep retrograde beds elsewhere in northern Greenland. Meanwhile, our results show that grounded outlet glaciers resting in shallower water and on prograde slopes (e.g. Harder, Academy, and Marie-Sophie: Chapter 3) were less sensitive to retreat, evident in lower magnitude retreat rates (averaging -24 m a^{-1} from 1948 to 2015) and little to no acceleration (Table 3.2). In line with previous studies, this suggests that the magnitude of retreat and adjustment to the glaciers force balance in northern Greenland is primarily controlled by bed slope. This substantiates previous findings that highlight the importance of bed topography on modulating glacier sensitivity to past and future retreat [Catania *et al.*, 2018]. Ultimately, this means that improved estimates of bed topography at the grounding lines of outlet glaciers not only in Greenland, will provide more accurate projections of retreat and associated mass loss under future scenarios of climate warming.

Alongside the influence of lateral resistance provided by ice tongues on grounded ice, the bed topography at the grounding line can either enhance or limit the positive glacier feedback to a loss of buttressing [Joughin & Alley, 2011; Enderlin *et al.*, 2013]. In the case of unconfined ice shelves like C. H. Ostenfeld and Hagen Bræ, bed slope is likely to be the primary control on grounding line stability [Gudmundsson *et al.*, 2012; Åkesson *et al.*, 2018; Schoof, 2007]. Taken together, the limited lateral resistance and thus buttressing provided by these ice tongues, and the absence of a retrograde bed slope at the grounding line, are likely to have limited the glacier response to ice tongue collapse. The grounding line may have already been stable on a rise in bed topography prior to collapse, and the bed topography immediately inland did not promote retreat after ice tongue loss at these two glaciers. As a result, there was a reduction in annual retreat rates at both glaciers to $< 200 \text{ m a}^{-1}$ after they became grounded (Figure 3.6 in Chapter 3). Their inland bed topography also suggests that they are unlikely to be prone to rapid retreat in the future,

unlike glaciers elsewhere [e.g., Catania *et al.*, 2018; Brough *et al.*, 2019].

In the case of well-confined ice tongues, however, a loss of lateral resistance causes a greater initial perturbation in stresses at the grounding line, forcing initial retreat. Thereafter, where the bed is retrograde, retreat into deeper water can sustain the initial perturbation, leading to a positive feedback, and ultimately marine ice sheet instability [Joughin *et al.*, 2012a; Pattyn, 2018]. This positive feedback mechanism has been both observed and modelled in the Amundsen Sea region of West Antarctica [Favier *et al.*, 2014; Joughin *et al.*, 2010a, 2014; Rignot *et al.*, 2014], and also at Jakobshavn Isbræ, in response to ice shelf/tongue loss [Vieli & Nick, 2011]. However, research conducted in northern Greenland to date has not specifically assessed the potential for marine-ice sheet instability. At Zachariæ Isstrøm, retreat of the ice tongue between 2002 and 2015 forced the grounding line to retreat down a deepening section of the fjord (see Figure 3.11 in Chapter 3), which prolonged the dynamic imbalance and positive feedback once it became grounded [Mouginot *et al.*, 2015]. Numerical simulations also suggest unstable downslope retreat will continue to the end of the 21st century, with the potential to cause mass loss equivalent to 16 mm of global sea level rise under high rates of frontal melt [6 m day⁻¹: Choi *et al.*, 2017]. Similarly, the modelling experiments conducted in Chapter 5 at Petermann Glacier showed that ice tongue loss, particularly close to the grounding line, was able to perturb grounding line stresses and force it to retreat ~12 km inland (see Figure 5.9 in Chapter 5). However, retreat past this point was prevented by a rise in bed topography, which limited the potential for marine-ice sheet instability in response to ice tongue loss. Crucially, this also limited the global sea level rise contribution to < 1 mm after 100 years (Figure 5.9), which is less than future estimates at other glaciers that terminated in ice tongues [Bondzio *et al.*, 2017; Choi *et al.*, 2017]. However, this grounding line stability is consistent with future simulations at Nioghalvfjærdsfjorden, which drains the NEGIS [Choi *et al.*, 2017]. Projections at Nioghalvfjærdsfjorden also showed that mass loss over the next century (equating to only 1.12 mm of sea level rise by 2100), was limited by a step in bed topography and pinning points at the front of the tongue [Choi *et al.*, 2017]. In general, the results presented here show that bed topography at a number of outlets in northern Greenland prevented unstable retreat in response to ice tongue loss. In addition, prograde sloping beds further inland at the remaining ice tongues (Petermann and Nioghalvfjærdsfjorden) could also limit grounding line retreat in the future. Overall, this highlights the important role of bed topography on future glacier retreat and mass loss, and the need to assess bed topography at the grounding lines of glaciers elsewhere.

Alongside the role of bed topography it is also important to consider the nature of the ice flowing over the bed, i.e. basal slipperiness and ice rheology, which can also

control the glacier dynamic response to a perturbation at the terminus. Firstly, slippery beds can reduce effective pressure, leading to acceleration and glacier thinning [Cuffey & Paterson, 2010]. Indeed, basal sliding accounts for the majority of ice flow across the GrIS [Rignot & Mouginot, 2012; MacGregor *et al.*, 2016; Shapero *et al.*, 2016]. Ice rheology indicates the viscosity of ice flow that can also govern the amount of stress provided by the ice. In the case of removing stiff, viscous ice, there is greater loss of resistance and subsequent perturbation to flow. Some previous studies have examined the ice conditions across Greenland. For example Lee *et al.* [2015] estimated ice sheet wide basal slipperiness and ice rheology as part of model initialisation. In addition, estimates of bed temperature have been made [MacGregor *et al.*, 2016; Chu *et al.*, 2018]. While ice-bed conditions were not considered on a region wide scale in this thesis, inversions of surface velocities at Petermann Glacier gave some insight into the basal conditions (see Figure 5.3 in Chapter 5). This revealed a region of slippery ice inland of the grounding line which is likely to have promoted rapid grounding line retreat over this portion of the bed. In addition, the temperature-dependent ice rheology parameter (A), revealed alternating bands of stiff/soft ice approximately 60 km inland of the grounding line (Figure 5.3) that coincide with regions of frozen/thawed ice identified by Chu *et al.* [2018]. These bands are thermally controlled due to frictional heating and meltwater availability, which means the onset region of Petermann Glacier is susceptible to inland migration under future warming [Chu *et al.*, 2018]. Crucially, bed strength is an important additional control (to bed topography) on glacier dynamics [Shapero *et al.*, 2016], and future work could use numerical models to invert for ice/bed conditions to better assess glacier dynamics in northern Greenland.

6.4 Future work

While this thesis has provided new insight into the behaviour of outlet glaciers in northern Greenland, a number of key areas for future research are also highlighted below:

- **Drivers of northern Greenland glacier retreat.** Determining the precise drivers of regional/individual glacier retreat in northern Greenland is an important area of future research. In the far northern regions, improved air temperature measurements and estimates of surface melt and subglacial discharge would help to better determine the link between subglacial discharge and submarine melt rates beneath floating ice tongues. In the northwest and northeast regions of Greenland, improved *in-situ* measurements of ocean temperatures would aid calculations of melt rates at

calving faces or along the underside of the remaining floating ice tongues. Alongside this, coupled ice-ocean model experiments at individual glaciers would be useful to quantify the impact of varying ocean conditions on glacier dynamics. Crucially, both observations and modelling of glacier sensitivity to a whole range of ocean or climate forcing in northern Greenland would provide valuable insight into their potential response to future climate warming.

- **Assessing the role of bed topography and grounded ice calving.** This thesis has assessed the role of ice tongues and showed that a number of glaciers were insensitive to recent ice tongue loss, primarily due to their unconfined nature, and steep bed topography inland of the grounding line. However, their response to further retreat (now they have become grounded) remains uncertain. Firstly, this requires improved observations (radar flight lines) to help better constrain bed topography in northern Greenland. This will allow a better assessment of the inland topography which may promote or limit glacier retreat, depending on the depth and slope of the bed [Catania *et al.*, 2018]. Bathymetric surveys in fjords in northern Greenland will also improve understanding of how deep ocean water is transported to glacier fronts, similar to recent surveys at Petermann Glacier [Jakobsson *et al.*, 2018]. In addition, modelling studies of individual glaciers are needed to examine their dynamic response to further retreat/calving forced by varying levels of external climate forcing, e.g. will these glaciers remain stable due to their bed topography despite extreme warming? Ultimately, improved understanding of glacier sensitivity to bed topography and future warming will improve future projections of sea level rise from these outlets.
- **Improved measurements of ocean temperatures and submarine melt rates.** There are currently three remaining ice tongues in northern Greenland. Some recent work has modelled their potential future response to ice tongue loss [Choi *et al.*, 2017; Rathmann *et al.*, 2017; Nick *et al.*, 2012] including the experiments presented in Chapters 4 and 5 of this thesis [Hill *et al.*, 2018b]. However, additional studies are needed that take into account varying ocean conditions and submarine melt rates. Wilson *et al.* [2017] recently estimated single average melt rates beneath these ice tongues during 2011 to 2015, which built upon previous steady-state estimates of melt beneath Petermann Glacier's ice tongue [Rignot & Steffen, 2008]. However, recent estimates of melt rates are isolated in time and there is a need for temporally resolved melt rates to determine links between recent ocean-climate warming and melt and thinning of ice tongues. In addition, forward modelling experiments are needed to determine the future response of these glaciers once they become grounded.

- **Predictions of future sea level rise from northern Greenland and the entire ice sheet** Alongside improved process understanding at individual glaciers, there is a need for improved predictions of sea level rise from both northern Greenland specifically and across the whole Greenland ice sheet. Current model simulations often exclude glacier retreat and calving in response to external forcing, due to the complex nature, and heterogeneity between individual glacier response. In northern Greenland, the presence of ice tongues complicates this further, as for example, the response to ocean warming and submarine melt is different underneath an ice tongue vs direct melt along a calving face. Given the distinct differences between grounded and floating termini identified in this thesis (Chapter 3), it is appropriate for glacier specific studies to examine the response of remaining ice tongue loss. Indeed this has been in part addressed with the work in Chapters 4 and 5. While it would be desirable to perform detailed glacier specific studies to determine their response to external forcing, perhaps even using coupled ice-ocean simulations, it is not feasible to conduct individual glacier studies on an ice sheet wide scale. Hence, new simple parameterizations have been developed to force tidewater glacier retreat as a simple linear function of changes in submarine melt [Cowton *et al.*, 2018; Slater *et al.*, 2019]. Indeed if the remaining ice tongues are lost in the near future (potentially without significant impact on inland ice), it may then be possible to model the response of these glaciers in the same way as tidewater outlets elsewhere on the ice sheet. However, the oversimplified nature of these parameterizations mean they are unable to capture non-linearity in glacier retreat. Instead it may be more appropriate to parameterize frontal melt rates, and use calving laws to allow for fully dynamic evolution of the terminus position through time [Morlighem *et al.*, 2016a; Bondzio *et al.*, 2016]. While this may provide a more complete picture of marine-terminating glacier retreat, it is computationally expensive on a continent wide scale. It remains an active field of research to balance computational expense and accurate projections of marine-terminating outlet glacier retreat across Greenland.
- **Glacier surging in northern Greenland.** This thesis has identified the role of glacier surging in northern Greenland (see Sections 2.4.4 and 3.5.4), and how this complicates the signal of retreat in response to climate-forcing. Some recent work has examined surging in northeast Greenland [Mouginot *et al.*, 2018], but there remains a need to provide a more comprehensive analysis of the role of glacier surging in Greenland. In particular, future work could usefully focus on Ryder Glacier, which unlike other glaciers in northern Greenland has not recently retreated. Instead, it has been referred to as surge-type, and showed a periodic advance and retreat of its floating terminus (see Figure 3.8). Hence, more detailed analysis is needed to determine if it is indeed surge-type, or is undergoing a tidewater glacier cycle.

Chapter 7

Conclusions

Northern Greenland is an important region as it drains a substantial portion of the ice sheet [$\sim 40\%$ by area: Rignot & Kanagaratnam, 2006] and has the potential to become destabilised by the amplified warming that the Arctic will experience in the future [Gregory & Huybrechts, 2006; Born & Nisancioglu, 2012]. It is also the last region of the GrIS where a number of glaciers terminate in long floating ice tongues, but remains poorly studied in comparison to other areas of the ice sheet. The first objective of this thesis was achieved by providing a review of previously published work on outlet glacier behaviour in northern Greenland (Chapter 2). This concluded that while there appeared to have been increased retreat, and in some cases accelerated ice flow, the region-wide glacier response to forcing (ocean-climate), local geometry (fjord width and depth) and, in particular, the collapse of floating ice tongues remained uncertain. Hence, more detailed observations and analysis were needed, which provided the motivation for the rest of the work conducted in this thesis. Thus, the primary aim of this thesis was twofold: 1) quantify outlet glacier change across northern Greenland, and 2) determine the role of floating ice tongues in modulating past and future glacier behaviour.

Quantifying regional outlet glacier change was achieved by using a combination of historical map charts and satellite imagery sources to provide a novel long-term record of terminus behaviour from 1948 to 2015 (Chapter 3). These data were then supplemented with annual ice velocities and elevation change datasets to assess the dynamic glacier response to changes at the terminus. The key conclusion is that accelerated retreat has occurred over the last two decades across northern Greenland, coincident with other regions of the ice sheet [e.g., Carr *et al.*, 2017b], and with the onset of regional ocean-climate warming. During 1948 to 1995 outlet glacier retreat rates averaged $+72 \text{ m a}^{-1}$ (advance).

However, after 1995 there was a clear switch to higher magnitude retreat averaging -445 m a^{-1} until 2015. Recent retreat over the last two decades (1995 to 2015) was dominated by the retreat and/or collapse of several ice tongues. By putting these recent changes into context over a longer timescale, this thesis shows that recent change was exceptional, rather than related to a cyclic advance and retreat of the glacier termini. This suggests that northern Greenland is undergoing rapid and likely irreversible change, which is largely in response to the onset of increased air and ocean temperatures in the region.

Despite region-wide accelerated retreat, the results presented in Chapter 3 also highlighted that terminus behaviour was heterogeneous. To determine the role of floating ice tongues in modulating glacier behaviour this thesis compared the dynamics of glaciers that are either grounded at their terminus or extend out into a floating ice tongue. This comparison showed that the magnitude and duration of retreat, alongside the dynamic response to terminus change was dependent on terminus type. This was primarily due to variations in resistive stresses acting on grounded ice depending on calving from a grounded or floating front.

Grounded outlets were characterised by sustained low magnitude retreat, alongside inland thinning and acceleration. This was due to a loss of basal resistance, during calving/retreat, which was amplified at glaciers where the terminus retreated down a retrograde bed slope. In general, glaciers terminating in floating ice tongues instead showed short-lived high magnitude stochastic retreat events. These calving events were followed by limited acceleration or thinning inland of the grounding line, suggesting that changes in ice tongue extent did not perturb the glacier force balance. This insensitivity to ice tongue loss is attributed primarily to limited lateral resistance and thus backstress provided by ice tongues that are weakly attached to their fjord walls. For example, satellite imagery revealed that ice tongues at C. H. Ostenfeld and Hagen Bræ were highly fragmented prior to collapse, suggesting they were already dynamically decoupled from grounded ice. In addition, the absence of a retrograde bed slope at the grounding lines prevented unstable downslope retreat during or after ice tongue loss. This highlights the importance of local glacier topography on modulating the glacier response to changes at the terminus. From these results, one of the key conclusions of this thesis is that unlike large ice shelves in Antarctica, outlet glaciers in northern Greenland were generally insensitive to recent collapse. However, now these glaciers have become grounded, it is important to focus on their future response to calving at a grounded terminus, that could accelerate ice flow, increase ice discharge and cause northern Greenland to become a more important contributor to sea level rise in the future.

While glaciers in northern Greenland appeared insensitive to past ice tongue loss, the

laterally confined nature of the remaining ice tongues (Petermann and Nioghalvfjærdsfjorden), suggests that they may respond more dynamically to future retreat and/or collapse [Nick *et al.*, 2012; Choi *et al.*, 2017], which could accelerate mass loss from these outlets. To assess this future sensitivity, and support the observations presented in Chapter 3, this thesis also used an ice flow model to simulate ice tongue loss (Objective 3: Chapters 4 and 5). These experiments were conducted on Petermann Glacier, which terminates in one of the last remaining floating ice tongues in Greenland. Two main conclusions can be drawn from these experiments. First, in line with our observations elsewhere in northern Greenland, the dynamic response of Petermann Glacier to ice tongue loss is primarily related to varying amounts of lateral resistance that apply buttressing to grounded ice. The lower fragmented parts of the tongue were passive, i.e. removing them did not perturb stresses at the grounding line. However calving from laterally confined portions of the tongue closer to the grounding line, is likely to cause thinning, acceleration, and an increase in grounded ice discharge. Secondly, while acceleration and thinning are likely to follow ice tongue loss at Petermann Glacier, the long-term response over 100-years appears muted. Compared to the response to ice shelf collapse in Antarctica the impact of losing Petermann Glacier ice tongue may be minimal in terms of sea-level rise (< 1 mm). This limited response is attributed to stability of the grounding line at a rise in bed topography. Overall, in line with the conclusions drawn from Chapter 3, these results suggest that Petermann Glacier may too be relatively insensitive to future collapse. However, future work could usefully focus on simulating varying levels of ocean-climate forcing on Petermann Glacier to see whether the glacier can retreat further inland, if it remains stable, or if the floating ice tongue could regrow.

Overall this thesis has provided new insight into the behaviour of marine-terminating outlet glaciers in northern Greenland and their sensitivity to changes in the extent of their ice tongues. Taken together, the findings from our observational record and numerical modelling highlight that glaciers in northern Greenland were generally insensitive to recent ice tongue collapse. Importantly this was due to their unconfined nature, and limiting inland bed topography, i.e. the absence of a deepening bed at the grounding line. Loss of the remaining ice tongues in northern Greenland may cause a greater perturbation on grounded ice, and increase ice discharge but, in the long-term their bed topography may limit further ice loss. Ultimately, it is now important to focus on the glacier response once previously floating termini become grounded and calve directly into the ocean. Crucially, this has the potential to increase the region-wide contribution to ice loss and global sea level rise over the 21st century.

Appendix A

Bed slope direction and errors in basal topography

Chapter 3 of this thesis considers the role of basal topography in governing a glaciers dynamic sensitivity (i.e. acceleration and thinning) to terminus retreat. While bed topography datasets have improved greatly in recent years, errors still remain, and as part of assessing glacier sensitivity to bed topography, it is important to examine the possible errors. Firstly, errors in bed topography were assessed using error maps provided in the BedMachine v3 dataset [Morlighem *et al.*, 2017]. Figure A.1 shows the source of bed topography for northern Greenland alongside the errors. Bed topography is well constrained at the majority of outlets in northern Greenland, where errors along the glacier centerline profiles are generally < 100 m (Table A.1). Exceptions are glaciers in northeast Greenland (Kofoed-Hansen Bræ, Storstrømmen, and L. Bistrup Bræ), which have higher errors due to being derived from Kriging interpolation rather than being well constrained by the mass conservation method. While recent improvements in fjord bathymetry [Morlighem *et al.*, 2017] and in particular topography at the transition from grounded ice to the ocean [Williams *et al.*, 2017] have been made, errors in fjord bathymetry are greater than on grounded ice at all glaciers in northern Greenland. This highlights the need for improved measurements of fjord bathymetry across the region, in line with recent surveys as part of NASA’s Ocean Melting Greenland project elsewhere around the ice sheet [Morlighem *et al.*, 2016b].

Chapter 3 also presented the nature of the bed slope (inland or seaward sloping: see Table 3.4) along the first 20 km inland of the grounding line of each study glacier in northern Greenland. This was done by fitting the bed topography along each glacier centerline

with a linear regression model to determine the slope of the linear fit (see Figure A.2).

| Glacier | Mean grounded bed topography error (m) | Mean bathymetry error (m) |
|-----------------------|--|---------------------------|
| Harald Moltke Bræ | 40.94 | 252.64 |
| Heilprin | 53.62 | 75.30 |
| Tracy | 86.54 | 184.60 |
| Humboldt | 31.36 | 188.82 |
| Petermann | 25.14 | 111.86 |
| Steensby | 44.84 | 194.99 |
| Ryder | 33.88 | 196.03 |
| Ostenfeld | 70.82 | 283.94 |
| Harder | 78.93 | 143.33 |
| Brikkerne | 146.45 | 236.65 |
| Marie Sophie | 87.14 | 85.82 |
| Academy | 46.48 | 181.31 |
| Hagen Bræ | 63.24 | 245.75 |
| Nioghalvfjærdsfjorden | 42.94 | 15.57 |
| Zachariae Isstrøm | 52.59 | 17.47 |
| Kofoed-Hansen Bræ | 215.93 | 104.88 |
| Storstrømmen | 116.07 | 117.54 |
| L. Bistrup Bræ | 112.36 | 169.52 |

Table A.1: Mean elevation error for each glacier across either the grounded portion of the glacier centreline profile, or the seaward (bathymetry) section of the glacier centreline profile

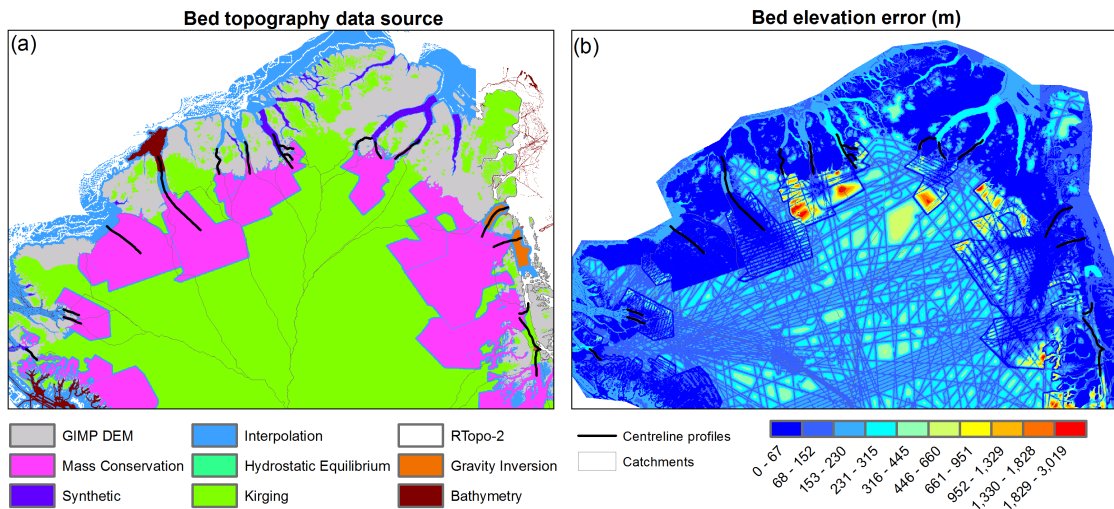


Figure A.1: (a) categorised source data of bed topography from the BedMachine v3 for northern Greenland (b) bed elevation error (m) map from the BedMachine v3 dataset. Grey outlines show glacier surface drainage catchments, and black lines show glacier centreline profiles.

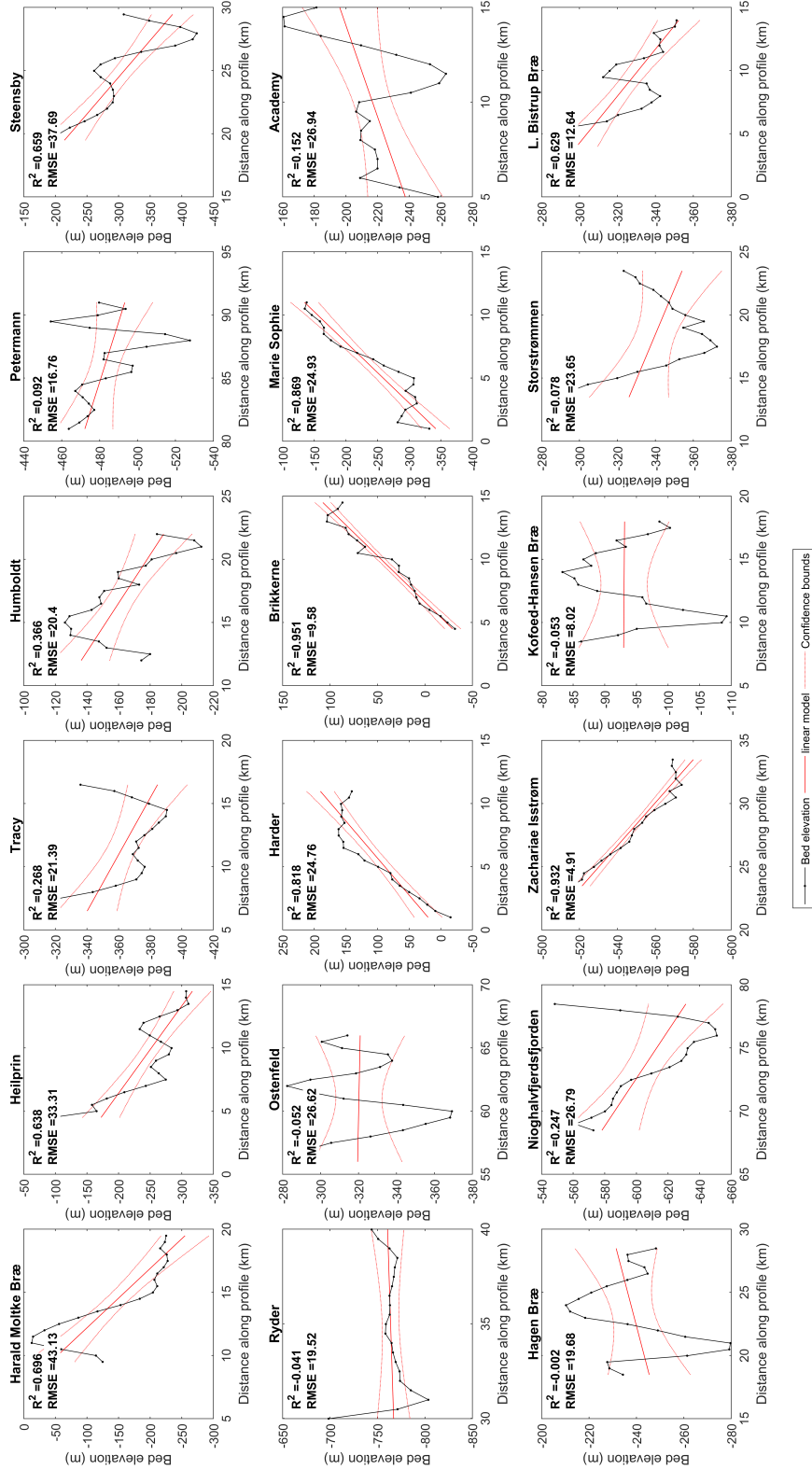


Figure A.2: Bed topography profiles for each of 18 study outlet glaciers in northern Greenland. Bed topography was sampled along glacier centreline profiles and subsampled from the grounding line to 20 km inland to determine the local bed slope direction inland of the grounding line. Each profile was fit with a linear regression model (red). The direction of the linear fit was used to determine if the bed slope was seaward or landward sloping

Appendix B

Sensitivity of our model results to the slipperiness exponent value (m) in the Weertman sliding law

The ice flow model used in this thesis ($\dot{U}a$) inverts for the basal slipperiness parameter C by employing a Weertman sliding law which takes the form

$$\tau_b = C^{-1/m} |\nu_b|^{1/m-1} \nu_b \quad (\text{B.1})$$

where C is the basal slipperiness, τ_b is the tangential basal traction, ν_b is the basal velocity, and m is the stress exponent.

The flow of fast flowing glaciers and ice streams is primarily controlled by basal motion i.e. deformation. However, estimates of basal slipperiness (C) and the stress exponent in the Weertman sliding law (m) have not been directly observed and instead rely on numerical estimates, often from inverting surface velocity measurements. In particular, the most appropriate value for m remains uncertain. To assess whether our results are independent of the value of m input into our sliding law, we repeated both our diagnostic and transient modelling experiments at Petermann Glacier using different values of m .

B.1 Diagnostic experiments

To assess impact of varying the value of m the velocity response of Petermann Glacier to perturbations of its calving front we repeated two of the previous diagnostic experiments: 1) removing the iceberg that calved in 2010, 2) removing the entire ice tongue. First, we invert pre-calving observed velocities (winter 2009/10) for basal slipperiness where we varied the stress exponent (m) between 1 and 9 ($m = 1, 2, 3, 5, 7, 9$). We then input each estimate of basal slipperiness into a diagnostic forward experiment. To assess the impact of different slipperiness distributions on inland ice flow speeds, we look at the normalized change in speed across a centerline profile from the grounding line to 40 km inland for each value of m and for both 2010 calving and entire ice tongue loss (left and middle panels of Figure B.1). In both cases, velocity increases are greatest at the grounding line and decrease with distance inland. The final panel shows the percentage change in speeds at the grounding line relative to initial flow speeds for both experiments. Importantly the impact of removing the entire ice tongue is distinctly different to removing the 2010 iceberg. Therefore, we can conclude that varying the value of m does not impact the results of our diagnostic experiments.

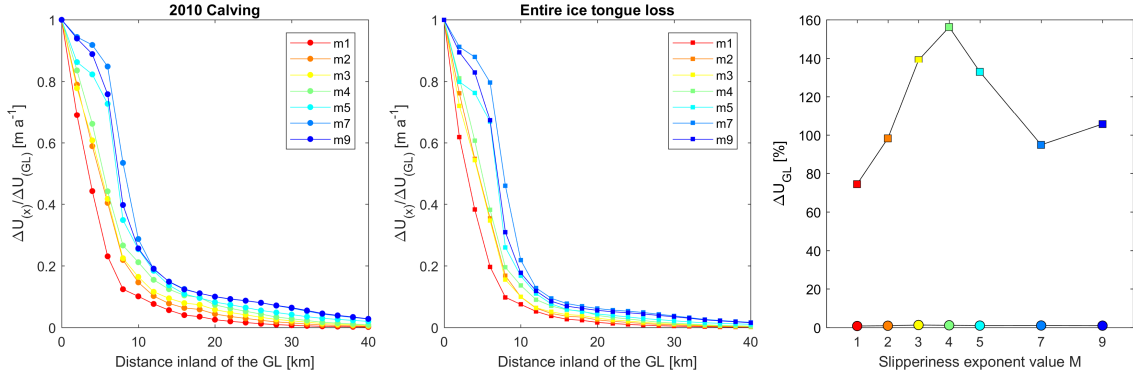


Figure B.1: Left two panels show normalized increase in speed along the Petermann Glacier centerline from the grounding line to 40 km inland where $\Delta U_{(x)}$ is the change in velocity at each point along the transect and $\Delta U_{(GL)}$ is the change in speed at the grounding line. Each colored line is a different value of m . The final panel shows the percentage change in speed at the grounding line $\Delta U_{(GL)}$ for each slipperiness exponent value of m . Circles show percentage change after the 2010 calving event and squares after removing the entire ice tongue

B.2 Transient experiments

As with our diagnostic experiment, we first invert the model using several different values for m (2,3,4). As for our initial inversion (see Section 5.3.1), we set the slipperiness

beneath the ice tongue to the average value 10 km inland of the grounding line to avoid an unrealistic sharp transition to high basal drag in the case of grounding line advance. We then input estimates of slipperiness (C) and ice rheology (A) into both our control run and most extreme scenario run (basal melt and episodic calving) to assess the variability in ice volume above flotation depending on the value of m used. Figure B.2 show the results of these sensitivity experiments. During the the early stages of each run there was little variability in VAF, although this increased with time. In the control run, final VAF values after 100 years ranged from -160 to -196 Gt, with an average difference of 20%. While the perturbed run showed greater variability in VAF depending on the value of m used, importantly the different distributions of basal slipperiness were not able to force grounding line retreat further inland, and in fact limited the VAF lost in comparison to using $m = 3$.

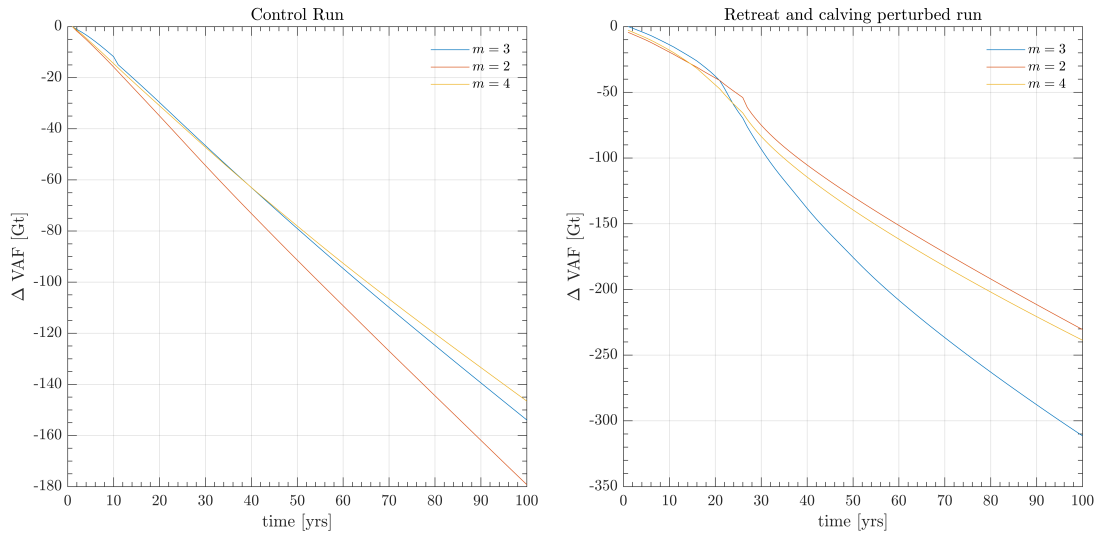


Figure B.2: Left panel shows volume above flotation (VAF) loss during our control run for different values of m . Right panel, same as left but for our perturbed model run, incorporating both enhanced basal melt rates and episodic calving of Petermann Glacier’s ice tongue.

References

- ABDALATI, W., KRABILL, W., FREDERICK, E., MANIZADE, S., MARTIN, C., SONNTAG, J., SWIFT, R., THOMAS, R., WRIGHT, W. & YUNGEL, J. 2001 Outlet glacier and margin elevation changes: Near-coastal thinning of the Greenland ice sheet. *Journal of Geophysical Research Atmospheres* **106** (D24), 33729–33741.
- AHLSTRØM, A. P., ANDERSEN, S. B., ANDERSEN, M. L., MACHGUTH, H., NICK, F. M., JOUGHIN, I., REIJMER, C. H., VAN DE WAL, R. S., MERRYMAN BONCORI, J. P., BOX, J. E., CITTERIO, M., VAN AS, D., FAUSTO, R. S. & HUBBARD, A. 2013 Seasonal velocities of eight major marine-terminating outlet glaciers of the Greenland ice sheet from continuous in situ GPS instruments. *Earth System Science Data* **5** (2), 277–287.
- AHNERT, F. 1963 The Terminal Disintegration of Steensby Gletscher, North Greenland. *Journal of Glaciology* **4** (35), 537–545.
- ÅKESSON, H., NISANCIOGLU, K. H. & NICK, F. M. 2018 Impact of Fjord Geometry on Grounding Line Stability. *Frontiers in Earth Science* **6** (June), 1–16.
- ALLEY, R. B. 1991 Sedimentary processes may cause fluctuations of tidewater glaciers. *Annals of Glaciology* **15** (19), 119–124.
- ALLEY, R. B., BLANKENSHIP, D. D., BENTLEY, C. R. & ROONEY, S. T. 1986 Deformation of till beneath ice stream B, West Antarctica. *Nature* **322** (6074), 57–59.
- AMUNDSON, J. M., FAHNESTOCK, M., TRUFFER, M., BROWN, J., LÜTHI, M. P. & MOTYKA, R. J. 2010 Ice mélange dynamics and implications for terminus stability, Jakobshavn Isbræ, Greenland. *Journal of Geophysical Research: Earth Surface* **115** (1), 1–12.
- ANDERSEN, M. L., STENSENG, L., SKOURUP, H., COLGAN, W., KHAN, S. A., KRISTENSEN, S. S., ANDERSEN, S. B., BOX, J. E., AHLSTRØM, A. P., FETTWEIS, X. & FORSBERG, R. 2015 Basin-scale partitioning of Greenland ice sheet mass balance components (2007–2011). *Earth and Planetary Science Letters* **409**, 89–95.

- BAMBER, J. L., GRIGGS, J. A., HURKMANS, R. T. W. L., DOWDESWELL, J. A., GOGINENI, S. P., HOWAT, I., MOUGINOT, J., PADEN, J., PALMER, S., RIGNOT, E. & STEINHAGE, D. 2013 A new bed elevation dataset for Greenland. *Cryosphere* **7** (2), 499–510.
- BAMBER, J. L., OPPENHEIMER, M., KOPP, R. E., ASPINALL, W. P. & COOKE, R. M. 2019 Ice sheet contributions to future sea-level rise from structured expert judgment. *Proceedings of the National Academy of Sciences of the United States of America* **116** (23), 11195–11200.
- BANWELL, A. F., MACAYEAL, D. R. & SERGIENKO, O. V. 2013 Breakup of the Larsen B Ice Shelf triggered by chain reaction drainage of supraglacial lakes. *Geophysical Research Letters* **40** (22), 5872–5876.
- BARTHOLOMEW, I., NIENOW, P., MAIR, D., HUBBARD, A., KING, M. A. & SOLE, A. 2010 Seasonal evolution of subglacial drainage and acceleration in a Greenland outlet glacier. *Nature Geoscience* **3** (6), 408–411.
- BENN, D. I., WARREN, C. R. & MOTTRAM, R. H. 2007 Calving processes and the dynamics of calving glaciers. *Earth-Science Reviews* **82** (3-4), 143–179.
- BEVAN, S. L., LUCKMAN, A. J. & MURRAY, T. 2012 Glacier dynamics over the last quarter of a century at Helheim, Kangerdlugssuaq and 14 other major Greenland outlet glaciers. *Cryosphere* **6** (5), 923–937.
- BINDSCHADLER, R., BAMBER, J. & ANANDAKRISHNAN, S. 2001 Onset of Streaming Flow in the Siple Coast Region, West Antarctica. In *The West Antarctic Ice Sheet: Behavior and Environment* (ed. R. B. Alley & R. A. Bindschadler), , vol. 77, pp. 123–136. Washington, DC: Wiley Online Library.
- BINDSCHADLER, R. A., STEPHENSON, S. N., MACAYEAL, D. R. & SHABTAIE, S. 1987 Ice dynamics at the mouth of ice stream B, Antarctica. *Journal of Geophysical Research* **92** (B9), 8885–8894.
- BJØRK, A. A., KJÆR, K. H., KORSGAARD, N. J., KHAN, S. A., KJELDSSEN, K. K., ANDRESEN, C. S., BOX, J. E., LARSEN, N. K. & FUNDER, S. 2012 An aerial view of 80 years of climate-related glacier fluctuations in southeast Greenland. *Nature Geoscience* **5** (6), 427–432.
- BONDZIO, J. H., MORLIGHEM, M., SEROUSSI, H., KLEINER, T., RÜCKAMP, M., MOUGINOT, J., MOON, T., LAROUE, E. Y. & HUMBERT, A. 2017 The mechanisms behind Jakobshavn Isbræ’s acceleration and mass loss: A 3-D thermomechanical model study. *Geophysical Research Letters* **44** (12), 6252–6260.

- BONDZIO, J. H., SEROUSSI, H., MORLIGHEM, M., KLEINER, T., RÜCKAMP, M., HUMBERT, A. & LAROUE, E. Y. 2016 Modelling calving front dynamics using a level-set method: application to jakobshavn isbræ, west greenland. *The Cryosphere* **10** (2), 497–510.
- BORN, A. & NISANCIOGLU, K. H. 2012 Melting of Northern Greenland during the last interglaciation. *Cryosphere* **6** (6), 1239–1250.
- BORSTAD, C. P., RIGNOT, E., MOUGINOT, J. & SCHODLOK, M. P. 2013 Creep deformation and buttressing capacity of damaged ice shelves: Theory and application to Larsen C ice shelf. *Cryosphere* **7** (6), 1931–1947.
- BOUGAMONT, M., CHRISTOFFERSEN, P., HUBBARD, A. L., FITZPATRICK, A. A., DOYLE, S. H. & CARTER, S. P. 2014 Sensitive response of the Greenland Ice Sheet to surface melt drainage over a soft bed. *Nature Communications* **5** (5052).
- BOX, J. E. & COLGAN, W. 2013 Greenland ice sheet mass balance reconstruction. Part III: Marine ice loss and total mass balance (1840-2010). *Journal of Climate* **26** (18), 6990–7002.
- BOX, J. E. & DECKER, D. T. 2011 Greenland marine-terminating glacier area changes: 2000-2010. *Annals of Glaciology* **52** (59), 91–98.
- BOX, J. E., YANG, L., BROMWICH, D. H. & BAI, L. S. 2009 Greenland ice sheet surface air temperature variability: 1840-2007. *Journal of Climate* **22** (14), 4029–4049.
- VAN DEN BROEKE, M., BAMBER, J., ETTEMA, J., RIGNOT, E., SCHRAMA, E., VAN BERG, W. J. D., VAN MEIJGAARD, E., VELICOGNA, I. & WOUTERS, B. 2009 Partitioning recent Greenland mass loss. *Science* **326** (5955), 984–986.
- VAN DEN BROEKE, M. R., ENDERLIN, E. M., HOWAT, I. M., KUIPERS MUNNEKE, P., NOËL, B. P., JAN VAN DE BERG, W., VAN MEIJGAARD, E. & WOUTERS, B. 2016 On the recent contribution of the Greenland ice sheet to sea level change. *Cryosphere* **10** (5), 1933–1946.
- BROUGH, S., CARR, J. R., ROSS, N. & LEA, J. M. 2019 Exceptional Retreat of Kangerlussuaq Glacier, East Greenland, Between 2016 and 2018. *Frontiers in Earth Science* **7** (May), 1–11.
- BUNCE, C., CARR, J. R., NIENOW, P. W., ROSS, N. & KILLICK, R. 2018 Ice front change of marine-terminating outlet glaciers in northwest and southeast Greenland during the 21st century. *Journal of Glaciology* **64** (246), 523–535.

- CAI, C., RIGNOT, E., MENEMENLIS, D. & NAKAYAMA, Y. 2017 Observations and modeling of ocean-induced melt beneath Petermann Glacier Ice Shelf in northwestern Greenland. *Geophysical Research Letters* **44** (16), 8396–8403.
- CAPPELEN, J., LAURSEN, E. V., JØRGENSEN, P. V. & KERN-HANSEN, C. 2010 DMI Monthly Climate Data Collection 1768–2009, Denmark, The Faroe Islands and Greenland. *Technical Report 10-05* .
- CARR, J., VIELI, A., STOKES, C., JAMIESON, S., PALMER, S., CHRISTOFFERSEN, P., DOWDESWELL, J., NICK, F., BLANKENSHIP, D. & YOUNG, D. 2015 Basal topographic controls on rapid retreat of Humboldt Glacier, northern Greenland. *Journal of Glaciology* **61** (225), 137–150.
- CARR, J. R., BELL, H., KILLICK, R. & HOLT, T. 2017a Exceptional retreat of Novaya Zemlya’s marine-terminating outlet glaciers between 2000 and 2013. *Cryosphere* **11** (5), 2149–2174.
- CARR, J. R., STOKES, C. & VIELI, A. 2014 Recent retreat of major outlet glaciers on Novaya Zemlya, Russian Arctic, influenced by fjord geometry and sea-ice conditions. *Journal of Glaciology* **60** (219), 155–170.
- CARR, J. R., STOKES, C. R. & VIELI, A. 2013a Recent progress in understanding marine-terminating Arctic outlet glacier response to climatic and oceanic forcing: Twenty years of rapid change. *Progress in Physical Geography* **37** (4), 436–467.
- CARR, J. R., STOKES, C. R. & VIELI, A. 2017b Threefold increase in marine-terminating outlet glacier retreat rates across the Atlantic Arctic: 1992–2010. *Annals of Glaciology* **58** (74), 72–91.
- CARR, J. R., VIELI, A. & STOKES, C. 2013b Influence of sea ice decline, atmospheric warming, and glacier width on marine-terminating outlet glacier behavior in northwest Greenland at seasonal to interannual timescales. *Journal of Geophysical Research: Earth Surface* **118** (3), 1210–1226.
- CASSOTTO, R., FAHNESTOCK, M., AMUNDSON, J. M., TRUFFER, M. & JOUGHIN, I. 2015 Seasonal and interannual variations in ice melange and its impact on terminus stability, Jakobshavn Isbræ, Greenland. *Journal of Glaciology* **61** (225), 76–88.
- CATANIA, G. A., STEARNS, L. A., SUTHERLAND, D. A., FRIED, M. J., BARTHOLOMAUS, T. C., MORLIGHEM, M., SHROYER, E. & NASH, J. 2018 Geometric Controls on Tidewater Glacier Retreat in Central Western Greenland. *Journal of Geophysical Research: Earth Surface* **123** (8), 2024–2038.

- CHOI, Y., MORLIGHEM, M., RIGNOT, E., MOUGINOT, J. & WOOD, M. 2017 Modeling the Response of Nioghalvfjærdsfjorden and Zachariae Isstrøm Glaciers, Greenland, to Ocean Forcing Over the Next Century. *Geophysical Research Letters* **44** (21), 071–11.
- CHRISTIANSON, K., PETERS, L. E., ALLEY, R. B., ANANDAKRISHNAN, S., JACOBEL, R. W., RIVERMAN, K. L., MUTO, A. & KEISLING, B. A. 2014 Dilatant till facilitates ice-stream flow in northeast Greenland. *Earth and Planetary Science Letters* **401**, 57–69.
- CHRISTOFFERSEN, P., MUGFORD, R. I., HEYWOOD, K. J., JOUGHIN, I., DOWDESWELL, J. A., SYVITSKI, J. P., LUCKMAN, A. & BENHAM, T. J. 2011 Warming of waters in an East Greenland fjord prior to glacier retreat: Mechanisms and connection to large-scale atmospheric conditions. *Cryosphere* **5** (3), 701–714.
- CHU, W., SCHROEDER, D. M., SEROUSSI, H., CREYTS, T. T. & BELL, R. E. 2018 Complex Basal Thermal Transition Near the Onset of Petermann Glacier, Greenland. *Journal of Geophysical Research: Earth Surface* **123** (5), 985–995.
- CHURCH, J. A., CLARK, P., CAZENAVE, A., GREGORY, J., JEVREJEVA, S., LEVERMANN, A., MERRIFIELD, M., MILNE, G., NEREM, R., NUNN, P., PAYNE, A., PFEFFER, W., STAMMER, D. & UNNIKRISHNAN, A. 2013 Sea level change. In *Climate Change 2013: The Physical Science Basis. Contribution of Working Group I to the Fifth Assessment Report of the Intergovernmental Panel on Climate Change* (ed. T. Stocker, D. Qin, G.-K. Plattner, M. Tignor, S. Allen, J. Boschung, A. Nauels, Y. Xia, V. Bex & P. Midgley), pp. 1137–1216. Cambridge, United Kingdom and New York, NY, USA: Cambridge University Press.
- COLLINS, M., KNUTTI, R., ARBLASTER, J., DUFRESNE, J.-L., FICHEFET, T., FRIEDLINGSTEIN, P., GAO, X., GUTOWSKI, W., JOHNS, T., KRINNER, G., SHONGWE, M., TEBALDI, C., WEAVER, A. & WEHNER, M. 2013 Long-term Climate Change: Projections, Commitments and Irreversibility. In *Climate Change 2013: The Physical Science Basis. Contribution of Working Group I to the Fifth Assessment Report of the Intergovernmental Panel on Climate Change* (ed. T. Stocker, D. Qin, G.-K. Plattner, M. Tignor, S. Allen, J. Boschung, A. Nauels, Y. Xia, V. Bex & P. Midgley), pp. 1029–1136. Cambridge, United Kingdom and New York, NY, USA: Cambridge University Press.
- COOK, A. J., COPLAND, L., NOËL, B. P. Y., STOKES, C. R., BENTLEY, M. J., SHARP, M. J., BINGHAM, R. G. & VAN DEN BROEKE, M. R. 2019 Atmospheric forcing of rapid marine-terminating glacier retreat in the Canadian Arctic Archipelago. *Science Advances* **5** (3).

- COOK, A. J., VAUGHAN, D. G., LUCKMAN, A. J. & MURRAY, T. 2014 A new Antarctic Peninsula glacier basin inventory and observed area changes since the 1940s. *Antarctic Science* **26** (6), 614–624.
- COWTON, T. R., SOLE, A. J., NIENOW, P. W., SLATER, D. A. & CHRISTOFFERSEN, P. 2018 Linear response of east Greenland’s tidewater glaciers to ocean/atmosphere warming. *Proceedings of the National Academy of Sciences* **115** (31), 7907–7912.
- CSATHO, B. M., SCHENK, A. F., VAN DER VEEN, C. J., BABONIS, G., DUNCAN, K., REZVANBEHBAHANI, S., VAN DEN BROEKE, M. R., SIMONSEN, S. B., NAGARAJAN, S. & VAN ANGELEN, J. H. 2014 Laser altimetry reveals complex pattern of Greenland Ice Sheet dynamics. *Proceedings of the National Academy of Sciences* **111** (52), 18478–18483.
- CUFFEY, K. & PATERSON, W. S. B. 2010 *The Physics of Glaciers*, 4th edn. Academic Press.
- DAS, S. B., JOUGHIN, I., BEHN, M. D., HOWAT, I. M., KING, M. A., LIZARRALDE, D. & BHATIA, M. P. 2008 Fracture propagation to the base of the Greenland ice sheet during supraglacial lake drainage. *Science* **320** (5877), 778–781.
- DAVIES, W. E. & KRINSLEY, D. B. 1962 The recent regime of the ice cap margin in north Greenland. *International Association of Hydrological Sciences* **58**, 119–130.
- DAWES, P. R. & AS, D. V. 2010 An advancing glacier in a recessive ice regime : Berlingske Bræ , North-West Greenland. *Geological Survey Of Denmark And Greenland Bulletin* pp. 79–82.
- DE RYDT, J., GUDMUNDSSON, G. H., ROTT, H. & BAMBER, J. L. 2015 Modeling the instantaneous response of glaciers after the collapse of the Larsen B Ice Shelf. *Geophysical Research Letters* **42** (13), 5355–5363.
- DOWDESWELL, J. A. & JEFFRIES, M. O. 2017 Arctic Ice Shelves: An Introduction. In *Arctic Ice Shelves and Ice Islands* (ed. L. Copland & D. Mueller), pp. 3–21. Dordrecht: Springer Netherlands.
- DOYLE, S. H., HUBBARD, A., VAN DE WAL, R. S., BOX, J. E., VAN AS, D., SCHARRER, K., MEIERBACHTOL, T. W., SMEETS, P. C., HARPER, J. T., JOHANSSON, E., MOTTRAM, R. H., MIKKELSEN, A. B., WILHELMS, F., PATTON, H., CHRISTOFFERSEN, P. & HUBBARD, B. 2015 Amplified melt and flow of the Greenland ice sheet driven by late-summer cyclonic rainfall. *Nature Geoscience* **8**, 647–653.
- DUNBAR, M. 1978 Petermann Gletscher: possible source of a tabular iceberg off the coast of Newfoundland. *Journal of Glaciology* **20** (84), 595–597.

- DURAND, G., GAGLIARDINI, O., ZWINGER, T., MEUR, E. L. & HINDMARSH, R. C. 2009 Full Stokes modeling of marine ice sheets: Influence of the grid size. *Annals of Glaciology* **50** (52), 109–114.
- ENDERLIN, E. M., HOWAT, I. M., JEONG, S., NOH, M. J., VAN ANGELEN, J. H. & VAN DEN BROEKE, M. R. 2014 An improved mass budget for the Greenland ice sheet. *Geophysical Research Letters* **41** (3), 866–872.
- ENDERLIN, E. M., HOWAT, I. M. & VIELI, A. 2013 High sensitivity of tidewater outlet glacier dynamics to shape. *Cryosphere* **7** (3), 1007–1015.
- ENGWIRDA, D. 2014 Locally optimal Delaunay-refinement and optimisation-based mesh generation. In *Ph.D Thesis*. School of Mathematics and Statistics, University of Sydney.
- ETTEMA, J., VAN DEN BROEKE, M. R., VAN MEIJGAARD, E., VAN DE BERG, W. J., BAMBER, J. L., BOX, J. E. & BALES, R. C. 2009 Higher surface mass balance of the Greenland ice sheet revealed by high-resolution climate modeling. *Geophysical Research Letters* **36** (12), 4–8.
- FALKNER, K. K., MELLING, H., MNCHOW, A. M., BOX, J. E., WOHLLEBEN, T., JOHNSON, H. L., GUDMANDSEN, P., SAMELSON, R., COPLAND, L., STEFFEN, K., RIGNOT, E. & HIGGINS, A. K. 2011 Context for the recent massive Petermann Glacier calving event. *Eos* **92** (14), 117–118.
- FAVIER, L., DURAND, G., CORNFORD, S. L., GUDMUNDSSON, G. H., GAGLIARDINI, O., GILLET-CHAULET, F., ZWINGER, T., PAYNE, A. J. & LE BROCCQ, A. M. 2014 Retreat of Pine Island Glacier controlled by marine ice-sheet instability. *Nature Climate Change* **4** (2), 117–121.
- FELIKSON, D., BARTHOLOMAUS, T. C., CATANIA, G. A., KORSGAARD, N. J., KJÆR, K. H., MORLIGHEM, M., NOËL, B., VAN DEN BROEKE, M., STEARNS, L. A., SHROYER, E. L., SUTHERLAND, D. A. & NASH, J. D. 2017 Inland thinning on the Greenland ice sheet controlled by outlet glacier geometry. *Nature Geoscience* **10** (5), 366–369.
- FETTWEIS, X., BOX, J. E., AGOSTA, C., AMORY, C., KITTEL, C., LANG, C., VAN AS, D., MACHGUTH, H. & GALLÉE, H. 2017 Reconstructions of the 1900–2015 Greenland ice sheet surface mass balance using the regional climate MAR model. *Cryosphere* **11** (2), 1015–1033.
- FETTWEIS, X., FRANCO, B., TEDESCO, M., VAN ANGELEN, J. H., LENAERTS, J. T., VAN DEN BROEKE, M. R. & GALLÉE, H. 2013 Estimating the Greenland ice sheet

- surface mass balance contribution to future sea level rise using the regional atmospheric climate model MAR. *Cryosphere* **7** (2), 469–489.
- FOWLER, A. C., MURRAY, T. & NG, F. S. 2001 Thermally controlled glacier surging. *Journal of Glaciology* **47** (159), 527–538.
- FRANCO, B., FETTWEIS, X., ERPICUM, M. & NICOLAY, S. 2011 Present and future climates of the Greenland ice sheet according to the IPCC AR4 models. *Climate Dynamics* **36** (9–10), 1897–1918.
- FÜRST, J. J., DURAND, G., GILLET-CHAULET, F., TAVARD, L., RANKL, M., BRAUN, M. & GAGLIARDINI, O. 2016 The safety band of Antarctic ice shelves. *Nature Climate Change* **6** (5), 479–482.
- FÜRST, J. J., GOELZER, H. & HUYBRECHTS, P. 2015 Ice-dynamic projections of the Greenland ice sheet in response to atmospheric and oceanic warming. *Cryosphere* **9** (3), 1039–1062.
- GEUZAIN, C. & REMACLE, J. F. 2009 Gmsh: A 3-D finite element mesh generator with built-in pre- and post-processing facilities. *International Journal for Numerical Methods in Engineering* **79** (11), 1309–1331.
- GOELZER, H., HUYBRECHTS, P., FÜRST, J., NICK, F., ANDERSEN, M., EDWARDS, T., FETTWEIS, X., PAYNE, A. & SHANNON, S. 2013 Sensitivity of Greenland Ice Sheet Projections to Model Formulations. *Journal of Glaciology* **59** (216), 733–749.
- GOLDBERG, D., HOLLAND, D. M. & SCHOOF, C. 2009 Grounding line movement and ice shelf buttressing in marine ice sheets. *Journal of Geophysical Research: Earth Surface* **114** (4).
- GREGORY, J. M. & HUYBRECHTS, P. 2006 Ice-sheet contributions to future sea-level change. *Philosophical Transactions of the Royal Society A: Mathematical, Physical and Engineering Sciences* **364** (1844), 1709–1731.
- GREGORY, J. M., HUYBRECHTS, P. & RAPER, S. C. B. 2004 Threatened loss of the Greenland ice-sheet. *Nature* **428** (6983), 616–616.
- GUDMUNDSSON, G. H. 2003 Transmission of basal variability to a glacier surface. *Journal of Geophysical Research: Solid Earth* **108** (B5), 1–19.
- GUDMUNDSSON, G. H. 2013 Ice-shelf buttressing and the stability of marine ice sheets. *Cryosphere* **7** (2), 647–655.

- GUDMUNDSSON, G. H., KRUG, J., DURAND, G., FAVIER, L. & GAGLIARDINI, O. 2012 The stability of grounding lines on retrograde slopes. *Cryosphere* **6** (6), 1497–1505.
- HANNA, E., HUYBRECHTS, P., STEFFEN, K., CAPPELEN, J., HUFF, R., SHUMAN, C., IRVINE-FYNN, T., WISE, S. & GRIFFITHS, M. 2008 Increased runoff from melt from the Greenland Ice Sheet: A response to global warming. *Journal of Climate* **21** (2), 331–341.
- HASELOFF, M. & SERGIENKO, O. V. 2018 The effect of buttressing on grounding line dynamics. *Journal of Glaciology* **64** (245), 417–431.
- HELK, J. & DUNBAR, M. 2014 Ice Islands: Evidence from North Greenland. *Arctic* **6** (4), 263–271.
- HELM, V., HUMBERT, A. & MILLER, H. 2014 Elevation and elevation change of Greenland and Antarctica derived from CryoSat-2. *Cryosphere* **8** (4), 1539–1559.
- HIGGINS, A. K. 1989 North greenland ice islands. *Polar Record* **25** (154), 207–212.
- HIGGINS, A. K. 1990 North Greenland glacier velocities and calf ice production. *Polarforschung* **60** (1), 1–23.
- HILL, E. A., CARR, J. R. & STOKES, C. R. 2017 A Review of Recent Changes in Major Marine-Terminating Outlet Glaciers in Northern Greenland. *Frontiers in Earth Science* **4** (111), 1–23.
- HILL, E. A., CARR, J. R., STOKES, C. R. & GUDMUNDSSON, G. H. 2018a Dynamic changes in outlet glaciers in northern Greenland from 1948 to 2015. *Cryosphere* **12** (10), 3243–3263.
- HILL, E. A., GUDMUNDSSON, G. H., CARR, J. R. & STOKES, C. R. 2018b Velocity response of Petermann Glacier, northwest Greenland, to past and future calving events. *Cryosphere* **12** (12), 3907–3921.
- HOGG, A. E. & GUDMUNDSSON, G. H. 2017 Commentary: Impacts of the Larsen-C Ice Shelf calving event. *Nature Climate Change* **7** (8), 540–542.
- HOGG, A. E., SHEPHERD, A., GOURMELEN, N. & ENGBAHL, M. 2016 Grounding line migration from 1992 to 2011 on Petermann Glacier, North-West Greenland. *Journal of Glaciology* **62** (236), 1104–1114.
- HOLLAND, D. M., THOMAS, R. H., DE YOUNG, B., RIBERGAARD, M. H. & LYBERTH, B. 2008 Acceleration of Jakobshavn Isbr triggered by warm subsurface ocean waters. *Nature Geoscience* **1** (10), 659–664.

- HOWAT, I. 2017 MEaSURES Greenland Ice Velocity: Selected Glacier Site Velocity Maps from Optical Images, Version 2. OPT_E66.50N and OPT_E68.80N Boulder, CO, USA. *NASA National Snow and Ice Data Center Distributed Active Archive Center*.
- HOWAT, I. M. & EDDY, A. 2011 Multi-decadal retreat of Greenland's marine-terminating glaciers. *Journal of Glaciology* **57** (203), 389–396.
- HOWAT, I. M., JOUGHIN, I., FAHNESTOCK, M., SMITH, B. E. & SCAMBOS, T. A. 2008 Synchronous retreat and acceleration of southeast Greenland outlet glaciers 2000–06: Ice dynamics and coupling to climate. *Journal of Glaciology* **54** (187), 646–660.
- HOWAT, I. M., JOUGHIN, I. & SCAMBOS, T. A. 2007 Rapid changes in ice discharge from Greenland outlet glaciers. *Science* **315** (5818), 1559–1561.
- HOWAT, I. M., JOUGHIN, I., TULACZYK, S. & GOGINENI, S. 2005 Rapid retreat and acceleration of Helheim Glacier, east Greenland. *Geophysical Research Letters* **32** (22), 1–4.
- HOWAT, I. M., NEGRETE, A. & SMITH, B. E. 2014 The Greenland Ice Mapping Project (GIMP) land classification and surface elevation data sets. *Cryosphere* **8** (4), 1509–1518.
- IGNÉCZI, Á., SOLE, A. J., LIVINGSTONE, S. J., LEESON, A. A., FETTWEIS, X., SELMES, N., GOURMELEN, N. & BRIGGS, K. 2016 Northeast sector of the Greenland Ice Sheet to undergo the greatest inland expansion of supraglacial lakes during the 21st century. *Geophysical Research Letters* **43** (18), 9729–9738.
- JAKOBSSON, M., HOGAN, K. A., MAYER, L. A., MIX, A., JENNINGS, A., STONER, J., ERIKSSON, B., JERRAM, K., MOHAMMAD, R., PEARCE, C., REILLY, B. & STRANNE, C. 2018 The Holocene retreat dynamics and stability of Petermann Glacier in northwest Greenland. *Nature Communications* **9** (1), 1–11.
- JAMIESON, S. S., VIELI, A., LIVINGSTONE, S. J., COFAIGH, C. , STOKES, C., HILLENBRAND, C. D. & DOWDESWELL, J. A. 2012 Ice-stream stability on a reverse bed slope. *Nature Geoscience* **5** (11), 799–802.
- JENKINS, A. 2011 Convection-Driven Melting near the Grounding Lines of Ice Shelves and Tidewater Glaciers. *Journal of Physical Oceanography* **41** (12), 2279–2294.
- JENKINS, A., SHOOSMITH, D., DUTRIEUX, P., JACOBS, S., KIM, T. W., LEE, S. H., HA, H. K. & STAMMERJOHN, S. 2018 West Antarctic Ice Sheet retreat in the Amundsen Sea driven by decadal oceanic variability. *Nature Geoscience* **11** (10), 733–738.

- JENSEN, T. S., BOX, J. E. & HVIDBERG, C. S. 2016 A sensitivity study of annual area change for Greenland ice sheet marine terminating outlet glaciers: 1999-2013. *Journal of Glaciology* **62** (231), 72–81.
- JISKOOT, H., MURRAY, T. & LUCKMAN, A. 2003 Surge potential and drainage-basin characteristics in East Greenland. *Annals of Glaciology* **36**, 142–148.
- JOHANNESSEN, O. M., BABIKER, M. & MILES, M. W. 2013 Unprecedented Retreat in a 50-Year Observational Record for Petermann Glacier, North Greenland. *Atmospheric and Oceanic Science Letters* **6** (5), 259–265.
- JOHNSON, H. L., MÜNCHOW, A., FALKNER, K. K. & MELLING, H. 2011 Ocean circulation and properties in Petermann Fjord, Greenland. *Journal of Geophysical Research: Oceans* **116** (1), 1–18.
- JOUGHIN, I., ABDALATI, W. & FAHNESTOCK, M. 2004 Large fluctuations in speed on Greenland’s Jakobshavn Isbræ glacier. *Nature* **432** (7017), 608–610.
- JOUGHIN, I. & ALLEY, R. B. 2011 Stability of the West Antarctic ice sheet in a warming world. *Nature Geoscience* **4** (8), 506–513.
- JOUGHIN, I., ALLEY, R. B. & HOLLAND, D. M. 2012a Ice-sheet response to oceanic forcing. *Science* **338** (6111), 1172–1176.
- JOUGHIN, I., FAHNESTOCK, M., KWOK, R., GOGINENI, P. & ALLEN, C. 1999 Ice flow of Humboldt, Petermann and Ryder Gletscher, northern Greenland. *Journal of Glaciology* **45** (150), 231–241.
- JOUGHIN, I., FAHNESTOCK, M., MACAYEAL, D., BAMBER, J. L. & GOGINENI, P. 2001 Observation and analysis of ice flow in the largest Greenland ice stream. *Journal of Geophysical Research: Atmospheres* **106** (D24), 34021–34034.
- JOUGHIN, I., HOWAT, I., ALLEY, R. B., EKSTROM, G., FAHNESTOCK, M., MOON, T., NETTLES, M., TRUFFER, M. & TSAI, V. C. 2008a Ice-front variation and tidewater behavior on Helheim and Kangerdlugssuaq Glaciers, Greenland. *Journal of Geophysical Research: Earth Surface* **113** (1), 1–11.
- JOUGHIN, I., HOWAT, I. M., FAHNESTOCK, M., SMITH, B., KRABILL, W., ALLEY, R. B., STERN, H. & TRUFFER, M. 2008b Continued evolution of Jakobshavn Isbrae following its rapid speedup. *Journal of Geophysical Research: Earth Surface* **113** (4), 1–14.

- JOUGHIN, I., KWOK, R. & FAHNESTOCK, M. 1996a Estimation of ice-sheet motion using satellite radar interferometry: Method and error analysis with application to Humboldt Glacier, Greenland. *Journal of Glaciology* **42** (142), 564–575.
- JOUGHIN, I., SMITH, B. E. & HOLLAND, D. M. 2010a Sensitivity of 21st century sea level to ocean-induced thinning of Pine Island Glacier, Antarctica. *Geophysical Research Letters* **37** (20), 1–5.
- JOUGHIN, I., SMITH, B. E., HOWAT, I. M., FLORICIOIU, D., ALLEY, R. B., TRUFFER, M. & FAHNESTOCK, M. 2012b Seasonal to decadal scale variations in the surface velocity of Jakobshavn Isbrae, Greenland: Observation and model-based analysis. *Journal of Geophysical Research: Earth Surface* **117** (2), 1–20.
- JOUGHIN, I., SMITH, B. E., HOWAT, I. M., SCAMBOS, T. & MOON, T. 2010b Greenland flow variability from ice-sheet-wide velocity mapping. *Journal of Glaciology* **56** (197), 415–430.
- JOUGHIN, I., SMITH, B. E. & MEDLEY, B. 2014 Marine ice sheet collapse potentially under way for the Thwaites Glacier basin, West Antarctica. *Science* **344** (6185), 735–738.
- JOUGHIN, I., TULACZYK, S., FAHNESTOCK, M. & KWOK, R. 1996b A mini-surge on the Ryder Glacier, Greenland, observed by satellite radar interferometry. *Science* **274** (5285), 228–230.
- KAMB, B., RAYMOND, C. F., HARRISON, W. D., ENGELHARDT, H., ECHELMMEYER, K. A., HUMPHREY, N., BRUGMAN, M. M. & PFEFFER, T. 1985 Glacier surge mechanism: 1982–1983 surge of Variegated Glacier, Alaska. *Science* **227** (4686), 469–479.
- KHAN, S. A., ASCHWANDEN, A., BJØRK, A. A., WAHR, J., KJELDSSEN, K. K. & KJÆR, K. H. 2015 Greenland ice sheet mass balance: A review. *Reports on Progress in Physics* **78** (4), 1–26.
- KHAN, S. A., KJÆR, K. H., BEVIS, M., BAMBER, J. L., WAHR, J., KJELDSSEN, K. K., BJØRK, A. A., KORSGAARD, N. J., STEARNS, L. A., VAN DEN BROEKE, M. R., LIU, L., LARSEN, N. K. & MURESAN, I. S. 2014 Sustained mass loss of the northeast Greenland ice sheet triggered by regional warming. *Nature Climate Change* **4** (4), 292–299.
- KHVOROSTOVSKY, K. S. 2012 Merging and analysis of elevation time series over Greenland ice sheet from satellite radar altimetry. *IEEE Transactions on Geoscience and Remote Sensing* **50** (1), 23–36.

- KILLICK, R., FEARNHEAD, P. & ECKLEY, I. A. 2012 Optimal detection of change-points with a linear computational cost. *Journal of the American Statistical Association* **107** (500), 1590–1598.
- KJELDSSEN, K. K., KORSGAARD, N. J., BJØRK, A. A., KHAN, S. A., BOX, J. E., FUNDER, S., LARSEN, N. K., BAMBER, J. L., COLGAN, W., VAN DEN BROEKE, M., SIGGAARD-ANDERSEN, M. L., NUTH, C., SCHOMACKER, A., ANDRESEN, C. S., WILLERSLEV, E. & KJÆR, K. H. 2015 Spatial and temporal distribution of mass loss from the Greenland Ice Sheet since AD 1900. *Nature* **528** (7582), 396–400.
- KOCH, L. 1928 Contributions to the Glaciology of North Greenland. *Meddelelser om Gronland* **65**, 184–464.
- KOLLMAYER, R. C. 1980 West Greenland outlet glaciers: an inventory of the major iceberg producers. *Cold Regions Science and Technology* **1** (3-4), 175–181.
- KORSGAARD, N. J., NUTH, C., KHAN, S. A., KJELDSSEN, K. K., BJØRK, A. A., SCHOMACKER, A. & KJÆR, K. H. 2016 Digital elevation model and orthophotographs of Greenland based on aerial photographs from 1978–1987. *Scientific Data* **3**, 1–15.
- KRABILL, W., ABDALATI, W., FREDERICK, E., MANIZADE, S., MARTIN, C., SONNTAG, J., SWIFT, R., THOMAS, R., WRIGHT, W. & YUNGEL, J. 2000 Greenland Ice Sheet: High-elevation balance and peripheral thinning. *Science* **289** (5478), 428–430.
- KRABILL, W., HANNA, E., HUYBRECHTS, P., ABDALATI, W., CAPPELEN, J., CSATHO, B., FREDERICK, E., MANIZADE, S., MARTIN, C., SONNTAG, J., SWIFT, R., THOMAS, R. & YUNGEL, J. 2004 Greenland Ice Sheet: Increased coastal thinning. *Geophysical Research Letters* **31** (24), 1–4.
- LAVIELLE, M. 2005 Using penalized contrasts for the change-point problem. *Signal Processing* **85** (8), 1501–1510.
- LAYBERRY, R. L. & BAMBER, J. L. 2001 A new ice thickness and bed data set for the Greenland ice sheet: 2. Relationship between dynamics and basal topography. *Journal of Geophysical Research: Atmospheres* **106** (D24), 33781–33788.
- LEA, J. M., MAIR, D. W. F. & REA, B. R. 2014 Instruments and Methods :Evaluation of existing and new methods of tracking glacier terminus change. *Journal of Glaciology* **60** (220), 323–332.
- LEE, V., CORNFORD, S. L. & PAYNE, A. J. 2015 Initialization of an ice-sheet model for present-day Greenland. *Annals of Glaciology* **56** (70), 129–140.

- LEMOS, A., SHEPHERD, A., McMILLAN, M., HOGG, A. E., HATTON, E. & JOUGHIN, I. 2018 Ice velocity of Jakobshavn Isbræ, Petermann Glacier, Nioghalvfjerdsfjorden, and Zachariæ Isstrøm, 2015-2017, from Sentinel 1-a/b SAR imagery. *Cryosphere* **12** (6), 2087–2097.
- LIU, Y., MOORE, J. C., CHENG, X., GLADSTONE, R. M., BASSIS, J. N., LIU, H., WEN, J. & HUI, F. 2015 Ocean-driven thinning enhances iceberg calving and retreat of Antarctic ice shelves. *Proceedings of the National Academy of Sciences* **112** (11), 3263–3268.
- LUCKMAN, A., MURRAY, T., DE LANGE, R. & HANNA, E. 2006 Rapid and synchronous ice-dynamic changes in East Greenland. *Geophysical Research Letters* **33** (3), 1–4.
- LÜTHI, M., VIELI, A., MOREAU, L., JOUGHIN, I., REISSER, M., SMALL, D. & STOBER, M. 2016 A century of geometry and velocity evolution at Eqip Sermia, West Greenland. *Journal of Glaciology* **62** (234), 640–654.
- MACAYEAL, D. R. 1989 Large-scale ice flow over a viscous basal sediment: Theory and application to ice stream B, Antarctica. *Journal of Geophysical Research: Solid Earth* **94** (B4), 4071–4087.
- MACDONALD, G. J., BANWELL, A. F. & MACAYEAL, D. R. 2018 Seasonal evolution of supraglacial lakes on a floating ice tongue, Petermann Glacier, Greenland. *Annals of Glaciology* **59** (76pt1), 56–65.
- MACGREGOR, J. A., CATANIA, G. A., MARKOWSKI, M. S. & ANDREWS, A. G. 2012 Widespread rifting and retreat of ice-shelf margins in the eastern Amundsen Sea Embayment between 1972 and 2011. *Journal of Glaciology* **58** (209), 458–466.
- MACGREGOR, J. A., FAHNESTOCK, M. A., CATANIA, G. A., ASCHWANDEN, A., CLOW, G. D., COLGAN, W. T., GOGINENI, S. P., MORLIGHEM, M., NOWICKI, S. M., PADEN, J. D., PRICE, S. F. & SEROUSSI, H. 2016 A synthesis of the basal thermal state of the Greenland Ice Sheet. *Journal of Geophysical Research: Earth Surface* **121** (7), 1328–1350.
- MAYER, C., REEH, N., JUNG-ROTHENHÄUSLER, F., HUYBRECHTS, P. & OERTER, H. 2000 The subglacial cavity and implied dynamics under Nioghalvfjerdsfjorden glacier, NE-Greenland. *Geophysical Research Letters* **27** (15), 2289–2292.
- MCFADDEN, E. M., HOWAT, I. M., JOUGHIN, I., SMITH, B. E. & AHN, Y. 2011 Changes in the dynamics of marine terminating outlet glaciers in west Greenland (2000-2009). *Journal of Geophysical Research: Earth Surface* **116** (2), 1–16.

- MEIER, M., LUNDSTROM, S., STONE, D., KAMB, B., ENGELHARDT, H., HUMPHREY, N., DUNLAP, W. W., FAHNESTOCK, M., KRIMMEL, R. M. & WALTERS, R. 1994 Mechanical and hydrologic basis for the rapid motion of a large tidewater glacier: 1. Observations. *Journal of Geophysical Research* **99** (B8), 15219.
- MEIER, M. F. & POST, A. 1969 What are glacier surges? *Canadian Journal of Earth Sciences* **6** (4), 807–817.
- MEIER, M. F. & POST, A. 1987 Fast tidewater glaciers. *Journal of Geophysical Research* **92** (B9), 9051–9058.
- MERCER, J. H. 1978 West antarctic ice sheet and co2 greenhouse effect: a threat of disaster. *Nature* **271** (5643), 321.
- MERNILD, S. H., LISTON, G. E., HIEMSTRA, C. A. & CHRISTENSEN, J. H. 2009 Greenland Ice Sheet Surface Mass-Balance Modeling in a 131-Yr Perspective, 1950-2080. *Journal of Hydrometeorology* **11** (1), 3–25.
- MILES, B., STOKES, C. & JAMIESON, S. 2018 Velocity increases at Cook Glacier, East Antarctica, linked to ice shelf loss and a subglacial flood event. *Cryosphere* **12** (10), 3123–3136.
- MILES, B. W. J., STOKES, C. R. & JAMIESON, S. S. R. 2016 Pan-ice-sheet glacier terminus change in East Antarctica reveals sensitivity of Wilkes Land to sea-ice changes. *Science Advances* **2** (5), e1501350.
- MILLAN, R., RIGNOT, E., MOUGINOT, J., WOOD, M., BJØRK, A. A. & MORLIGHEM, M. 2018 Vulnerability of Southeast Greenland Glaciers to Warm Atlantic Water From Operation IceBridge and Ocean Melting Greenland Data. *Geophysical Research Letters* **45** (6), 2688–2696.
- MOCK, S. J. 1966 Fluctuations of the Terminus of the Harald Moltke Bræ, Greenland. *Journal of Glaciology* **6** (45), 369–373.
- MOHR, J. J., REEH, N. & MADSEN, S. N. 1998 Three-dimensional glacial flow and surface elevation measured with radar interferometry. *Nature* **391** (6664), 273–276.
- MOON, T. & JOUGHIN, I. 2008 Changes in ice front position on Greenland’s outlet glaciers from 1992 to 2007. *Journal of Geophysical Research: Earth Surface* **113** (2), 1–10.
- MOON, T., JOUGHIN, I. & SMITH, B. 2015 Seasonal to multiyear variability of glacier surface velocity, terminus position, and sea ice/ice mélange in northwest Greenland. *Journal of Geophysical Research: Earth Surface* **120** (5), 818–833.

- MOON, T., JOUGHIN, I., SMITH, B. & HOWAT, I. 2012 21st-century evolution of Greenland outlet glacier velocities. *Science* **336** (6081), 576–578.
- MORLAND, L. W. 1987 Unconfined Ice-Shelf Flow. In *Dynamics of the West Antarctic Ice Sheet* (ed. C. J. der Veen & J. Oerlemans), pp. 99–116. Dordrecht: Springer Netherlands.
- MORLIGHEM, M., BONDZIO, J., SEROUSSI, H., RIGNOT, E., LAROUR, E., HUMBERT, A. & REBUFFI, S. 2016a Modeling of Store Gletscher’s calving dynamics, West Greenland, in response to ocean thermal forcing. *Geophysical Research Letters* **43** (6), 2659–2666.
- MORLIGHEM, M., RIGNOT, E., MOUGINOT, J., SEROUSSI, H. & LAROUR, E. 2014 Deeply incised submarine glacial valleys beneath the Greenland ice sheet. *Nature Geoscience* **7** (6), 418–422.
- MORLIGHEM, M., RIGNOT, E. & WILLIS, J. 2016b Improving Bed Topography Mapping of Greenland Glaciers Using NASA’s Oceans Melting Greenland (OMG) Data. *Oceanography* **29** (4), 62–71.
- MORLIGHEM, M., WILLIAMS, C. N., RIGNOT, E., AN, L., ARNDT, J. E., BAMBER, J. L., CATANIA, G., CHAUCHÉ, N., DOWDESWELL, J. A., DORSCHER, B., FENTY, I., HOGAN, K., HOWAT, I., HUBBARD, A., JAKOBSSON, M., JORDAN, T. M., KJELDSEN, K. K., MILLAN, R., MAYER, L., MOUGINOT, J., NOËL, B. P., O’COFAIGH, C., PALMER, S., RYSGAARD, S., SEROUSSI, H., SIEGERT, M. J., SLABON, P., STRANEO, F., VAN DEN BROEKE, M. R., WEINREBE, W., WOOD, M. & ZINGLERSSEN, K. B. 2017 BedMachine v3: Complete Bed Topography and Ocean Bathymetry Mapping of Greenland From Multibeam Echo Sounding Combined With Mass Conservation. *Geophysical Research Letters* **44** (21), 051–11.
- MOTYKA, R. J., DRYER, W. P., AMUNDSON, J., TRUFFER, M. & FAHNESTOCK, M. 2013 Rapid submarine melting driven by subglacial discharge, LeConte Glacier, Alaska. *Geophysical Research Letters* **40** (19), 5153–5158.
- MOTYKA, R. J., HUNTER, L., ECHELMAYER, K. A. & CONNOR, C. 2003 Submarine melting at the terminus of a temperate tidewater glacier, LeConte Glacier, Alaska, U.S.A. *Annals of Glaciology* **36**, 57–65.
- MOTYKA, R. J., TRUFFER, M., FAHNESTOCK, M., MORTENSEN, J., RYSGAARD, S. & HOWAT, I. 2011 Submarine melting of the 1985 Jakobshavn Isbræ floating tongue and the triggering of the current retreat. *Journal of Geophysical Research: Earth Surface* **116**.

- MOUGINOT, J., BJØRK, A. A., MILLAN, R., SCHEUCHL, B. & RIGNOT, E. 2018 Insights on the Surge Behavior of Storstrømmen and L. Bistrup Bræ, Northeast Greenland, Over the Last Century. *Geophysical Research Letters* **45** (20), 197–11.
- MOUGINOT, J., RIGNOT, E., BJØRK, A. A., VAN DEN BROEKE, M., MILLAN, R., MORLIGHEM, M., NOËL, B., SCHEUCHL, B. & WOOD, M. 2019 Forty-six years of Greenland Ice Sheet mass balance from 1972 to 2018. *Proceedings of the National Academy of Sciences* **116** (19), 9239–9244.
- MOUGINOT, J., RIGNOT, E., SCHEUCHL, B., FENTY, I., KHAZENDAR, A., MORLIGHEM, M., BUZZI, A. & PADEN, J. 2015 Fast retreat of Zachariæ Isstrøm, northeast Greenland. *Science* **350** (6266), 1357–1361.
- MÜNCHOW, A., FALKNER, K., MELLING, H., RABE, B. & JOHNSON, H. 2011 Ocean Warming of Nares Strait Bottom Waters off Northwest Greenland, 2003-2009. *Oceanography* **24** (3), 114–123.
- MÜNCHOW, A., PADMAN, L. & FRICKER, H. A. 2014 Interannual changes of the floating ice shelf of Petermann Gletscher, North Greenland, from 2000 to 2012. *Journal of Glaciology* **60** (221), 489–499.
- MÜNCHOW, A., PADMAN, L., WASHAM, P. & NICHOLLS, K. 2016 The Ice Shelf of Petermann Gletscher, North Greenland, and Its Connection to the Arctic and Atlantic Oceans. *Oceanography* **29** (4), 84–95.
- MURRAY, T., SCHARRER, K., JAMES, T. D., DYE, S. R., HANNA, E., BOOTH, A. D., SELMES, N., LUCKMAN, A., HUGHES, A. L., COOK, S. & HUYBRECHTS, P. 2010 Ocean regulation hypothesis for glacier dynamics in southeast Greenland and implications for ice sheet mass changes. *Journal of Geophysical Research: Earth Surface* **115** (3), 1–15.
- MURRAY, T., SCHARRER, K., SELMES, N., BOOTH, A. D., JAMES, T. D., BEVAN, S. L., BRADLEY, J., COOK, S., LLANA, L. C., DROCOURT, Y., DYKE, L., GOLDSACK, A., HUGHES, A. L., LUCKMAN, A. J. & MCGOVERN, J. 2015 Extensive retreat of Greenland tidewater glaciers, 2000-2010. *Arctic, Antarctic, and Alpine Research* **47** (3), 427–447.
- MURRAY, T., STROZZI, T., LUCKMAN, A., JISKOOT, H. & CHRISTAKOS, P. 2003 Is there a single surge mechanism? Contrasts in dynamics between glacier surges in Svalbard and other regions. *Journal of Geophysical Research: Solid Earth* **108** (B5), –.

- NAGLER, T., HAUGLUND, K., FORSBERG, R. & ENGDAHL, M. 2016 Product User Guide (PUG). *Greenland Ice Sheet project of ESA's Climate Change Initiative* **version 2**. (June 2016), 1–91.
- NAGLER, T., ROTT, H., HETZENECKER, M., WUITE, J. & POTIN, P. 2015 The Sentinel-1 mission: New opportunities for ice sheet observations. *Remote Sensing* **7** (7), 9371–9389.
- NICK, F., LUCKMAN, A., VIELI, A., VAN DER VEEN, C., VAN AS, D., VAN DE WAL, R., PATTYN, F., HUBBARD, A. & FLORICIOIU, D. 2012 The response of Petermann Glacier, Greenland, to large calving events, and its future stability in the context of atmospheric and oceanic warming. *Journal of Glaciology* **58** (208), 229–239.
- NICK, F. M., VAN DER VEEN, C. J. & OERLEMANS, J. 2007 Controls on advance of tidewater glaciers: Results from numerical modeling applied to Columbia Glacier. *Journal of Geophysical Research: Earth Surface* **112** (3), 1–11.
- NICK, F. M., VAN DER VEEN, C. J., VIELI, A. & BENN, D. I. 2010 A physically based calving model applied to marine outlet glaciers and implications for the glacier dynamics. *Journal of Glaciology* **56** (199), 781–794.
- NICK, F. M., VIELI, A., ANDERSEN, M. L., JOUGHIN, I., PAYNE, A., EDWARDS, T. L., PATTYN, F. & VAN DE WAL, R. S. 2013 Future sea-level rise from Greenland's main outlet glaciers in a warming climate. *Nature* **497** (7448), 235–238.
- NICK, F. M., VIELI, A., HOWAT, I. M. & JOUGHIN, I. 2009 Large-scale changes in Greenland outlet glacier dynamics triggered at the terminus. *Nature Geoscience* **2** (2), 110–114.
- NOËL, B., JAN VAN DE BERG, W., MACHGUTH, H., LHERMITTE, S., HOWAT, I., FETTWEIS, X. & VAN DEN BROEKE, M. R. 2016 A daily, 1 km resolution data set of downscaled Greenland ice sheet surface mass balance (1958–2015). *Cryosphere* **10** (5), 2361–2377.
- O'LEARY, M. & CHRISTOFFERSEN, P. 2013 Calving on tidewater glaciers amplified by submarine frontal melting. *Cryosphere* **7** (1), 119–128.
- PALMER, S., SHEPHERD, A., NIENOW, P. & JOUGHIN, I. 2011 Seasonal speedup of the Greenland Ice Sheet linked to routing of surface water. *Earth and Planetary Science Letters* **302** (3–4), 423–428.
- PAOLO, F. S., FRICKER, H. A. & PADMAN, L. 2015 Volume loss from Antarctic ice shelves is accelerating. *Science* **348** (6232), 327–331.

- PATTYN, F. 2018 The paradigm shift in Antarctic ice sheet modelling. *Nature Communications* **9** (2728).
- PATTYN, F., RITZ, C., HANNA, E., ASAY-DAVIS, X., DECONTO, R., DURAND, G., FAVIER, L., FETTWEIS, X., GOELZER, H., GOLLEDGE, N. R., KUIPERS MUNNEKE, P., LENAERTS, J. T., NOWICKI, S., PAYNE, A. J., ROBINSON, A., SEROUSSI, H., TRUSEL, L. D. & VAN DEN BROEKE, M. 2018 The Greenland and Antarctic ice sheets under 1.5 °C global warming. *Nature Climate Change* **8** (12), 1053–1061.
- PATTYN, F., SCHOOF, C., PERICHON, L., HINDMARSH, R. C., BUELER, E., DE FLEURIAN, B., DURAND, G., GAGLIARDINI, O., GLADSTONE, R., GOLDBERG, D., GUDMUNDSSON, G. H., HUYBRECHTS, P., LEE, V., NICK, F. M., PAYNE, A. J., POLLARD, D., RYBAK, O., SAITO, F. & VIELI, A. 2012 Results of the marine ice sheet model intercomparison project, MISMIP. *Cryosphere* **6** (3), 573–588.
- PEARY, R. E. 1892 The North Greenland Expedition of 1891-92. *Journal of the American Geographical Society of New York* **24** (3), 536.
- PEGLER, S. S. 2016 The dynamics of confined extensional flows. *Journal of Fluid Mechanics* **804**, 24–57.
- PEGLER, S. S., KOWAL, K. N., HASENCLEVER, L. Q. & WORSTER, M. G. 2013 Lateral controls on grounding-line dynamics. *Journal of Fluid Mechanics* **722**, 1–12.
- PFEFFER, W. T. 2007 A simple mechanism for irreversible tidewater glacier retreat. *Journal of Geophysical Research: Earth Surface* **112** (3), 1–12.
- PHILLIPS, T., RAJARAM, H. & STEFFEN, K. 2010 Cryo-hydrologic warming: A potential mechanism for rapid thermal response of ice sheets. *Geophysical Research Letters* **37** (20), 1–5.
- PIMENTEL, S. & FLOWERS, G. E. 2010 A numerical study of hydrologically driven glacier dynamics and subglacial flooding. *Proceedings of the Royal Society A: Mathematical, Physical and Engineering Sciences* **467** (2126), 537–558.
- PODRASKY, D., TRUFFER, M., FAHNESTOCK, M., AMUNDSON, J. M., CASSOTTO, R. & JOUGHIN, I. 2012 Outlet glacier response to forcing over hourly to interannual timescales, Jakobshavn Isbræ, Greenland. *Journal of Glaciology* **58** (212), 1212–1226.
- PORTER, D. F., TINTO, K. J., BOGHOSIAN, A., COCHRAN, J. R., BELL, R. E., MANIZADE, S. S. & SONNTAG, J. G. 2014 Bathymetric control of tidewater glacier mass loss in northwest Greenland. *Earth and Planetary Science Letters* **401**, 40–46.

- POST, A. 1975 Preliminary hydrography and historic terminal changes of Columbia Glacier, Alaska. *Hydrologic Atlas* **559**.
- POST, A., O'NEEL, S., MOTYKA, R. J. & STREVELER, G. 2011 A complex relationship between calving glaciers and climate. *Eos* **92** (37), 305–307.
- POWELL, R. D. 1990 Glacimarine processes at grounding-line fans and their growth to ice-contact deltas. *Geological Society, London, Special Publications* **53** (1), 53–73.
- PRICE, S. F., PAYNE, A. J., HOWAT, I. M. & SMITH, B. E. 2011 Committed sea-level rise for the next century from Greenland ice sheet dynamics during the past decade. *Proceedings of the National Academy of Sciences* **108** (22), 8978–8983.
- PRITCHARD, H., MURRAY, T., LUCKMAN, A., STROZZI, T. & BARR, S. 2005 Glacier surge dynamics of Sortebræ, east Greenland, from synthetic aperture radar feature tracking. *Journal of Geophysical Research: Earth Surface* **110** (3), 1–13.
- PRITCHARD, H. D., ARTHURN, R. J., VAUGHAN, D. G. & EDWARDS, L. A. 2009 Extensive dynamic thinning on the margins of the Greenland and Antarctic ice sheets. *Nature* **461** (7266), 971–975.
- PRITCHARD, H. D., LIGTENBERG, S. R., FRICKER, H. A., VAUGHAN, D. G., VAN DEN BROEKE, M. R. & PADMAN, L. 2012 Antarctic ice-sheet loss driven by basal melting of ice shelves. *Nature* **484** (7395), 502–505.
- RASMUSSEN, K. 1919 The Second Thule Expedition to Northern Greenland, 1916–1918. *Geographical Review* **8** (2), 116–125.
- RASMUSSEN, K. J. V. 1912 Report of the First Thule Expedition 1912. In *Meddelelser om Grønland*. C.A. Reitzels Forlag.
- RATHMANN, N. M., HVIDBERG, C. S., SOLGAARD, A. M., GRINSTED, A., GUDMUNDSSON, G. H., LANGEN, P. L., NIELSEN, K. P. & KUSK, A. 2017 Highly temporally resolved response to seasonal surface melt of the Zachariae and 79N outlet glaciers in northeast Greenland. *Geophysical Research Letters* **44** (19), 9805–9814.
- RAYMOND, C. 1996 Shear margins in glaciers and ice sheets. *Journal of Glaciology* **42** (140), 90–102.
- REEH, N. 2017 Greenland Ice Shelves and Ice Tongues. In *Arctic Ice Shelves and Ice Islands* (ed. L. Copland & D. Mueller), pp. 75–106. Dordrecht: Springer Netherlands.
- REEH, N., BOGGILD, C. E. & OERTER, H. 1994 Surge of Storstrømmen, a large outlet glacier from the inland ice of north-east Greenland. *Grønlands Geologisk undersøgelse* .

- REEH, N., MAYER, C., MILLER, H., THOMSEN, H. H. & WEIDICK, A. 1999 Present and past climate control on fjord glaciations in Greenland: Implications for IRD-deposition in the sea. *Geophysical Research Letters* **26** (8), 1039–1042.
- REEH, N., MOHR, J. J., MADSEN, S. N., OERTER, H. & GUNDESTRUP, N. S. 2003 Three-dimensional surface velocities of Storstrømmen Glacier, Greenland, derived from radar interferometry and ice-sounding radar measurements. *Journal of Glaciology* **49** (165), 201–209.
- REEH, N., THOMSEN, H. H., HIGGINS, A. K. & WEIDICK, A. 2001 Sea ice and the stability of north and northeast Greenland floating glaciers. *Annals of Glaciology* **33**, 474–480.
- REESE, R., GUDMUNDSSON, G. H., LEVERMANN, A. & WINKELMANN, R. 2018a The far reach of ice-shelf thinning in Antarctica. *Nature Climate Change* **8** (1), 53–57.
- REESE, R., WINKELMANN, R. & HILMAR GUDMUNDSSON, G. 2018b Grounding-line flux formula applied as a flux condition in numerical simulations fails for buttressed Antarctic ice streams. *Cryosphere* **12** (10), 3229–3242.
- RIGNOT, E. 1996 Tidal motion, ice velocity and melt rate of Petermann Gletscher, Greenland, measured from radar interferometry. *Journal of Glaciology* **42** (142), 476–485.
- RIGNOT, E., BOX, J. E., BURGESS, E. & HANNA, E. 2008 Mass balance of the Greenland ice sheet from 1958 to 2007. *Geophysical Research Letters* **35** (20), 1–5.
- RIGNOT, E., BRAATEN, D., GOGINENI, S. P., KRABILL, W. B. & MCCONNELL, J. R. 2004 Rapid ice discharge from southeast Greenland glaciers. *Geophysical Research Letters* **31** (10), 2–5.
- RIGNOT, E., FENTY, I., XU, Y., CAI, C. & KEMP, C. 2015 Undercutting of marine-terminating glaciers in West Greenland. *Geophysical Research Letters* **42** (14), 5909–5917.
- RIGNOT, E., GOGINENI, S., JOUGHIN, I. & KRABILL, W. 2001 Contribution to the glaciology of northern Greenland from satellite radar interferometry. *Journal of Geophysical Research: Atmospheres* **106** (D24), 34007–34019.
- RIGNOT, E., JACOBS, S., MOUGINOT, J. & SCHEUCHL, B. 2013 Ice-shelf melting around Antarctica. *Science* **341** (6143), 266–70.
- RIGNOT, E. & KANAGARATNAM, P. 2006 Changes in the velocity structure of the Greenland Ice Sheet. *Science* **311** (5763), 986–990.

- RIGNOT, E., KOPPEL, M. & VELICOGNA, I. 2010 Rapid submarine melting of the calving faces of West Greenland glaciers. *Nature Geoscience* **3** (3), 187–191.
- RIGNOT, E. & MOUGINOT, J. 2012 Ice flow in Greenland for the International Polar Year 2008–2009. *Geophysical Research Letters* **39** (11), 1–7.
- RIGNOT, E., MOUGINOT, J., MORLIGHEM, M., SEROUSSI, H. & SCHEUCHL, B. 2014 Widespread, rapid grounding line retreat of Pine Island, Thwaites, Smith, and Kohler glaciers, West Antarctica, from 1992 to 2011. *Geophysical Research Letters* **41** (10), 3502–3509.
- RIGNOT, E. & STEFFEN, K. 2008 Channelized bottom melting and stability of floating ice shelves. *Geophysical Research Letters* **35** (2), 2–6.
- RIGNOT, E., VELICOGNA, I., VAN DEN BROEKE, M. R., MONAGHAN, A. & LENAERTS, J. 2011 Acceleration of the contribution of the Greenland and Antarctic ice sheets to sea level rise. *Geophysical Research Letters* **38** (5), 1–5.
- RIGNOT, E. J., GOGINENI, S. P., KRABILL, W. B. & EKHOLM, S. 1997 North and north-east Greenland ice discharge from satellite radar interferometry. *Science* **276** (5314), 934–937.
- ROSENAU, R., SCHEINERT, M. & DIETRICH, R. 2015 A processing system to monitor Greenland outlet glacier velocity variations at decadal and seasonal time scales utilizing the Landsat imagery. *Remote Sensing of Environment* **169**, 1–19.
- ROTT, H., RACK, W., SKVARCA, P. & DE ANGELIS, H. 2002 Northern Larsen Ice Shelf, Antarctica: Further retreat after collapse. *Annals of Glaciology* **34**, 277–282.
- RÜCKAMP, M., NECKEL, N., BERGER, S., HUMBERT, A. & HELM, V. 2019 Calving Induced Speedup of Petermann Glacier. *Journal of Geophysical Research: Earth Surface* **124** (1), 216–228.
- SASGEN, I., VAN DEN BROEKE, M., BAMBER, J. L., RIGNOT, E., SØRENSEN, L. S., WOUTERS, B., MARTINEC, Z., VELICOGNA, I. & SIMONSEN, S. B. 2012 Timing and origin of recent regional ice-mass loss in Greenland. *Earth and Planetary Science Letters* **333–334**, 293–303.
- SCAMBOS, T. A., BOHLANDER, J. A., SHUMAN, C. A. & SKVARCA, P. 2004 Glacier acceleration and thinning after ice shelf collapse in the Larsen B embayment, Antarctica. *Geophysical Research Letters* **31** (18), 2001–2004.
- SCHILD, K. M. & HAMILTON, G. S. 2013 Seasonal variations of outlet glacier terminus position in Greenland. *Journal of Glaciology* **59** (216), 759–770.

- SCHOOF, C. 2007 Ice sheet grounding line dynamics: Steady states, stability, and hysteresis. *Journal of Geophysical Research: Earth Surface* **112** (3), 1–19.
- SCHOOF, C., DAVIS, A. D. & POPA, T. V. 2017 Boundary layer models for calving marine outlet glaciers. *Cryosphere* **11** (5), 2283–2303.
- SCHWANGHART, W. & KUHN, N. J. 2010 TopoToolbox: A set of Matlab functions for topographic analysis. *Environmental Modelling and Software* **25** (6), 770–781.
- SCIASCIA, R., STRANEO, F., CENEDESE, C. & HEIMBACH, P. 2013 Seasonal variability of submarine melt rate and circulation in an East Greenland fjord. *Journal of Geophysical Research: Oceans* **118** (5), 2492–2506.
- SEALE, A., CHRISTOFFERSEN, P., MUGFORD, R. I. & O’LEARY, M. 2011 Ocean forcing of the Greenland Ice Sheet: Calving fronts and patterns of retreat identified by automatic satellite monitoring of eastern outlet glaciers. *Journal of Geophysical Research: Earth Surface* **116** (3), 1–16.
- SERREZE, M. C. & MEIER, W. N. 2019 The Arctic’s sea ice cover: trends, variability, predictability, and comparisons to the Antarctic. *Annals of the New York Academy of Sciences* **1436** (1), 36–53.
- SHAPERO, D. R., JOUGHIN, I. R., POINAR, K., MORLIGHEM, M. & GILLET-CHAULET, F. 2016 Basal resistance for three of the largest Greenland outlet glaciers. *Journal of Geophysical Research: Earth Surface* **121** (1), 168–180.
- SHARP, M. 1988 Surging glaciers: Behaviour and mechanisms. *Progress in Physical Geography* **12** (3), 349–370.
- SHEPHERD, A., IVINS, E. R., GERUO, A., BARLETTA, V. R., BENTLEY, M. J., BETTADPUR, S., BRIGGS, K. H., BROMWICH, D. H., FORSBERG, R., GALIN, N., HORWATH, M., JACOBS, S., JOUGHIN, I., KING, M. A., LENAERTS, J. T., LI, J., LIGHTENBERG, S. R., LUCKMAN, A., LUTHCKE, S. B., McMILLAN, M., MEISTER, R., MILNE, G., MOUGINOT, J., MUIR, A., NICOLAS, J. P., PADEN, J., PAYNE, A. J., PRITCHARD, H., RIGNOT, E., ROTT, H., SØRENSEN, L. S., SCAMBOS, T. A., SCHEUCHL, B., SCHRAMA, E. J., SMITH, B., SUNDAL, A. V., VAN ANGELEN, J. H., VAN DE BERG, W. J., VAN DEN BROEKE, M. R., VAUGHAN, D. G., VELICOGNA, I., WAHR, J., WHITEHOUSE, P. L., WINGHAM, D. J., YI, D., YOUNG, D. & ZWALLY, H. J. 2012 A reconciled estimate of ice-sheet mass balance. *Science* **338** (6111), 1183–1189.
- SHREVE, R. L. 1972 Movement of Water in Glaciers. *Journal of Glaciology* **11** (62), 205–214.

- SHROYER, E. L., PADMAN, L., SAMELSON, R. M., MÜNCHOW, A. & STEARNS, L. A. 2017 Seasonal control of Petermann Gletscher ice-shelf melt by the ocean's response to sea-ice cover in Nares Strait. *Journal of Glaciology* **63** (238), 324–330.
- SIMONSEN, S. B. & SØRENSEN, L. S. 2017 Implications of changing scattering properties on Greenland ice sheet volume change from Cryosat-2 altimetry. *Remote Sensing of Environment* **190**, 207–216.
- SLATER, D., STRANEO, F., FELIKSON, D., LITTLE, C., GOELZER, H., FETTWEIS, X. & HOLTE, J. 2019 Past and future response of Greenland's tidewater glaciers to submarine melting. *The Cryosphere Discussions* **in review**.
- SLATER, D. A., NIENOW, P. W., COWTON, T. R., GOLDBERG, D. N. & SOLE, A. J. 2015 Effect of near-terminus subglacial hydrology on tidewater. *Geophysical Research Letters* **42**, 2861–2868.
- SOHN, H. G., JEZEK, K. C. & VAN DER VEEN, C. J. 1998 Jakobshavn Glacier, West Greenland: 30 years of spaceborne observations. *Geophysical Research Letters* **25** (14), 2699–2702.
- SOLE, A., NIENOW, P., BARTHOLOMEW, I., MAIR, D., COWTON, T., TEDSTONE, A. & KING, M. A. 2013 Winter motion mediates dynamic response of the Greenland Ice Sheet to warmer summers. *Geophysical Research Letters* **40** (15), 3940–3944.
- SØRENSEN, L. S., SIMONSEN, S. B., MEISTER, R., FORSBERG, R., LEVINSSEN, J. F. & FLAMENT, T. 2015 Envisat-derived elevation changes of the Greenland ice sheet, and a comparison with ICESat results in the accumulation area. *Remote Sensing of Environment* **160**, 56–62.
- STEIGER, N., NISANCIOGLU, K. H., ÅKESSON, H., DE FLEURIAN, B. & NICK, F. M. 2018 Simulated retreat of Jakobshavn Isbræ since the Little Ice Age controlled by geometry. *Cryosphere* **12** (7), 2249–2266.
- STRANEO, F. & HEIMBACH, P. 2013 North Atlantic warming and the retreat of Greenland's outlet glaciers. *Nature* **504** (7478), 36–43.
- STRANEO, F., HEIMBACH, P., SERGIENKO, O., HAMILTON, G., CATANIA, G., GRIFFIES, S., HALLBERG, R., JENKINS, A., JOUGHIN, I., MOTYKA, R., PFEFFER, W. T., PRICE, S. F., RIGNOT, E., SCAMBOS, T., TRUFFER, M. & VIELI, A. 2013 Challenges to Understanding the Dynamic Response of Greenland's Marine Terminating Glaciers to Oceanic and Atmospheric Forcing. *Bulletin of the American Meteorological Society* **94** (8), 1131–1144.

- TEDESCO, M., MOTE, T., FETTWEIS, X., HANNA, E., JEYARATNAM, J., BOOTH, J. F., DATTA, R. & BRIGGS, K. 2016 Arctic cut-off high drives the poleward shift of a new Greenland melting record. *Nature Communications* **7** (11723), 1–6.
- TEDSTONE, A. J., NIENOW, P. W., GOURMELEN, N., DEHECQ, A., GOLDBERG, D. & HANNA, E. 2015 Decadal slowdown of a land-terminating sector of the Greenland Ice Sheet despite warming. *Nature* **526**, 692–695.
- THOMAS, R., FREDERICK, E., KRABILL, W., MANIZADE, S. & MARTIN, C. 2009 Recent changes on Greenland outlet glaciers. *Journal of Glaciology* **55** (189), 147–162.
- THOMAS, R., FREDERICK, E., LI, J., KRABILL, W., MANIZADE, S., PADEN, J., SONNTAG, J., SWIFT, R. & YUNGEL, J. 2011 Accelerating ice loss from the fastest Greenland and Antarctic glaciers. *Geophysical Research Letters* **38** (10), 1–6.
- THOMAS, R. H. 2004 Force-perturbation analysis of recent thinning and acceleration of Jakobshavn Isbræ, Greenland. *Journal of Glaciology* **50** (168), 57–66.
- THOMSEN, H. H., REEH, N., OLESEN, O. B., BOGGILD, C. E., STARZER, W., WEIDICK, A. & HIGGINS, A. K. 1997 The Nioghalvfjerdsfjorden glacier project, North-East Greenland: a study of ice sheet response to climatic change. *Geol. Surv. Greenland Bull.* **179**, 95–103.
- VAUGHAN, D., COMISO, J., ALLISON, I., CARRASCO, J., KASER, G., KWOK, R., MOTE, P., MURRAY, T., PAUL, F., REN, J., RIGNOT, E., SOLOMINA, O., STEFFEN, K. & ZHANG, T. 2013 Observations: Cryosphere. In *Climate Change 2013: The Physical Science Basis. Contribution of Working Group I to the Fifth Assessment Report of the Intergovernmental Panel on Climate Change* (ed. T. Stocker, D. Qin, G.-K. Plattner, M. Tignor, S. Allen, J. Boschung, A. Nauels, Y. Xia, V. Bex & P. Midgley), pp. 317–382. Cambridge, United Kingdom and New York, NY, USA: Cambridge University Press.
- VAUGHAN, D. G. & ARTHURN, R. 2007 Why is it hard to predict the future of ice sheets? *Science* **315** (5818), 1503–1504.
- VAN DER VEEN, C., PLUMMER, J. C. & STEARNS, L. 2011 Controls on the recent speed-up of Jakobshavn Isbræ, West Greenland. *Journal of Glaciology* **57** (204), 770–782.
- VAN DER VEEN, C. J. 1996 Tidewater calving. *Journal of Glaciology* **42** (6), 375–385.
- VAN DER VEEN, C. J. 1998 Fracture mechanics approach to penetration of bottom crevasses on glaciers. *Cold Regions Science and Technology* **27** (3), 213–223.
- VAN DER VEEN, C. J. 2007 Fracture propagation as means of rapidly transferring surface meltwater to the base of glaciers. *Geophysical Research Letters* **34** (1), 1–5.

- VELICOGNA, I., SUTTERLEY, T. C. & VAN DEN BROEKE, M. R. 2014 Geophysical Research Letters Regional acceleration in ice mass loss from Greenland and Antarctica using GRACE time-variable gravity data. *J. Geophys. Res. Space Physics* **41** (January 2003), 8130–8137.
- VIELI, A. & NICK, F. M. 2011 Understanding and Modelling Rapid Dynamic Changes of Tidewater Outlet Glaciers: Issues and Implications. *Surveys in Geophysics* **32** (4-5), 437–458.
- WALSH, K. M., HOWAT, I. M., AHN, Y. & ENDERLIN, E. M. 2012 Changes in the marine-terminating glaciers of central east Greenland, 2000-2010. *Cryosphere* **6** (1), 211–220.
- WALTER, F., CHAPUT, J. & LÜTHI, M. P. 2014 Thick sediments beneath Greenland’s ablation zone and their potential role in future ice sheet dynamics. *Geology* **42** (6), 487–490.
- WARREN, C. R. & GLASSER, N. F. 2006 Contrasting Response of South Greenland Glaciers to Recent Climatic Change. *Arctic and Alpine Research* **24** (2), 124.
- WASHAM, P., MÜNCHOW, A. & NICHOLLS, K. W. 2018 A Decade of Ocean Changes Impacting the Ice Shelf of Petermann Gletscher, Greenland. *Journal of Physical Oceanography* **48** (10), 2477–2493.
- WEIDICK, A., ANDREASEN, C., OERTER, H. & REEH, N. 1994 Neoglacial glacier changes around Storstrømmen, north-east Greenland. *Polarforschung* **64** (3), 95–108.
- WEIDICK, A., WILLIAMS, R. S. & FERRIGNO, J. G. 1995 *Satellite image atlas of glaciers of the world: Greenland*. US Government Printing Office Washington, DC.
- WILLIAMS, C. N., CORNFORD, S. L., JORDAN, T. M., DOWDESWELL, J. A., SIEGERT, M. J., CLARK, C. D., SWIFT, D. A., SOLE, A., FENTY, I. & BAMBER, J. L. 2017 Generating synthetic fjord bathymetry for coastal Greenland. *Cryosphere* **11** (1), 363–380.
- WILLIS, J., CARROLL, D., FENTY, I., KOHLI, G., KHAZENDAR, A., RUTHERFORD, M., TRENHOLM, N. & MORLIGHEM, M. 2018 Ocean-Ice Interactions in Inglefield Gulf: Early Results from NASA’s Oceans Melting Greenland Mission. *Oceanography* **31** (2).
- WILSON, N., STRANEO, F. & HEIMBACH, P. 2017 Satellite-derived submarine melt rates and mass balance (2011-2015) for Greenland’s largest remaining ice tongues. *Cryosphere* **11** (6), 2773–2782.

- WILSON, N. J. & STRANEO, F. 2015 Water exchange between the continental shelf and the cavity beneath Nioghalvfjærdsbræ (79 North Glacier). *Geophysical Research Letters* **42** (18), 7648–7654.
- WOOD, M., RIGNOT, E., FENTY, I., MENEMENLIS, D., MILLAN, R., MORLIGHEM, M., MOUGINOT, J. & SEROUSSI, H. 2018 Ocean-Induced Melt Triggers Glacier Retreat in Northwest Greenland. *Geophysical Research Letters* **45** (16), 8334–8342.
- WRIGHT, J. W. 1939 *Contributions to the glaciology of North-West Greenland*. København: Reitzel.
- XU, Y., RIGNOT, E., MENEMENLIS, D. & KOPPES, M. 2012 Numerical experiments on subaqueous melting of Greenland tidewater glaciers in response to ocean warming and enhanced subglacial discharge. *Annals of Glaciology* **53** (60), 229–234.
- ZWALLY, H. J., ABDALATI, W., HERRING, T., LARSON, K., SABA, J. & STEFFEN, K. 2002 Surface melt-induced acceleration of Greenland ice-sheet flow. *Science* **297**, 218–222.